UCSF
UC San Francisco Electronic Theses and Dissertations

Title
Dynamic Tuning of CD4+ T cells by Tonic Signals

Permalink
https://escholarship.org/uc/item/6r11z6ft

Author
Myers, Darienne Ross

Publication Date
2017

Peer reviewed|Thesis/dissertation

eScholarship.org Powered by the California Digital Library
University of California

Dynamic Tuning of CD4+ T cells by Tonic Signals

by

Darienne Myers

DISSERTATION

Submitted in partial satisfaction of the requirements for the degree of

DOCTOR OF PHILOSOPHY

in

Biomedical Sciences

in the

GRADUATE DIVISION

of the

UNIVERSITY OF CALIFORNIA, SAN FRANCISCO

Copyright 2017
by
Darienne R. Myers

DEDICATION AND ACKNOWLEDGEMENTS

Chapter 1 of this dissertation is a reprint of material published in Myers, D.R., Roose, J.P., 2016. Kinase and Phosphatase Pathways in T Cells. Ratcliffe, M.J.H. (Editor in Chief), Encyclopedia of Immunobiology, Vol. 3, pp. 25-37. Oxford: Academic Press. Chapter 6 is a reprint of Daley et al, *Rasgrp1* mutation increases naïve T-cell CD44 expression and drives mTOR-dependent accumulation of Helios^{+} T cells and autoantibodies. eLIFE 2013; 2:e01020.

The research presented in this dissertation is the result of hard work, and it could not have been done without the support of many people. First, I would like to thank my mentor, Jeroen Roose. Jeroen, thank you for everything. You have taught me so much about being a scientist: how to think critically and strategically about experimental design and analysis, how to write, how to give clear and interesting presentations, and how to share my knowledge with my own mentees. I appreciate how you set me up with three fascinating projects and gave me the freedom to explore the questions I found most interesting, always providing me with guidance when I needed it. Thank you for always telling me to dream big. And, most importantly, thank you for encouraging me to have fun while doing all of that! I feel incredibly fortunate to have had the chance to work with you – your intellect, strong leadership, and positivity are admirable, and I hope I can channel these qualities as I move forward in my career. Additionally, thank you for building a lab full of smart, kind, and fun people – it was always a pleasure coming to work and I greatly value the friendships I have made as a member of the Roose lab.

I would also like to thank every member of the Roose lab whom I've had the chance to work with over these past several years, and I'd like to specifically acknowledge a few people here. Olga Ksionda, thank you for being an incredible friend and mentor. You always answered my questions no matter how busy you were, and I had great fun with you swapping recipes and chatting in our bay. Yvonne Vercoulen, I admire your energy and organizational skills so much, thank you for teaching me how to handle big experiments and for contributing your interesting

data on basal Rasgrp1 signaling to my Anaef manuscript. And, thanks for being the BEST conference buddy! Andre Limnander, thanks for getting me set up in the lab with the Anaef project and for being the ultimate SF restaurant guru. Marsilius Mues, thanks for teaching me flow cytometry, for always being willing to lend a hand, and for all the laughs! Philippe Depeille and Jesse Jun, you have both been in the lab with me the entire time, and I am so happy I had you both as friends and mentors these past few years. Jesse, thanks for answering my endless questions about signaling assays, and Philippe, thanks for being my friend despite me never listening to you about why researching the intestine is the best! Emilia Norlin, it has been so wonderful working with you on the Anaef project these past couple years – thanks for your energy and hard work, and for your warmth and friendship. Tannia Lau, thanks for working with me on the HDAC story and for being such a fun presence in the lab. I would also like to thank my rotation students, Jorge Ortiz-Carpena, Casey Beppler, Ian Boothby, and Anthony Venida for their hard work and creative thinking on the Rasgrp1-metabolism project presented in Chapter 8.

I also received invaluable mentorship from several UCSF faculty members. Thanks to Mark Ansel, Julie Zikherman, and Davide Ruggero for being on my qualifying exam and thesis committees – your ideas and feedback at our meetings were incredibly helpful as I drove my projects forward. Thank you to Art Weiss and the Weiss lab for your comments and suggestions at our joint lab meetings.

Prior to starting my Ph.D. at UCSF, I received fantastic research training as an undergraduate at Amherst College by Dr. Dominic Poccia and Dr. David Ratner. Following that, I was first exposed to the exciting world of immunology research in Dr. Frederick Alt's lab. Thanks to Fred for giving me the opportunity to work in his lab, to Roberto Chiarle for mentoring me on a challenging and engaging project, and to Chunguang Guo for his mentorship and friendship.

Science is hard work, and I couldn't have made it through graduate school without my amazing friends. Thank you for sharing so many meals, cups of coffee, movies, hikes and boxing classes with me! All my love to Kathryn Cubria, Stacey Frumm, my Cooley Dorm roomies, my SF roommate Bevin English, and my BMS and MSTP friends.

Max, thank you for being my partner, friend, and the love of my life. I could not have done this without you. Whether we're at the top of a mountain or dancing in the kitchen, every moment with you is full of love and joy and laughter. I can't wait to go on more adventures with you for the rest of our lives.

Thank you to my family – mom, dad, and Jenna, I love you more than words can express. Thank you for encouraging me every step of the way, for supporting me as I moved across the country to pursue grad school, and for all the fun and laughter when we are together! Mom, thanks for the daily walk-to-work phone calls, talking with you always brightens my day. Thank you for being my best friend, and for all of your love, always.

ABSTRACT

Dynamic Tuning of CD4$^+$ T cells by Tonic Signals

Darienne R. Myers

To maintain immunological tolerance and prevent autoimmunity, naïve CD4$^+$ T cells need to be able to discriminate between self and nonself. In addition, naïve T cells need to remain quiescent and prevent spontaneous activation or differentiation, yet they also must be primed to efficiently respond when they do encounter foreign antigen. These features suggest that there must be active mechanisms to regulate the naïve state of CD4$^+$ T cells. We have uncovered that tonic (basal) signaling pathways in peripheral CD4$^+$ T cells dynamically maintain this primed-yet-quiescent state in three manners: transcriptional, translational, and metabolic programs.

We identified a tonic pathway involving the adapter LAT that dynamically controls a transcriptional program in naïve CD4$^+$ T cells. LAT perturbation in T cells leads to a spontaneous Th2-biased lymphoproliferative disease. We found that LAT is critical for tonic regulation of the repressor HDAC7. Tonic signals lead to phosphorylation and cytoplasmic localization of HDAC7, where it does not de-acetylate and repress its target genes. Without basal LAT function, HDAC7 is dephosphorylated and resides in the nucleus, where it represses target genes such as *Nur77* and *Irf4.* Appropriate expression of these genes is important for preventing spontaneous proliferation of CD4$^+$ T cells and differentiation to Th2.

Second, we identified a connection between tonic Rasgrp1-mTOR signals and translational programs. CD4$^+$ T cells with a point mutation in the Ras activator Rasgrp1, called Rasgrp1^{Anaef}, exhibit increased basal mTOR signaling and as a result the mice develop autoimmune features.

We found that *Rasgrp1*^{Anaef} CD4^{+} T cells have an autoreactive TCR repertoire and show increased differentiation to the Tfh- and Th2- lineages, with concomitant increase in Gata3 protein levels that we hypothesize is caused by increased translation. We are currently investigating what global basal translation programs are regulated by tonic Rasgrp1-mTOR signals in naïve T cells.

Additionally, we are following up on findings that tonic mTOR signals control the metabolic state of naïve T cells and allow for efficient switching of metabolic programs upon T cell activation. Overall, our results provide novel insights into the role of tonic signaling pathways in controlling naïve CD4^{+} T cells and how point mutations in signaling proteins can disrupt these tonic pathways, leading to perturbed immune function.

TABLE OF CONTENTS

Chapter 1: Kinase and Phosphatase Effector Pathways in T cells 1

Abstract 2

Introduction 3

Main text 4

Concluding remarks 26

Figures 28

References 38

Chapter 2: Tonic Signals in T Cells and their Role in Immune Function 46

Introduction: Tonic Signals in Lymphocytes 47

Main text 47

Conclusions and Perspectives 57

References 59

Chapter 3: mTOR Signaling in T Cells 61

Introduction 62

Main Text 62

Closing Remarks 74

Figures 75

References 77

Chapter 4: Aims of My Ph.D. Studies 81

Chapter 5: Tonic LAT-HDAC7 signals sustain *Nur77* and *Irf4* expression to tune naïve CD4$^+$ T cells 84

Abstract 85

Introduction 86

Results 88

Discussion 96

Figures 99

Methods 118

References 124

Chapter 6: *Rasgrp1* mutation increases naïve T-cell CD44 expression and drives mTOR-dependent accumulation of Helios$^+$ T cells and autoantibodies 128

Abstract 129

Introduction 130

Results 133

Discussion 144

Figures 149

Methods 189

References 195

Chapter 7: Naïve CD4$^+$ T Cells Feature Tonic Rasgrp1-mTORC1 Signals that Control mRNA Translation 200

Abstract 201

Introduction 202

Results 205

Future Directions 212
Discussion 213
Figures 216
Methods 228
References 234

Chapter 8: Future Directions. A Role for Tonic and Inducible Rasgrp1-mTOR Signals in T Cell Metabolism 238
Introduction 239
Preliminary Results 241
Future Directions 244
Figures 247
Methods 255
References 257

LIST OF FIGURES

Figure 1.1: TCR stimulation and proximal signaling events result in the recruitment of PLCγ1 and the generation of second messenger molecules IP3 and DAG 28

Figure 1.2: Diacylglycerol allows for the recruitment of PKC θ and RasGRP1 via their DAG-binding C1 domain 30

Figure 1.3: Generation of calcium signals in T cells resulting in NFAT transcriptional responses 33

Figure 1.4: Autoinhibition of RasGRP1 and activation by DAG and calcium. 35

Figure 1.5: Co-expression of RasGRP1 and SOS1 in lymphocytes allows for choices in analog or digital Ras-ERK signaling 37

Figure 3.1: Schematic of mTOR Signaling 76

Figure 5.1: A paradoxical TH2 hyperproliferative syndrome 99

Figure 5.2: A panel of immediate early response genes is maintained by LAT and repressed by HDAC7 101

Figure 5.3: HDAC7 represses IFN-γ and is constitutively phosphorylated in $CD4^+$ T cells.....103

Figure 5.4: A tonic LAT-PLCγ1-DAG signal regulates constitutive phosphorylation and nuclear export of HDAC-5 and -7.....105

Figure 5.5: Tonic signals in $CD4^+$ T cells dynamically regulate HDAC7 and its target Nur77 to limit proliferation 107

Figure 5.6: Irf4 expression is under tonic signal regulation and curbs T_H2 polarization of $CD4^+$ T cells 109

Supplemental Figure S1 – Gene expression alterations in $CD44^{LOW}CD4^+$ T cells with LAT perturbations induced by either 1-week or 4-weeks of tamoxifen treatment.....112

Supplemental Figure S2 – Gene expression alterations in $CD44^{LOW}CD4^{+}$ T cells with one week LAT perturbations....114

Supplemental Figure S3 – Gene expression alterations in $CD44^{LOW}CD4^{+}$ T cells with one week LAT perturbations....116

Figure 6.1: An ENU mouse mutant with increased CD44hi CD4 cells and anti-nuclear autoantibodies....150

Figure 6.1 – Supplemental Figure 1: Mapping and genotyping of the Rasgrp1 mutation in ENU mutant mice with anti-nuclear antibodies and CD44hi phenotype....152

Figure 6.2: Mapping of the ENU mutation to the autoinhibitory second EF hand domain in Rasgrp1....154

Figure 6.3: *Rasgrp1*^{Anaef} differs from *Rasgrp1*^{null} by preserving T cell selection in the thymus....156

Figure 6.3 – Supplemental Figure 2: Comparison of thymocyte maturation kinetics in WT and *Rasgrp1*^{Anaef}....159

Figure 6.4: Rasgrp1^{Anaef} diminishes *in vitro* signaling to Ras and ERK....161

Figure 6.4 – Supplemental Figure 3: Biochemical aspects of the *Rasgrp1*^{Anaef} allele....163

Figure 6.5: *Rasgrp1*^{Anaef} signaling characteristics of *in vitro* stimulated thymocytes....165

Figure 6.5 - Supplemental Figure 4: Signaling characteristics of *Rasgrp1*^{Anaef} thymocytes....167

Figure 6.5 - Supplemental Figure 5: Thymic selection in *Rasgrp1*^{Anaef} mice carrying transgenic TCRs....169

Figure 6.6: *Rasgrp1*^{Anaef} results in intrinsic dysregulation of peripheral CD4 T cells....171

Figure 6.7: Role of B and T cells in *Rasgrp1*^{Anaef}-induced PD-1^{+} $CD4^{+}$ T cell and autoantibody formation....173

Figure 6.8: CD44 is a sensitive reporter of mTOR activity in immature and naïve $CD4^{+}$ T cells....175

Figure 6.8 - Supplemental Figure S6: Alignment of HEAT5 domains in mTOR....178

Figure 6.9: Selective and cell-autonomous increase in CD44 expression in *Rasgrp1*^{Anaef} CD4^{+} T cells 180

Figure 6.9 - Supplemental Figure S7: CD44 and P-S6 expression in thymocytes 182

Figure 6.10: Increased tonic mTOR-S6 signals in *Rasgrp1*^{Anaef} thymocytes and T cells 184

Figure 6.10 - Supplementary Figure S8: Testing the role of MHCII recognition in constitutive CD44 overexpression by *Rasgrp1*^{Anaef} naive CD4 T cells 186

Figure 6.11: *Mtor* hypomorphic mutation corrects *Rasgrp1*^{Anaef}–induced increase in naive T-cell CD44 expression and accumulation of CD44^{+}Helios^{+}PD-1^{+}CD4^{+} cells and autoantibodies 188

Figure 7.1: Robust Tonic Rasgrp1-mTORC1-S6 Signals in Naïve CD4^{+} T Cells 217

Figure 7.2: Altered Selection and Autoimmune Features in Aging Anaef Mice 219

Figure 7.3: Anaef T Cells Exhibit Altered Helper T Cell Differentiation 221

Figure 7.4: Tonic mTORC1 Signals Affect Th2 Differentiation 223

Figure 7.5: Tonic mTORC1 Signaling Controls Translation of Specific Targets 225

Supplemental Figure 1: Rasgrp1^{Anaef} Thymocytes and T Cells have an Autoreactive TCR Repertoire 227

Figure 8.1: Rasgrp1^{Anaef} and Rasgrp1-deficient Cells have Impaired Receptor-induced mTORC1 Activation 248

Figure 8.2: Rasgrp1^{Anaef} CD4^{+} T Cells have Impaired TCR-induced Activation and Proliferation 250

Figure 8.3: Rasgrp1^{Anaef} CD4^{+} T Cells have Impaired TCR-induced Upregulation of Trophic Receptors 252

Figure 8.4: Rasgrp1 has a Role in Nutrient Sensing in Lymphocytes 254

Chapter 1

Kinase and Phosphatase Effector Pathways in T cells

ABSTRACT

Multiple interconnected effector pathways mediate the activation of T cells following recognition of cognate antigen. These kinase and phosphatase pathways link proximal T cell receptor (TCR) signaling to changes in gene expression and cell physiology. A key step in the TCR signaling cascade is the generation of the second messenger molecules inositol trisphosphate (IP3) and diacylglycerol (DAG). IP3 triggers calcium signaling, leading to activation of the transcription factor NFAT, while DAG activates PKCθ and RasGRP1, which couple to the transcription factors NFκB and AP-1, respectively. The coordinated binding of these three transcription factors, NFAT, NFκB, and AP-1, to the promoter of the T cell survival cytokine interleukin-2 is a critical step in T cell activation. In this chapter, we cover the kinase and phosphatase pathways downstream of second messenger generation and discuss the role of these effectors in T cell development, activation and differentiation.

Introduction

When a T cell interacts with an antigen presenting cell (APC) bearing cognate antigen, a number of signaling and cell biological events occur that lead to full activation of the T cell. The site of contact between the T cell and the APC is known as the immunological synapse (IS), and a number of studies have shown that signaling molecules are recruited to or excluded from the IS in a coordinated, regulated manner. This spatial reorganization facilitates transduction of signals from the T cell receptor (TCR) and costimulatory molecules in a multistep fashion to eventually instruct transcription factors in the nucleus to induce gene expression. Receptor signals trigger the activation of proximal tyrosine kinases and the phosphorylation and assembly of adaptor complexes so that distal kinase and phosphatase effector pathways can be subsequently engaged to activate a number of important transcription factors. These transcription factors include nuclear factor of activated T cells (NFAT), nuclear factor kappa B (NFκB), and activator protein 1 (AP-1), which are of particular importance for T cells because of their role in inducing transcription of the T cell survival cytokine IL-2 (interleukin 2). Namely, there are binding sites for all three transcription factors in the *IL-2* promoter, and their coordinated binding is required for *IL-2* gene expression (Smith-Garvin et al. 2009; Navarro & Cantrell 2014).

TCR- and costimulatory- signals, such as CD28, also act in concert with specific cytokine receptor signals to establish differentiation of naïve $CD4^+$ T cells into appropriate effector T cell subsets. Depending on the type of pathogen and local cytokine environment, naïve $CD4^+$ T cells can for instance differentiate into T helper type 1 (Th1) cells that are important for clearing bacterial and viral infections or into T helper type 2 (Th2) cells that are important for clearing helminth infections but can be pathogenic in asthma. Th17 cells are pro-

inflammatory, while iTregs express the master transcription factor FoxP3 and are important for suppressing other T cells (O'Shea & Paul 2010). A key function of these differentiated cells is to produce cytokines such as IFNγ (for Th1) and IL-4 (for Th2).

In this chapter we will focus on the different serine/threonine kinase and phosphatase effector pathways that lie downstream of the proximal tyrosine kinases and assembled adaptor complexes and are triggered by second messenger molecules. We will discuss the role of these kinase pathways in $CD4^+$ T cells.

Second messenger molecules: Connecting proximal TCR signaling to effector kinase and phosphatase pathways

Many molecular events have been defined to occur when the T cell receptor is ligated by cognate antigen and the IS is formed. In short, the initiation of proximal TCR signaling first involves phosphorylation of the ITAMs (immunoreceptor tyosine-based activation motifs) of the TCR. Zeta-associated protein of 70 kDa (Zap70) is recruited to the phosphorylated ITAMs, and in turn this leads to the phosphorylation of a number of effectors. Two of these are the transmembrane adapter linker for activation of T cells (LAT) and the cytosolic adapter SH2-domain containing leukocyte phosphoprotein of 76kDa (SLP-76). Coordinated assembly of LAT, SLP-76, and other molecules forms a structure called the LAT signalosome. The formation of the LAT signalosome ultimately leads to the binding and activation of the enzyme PLCγ1 (phospholipase C gamma 1) at tyrosine 136 (murine LAT; Y132 for human LAT) (**Figure 1**). The importance of PLCγ1 in a number of thymocyte and T cell processes was demonstrated using mice where *PLCγ1* is deleted exclusively in T cells (Fu et al. 2010). Deletion of *PLCγ1* results in reduced numbers of thymocytes due to defects in positive and negative selection, and very few

T cells populate the secondary lymphoid organs. Those T cells that do make it to lymphoid organs have defects in proliferation and IL-2 production, and the mice develop an autoimmune, inflammatory disease. With respect to biochemical signals, *PLCγ1*-deficient T cells are impaired in their ability to activate the transcription factors NFAT, NFκB, and AP-1. Of note, PLCγ2 plays a similarly critical role in B lymphocytes (Wang et al. 2000), but we focus on T cells here.

How does PLCγ1 connect to activation of NFAT, NFκB, and AP-1? PLCγ1 hydrolyzes the phospholipid PIP2 (phosphatidylinositol 4,5-bisphosphate) at the plasma membrane (PM), generating two important second messenger molecules: the hydrophilic inositol trisphosphate (IP3), which diffuses into the cytosol (Huang & Sauer 2010), and the hydrophobic diacylglycerol (DAG), which embeds in the plasma membrane (and other endomembranes) (Almena & Merida 2011)) (**Figure 1.1**). IP3 activates calcium (Ca^{2+}) signaling and the transcription factor NFAT, and DAG activates effector proteins such as the protein kinase C family (PKCs) and the Ras guanine nucleotide releasing protein (RasGRP) family members, which can couple to the NFκB and AP-1 pathways, respectively (**Figure 1.2**). In the next sections, we will discuss kinase and phosphatase signaling pathways downstream of IP3 and DAG and highlight their role in thymocyte development and T cell activation and function.

Calcium fluxes and calcium-trigger signals in T cells

Calcium is a critical second messenger and mediates a number of important biochemical and cell biological functions in T cells and other cells (Huang & Sauer 2010; Feske 2007; Hogan et al. 2010). Resting T cells maintain cytoplasmic stores of Ca^{2+} at ~100nM concentration (Feske 2007; Hogan et al. 2010), and upon receptor ligation, activated T cells flux Ca^{2+} and the intracellular concentration rises to ~1 μM. This is due to (1) release of Ca^{2+} that is stored in the

endoplasmic reticulum (ER) into the cytosol as well as (2) influx of Ca^{2+} from the extracellular space to the inside of the cell (Feske 2007; Hogan et al. 2010; Feske et al. 2015). There are a number of cellular proteins whose activation is controlled by binding to calcium, and many of these harbor a protein domain called the EF hand. EF hands typically come in pairs and have a helix-loop-helix structure. Each EF hand can bind one calcium ion, and Ca^{2+} binding typically induces a conformational change in the protein that facilitates subsequent signal transduction (Gifford et al. 2007). In the next sections we will highlight the Ca^{2+} signaling pathway downstream of TCR-IP3 signals that culminates in NFAT activation, point out EF hand-containing proteins therein, and discuss the role of these Ca^{2+} effectors in T cell biology.

Release of calcium stores from the ER–Role of the IP3 Receptor

Generation of the second messenger IP3 from PIP2 at the PM is the first step in activating Ca^{2+} signaling. The soluble, hydrophilic IP3 molecule diffuses throughout the cytosol and binds to IP3-receptors (IP3Rs), which are channels located on the ER. IP3Rs also bind calcium, and it is thought that the combined binding of IP3 and Ca^{2+} leads to a conformational change, activating and opening the IP3R. This is followed by a rapid efflux of Ca^{2+} ions from the ER lumen into the cytosol (Taylor et al. 2009) (**Figure 1.3**). Three genes (*ITPR1*, *2*, and *3*) encode the three IP3R homologs, which are ubiquitously expressed (Taylor et al. 2009). Experiments utilizing a chicken B cell line deficient for all *ITPR* genes clearly demonstrated that IP3-receptors are critical for calcium flux downstream of B cell receptor activation (Sugawara et al. 1997). A mouse model in which all three *ITPR* genes are deleted in T cells revealed a role for IP3R signaling in thymocyte development at the double negative (DN) to double positive (DP) transition. Interestingly, these knockout mice also develop thymic tumors that resemble T cell acute lymphoblastic leukemia/lymphoma (T-ALL) (Ouyang et al. 2014). These studies demonstrate an important role for IP3Rs and release of stored calcium in controlling lymphocyte development and activation.

Calcium entry from outside the cell—STIM and ORAI

Release of stored calcium from the ER downstream of TCR→IP3 signals results in the opening of CRAC (calcium release-activated calcium) channels at the PM. Open CRAC channels allow for influx of calcium from the outside of the cell into the cytosol. This influx is known as SOCE, or store operated calcium entry. Several tools aided researchers in studying SOCE and calcium signaling in T cells, such as thapsigargin, an agent that leads to depletion of ER calcium stores, and ionomycin, a calcium ionophore (Hogan et al. 2010). It was known since the 1970s that activated T cells take up extracellular calcium, but the molecular players that physically form the channel the Ca^{2+} ions enter through were not identified until the mid-2000s. Seminal papers describe their discovery: these studies involved RNAi screens in *Drosophila* and HeLa cells, and the analysis of patients with primary immunodeficiency and CRAC channel activation (Hogan et al. 2010; Feske 2007; Feske et al. 2015). These players are now known to be STIM (stromal interaction molecule) and ORAI (ORAI calcium release-activated calcium channel modulator). We will provide a brief summary of how STIM and ORAI function in T cells, and for further details on this topic we point the readers to these excellent reviews (Hogan et al. 2010; Feske et al. 2015).

STIM1 is a single-pass transmembrane protein that is predominantly localized to the ER. Lymphocytes and other cells also express another STIM family member, STIM2, although mouse models with deficiencies in *STIM1* or *STIM2* reveal that STIM1 appears to be more important for Ca^{2+} signaling in T cells (Oh-hora et al. 2008). The portion of the STIM1 protein that resides in the ER lumen contains a pair of EF hands (Stathopulos et al. 2008). STIM1 is a calcium-sensing protein: in resting lymphocytes, the EF hands of STIM1 bind Ca^{2+} which is present in high concentration in the ER. Upon TCR ligation and depletion of ER Ca^{2+} stores,

Ca^{2+} dissociates from STIM1, inducing a conformational change in the protein (Stathopulos et al. 2008). Total internal reflection fluorescence microscopy (TIRF) and electron microscopy (EM) studies demonstrated that STIM oligomers cluster at individual spots, called puncta. These puncta are found at sites where the ER and the PM are closely apposed, and calcium entry follows their formation (Wu 2006). STIM1 recruits ORAI1 to these puncta by binding to the C-terminus of ORAI1 (Park et al. 2009), and STIM1 activates ORAI1 via an additional interaction (possibly the ORAI N terminus) (Hogan et al. 2010) **Figure 3**. The *ORAI1* gene encodes the protein that forms the CRAC channel (specifically, the pore subunit of the CRAC channel), which is very selective for Ca^{2+} (Prakriya et al. 2006). The pore is not active and does not allow Ca^{2+} entry, however, until it complexes with STIM1. Of note, there are two *ORAI1* homologs, *ORAI2* and *ORAI3*, although their role in lymphocytes is still unclear (Feske et al. 2015).

Analysis of human patients with primary immunodeficiency and of genetic mouse models revealed critical physiological functions for STIM and ORAI. Several families were identified that had severe combined immunodeficiency (SCID) accompanied by impaired CRAC channel activity (these disorders are also referred to as “CRAC channelopathies”). These families were found to have mutations in *STIM1* (Fuchs et al. 2012; Picard et al. 2009) and *ORAI1* (Feske et al. 2006) that either abolish protein expression or lead to loss-of-function variants. Patients with *STIM1*- and *ORAI1*-mutated immunodeficiencies have similar clinical phenotypes that include recurrent infections (especially at a young age), autoimmunity later in life, muscular hypotonia and ectodermal dysplasia (Feske et al. 2015). Interestingly, lymphocyte development is normal in these patients, but their peripheral T cells are functionally impaired: these T cells do not flux Ca^{2+}, do not proliferate well in response to stimulation, and do not activate NFAT. These T cells also have impaired production of NFAT-responsive cytokines such as IL-2 (Hogan et al. 2010; Feske et al. 2015). Reconstituting the patient cells with WT *ORAI1* restores CRAC channel function.

Mouse models with gene deletions in STIM and ORAI (*STIM1*$^{-/-}$ *STIM2*$^{-/-}$ and *ORAI1*$^{-/-}$) or with a patient variant (*ORAI1*^{R93W}) knocked into the endogenous *ORAI1* locus were subsequently generated (Oh-hora et al. 2008; Gwack et al. 2008; Vig et al. 2007). These mice phenotypically resemble the human patients, in that thymocyte development is intact yet peripheral $CD4^+$ T cells display profound defects in SOCE, NFAT activation, and NFAT-dependent cytokine production. These mice have been powerful tools for aiding our understanding of the roles STIM and ORAI play in a number of T cell effector functions (Oh-hora et al. 2008; Ma et al. 2010; Gwack et al. 2008; McCarl et al. 2010; Feske et al. 2015; Hogan et al. 2010).

A calcium-calmodulin-calcineurin phosphatase pathway regulates NFAT activation

A key downstream consequence of calcium signaling is activation of the transcription factor family NFAT. The biochemical details of this pathway have been well-studied and involve the sequential activation of the Ca^{2+} sensor calmodulin and the phosphatase calcineurin. Calmodulin contains four canonical EF hands, and these become fully occupied (each binding one Ca^{2+} ion) when the cytosolic concentration rises following SOCE. Ca^{2+}-bound calmodulin undergoes a conformational change, exposing a site necessary for interaction with its binding partners, including calcineurin (Babu et al. 1988; James et al. 1995). Calcineurin is a heterodimeric phosphatase comprised of a catalytic subunit (A) and a regulatory subunit (B), which heterodimerize, but the dimer is not fully active until it binds calmodulin. (**Figure 3**). Calcineurin A consists of an N-terminal catalytic domain, a calcineurin B binding region, a calmodulin binding segment, and an autoinhibitory region. Calcineurin B also contains four EF hands, which have roles in both calcium sensing and in conferring stability on the heterodimer (Li et al. 2011). Calmodulin binding leads to a conformational change in calcineurin by

displacing the autoinhibitory domain (Marshall et al. 2015). The importance of calcineurin in T cell activation is underscored by the fact that two clinically important immunosuppressive agents, cyclosporine A (CsA) and tacrolimus (also called FK506), were shown to be inhibitors of calcineurin (J. Liu et al. 1991). These drugs are extensively used in the clinic to treat autoimmunity and to improve survival following transplantation.

Upon activation, calcineurin docks onto NFAT in order to dephosphorylate and activate the transcription factor. NFAT proteins contain a transactivation domain, a regulatory domain, a DNA-binding domain, and a C-terminal domain. Within the regulatory domain lie several serine-rich motifs, and these are heavily phosphorylated in resting T cells by several kinases (Hogan et al. 2003; Macian 2005; Müller & Rao 2010). When these serines are phosphorylated, NFAT is in such a conformation that its nuclear localization signal (NLS) is masked (Macian 2005). Upon antigen receptor stimulation and Ca^{2+} signaling, active calcineurin dephosphorylates NFAT, exposing the NLS. This permits the nuclear translocation of NFAT and induction of its target genes (**Figure 1.3)**. Thus, NFAT serves as a molecular link between Ca^{2+} signaling and gene expression. NFAT typically partners with other transcription factors via protein-protein interactions to regulate specific gene expression patterns. AP-1 (downstream of Ras-ERK signaling, discussed below) is a common partner of NFAT in activated T cells (Jain et al. 1992); as such, T cells integrate kinase pathways downstream of IP3 and DAG for full activation. Upon termination of cell activation, NFAT can be re-phosphorylated in the nucleus by export kinases to promote its export from the nucleus into the cytosol (Macian 2005; Müller & Rao 2010).

There are five NFAT family members (NFAT1-5), but we discuss NFAT1, 2, and 4 (which we collectively refer to as “NFAT”) here, as NFAT3 is not expressed in T cells and, unlike NFATs 1-4, NFAT5 is not regulated by Ca^{2+} (Macian 2005). The various NFAT proteins seem to have redundant functions in T cells, as individual gene knockout mice have a mild impact on the

immune system. Data from the study of mice deficient in multiple NFAT family members have revealed roles for NFAT in thymocyte positive selection, T cell differentiation, and anergy. For example, *NFAT1*$^{-/-}$ *NFAT2*$^{-/-}$ mice have profound defects in the production of IL-2 and other cytokines, and *NFAT1*$^{-/-}$ *NFAT4*$^{-/-}$ mice have hyperactive T cells and increased Th2 responses (Macian 2005). For a thorough discussion of the role of NFAT in these effector functions, we point readers to several excellent reviews (Hogan et al. 2003; Macian 2005; Müller & Rao 2010).

As described here, signaling downstream of the TCR can lead to activation of NFAT through generation of the second messenger IP3 and Ca^{2+} signaling. However, to fully activate T cells and induce IL-2 production, NFAT needs to bind in a coordinated fashion to the *IL-2* promoter along with the transcription factors NFκB and AP-1, which are triggered downstream of DAG. The role of DAG and its downstream effector pathways in T cells will be discussed next.

Diacylglycerol (DAG) and C1 domains

Diacylglycerol (DAG) is a glycerol molecule joined to two long chain fatty acids through ester linkages; it is a hydrophobic molecule and thus embeds in cellular membranes such as the plasma membrane (PM) (Carrasco & Merida 2007; Krishna & Zhong 2013). DAG is an important lipid for lymphocytes and other cell types both because it can be metabolized and used as a source of fatty acids, which are important for growth and development (Carrasco & Merida 2007), and because it can act as a second messenger for activation of signaling pathways such as NFκB and AP-1 (**Figure 1.2**). How exactly does DAG generation downstream of the TCR trigger NFκB and AP-1 signaling pathways, ultimately leading to T cell activation? This is primarily achieved through the recruitment and allosteric activation of effector proteins

that harbor a “typical C1 domain”, which can bind to DAG. C1 domains have a conserved 50 amino acid sequence and a well-characterized structure; they contain a hydrophobic base and a groove that form a cup-like structure to bind DAG. Binding of the C1 structure to DAG achieves membrane recruitment of proteins with such a domain (Carrasco & Merida 2004). Examples of signaling proteins with C1 domains include members of the protein kinase C (PKC) family, protein kinase D (PKD) (Spitaler et al. 2006), Ras guanine nucleotide releasing proteins (RasGRPs), chimaerin family proteins, and munc13 proteins (Krishna & Zhong 2013); PKCs (particularly PKCθ) and RasGRP1 will be discussed in greater detail subsequently (**Figure 1.2**).

Direct biochemical measurement of DAG levels in cells, and how receptor stimulation alters these levels, is challenging. Elegant microscopy studies used the isolated C1 domains from various proteins as tools to investigate DAG in cells (Carrasco & Merida 2004; Spitaler et al. 2006; Quann et al. 2009). These tools, referred to as C1 domain probes, typically consist of the isolated C1 domain fused to GFP (green fluorescent protein). The C1 binds DAG and the associated GFP reports the subcellular location of DAG and potentially the localization of the protein whose C1 domain was used (though other protein domains can contribute to localization as well). These tools revealed that DAG and DAG effector proteins accumulate at the plasma membrane and within the IS in an organized way. For more detailed reading on subsequent studies and approaches we refer the reader to these additional studies (Sato et al. 2006; Kunkel & Newton 2010; Almena & Merida 2011).

Generation and turnover of DAG – Regulation is critical

In the 1980’s it became clear that DAG is a potent T cell stimulant. Evidence for this came from experiments showing that phorbol esters (synthetic DAG mimetics) such as phorbol 12-myristate 13-acetate (PMA) are efficient T cell activators (Smith-Garvin et al. 2009). Cells

cannot metabolize PMA, so upon administration it embeds in the plasma membrane and fully activates AP-1 and NFκB signaling to drive T cell effector functions, such as cytokine production (Weiss et al. 1984). For certain cell responses, PMA stimulation entirely bypasses the need for TCR stimulation or proximal TCR signaling components such as the tyrosine kinase ZAP70 or the adapter molecule LAT. Because of this, in the 90's PMA became a useful tool to help delineate the TCR signaling pathway. Occurring in parallel in the 80's, cancer researchers uncovered that 12-O-tetradecanoylphorbol-13-acetate (TPA), a phorbol ester similar to PMA, could be used to promote tumor formation in various cancer settings, particularly in mouse models of skin cancer where TPA is painted on the skin (Takigawa et al. 1983). These studies inspired the hunt for DAG/PMA-responsive effector molecules, which we will discuss later.

The above-mentioned studies indirectly implied that DAG levels must be strictly regulated to ensure signaling occurs in the appropriate context. DAG is present at low levels in resting (unstimulated) lymphocytes; it can be generated by *de novo* synthesis or can be produced from cellular intermediates by the activity of several enzymes such as sphingomyelin synthase, phospholipase D (PLD), and phospholipase C (PLC). DAG is rapidly generated in response to TCR ligation. The PLC family member PLCγ1 is particularly important for DAG generation from PIP2 in TCR-activated T cells (**Figure 1.1**). It is of interest to note that PIP2 comprises less than 1% of the plasma membrane (Spitaler et al. 2006; Huang & Sauer 2010), yet its hydrolysis has profound effects on the activation status of lymphocytes. This is achieved because newly generated DAG is not equally distributed but forms a gradient and accumulates at the IS. The localized clustering of DAG-responsive signaling molecules at the IS is important for the robust activation of downstream pathways and is functionally important for T cell polarization, activation, development, and differentiation (Smith-Garvin et al. 2009; Quann et al. 2011).

Conversely, DAG can be phosphorylated by a class of proteins called diacylglycerol kinases (DGKs), producing PA (phosphatidic acid), and this can serve as a mechanism to dampen or turn off DAG signaling. Mouse models with T cell specific deletions of *DGK*α and *DGK*ζ (the DGK family members expressed in T cells), which effectively constitutively activate DAG signaling due to the inability to "turn off" DAG, reveal a crucial role for these kinases in controlling thymocyte maturation and cell activation (Guo et al. 2008). *DGK*$\alpha^{-/-}$ *DGK*$\zeta^{-/-}$ mice have reduced numbers of single positive (SP) thymocytes concomitant with elevated levels of Ras-GTP and phosphorylated ERK. (Guo et al. 2008). It is still unclear whether this reduction is due to defects in positive selection or enhanced negative selection of thymocytes (Joshi & Koretzky 2013). Furthermore, older compound heterozygous *DGK*$\alpha^{+/-}$ *DGK*$\zeta^{+/-}$ mice that are engineered to carry a transgenic TCR on thymocytes develop thymic lymphomas. These cells exhibit elevated Ras-ERK signaling which likely drives the cellular transformation. These genetic approaches highlight the importance of regulated, controlled DAG generation and turnover to ensure proper thymocyte development and T cell proliferation (Krishna & Zhong 2013).

Protein Kinase C (PKC) Family – Classification and Structural Features

The PKC family of serine/threonine kinases harbor two tandem C1-domains (C1a and C1b) and thus are capable of binding DAG. This family consists of at least 9 isoforms (α, β, γ, δ, ε, η, θ, ζ, ι), 8 of which (all but γ) are expressed in T lymphocytes. The isoforms are further categorized into three groups. The (1) conventional PKCs (α, β, γ) require both DAG and Ca^{2+} for activation; the (2) novel PKCs (δ, ε, η, θ) require DAG but not Ca^{2+} for activation; the (3)

atypical PKCs (ζ, ι) are activated via protein-protein interactions independently of both DAG and Ca^{2+} (Melowic et al. 2007; Quann et al. 2009; Pfeifhofer et al. 2003).

All PKCs contain C1 domains, but PKCθ is the dominant isoform to get recruited to the IS upon T-cell contact with an APC (Monks et al. 1997). This IS localization occurs in an antigen-specific manner and is dependent on PLCγ1-derived DAG, as treatment of cells with a PLCγ1 inhibitor, or with calphostin c (which competes for DAG binding) blocks PKCθ translocation to the plasma membrane (Diaz-Flores et al. 2003; Carrasco & Merida 2004). Thus, DAG plays a critical role in the regulation of PKCθ translocation. Additional studies revealed that various structural domains of PKCθ in addition to the C1 domain are important for controlling its activation and membrane localization. PKCθ has a C2 domain at its N-terminus, followed by a pseudosubstrate (PS) domain, tandem C1 domains (C1a and C1b), a V3 (hinge region), and C-terminal kinase domains (**Figure 1.2**). In resting cells, PKCθ exists in a "closed/inactive" conformation in the cytosol; the PS domain forms an intramolecular interaction with the kinase (catalytic) domain, such that substrate cannot bind to PKCθ (Wang et al. 2012). The C2 domain is also thought to be important for this auto-inhibition (Melowic et al. 2007). This inhibition is relieved upon T cell activation: DAG binds to PKCθ, leading to plasma membrane translocation and inducing an allosteric change in the protein such that the activation loop can be phosphorylated and the kinase domain can be accessible by substrate. The membrane-associated protein is now in an "open/active" conformation and can bind and phosphorylate its substrates (Wang et al. 2012).

Specifically, it is the C1b domain that allows for plasma membrane targeting in response to PMA or TCR/CD28 stimulation (Carrasco & Merida 2004; Melowic et al. 2007) (**Figure 1.2**). Interestingly, in *in vitro* experiments the full length PKCθ protein remains at the T cell-APC

contact site for a longer period of time than the isolated C1 domains of PKCθ do, suggesting that other domains of PKCθ are also important for stable recruitment of PKCθ to the IS (Carrasco & Merida 2004). Specifically, it was shown that the V3 (hinge) region of PKCθ, which contains a proline-rich element, is important for IS localization and activation of downstream signaling pathways (Kong et al. 2011). In the current model, PKCθ is recruited to the IS in a transient, low-affinity manner via its C1b domain, and then binding of the V3 region to CD28 stabilizes PKCθ at the IS, allowing for signal propagation (Yokosuka et al. 2008; Kong et al. 2011).

PKCθ, NFκB and AP-1 Pathways, and T cell function

To understand the role of PKCθ *in vivo*, two groups independently generated *PKCθ* knockout mice using different gene targeting strategies and both reported a striking defect in T cell proliferation and production of the T cell survival cytokine IL-2 in response to TCR/CD28 stimulation (Sun et al. 2000; Pfeifhofer et al. 2003). These mice revealed an important role for PKCθ in T cell proliferation and IL-2 production; *PKCθ* knockout T cells demonstrated decreased activation of the transcription factors AP-1 and NFκB in response to CD3/CD28 stimulation, which fits with the notion that these transcription factors need to bind to the promoter region of the *IL-2* gene to induce IL-2 expression. Indeed, the proliferation defect could be rescued by administering IL-2 to *PKCθ* knockout T cells exogenously. These findings were corroborated by two studies using a Jurkat T cell lymphoma cell line; both groups found that PKCθ could activate NFκB and AP-1 luciferase reporters in response to CD3/CD28 stimulation, and this effect could be blocked with rottlerin, a PKCθ inhibitor (Coudronniere et al. 2000) and antisense oligos to PKCθ (Lin et al. 2000). More specifically, these groups found that PKCθ activity was important for activating IKKβ and for inducing degradation of IκB. One of these

groups (Lin et al. 2000) also revealed a critical role for CD28 costimulation in PKCθ-dependent NFκB activation, which agrees with the biochemical connection between CD28 and the V3 region of PKCθ to stabilize this kinase at the IS (Lin et al. 2000; Kong et al. 2011).

Biochemically, the classical NFκB pathway has been well-characterized in T lymphocytes (Thome et al. 2010; Hayden & Ghosh 2012). Briefly, in the basal state homo- or hetero-dimers of the transcription factor NFκB are sequestered in the cytosol due to their association with the inhibitory subunit IκB. Upon T cell receptor stimulation, a signaling cascade leads to the activation of the IKK complex (which consists of the regulatory protein NEMO and the kinases IKKα and IKKβ). Active IKKβ can then phosphorylate IκB family members (such as IκBα) on conserved serine residues. Phosphorylated IκBα is then ubiquitinated and degraded, releasing NFκB and exposing its nuclear localization signal. The liberated NFκB dimers can then translocate to the nucleus, bind to target genes, and initiate NFκB-driven transcription. Of note, it was not immediately clear how PKCθ couples to AP-1 activation. In a subsequent section we will discuss how it was uncovered that PKCθ phosphorylates RasGRP1, which in turn activates the Ras-ERK-AP-1 pathway (Roose et al. 2005) (**Figure 1.2**).

The molecular players upstream of the IKK complex can vary depending on the type of stimulation. In antigen receptor-stimulated lymphocytes, there is a pathway linking PKCθ to IKK/NFκB activation via the scaffold protein CARMA1 (also called CARD11). CARMA1 exists in a closed conformation in the cytosol. When CARMA1 becomes activated, it forms a complex (the CBM complex) with the scaffold protein MALT1 and the adaptor BCL10 (which are constitutively associated). Active PKCθ (and possibly other kinases) phosphorylates CARMA1 at specific serine residues, triggering a conformational change (to a more open form) that allows for CARMA1 to bind MALT1/BCL10 (via interactions of the CARD domains in CARMA1 and

BCL10). Complexed MALT1 and BCL10 subsequently become ubiquitinated, which leads to the recruitment and activation of IKK (Oeckinghaus et al. 2007). Other studies have shown that PKCθ may also have a role in recruiting IKK to CBM (K.-Y. Lee et al. 2005). Thus, a TCR-PKCθ-CBM pathway exists that leads to NFκB activation in T cells. For a more in-depth discussion of NFκB signaling, we point the readers to two excellent reviews (Thome et al. 2010; Hayden & Ghosh 2012).

A number of studies have documented important roles for PKCθ in various aspects of T cell mediated immunity. In the appropriate cytokine milieu, activated T cells can differentiate into a number of effector subsets (including Th1, Th2, Th17 and iTreg) that mediate different functions (O'Shea & Paul 2010). PKCθ has an important role in Th2 cells, as *PKCθ* knockout mice cannot efficiently clear *Nippostrongylus brasiliensis* worm infections due to impaired Th2 cell activity, and *PKCθ*–deficient mice do not develop allergic airway disease (Marsland 2004; Salek-Ardakani et al. 2004). More subtle effects on Th17 and iTreg cells were observed (Salek-Ardakani et al. 2005; Tan et al. 2006), whereas PKCθ appears to be dispensable for Th1 cells. These studies reveal an important yet complex role for PKCθ signals in helper T cell differentiation and function, and at this point it is not understood why Th2 cells are most affected when PKCθ is absent.

A DAG-induced Ras-ERK Signaling Pathway in T cells

As mentioned earlier, DAG as a signaling molecule caught the attention of both cancer biologists and immunologists in the 1980's. A seminal paper from Julian Downward and Doreen Cantrell described the increased levels of active Ras-GTP when lymphocytes were stimulated with phorbol ester (Downward et al. 1990); this was the first time that signal-induced Ras

activation was observed in non-cancerous cells. Ras is a small GTPase that cycles between an inactive, GDP-bound state and an active, GTP-bound state (**Figure 1.4**). Ras is turned on when it is bound to GTP, as GTP-bound (but not GDP-bound) Ras is capable of binding downstream effector proteins such as RAF, PI3K, and RalGDS, which then can become activated and propagate downstream signaling (Castellano & Downward 2010; Castellano & Downward 2011; Ahearn et al. 2012). Ras signaling can be turned off by hydrolysis of GTP into GDP. The nucleotide-bound states of Ras are regulated by two classes of proteins, RasGAPs (GTPase activating proteins) and RasGEFs (guanine nucleotide exchange factors) (Jun, Rubio, et al. 2013). Ras by itself has limited GTPase activity, and RasGAP proteins turn off Ras signaling by enhancing the GTPase activity of Ras, leading to GTP hydrolysis and Ras adopting a conformation such that it is unable to bind downstream effectors. Conversely, GEFs activate Ras by binding it and inducing a conformational change such that GDP is released; empty Ras subsequently associates with GTP, which is available at higher levels than GDP in the cytoplasm (Vetter & Wittinghofer 2001; Bos et al. 2007). Lymphocytes express three families of GEFs, RasGRPs (Ras guanine nucleotide releasing proteins), SOS (son of sevenless), and RasGRFs (Ras guanine nucleotide releasing factors). However, RasGRFs appear to have a very limited role in Ras-ERK activation in T cells (Jun, Rubio, et al. 2013; Ksionda et al. 2013), so in this review we will focus on the role of RasGRPs and SOS. Both of these RasGEFs activate Ras by inducing a conformational change that causes the release of otherwise tightly bound nucleotide (Boriack-Sjodin et al. 1998).

Briefly, the classical MAP kinase pathway downstream of Ras activation proceeds as follows: Ras-GTP binds the kinase RAF, and active RAF phosphorylates MEK (mitogen-activated protein kinase kinase), which in turn phosphorylates ERK1/2 (extracellular signal regulated kinase 1/2) on tyrosine and threonine residues (Ahearn et al. 2012). ERK1/2 are serine/threonine kinases and are able to activate a number of cytosolic proteins and

transcription factors through phosphorylation, including the transcription factor ELK1, which in turn leads to activation of AP-1 (**Figure 1.2**). AP-1 consists of a heterodimer of the Jun/Fos transcription factors, and it (along with NFAT and NFκB, discussed above) contributes to IL-2 gene induction (Smith-Garvin et al. 2009).

The molecular components of the Ras-MAP kinase pathway have been shown to be important for T cells in studies using genetic mouse models. Generation of CD4 or CD8 single positive (SP) thymocytes, the most mature stages of developing T cells in the thymus, is reduced when mice express a dominant negative form of Ras (S17N) transgenically under the control of the Lck promoter (which turns on early in thymocyte development). This inability to progress from the $CD4^+$ $CD8^+$ double positive (DP) to the SP stage was shown to be due to impaired positive selection of these developing T cells (Swan et al. 1995). Consistent with a role for the Ras-RAF-MEK-ERK pathway, mice expressing catalytically inactive MEK1 in thymocytes as well as mice with thymocytes doubly deficient for *ERK1* and *ERK2* also have impaired positive selection and reduced SP cells (Alberola-Ila et al. 1995; Fischer et al. 2005).

The RasGRP family of Ras exchange factors and their role in Ras-ERK Signaling

As discussed, it was known since 1990 that phorbol esters such as DAG can activate Ras, however a direct molecular link remained elusive. For a substantial period, PKCs were thought to provide this link between DAG and Ras activation. However, thymocyte development (a process that, as discussed, requires intact Ras signaling) is normal in *PKCθ*-deficient mice (Sun et al. 2000). In 1998, the RasGEF RasGRP1 was identified by Jim Stone's group through a fibroblast transformation screen, surprisingly late in the cloning era (Ebinu 1998). Since the

sequence of RasGRP1 revealed both a Ras activation domain as well as a C1 domain, the link between DAG and Ras was quickly made.

Stone's group cloned *RasGRP1* from a cDNA library from the brain, indicating that *RasGRP1* is expressed in that tissue. Soon after, Robert Kay and colleagues also identified *RasGRP1* in a transformation screen, this time using a cDNA library from a T cell hybridoma line (Tognon et al. 1998). Subsequently, RasGRP1 was shown to be very highly expressed in thymocytes and T cells (Ebinu et al. 2000), and thus a large body of research has focused on RasGRP1 and its role in Ras activation in T cells. However it is of note that in addition to developing and mature T cells, *RasGRP1* is expressed in other hematopoietic cells such as B cells (Coughlin et al. 2005), mast cells (Y. Liu et al. 2007), neutrophils (la Luz Sierra et al. 2010) and natural killer cells (S. H. Lee et al. 2009). RasGRP1 is also expressed in non-hematopoietic cells, such as cells in several regions of the brain (Kawasaki et al. 1998), in keratinocytes of the skin (Rambaratsingh et al. 2003), and in intestinal epithelial cells (Depeille et al. 2015).

RasGRP1 is a member of the RasGRP family of Ras GEFs. This family is comprised of 4 members, RasGRP1, 2, 3, and 4. The four molecules all share several protein domains, including the catalytic module, consisting of a REM (Ras exchange motif) and a CDC25 domain, which binds Ras, C1 domains, and a pair of EF-hands (**Figure 1.4**). However, there are variations in these domains across the different RasGRPs, and the molecules thus seem to have distinct biochemical function and regulation. For further details on the different RasGRP proteins we refer you to a review (Ksionda et al. 2013). Here we exclusively focus on RasGRP1 because of its evident role in thymocytes and T cells.

RasGRP1's C1 domain has high homology to the C1 of PKCs and has high affinity for phorbol esters (Lorenzo et al. 2000). The earliest studies of RasGRP1 showed that the full-

length protein, but not a construct lacking the DAG-binding C1 domain, could be detected in membrane fractions after subcellular fractionation (Ebinu 1998). Later, it was shown using probes consisting of an isolated RasGRP1 C1 domain fused to GFP that RasGRP1 is found in the cytoplasm (often perinuclear) in resting Jurkat cells and translocates to the plasma membrane upon stimulation with TCR/CD28 or PMA (Carrasco & Merida 2004). The C1 domain was also shown to be important for RasGRP1's signaling capabilities, as cells harboring a RasGRP1 ΔC1 construct display reduced Ras-GTP loading, less phosphorylation of ERK (Ebinu 1998), and reduced cellular transformation (Tognon et al. 1998).

Classical EF hands (such as the pair found in calmodulin, discussed above) come in pairs, and each hand typically binds one calcium ion. Early studies showed that RasGRP1 was capable of binding calcium (Ebinu 1998), but it was noted that the EF hands of RasGRP1 are unique in that the region between the two EF hands is shorter than what is typically observed. Later, it was found that RasGRP1 only binds one Ca^{2+} ion, via the first EF hand (EF1) (Iwig et al. 2013) (**Figure 1.4**).

The presence of the DAG-binding C1 domain and the EF hands in RasGRP1 suggested that the protein is regulated by both of these second messengers. Our lab and the Kuriyan lab recently solved the crystal structure of RasGRP1, which led to a model for how RasGRP1 is autoinhibited in the basal state and activated upon receptor stimulation. The catalytic domain of RasGRP1 is intrinsically active (Iwig et al. 2013) so autoinhibition is critical to prevent spurious RasGRP1-Ras signaling. The C1 and EF hands play crucial regulatory roles here. The crystal structure revealed that RasGRP1 autoinhibition in the basal state is achieved via a dimer interface that prevents DAG binding and via a linker domain that blocks the Ras-binding site (Iwig et al. 2013). The autoinhibited dimer interface forms such that the C1 domain of each RasGRP1 monomer contacts the EF2 and CDC25 domains of the other, thereby burying the C1

domains (and presumably preventing its ability to bind DAG and translocate to the PM). The C-termini of two RasGRP1 molecules also form a coiled coil, providing an additional dimerization interface (**Figure 1.4**). The C-terminal tail domain of RasGRP1 appears to be functionally important as well, as mice where endogenous *RasGRP1* is replaced with a version that lacks the tail domain have impaired thymocyte development, T cell proliferation, and autoimmunity. This tail-deficient RasGRP1 is also impaired in PMA-induced PM translocation (Fuller et al. 2012). As noted, autoinhibition is further achieved by the presence of a CDC25-EF linker, which lies in the Ras binding site of RasGRP1.

How and in what order of events RasGRP1 is activated is unknown, but DAG, calcium, and RasGRP1 phosphorylation play a role (Roose et al. 2005; Iwig et al. 2013; Ksionda et al. 2013). NMR scattering studies imply that calcium binding to EF1 induces a conformational change from an autoinhibited dimer to an active dimer (Iwig et al. 2013) (**Figure 1.4**). RasGRP1 is inducibly phosphorylated by PKCθ following receptor stimulation (Roose et al. 2005; Zheng et al. 2005), however the biochemical and physiological relevance of this phosphorylation is still not well understood. Notably, this PKCθ-RasGRP1 connection may explain why PKCθ-deficient cells fail to activate the transcription factor AP-1 (Sun et al. 2000; Pfeifhofer et al. 2003) (**Figure 2**).

Strict regulation of RasGRP1-kinase Signals and consequences of perturbed regulation

RasGRP1-deficient mice were generated by Jim Stone's group in 2000 and revealed an important physiological role for RasGRP1 in thymocyte development (Dower et al. 2000). Strikingly, thymocytes from *RasGRP1* knockout mice are developmentally arrested at the double positive stage, leading to greatly reduced absolute numbers and percentages of $CD4^+$

and $CD8^+$ SP thymocytes. In line with the fact that so few thymocytes make it through development, *RasGRP1*-deficient mice also have very few mature T cells populating their spleen and lymph nodes. Biochemically, *RasGRP1*$^{-/-}$ thymocytes have impaired RasGRP1-Ras-ERK signaling, demonstrated by the inability to phosphorylate ERK in response to TCR or phorbol ester stimulation. *RasGRP1*-deficient Jurkat T cells similarly are impaired to induce P-ERK or upregulate the activation marker CD69 (Roose et al. 2005). Subsequent studies in which *RasGRP1*$^{-/-}$ mice were crossed to TCR transgenic mice revealed that RasGRP1 is required for thymocyte positive selection but, interestingly, RasGRP1 is not required for negative selection (Priatel et al. 2002).

Conversely, dysregulated RasGRP1 activity *in vivo* can lead to disease. RasGRP1 overexpression overwhelms basal autoinhibition and leads to T cell leukemia (Klinger et al. 2004; Oki et al. 2011; Hartzell et al. 2013). *RasGRP1*^{Anaef}, a mouse missense variant with a point-mutated EF2, weakens autoinhibition and follicular helper-like T cells (T_{FH}-like cells) aberrantly accumulate as a result of increased basal *RasGRP1*^{Anaef}-mTOR signaling (Daley et al. 2013). These cells aberrantly stimulate B cells to produce autoantibodies, driving a lupus-like disease. It is of interest to note that *RasGRP1* variants have been implicated in human autoimmune disease as well: splice variants in *RasGRP1* have been reported in SLE (Yasuda et al. 2007), and single nucleotide variants near *RasGRP1* have been identified in genome wide association studies of type 1 diabetes and Graves' disease (Qu et al. 2009; Plagnol et al. 2011).

A second Ras-ERK pathway that generates digital effector kinase signals

The SOS1 and SOS2 Ras GEFs are ubiquitously expressed in all cell types, including lymphoid cells. In T lymphocytes that are stimulated through the TCR, these RasGEFs are recruited to the membrane via the adapter molecule Grb2, which binds to phosphorylated tyrosines in LAT

(Jun, Rubio, et al. 2013). Like RasGRP1, SOS1 has a catalytic domain consisting of REM and CDC25 modules, which can bind and activate Ras. The identification of the DAG-RasGRP1-Ras pathway in T lymphocytes immediately brought up a conundrum as to why these cells would have two pathways, via SOS and via RasGRP, to activate Ras following stimulation of the same receptor (the TCR). The fact that *RasGRP1*-deficient mice display such a profound defect in thymocyte positive selection implies that SOS cannot compensate for RasGRP1 deficiency (Dower et al. 2000). Vice versa, SOS RasGEFs play a role at the TCRβ selection checkpoint, earlier in thymocyte development, and defects at this checkpoint observed in *SOS1*-deficient mice are not compensated for by RasGRP1 (Kortum et al. 2011).

Biochemical and computational studies on these two families of RasGEFs, aided by structural work, revealed that RasGRP and SOS can signal to Ras in distinct patterns. RasGRP1 activates Ras (and the downstream ERK kinase) in an analog manner: there is a linear correlation between signal input to RasGRP1 and Ras-ERK signal output (Roose et al. 2007; Das et al. 2009; Jun, Rubio, et al. 2013; Ksionda et al. 2013). By contrast, SOS1 can signal to Ras-ERK in a digital or bimodal manner: when the input signal to SOS1 crosses a threshold, a jump in the intensity of the Ras-ERK signal occurs (Roose et al. 2007; Das et al. 2009; Prasad et al. 2009; Jun, Yang, et al. 2013; Jun, Rubio, et al. 2013). The molecular basis for the digital Ras-ERK signal lies in a positive feedback loop on SOS1 (**Figure 1.5**). Crystal structures of SOS1 with Ras demonstrated that there is a second binding site for Ras on SOS1, distal of the catalytic pocket. Occupancy of this allosteric pocket by Ras-GTP increases the GEF activity of SOS1 *in vitro* (Margarit et al. 2003; Sondermann et al. 2004) (**Figure 1.5**). Since SOS1 itself generates Ras-GTP, this phenomenon creates a positive feedback loop that was demonstrated to exist in several cell types, including lymphocytes (Boykevisch et al. 2006; Roose et al. 2007; Das et al. 2009; Jun, Rubio, et al. 2013; Jeng et al. 2012; Depeille et al.

2015). RasGRP1 also facilitates engagement of this positive feedback loop over SOS by generating some initial Ras-GTP to prime SOS1 (Roose et al. 2007).

Thus, lymphocytes have a choice of signaling to Ras-ERK in an analog (only RasGRP) or digital (RasGRP & SOS) manner, but the true *in vivo* implication of analog versus digital Ras-ERK signals still needs to be elucidated. The phenotypes of the different genetic mouse models clearly indicated that these RasGEFs play distinct roles during thymocyte development (Dower et al. 2000; Kortum et al. 2011; Kortum et al. 2012). While this could be the consequence of altered analog or digital Ras-ERK signaling, it is also possible that the defects in thymocyte development are caused by impaired signals through other (non-Ras) pathways that depend on either RasGRP1 or on SOS1.

Concluding remarks

Here we have provided an overview of the effector kinase and phosphatase pathways that connect proximal T cell receptor signaling to NFAT, NFκB, and activator AP-1 transcription factors, and we discussed the role these pathways play in T cells. We want to emphasize that we did not attempt to cover all effector pathways but focused on the more established ones. For example, in many cancer settings PI3K (phosphoinositide 3-kinase) is an effector molecule of Ras-GTP (Castellano & Downward 2010; Castellano & Downward 2011). In T cells, CD28 costimulation is thought to enhance PI3K activation but the signaling pathways triggered by CD28 are poorly understood and the exact connection between CD28 and PI3K is controversial as well (Boomer & Green 2010). PI3K is a lipid kinase that converts PIP2 into PIP3 (phosphatidylinositol 3,4,5-triphosphate) at the membrane resulting into the recruitment of plextrin homology (PH)-domain containing proteins such as the kinase AKT. The PH domain

binds to PIP3. One of the pathways that AKT can activate involves mTOR (mammalian/mechanistic target of rapamycin), which regulates metabolic processes in cells and is covered elsewhere in *Encyclopedia of Immunobiology*.

Lastly, it is intuitive to focus on the catalytic activity of enzymes such as kinases, phosphatases and RasGEFs but it is important to keep in mind that these enzymes can also fulfill non-catalytic, adapter functions and couple to signaling proteins in an unanticipated manner. For example, we have identified a P38 kinase pathway that relies on the presence but not on the catalytic function of the RasGEF SOS1 (Jun, Yang, et al. 2013). Similarly, the *RasGRP1* variant *RasGRP1*^{Anaef} signals to mTOR at an increased intensity resulting in increased expression of the mTOR target gene CD44 (Daley et al. 2013). However, Ras target genes, such as CD69 and TCRβ, are expressed at normal levels in *RasGRP1*^{Anaef} T cells (Daley et al. 2013), arguing that there is also a non-canonical signaling pathway downstream of the RasGEF RasGRP1 to mTOR, revealed by the *RasGRP1*^{Anaef} variant.

FIGURES

All images for Figures 1.1-1.5 were generated by Anna Hupalowska.

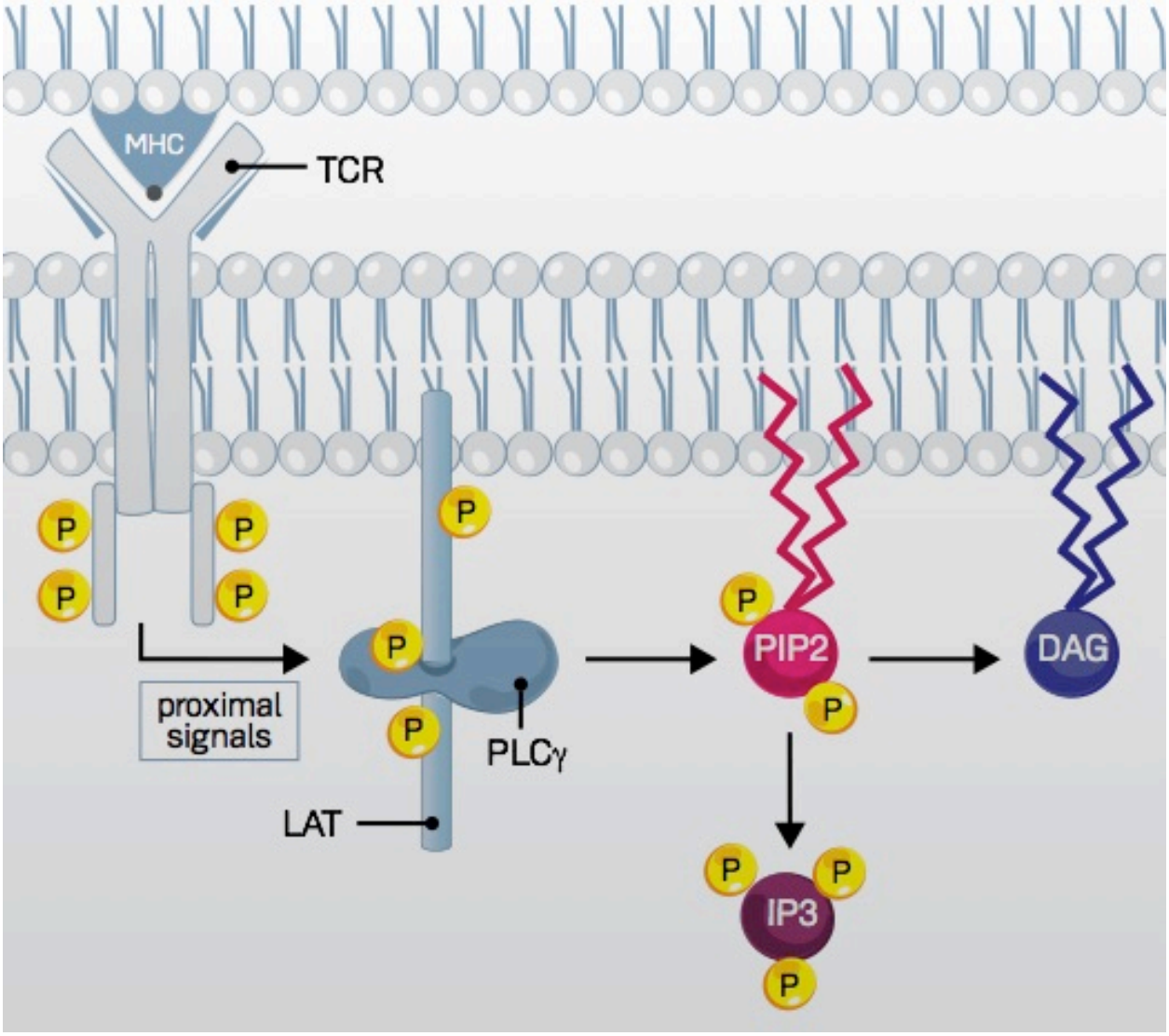


Figure 1.1: TCR stimulation and proximal signaling events result in the recruitment of PLCγ1 and the generation of second messenger molecules IP3 and DAG. Upon ligation of the T cell receptor (TCR) by cognate antigen bound to MHC, a number of proximal TCR signaling events (not depicted) are initiated that result in the formation of the LAT signalosome. PLCγ1 can bind to LAT, where it is activated by Tec kinases. Active PLCγ1 hydrolyzes the plasma membrane-associated phospholipid PIP2, leading to the production of two important second messengers: IP3 and DAG. IP3 is a soluble, hydrophilic molecule and diffuses into the cytosol. DAG is a hydrophobic molecule and embeds in the plasma membrane. It is recruited to the IS (immunological synapse), formed at the site of T cell : APC contact.

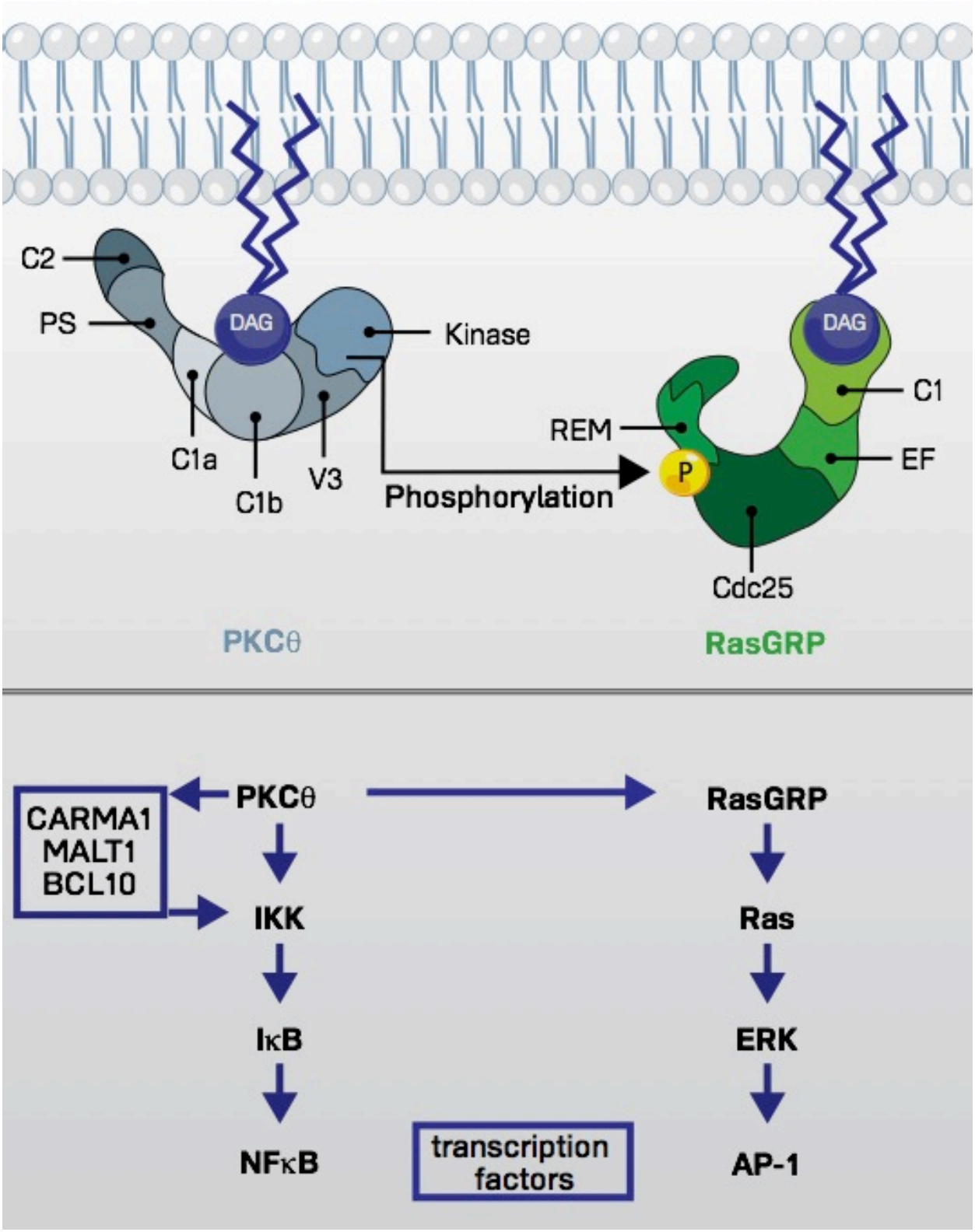

C2
PS
DAG
Kinase
C1a
C1b
V3
Phosphorylation
REM
P
DAG
C1
EF
Cdc25
PKCθ
RasGRP
CARMA1
MALT1
BCL10
PKCθ
IKK
IκB
NFκB
transcription factors
RasGRP
Ras
ERK
AP-1

Figure 1.2: Diacylglycerol allows for the recruitment of PKC θ and RasGRP1 via their DAG-binding C1 domain. Depiction of PKCθ and RasGRP1 with their protein domains and highlighting their role in propagating downstream signaling. Both proteins harbor typical C1 domains, which have a conformation that is compatible with binding to DAG. This C1-DAG interaction promotes recruitment of these effectors to the plasma membrane. Membrane-bound PKCθ activates the NFκB signaling pathway. DAG-bound RasGRP1 can interact with Ras and activate Ras-ERK-AP-1 signaling. PKCθ can also phosphorylate RasGRP1 at a threonine residue in the catalytic domain, though the role of this phosphorylation event is still unclear.

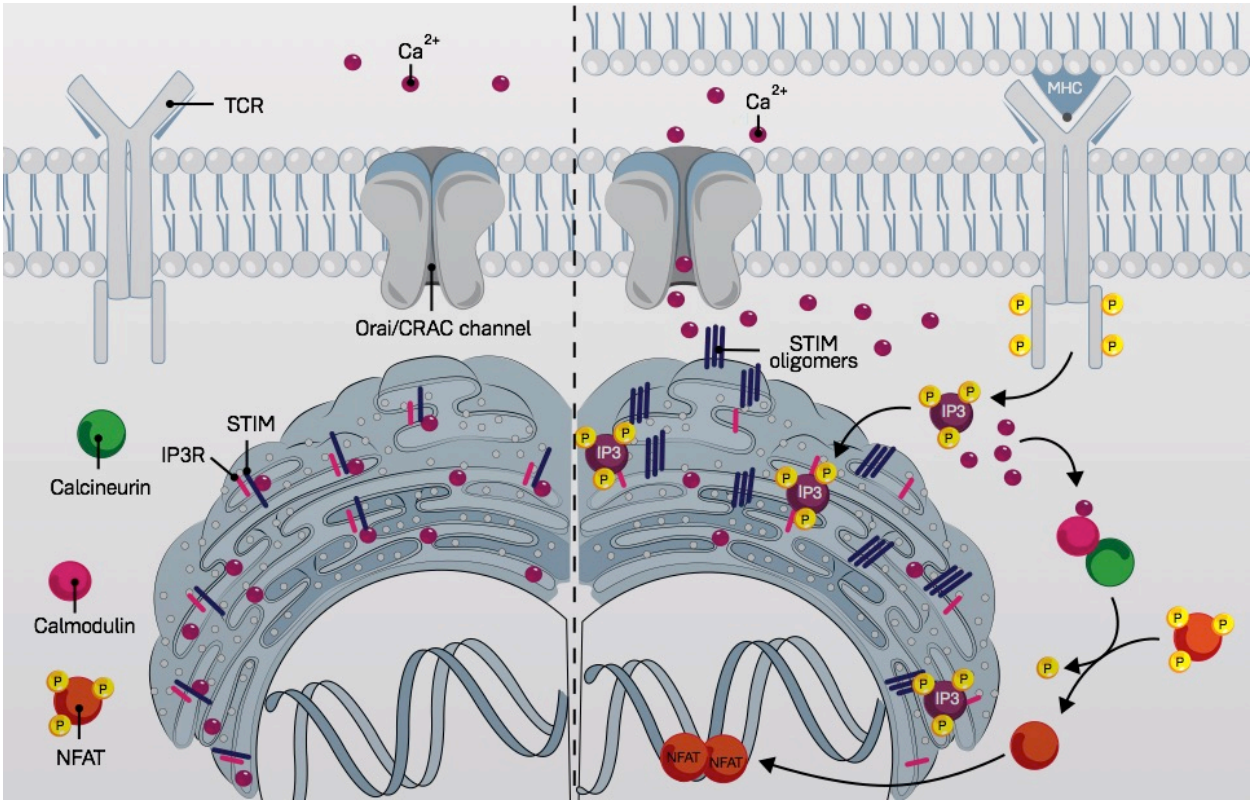

Ca2+
TCR
Orai/CRAC channel
Ca2+
MHC
STIM
oligomers
STIM
IP3R
Calcineurin
Calmodulin
NFAT
IP3
IP3
IP3
IP3
NFAT
NFAT

Figure 1.3: Generation of calcium signals in T cells resulting in NFAT transcriptional responses. Overview of calcium regulation in resting (left side) and receptor-activated (right side) T cells. In the basal state (left), there is little free calcium in the cytoplasm and instead it is stored in the endoplasmic reticulum (ER). Some of this calcium associates with the EF hands of STIM1 molecules, which span the ER membrane. Ca^{2+}-associated STIM molecules are inactive and do not form higher-order oligomers. The calcium-responsive transcription factor NFAT is sequestered in the cytoplasm via constitutive phosphorylation. Upon TCR activation (right), generated IP3 binds IP3 receptors (IP3Rs) on the ER membrane. These receptors open and release stored calcium into the cytosol. Ca^{2+} uncouples from STIM, and STIM oligomers form near the PM, where they interact with ORAI. ORAI molecules span the PM and are the pore-forming unit of the CRAC channel. STIM activates ORAI, opening the CRAC channel, allowing for the import of Ca^{2+} from outside the cell into the cytosol. One important consequence of this calcium flux is activation of NFAT. Calcium binds the EF hands of calmodulin, which activates calcineurin, a phosphatase. Activated calcineurin can de-phosphorylate NFAT, and NFAT translocates to the nucleus where it activates its target genes. Note that some of the molecular details are not included in the figure.

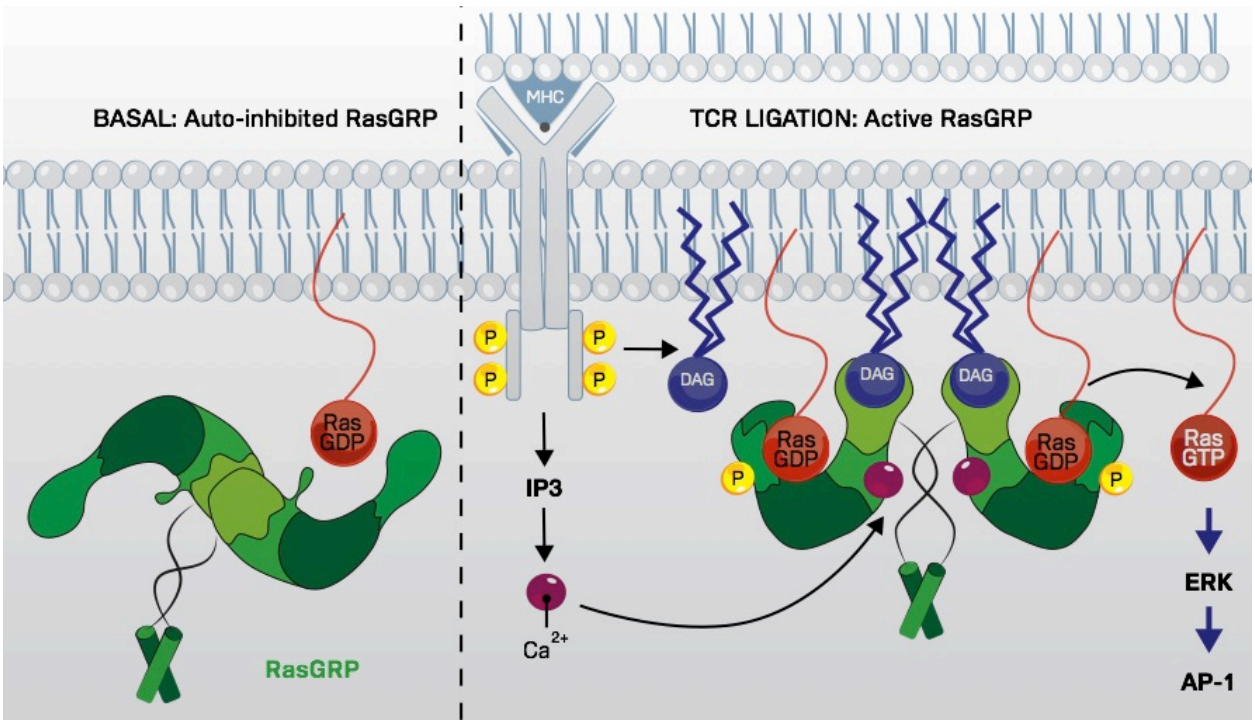

BASAL: Auto-inhibited RasGRP
MHC
TCR LIGATION: Active RasGRP
Ras GDP
RasGRP
P
P
P
P
DAG
IP3
Ca2+
DAG
DAG
Ras GDP
Ras GDP
P
P
Ras GTP
ERK
AP-1

Figure 1.4: Autoinhibition of RasGRP1 and activation by DAG and calcium. In the basal state (left), RasGRP1 molecules exist in the cytosol as auto-inhibited dimers. Dimerization is achieved via the C-terminal coiled-coil domain as well as by a C1-EF hand interface. This puts the protein in a closed conformation and buries the C1 domain of RasGRP1, so it is unable to bind DAG and be translocated to the plasma membrane, where it interacts with Ras. Autoinhibition is further achieved by the presence of a linker that blocks the Ras-binding domain of RasGRP1. When T cells are activated via the TCR (right), autoinhibition is relieved and RasGRP1 becomes activated. Calcium binds to the EF1 hand of RasGRP1, promoting a more open conformation and exposing the C1 domain. Open RasGRP1 molecules can translocate to the PM via C1-DAG binding, and at the PM they can bind to and activate Ras.

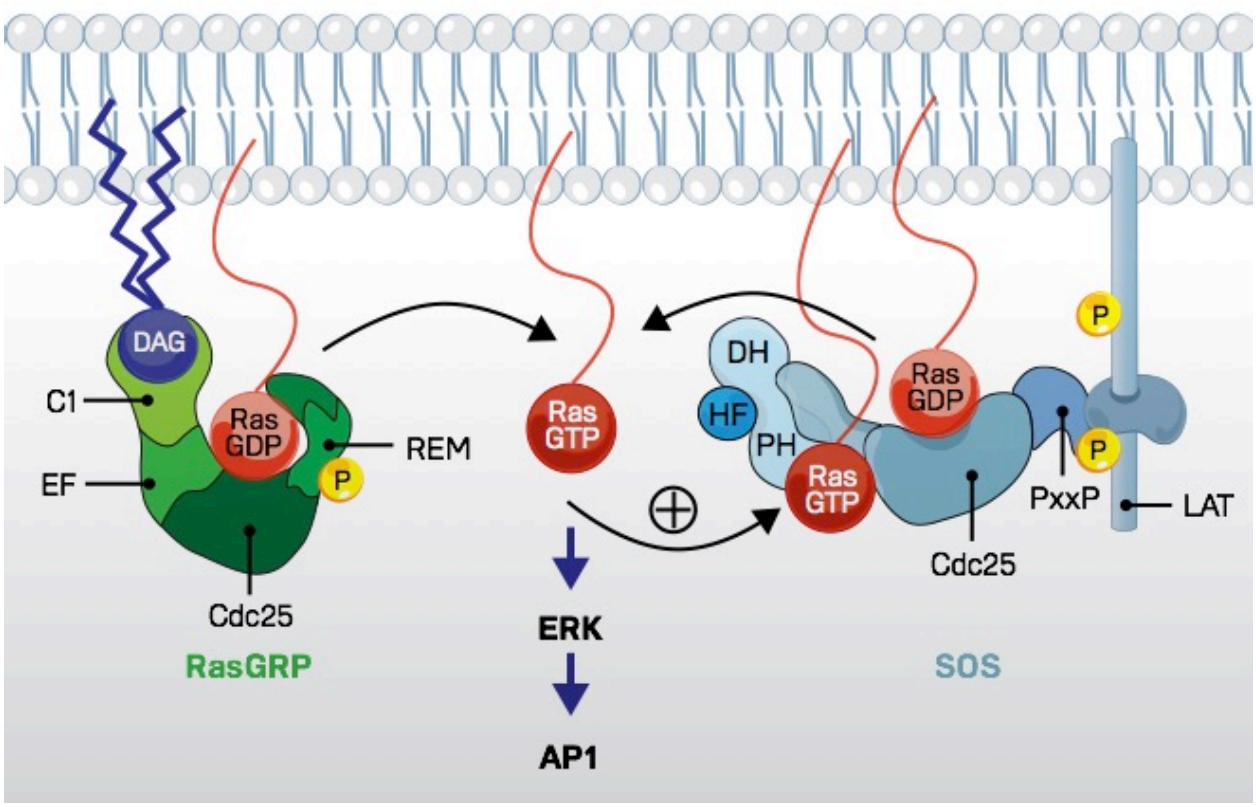

DAG
C1
Ras
GDP
REM
EF
P
Cdc25
RasGRP
Ras
GTP
ERK
AP1
DH
HF
PH
Ras
GTP
Ras
GDP
P
P
PxxP
LAT
Cdc25
SOS

Figure 1.5: Co-expression of RasGRP1 and SOS1 in lymphocytes allows for choices in analog or digital Ras-ERK signaling. The catalytic module of RasGRP1, the REM-CDC25 domains, can bind Ras and activate it, producing Ras-GTP. There is a linear relationship between the amount of signal input and the amount of Ras-ERK output. In contrast, SOS1 can bind Ras at two distinct sites, one in its catalytic domain (also comprised of REM-CDC25 domains) and another at an allosteric site distal to the catalytic module. The allosteric site binds Ras-GTP and when Ras-GTP is bound there it greatly enhances the GEF activity of SOS. SOS1 itself can initially generate Ras-GTP, that then positively feeds back on SOS1 by binding to the allosteric site. Additionally, RasGRP1 can provide this initial burst of Ras-GTP that binds to the allosteric site of SOS1. This positive feedback loop means that SOS1-Ras signaling occurs in a digital fashion: once a certain threshold of signal input is crossed, a jump in the intensity of the Ras-ERK-AP-1 output occurs.

REFERENCES

Ahearn, I.M. et al., 2012. Regulating the regulator: post-translational modification of RAS. *Nature Reviews Molecular Cell Biology*, 13(1), pp.39–51.

Alberola-Ila, J. et al., 1995. Selective requirement for MAP kinase activation in thymocyte differentiation. *Nature*, 373(6515), pp.620–623.

Almena, M.A. & Merida, I., 2011. Shaping up the membrane: diacylglycerol coordinates spatial orientation of signaling. *Trends in Biochemical Sciences*, 36(11), pp.593–603.

Babu, Y.S., Bugg, C.E. & Cook, W.J., 1988. Structure of calmodulin refined at 2.2 A resolution. *Journal of molecular biology*, 204(1), pp.191–204.

Boomer, J.S. & Green, J.M., 2010. An Enigmatic Tail of CD28 Signaling. *Cold Spring Harbor Perspectives in Biology*, 2(8), pp.a002436–a002436.

Boriack-Sjodin, P.A. et al., 1998. The structural basis of the activation of Ras by Sos. *Nature*, 394(6691), pp.337–343.

Bos, J.L., Rehmann, H. & Wittinghofer, A., 2007. GEFs and GAPs: Critical Elements in the Control of Small G Proteins. *Cell*, 129(5), pp.865–877.

Boykevisch, S. et al., 2006. Regulation of Ras Signaling Dynamics by Sos-Mediated Positive Feedback. *Current Biology*, 16(21), pp.2173–2179.

Carrasco, S. & Merida, I., 2007. Diacylglycerol, when simplicity becomes complex. *Trends in Biochemical Sciences*, 32(1), pp.27–36.

Carrasco, S. & Merida, I., 2004. Diacylglycerol-dependent Binding Recruits PKC□ and RasGRP1 C1 Domains to Specific Subcellular Localizations in Living T Lymphocytes. *Molecular Biology of the Cell*, 15, pp.2932–2942.

Castellano, E. & Downward, J., 2011. RAS Interaction with PI3K: More Than Just Another Effector Pathway. *Genes & Cancer*, 2(3), pp.261–274.

Castellano, E. & Downward, J., 2010. Role of RAS in the regulation of PI 3-kinase. *Current topics in microbiology and immunology*, 346, pp.143–169.

Coudronniere, N. et al., 2000. NF-kappa B activation induced by T cell receptor/CD28 costimulation is mediated by protein kinase C-theta. *Proceedings of the National Academy of Sciences of the United States of America*, 97(7), pp.3394–3399.

Coughlin, J.J. et al., 2005. RasGRP1 and RasGRP3 Regulate B Cell Proliferation by Facilitating B Cell Receptor-Ras Signaling. *The Journal of Immunology*, 175(11), pp.7179–7184.

Daley, S.R. et al., 2013. Rasgrp1 mutation increases naive T-cell CD44 expression and drives mTOR-dependent accumulation of Helios^{+} T cells and autoantibodies. *eLife*, 2, p.e01020.

Das, J. et al., 2009. Digital Signaling and Hysteresis Characterize Ras Activation in Lymphoid

Cells. *Cell*, 136(2), pp.337–351.

Depeille, P. et al., 2015. RasGRP1 opposes proliferative EGFR--SOS1--Ras signals and restricts intestinal epithelial cell growth. *Nature Cell Biology*, 17(6), pp.804–815.

Diaz-Flores, E. et al., 2003. Membrane Translocation of Protein Kinase C during T Lymphocyte Activation Requires Phospholipase C- -generated Diacylglycerol. *Journal of Biological Chemistry*, 278(31), pp.29208–29215.

Dower, N.A. et al., 2000. RasGRP is essential for mouse thymocyte differentiation and TCR signaling. *Nature immunology*, 1(4), pp.317–321.

Downward, J. et al., 1990. Stimulation of p21ras upon T-cell activation. *Nature*, 346(6286), pp.719–723.

Ebinu, J.O., 1998. RasGRP, a Ras Guanyl Nucleotide- Releasing Protein with Calcium- and Diacylglycerol-Binding Motifs. *Science (New York, N.Y.)*, 280(5366), pp.1082–1086.

Ebinu, J.O. et al., 2000. RasGRP links T-cell receptor signaling to Ras. *Blood*, 95(10), pp.3199–3203.

Feske, S., 2007. Calcium signalling in lymphocyte activation and disease. *Nature Publishing Group*, 7(9), pp.690–702.

Feske, S. et al., 2006. A mutation in Orai1 causes immune deficiency by abrogating CRAC channel function. *Nature Cell Biology*, 441(7090), pp.179–185.

Feske, S., Wulff, H. & Skolnik, E.Y., 2015. Ion Channels in Innate and Adaptive Immunity. *Annual Review of Immunology*, 33(1), pp.291–353.

Fischer, A.M. et al., 2005. The Role of Erk1 and Erk2 in Multiple Stages of T Cell Development. *Immunity*, 23(4), pp.431–443.

Fu, G. et al., 2010. Phospholipase C 1 is essential for T cell development, activation, and tolerance. *Journal of Experimental Medicine*, 207(2), pp.309–318.

Fuchs, S. et al., 2012. Antiviral and Regulatory T Cell Immunity in a Patient with Stromal Interaction Molecule 1 Deficiency. *The Journal of Immunology*, 188(3), pp.1523–1533.

Fuller, D.M. et al., 2012. Regulation of RasGRP1 Function in T Cell Development and Activation by Its Unique Tail Domain. *PLoS ONE*, 7(6), p.e38796.

Gifford, J.L., Walsh, M.P. & Vogel, H.J., 2007. Structures and metal-ion-binding properties of the Ca 2+-binding helix--loop--helix EF-hand motifs. *Biochemical Journal*, 405(2), pp.199–221.

Guo, R. et al., 2008. Synergistic control of T cell development and tumor suppression by diacylglycerol kinase alpha and zeta. *Proceedings of the National Academy of Sciences of the United States of America*, 105(33), pp.11909–11914.

Gwack, Y. et al., 2008. Hair Loss and Defective T- and B-Cell Function in Mice Lacking ORAI1. *Molecular and cellular biology*, 28(17), pp.5209–5222.

Hartzell, C. et al., 2013. Dysregulated RasGRP1 responds to cytokine receptor input in T cell leukemogenesis. *Science Signaling*, 6(268), p.ra21.

Hayden, M.S. & Ghosh, S., 2012. NF- B, the first quarter-century: remarkable progress and outstanding questions. *Genes & Development*, 26(3), pp.203–234.

Hogan, P.G. et al., 2003. Transcriptional regulation by calcium, calcineurin, and NFAT. *Genes & Development*, 17(18), pp.2205–2232.

Hogan, P.G., Lewis, R.S. & Rao, A., 2010. Molecular Basis of Calcium Signaling in Lymphocytes: STIM and ORAI. *Annual Review of Immunology*, 28(1), pp.491–533.

Huang, Y.H. & Sauer, K., 2010. Lipid Signaling in T-Cell Development and Function. *Cold Spring Harbor Perspectives in Biology*, 2(11), pp.a002428–a002428.

Iwig, J.S. et al., 2013. Structural analysis of autoinhibition in the Ras-specific exchange factor RasGRP1. *eLife*, 2(0), pp.e00813–e00813.

Jain, J. et al., 1992. Nuclear factor of activated T cells contains Fos and Jun. *Nature*, 356(6372), pp.801–804.

James, P., Vorherr, T. & Carafoli, E., 1995. Calmodulin-binding domains: just two faced or multi-faceted? *Trends in Biochemical Sciences*, 20(1), pp.38–42.

Jeng, H.-H., Taylor, L.J. & Bar-Sagi, D., 2012. Sos-mediated cross-activation of wild-type Ras by oncogenic Ras is essential for tumorigenesis. *Nature Communications*, 3, pp.1168–1168.

Joshi, R. & Koretzky, G., 2013. Diacylglycerol Kinases: Regulated Controllers of T Cell Activation, Function, and Development. *International Journal of Molecular Sciences*, 14(4), pp.6649–6673.

Jun, J.E., Rubio, I. & Roose, J.P., 2013. Regulation of ras exchange factors and cellular localization of ras activation by lipid messengers in T cells. *Frontiers in Immunology*, 4, p.239.

Jun, J.E., Yang, M., et al., 2013. Activation of extracellular signal-regulated kinase but not of p38 mitogen-activated protein kinase pathways in lymphocytes requires allosteric activation of SOS. *Molecular and cellular biology*, 33(12), pp.2470–2484.

Kawasaki, H. et al., 1998. A Rap guanine nucleotide exchange factor enriched highly in the basal ganglia. *Proceedings of the National Academy of Sciences of the United States of America*, 95(22), pp.13278–13283.

Klinger, M.B. et al., 2004. Deregulated expression of RasGRP1 initiates thymic lymphomagenesis independently of T-cell receptors. *Oncogene*, 24(16), pp.2695–2704.

Kong, K.-F. et al., 2011. A motif in the V3 domain of the kinase PKC- θ determines its localization in the immunological synapse and functions in T cells via association with CD28. *Nature immunology*, 12(11), pp.1105–1112.

Kortum, R.L. et al., 2012. Deconstructing Ras signaling in the thymus. *Molecular and cellular biology*.

Kortum, R.L. et al., 2011. Targeted Sos1 deletion reveals its critical role in early T-cell development. *Proceedings of the National Academy of Sciences of the United States of America*, 108(30), pp.12407–12412.

Krishna, S. & Zhong, X., 2013. Role of diacylglycerol kinases in T cell development and function. *Critical reviews in immunology*, 33(2), pp.97–118.

Ksionda, O., Limnander, A. & Roose, J.P., 2013. RasGRP Ras guanine nucleotide exchange factors in cancer. *Frontiers in Biology*, 8(5), pp.508–532.

Kunkel, M.T. & Newton, A.C., 2010. Calcium Transduces Plasma Membrane Receptor Signals to Produce Diacylglycerol at Golgi Membranes. *Journal of Biological Chemistry*, 285(30), pp.22748–22752.

la Luz Sierra, de, M. et al., 2010. The transcription factor Gfi1 regulates G-CSF signaling and neutrophil development through the Ras activator RasGRP1. *Blood*, 115(19), pp.3970–3979.

Lee, K.-Y. et al., 2005. PDK1 nucleates T cell receptor-induced signaling complex for NF-kappaB activation. *Science (New York, N.Y.)*, 308(5718), pp.114–118.

Lee, S.H. et al., 2009. RasGRP1 Is Required for Human NK Cell Function. *The Journal of Immunology*, 183(12), pp.7931–7938.

Li, H., Rao, A. & Hogan, P.G., 2011. Interaction of calcineurin with substrates and targeting proteins. *Trends in Cell Biology*, 21(2), pp.91–103.

Lin, X. et al., 2000. Protein kinase C-theta participates in NF-kappaB activation induced by CD3-CD28 costimulation through selective activation of IkappaB kinase beta. *Molecular and cellular biology*, 20(8), pp.2933–2940.

Liu, J. et al., 1991. Calcineurin is a common target of cyclophilin-cyclosporin A and FKBP-FK506 complexes. *Cell*, 66(4), pp.807–815.

Liu, Y. et al., 2007. An essential role for RasGRP1 in mast cell function and IgE-mediated allergic response. *Journal of Experimental Medicine*, 204(1), pp.93–103.

Lorenzo, P.S. et al., 2000. The guanine nucleotide exchange factor RasGRP is a high -affinity target for diacylglycerol and phorbol esters. *Molecular pharmacology*, 57(5), pp.840–846.

Ma, J. et al., 2010. T-cell-specific deletion of STIM1 and STIM2 protects mice from EAE by impairing the effector functions of Th1 and Th17 cells. *European Journal of Immunology*, 40(11), pp.3028–3042.

Macian, F., 2005. NFAT proteins: key regulators of T-cell development and function. *Nature Publishing Group*, 5(6), pp.472–484.

Margarit, S.M. et al., 2003. Structural evidence for feedback activation by Ras.GTP of the Ras-

specific nucleotide exchange factor SOS. *Cell*, 112(5), pp.685–695.

Marshall, C.B. et al., 2015. Biochemical and Biophysical Research Communications. *Biochemical and biophysical research communications*, 460(1), pp.5–21.

Marsland, B.J., 2004. Protein Kinase C Is Critical for the Development of In Vivo T Helper (Th)2 Cell But Not Th1 Cell Responses. *Journal of Experimental Medicine*, 200(2), pp.181–189.

McCarl, C.A. et al., 2010. Store-Operated Ca2+ Entry through ORAI1 Is Critical for T Cell-Mediated Autoimmunity and Allograft Rejection. *The Journal of Immunology*, 185(10), pp.5845–5858.

Melowic, H.R. et al., 2007. Mechanism of diacylglycerol-induced membrane targeting and activation of protein kinase Ctheta. *The Journal of biological chemistry*, 282(29), pp.21467–21476.

Monks, C.R. et al., 1997. Selective modulation of protein kinase C-theta during T-cell activation. *Nature*, 385(6611), pp.83–86.

Müller, M.R. & Rao, A., 2010. NFAT, immunity and cancer: a transcription factor comes of age. *Nature Publishing Group*, 10(9), pp.645–656.

Navarro, M.N. & Cantrell, D.A., 2014. Serine-threonine kinases in TCR signaling. *Nature immunology*, 15(9), pp.808–814.

O'Shea, J.J. & Paul, W.E., 2010. Mechanisms underlying lineage commitment and plasticity of helper CD4+ T cells. *Science (New York, N.Y.)*, 327(5969), pp.1098–1102.

Oeckinghaus, A. et al., 2007. Malt1 ubiquitination triggers NF-kappaB signaling upon T-cell activation. *The EMBO journal*, 26(22), pp.4634–4645.

Oh-hora, M. et al., 2008. Dual functions for the endoplasmic reticulum calcium sensors STIM1 and STIM2 in T cell activation and tolerance. *Nature immunology*, 9(4), pp.432–443.

Oki, T. et al., 2011. Aberrant expression of RasGRP1 cooperates with gain-of-function NOTCH1 mutations in T-cell leukemogenesis. *Leukemia*, 26(5), pp.1038–1045.

Ouyang, K. et al., 2014. R-dependent Ca. *Nature Communications*, 5, pp.1–12.

Park, C.Y. et al., 2009. STIM1 Clusters and Activates CRAC Channels via Direct Binding of a Cytosolic Domain to Orai1. *Cell*, 136(5), pp.876–890.

Pfeifhofer, C. et al., 2003. Protein Kinase C Affects Ca2+ Mobilization and NFAT Activation in Primary Mouse T Cells. *Journal of Experimental Medicine*, 197(11), pp.1525–1535.

Picard, C. et al., 2009. STIM1 mutation associated with a syndrome of immunodeficiency and autoimmunity. *The New England journal of medicine*, 360(19), pp.1971–1980.

Plagnol, V. et al., 2011. Genome-wide association analysis of autoantibody positivity in type 1 diabetes cases. *PLoS genetics*, 7(8), p.e1002216.

Prakriya, M. et al., 2006. Orai1 is an essential pore subunit of the CRAC channel. *Nature*,

443(7108), pp.230–233.

Prasad, A. et al., 2009. Origin of the sharp boundary that discriminates positive and negative selection of thymocytes. *Proceedings of the National Academy of Sciences of the United States of America*, 106(2), pp.528–533.

Priatel, J.J. et al., 2002. RasGRP1 transduces low-grade TCR signals which are critical for T cell development, homeostasis, and differentiation. *Immunity*, 17(5), pp.617–627.

Qu, H.Q. et al., 2009. Association of RASGRP1 with type 1 diabetes is revealed by combined follow-up of two genome-wide studies. *Journal of Medical Genetics*, 46(8), pp.553–554.

Quann, E.J. et al., 2011. A cascade of protein kinase C isozymes promotes cytoskeletal polarization in T cells. *Nature Publishing Group*, 12(7), pp.647–654.

Quann, E.J. et al., 2009. Localized diacylglycerol drives the polarization of the microtubule-organizing center in T cells. *Nature Publishing Group*, 10(6), pp.627–635.

Rambaratsingh, R.A. et al., 2003. RasGRP1 Represents a Novel Non-protein Kinase C Phorbol Ester Signaling Pathway in Mouse Epidermal Keratinocytes. *Journal of Biological Chemistry*, 278(52), pp.52792–52801.

Roose, J.P. et al., 2005. A Diacylglycerol-Protein Kinase C-RasGRP1 Pathway Directs Ras Activation upon Antigen Receptor Stimulation of T Cells. *Molecular and cellular biology*, 25(11), pp.4426–4441.

Roose, J.P. et al., 2007. Unusual Interplay of Two Types of Ras Activators, RasGRP and SOS, Establishes Sensitive and Robust Ras Activation in Lymphocytes. *Molecular and cellular biology*, 27(7), pp.2732–2745.

Salek-Ardakani, S. et al., 2004. Differential Regulation of Th2 and Th1 Lung Inflammatory Responses by Protein Kinase C. *The Journal of Immunology*, 173(10), pp.6440–6447.

Salek-Ardakani, S. et al., 2005. Protein Kinase C Controls Th1 Cells in Experimental Autoimmune Encephalomyelitis. *The Journal of Immunology*, 175(11), pp.7635–7641.

Sato, M., Ueda, Y. & Umezawa, Y., 2006. Imaging diacylglycerol dynamics at organelle membranes. *Nature methods*, 3(10), pp.797–799.

Smith-Garvin, J.E., Koretzky, G.A. & Jordan, M.S., 2009. T Cell Activation. *Annual Review of Immunology*, 27(1), pp.591–619.

Sondermann, H. et al., 2004. Structural analysis of autoinhibition in the Ras activator Son of sevenless. *Cell*, 119(3), pp.393–405.

Spitaler, M. et al., 2006. Diacylglycerol and Protein Kinase D Localization during T Lymphocyte Activation. *Immunity*, 24(5), pp.535–546.

Stathopulos, P.B. et al., 2008. Structural and Mechanistic Insights into STIM1-Mediated Initiation of Store-Operated Calcium Entry. *Cell*, 135(1), pp.110–122.

Sugawara, H. et al., 1997. Genetic evidence for involvement of type 1, type 2 and type 3 inositol

1,4,5-trisphosphate receptors in signal transduction through the B-cell antigen receptor. *The EMBO journal*, 16(11), pp.3078–3088.

Sun, Z. et al., 2000. PKC-theta is required for TCR-induced NF-kappaB activation in mature but not immature T lymphocytes. *Nature*, 404(6776), pp.402–407.

Swan, K.A. et al., 1995. Involvement of p21ras distinguishes positive and negative selection in thymocytes. *The EMBO journal*, 14(2), pp.276–285.

Takigawa, M. et al., 1983. Inhibition of mouse skin tumor promotion and of promoter-stimulated epidermal polyamine biosynthesis by alpha-difluoromethylornithine. *Cancer research*, 43(8), pp.3732–3738.

Tan, S.L. et al., 2006. Resistance to Experimental Autoimmune Encephalomyelitis and Impaired IL-17 Production in Protein Kinase C -Deficient Mice. *The Journal of Immunology*, 176(5), pp.2872–2879.

Taylor, C.W. et al., 2009. IP3 receptors: some lessons from DT40 cells. *Immunological reviews*, 231(1), pp.23–44.

Thome, M. et al., 2010. Antigen Receptor Signaling to NF- B via CARMA1, BCL10, and MALT1. *Cold Spring Harbor Perspectives in Biology*, 2(9), pp.a003004–a003004.

Tognon, C.E. et al., 1998. Regulation of RasGRP via a phorbol ester-responsive C1 domain. *Molecular and cellular biology*, 18(12), pp.6995–7008.

Vetter, I.R. & Wittinghofer, A., 2001. The guanine nucleotide-binding switch in three dimensions. *Science (New York, N.Y.)*, 294(5545), pp.1299–1304.

Vig, M. et al., 2007. Defective mast cell effector functions in mice lacking the CRACM1 pore subunit of store-operated calcium release--activated calcium channels. *Nature immunology*, 9(1), pp.89–96.

Wang, D. et al., 2000. Phospholipase Cgamma2 is essential in the functions of B cell and several Fc receptors. *Immunity*, 13(1), pp.25–35.

Wang, X. et al., 2012. Regulation of PKC- θ function by phosphorylation in T cell receptor signaling. *Frontiers in Immunology*, 3, p.197.

Weiss, A., Wiskocil, R.L. & Stobo, J.D., 1984. The role of T3 surface molecules in the activation of human T cells: a two-stimulus requirement for IL 2 production reflects events occurring at a pre-translational level. *Journal of immunology (Baltimore, Md. : 1950)*, 133(1), pp.123–128.

Wu, M.M., 2006. Ca2+ store depletion causes STIM1 to accumulate in ER regions closely associated with the plasma membrane. *The Journal of Cell Biology*, 174(6), pp.803–813.

Yasuda, S. et al., 2007. Defective expression of Ras guanyl nucleotide-releasing protein 1 in a subset of patients with systemic lupus erythematosus. *Journal of immunology (Baltimore, Md. : 1950)*, 179(7), pp.4890–4900.

Yokosuka, T. et al., 2008. Spatiotemporal Regulation of T Cell Costimulation by TCR-CD28 Microclusters and Protein Kinase C q Translocation. *Immunity*, 29(4), pp.589–601.

Zheng, Y. et al., 2005. Phosphorylation of RasGRP3 on threonine 133 provides a mechanistic link between PKC and Ras signaling systems in B cells. *Blood*, 105(9), pp.3648–3654.

Chapter 2

Tonic Signals in T Cells and their Role in Immune Function

Introduction: Tonic Signals in Lymphocytes

Chapter 1 outlines the kinase and phosphatase pathways that are activated downstream of antigen receptor ligation. However, it has been appreciated for many years that in the absence of these activating signals, some of the same signaling effectors exhibit low-level phosphorylation, thought to be driven by transient interactions between the TCR and self-peptide-MHC (pMHC) as peripheral T cells survey the lymphoid organs. This phenomenon is referred to as "basal" or "tonic" signaling. Tonic signals have been observed in both $CD4^+$ and $CD8^+$ T lymphocytes, but they have also been well-studied in B lymphocytes [1-5]. The focus here will primarily be on $CD4^+$ T cells. The basal signals themselves are observed in the form of low-level phosphorylation, which is thought to be due to the establishment of an equilibrium between positive and negative regulators of receptor signaling. TCR ligation disrupts the equilibrium in favor of positive regulators, leading to robust signal transduction [6]. Similar signaling events are likely involved in the tonic- and inducible-signaling pathways, though the precise nature of these signaling events (with respect to the effectors involved as well as their spatio-temporal localization) still remains an open research question. While less well studied than antigen-induced signaling, these tonic signaling pathways have been proposed to be important for a number of T cell effector functions. This chapter will outline what is known about tonic signaling pathways in lymphocytes and the recently-developed tools that have aided our ability to study these pathways and their role in lymphocyte biology in detail.

Thymocyte Selection: Setting the Stage for Self-recognition

The TCR's affinity for self is set in the thymus: developing thymocytes rearrange their TCRα and β chains to generate a functional receptor, and some of these rearranged TCRs are reactive against self-antigen. This TCR is "tested" for recognition of self pMHC, a key mechanism of

central tolerance. Cells with TCRs capable of recognizing self (and can productively generate a TCR-Ras signal) are positively selected, but cells bearing TCRs with too high of an affinity for self (autoreactive cells) are either negatively selected and die, or they are agonist-selected to become regulatory T cells (Tregs), CD8αα intra-epithelial lymphocytes (IELs), or invariant natural killer T (iNKT) cells [7]. The thymocytes that pass these developmental checkpoints exhibit a range of self-reactivity, and thus the T cell pool consists of cells with different degrees of tonic signaling. This leads to a peripheral, naïve T cell compartment that is very heterogeneous, comprised of T cells with TCRs of varying specificities and affinities for self.

Tonic Signals in T Cells: What is their Function?

The TCRs of T cells make transient contacts with self-pMHC as lymphocytes survey the peripheral lymphoid organs [8,9]. These contacts do not trigger T cell activation but instead generate the above-described tonic, sub-threshold signals. TCRs with varying degrees of affinity for self generate stronger or weaker tonic signals [3]. Early work characterizing this tonic pathway revealed that there is low-level phosphorylation of proximal TCR signaling components such as the TCRζ chain immunoreceptor tyrosine-based activation motifs (ITAMs) [1], and Zap70 can associate with pTCRζ in the basal state [2]. When cells are deprived of these tonic signals, such as when being rested *ex vivo* in PBS at 37ºC [1,10], when an MHC class II blocking antibody is administered to mice [11], or when T cells are isolated from blood (as opposed to lymphoid organs) [11], a loss of basal phospho-TCRζ levels can be observed. A set of conflicting studies in which T cells were deprived of tonic signals postulate that these signals either desensitize the TCR [12] (by recruiting negative regulators, raising the threshold required for activation) or that interactions with self-pMHC sensitize the TCR, lowering its activation threshold [9]. These studies suggest that tonic signals are mechanistically important for tuning the sensitivity of the TCR for when T cells do encounter foreign antigen and need to respond.

Receptor-Ablation Studies Indicate a Maintenance Role for Tonic TCR Signals

In addition to a possible functional role in "priming" the TCR to be able to respond to foreign antigen, additional evidence points to a role for tonic signals in lymphocyte survival and homeostasis. In B cells, tonic signals have been shown to be crucial for cell survival, as ablation of the BCR results in rapid cell-death [5] due to loss of BCR-PI3K survival signals [13]. However, unlike in B cells, tonic TCR signaling does not appear to be essential for T cell survival [14]. Inducible deletion of the TCR by treating $C\alpha^{fl/fl}$ Mx-Cre mice with poly(I):poly(C) (pI:C) reveals that both $CD4^+$ and $CD8^+$ T cells do not immediately die. Instead, they decay over time, with half-lives of 16 and 46 days, respectively [14]. The maintenance signal also requires MHC class II: when a WT B6 thymus is engrafted into a thymectomized $Rag2^{-/-}$ class $II^{-/-}$ recipient, $CD4^+$ T cells initially populate the periphery normally, but over time the pool of $CD4^+$ T cells decreases more rapidly in the $Rag2^{-/-}$ class $II^{-/-}$ recipients compared to $Rag2^{-/-}$ class $II^{+/+}$ recipients. This indicates that MHC class II is required for T cell maintenance, but not for T cell survival per se. Interestingly, peripheral T cells in the class II-deficient environment could proliferate normally (measured by Brdu incorporation), and they expressed a diverse set of TCRs (measured by Vα2 usage) even 6 months following engraftment. These cells failed to upregulate CD44 with age, suggesting that tonic TCR-class II interactions may impact the activation state of the cells as well [15]. Maintenance of naïve $CD8^+$ T cells also requires specific MHC class I molecules, as H-Y TCR transgenic cells decayed upon transfer into recipients deficient for relevant MHC class I ($H\text{-}2D^{b-}$ or $H2\text{-}D^{b-}$ $\beta2m^-$) hosts. Interestingly, this decay was much more rapid (on the order of days) than what is observed when $CD4^+$ T cells are in a class II-deficient environment. These $CD8^+$ T cells did not incorporate Brdu in the absence of antigen, indicating a requirement for self-recognition for homeostatic proliferation as

well [16]. Collectively, these data suggest that tonic TCR signals are important signals for maintaining T cell homeostasis.

The role of tonic TCR signaling in regulatory T cell survival has also been examined. When the TCR is ablated from Treg cells (by treating Mx1-Cre *Tcra*$^{fl/fl}$ mice with pI:C [17] or by treating FoxP3-Cre^{ERT2} *Trac*$^{fl/fl}$ mice with tamoxifen [18]), a reduced number of Tregs is observed. These Tregs do not proliferate, and they lose expression of activation markers, suggesting that tonic TCR signals are important for maintenance of Tregs as well as for conventional T cells. Interestingly, TCR-deficient Tregs lose their suppressive capabilities yet still maintain Treg "lineage-specifying" characteristics such as FoxP3 expression, Treg-specific DNA methylation patterns, and IL-2R signaling. This indicates that tonic signals are more important for Treg functionality than for Treg "identity." [17,18]. A number of genes were differentially expressed in TCR-deficient Tregs, suggesting that a tonic TCR-gene expression program exists in these cells that may contribute to their suppressive capacity.

Reporters of Tonic Signaling Levels Aid Functional Studies

Two important markers that read-out the level of basal signaling (level of TCR affinity for self) have been identified that have greatly aided our ability to perform functional studies comparing cells with different levels of tonic signaling. These markers are the surface receptor CD5 [8], a negative regulator of TCR signaling, and the orphan nuclear hormone receptor Nur77 [19,20]. CD5 levels are induced proportional to TCR signal strength during thymocyte selection and single-positive thymocytes express CD5 at levels that correspond to TCR avidity. Maintenance of CD5 levels on thymocytes as well as on both CD4$^+$ and CD8$^+$ peripheral T cells requires self-pMHC interactions [8]. Recent studies in which naïve CD4$^+$ cells were sorted based on the level of CD5 revealed that CD5^{high} cells had higher levels of pTCRζ compared to CD5^{low} cells [3], as

well as higher levels of P-S6 and P-Erk levels in the $CD5^{high}$ compartment [10]. *Nr4a1 (Nur77)* is an immediate-early gene that gets upregulated by TCR stimulation in thymocytes and T cells and by BCR stimulation in B cells. Two groups generated Nur77-GFP BAC-transgenic mice, in which enhanced green fluorescent protein (EGFP) is under control of the *Nur77* regulatory region [19,20]. The level of induced GFP reports the strength of TCR signaling, as *in vitro* stimulations with increasing doses of α-CD3 led to concomitant increases in GFP. GFP expression was also induced in thymocyte populations that have undergone signaling-dependent checkpoints during selection [20], and agonist-selected populations (Tregs, CD8αα IELs, and iNKT cells), postulated to derive from thymocytes from high-affinity TCRs, showed higher GFP levels than their conventional $CD4^+$ and $CD8^+$ counterparts [19]. In the basal state, genetic titration of TCR signaling (using an allelic series of the phosphatase CD45) sensitively altered GFP levels in T cells [20], and in the periphery, $CD4^+$ and $CD8^+$ T cells exhibited a range of GFP expression, consistent with the idea that T cells within the peripheral pool exhibit a continuum of self-reactivity [19,20]. Perhaps unsurprisingly, CD5 levels correlate with Nur77-GFP expression in $CD4^+$ and $CD8^+$ naïve T cells [4]. These tools have sparked a great deal of interest in deciphering how the level of tonic signal a cell receives impacts its ability to participate in an immune response. Additionally, these tools allow for study of how dysregulated tonic signaling could lead to T cell abnormalities.

Recently, several studies have begun to more clearly define the physiological role of these basal signals in several T cell subsets, including $CD4^+$ conventional T cells [3,10], $CD8^+$ cytotoxic T cells [4], and $CD4^+$ regulatory T cells [17,18]. Nonspecific stimulation of $CD5^{low}$ and $CD5^{high}$ T cells revealed that the $CD5^{high}$ cells have increased phosphorylation of Erk and produce more IL-2 than $CD5^{low}$ cells [21]. Tetramer studies revealed that $CD4^+$ conventional T cells with high tonic signaling ($CD5^{high}$) bind to foreign antigen better than their $CD5^{low}$ counterparts, suggesting that the degree of affinity for self-antigen parallels the degree of affinity

for foreign antigen. Consistent with this, when congenically marked, sorted $CD5^{low}$ and $CD5^{high}$ cells were transferred into recipients prior to infection (with influenza A, lymphocytic choriomeningitis virus Armstrong (LCMV), or *Listeria monocytogenes* (LM)), the $CD5^{high}$ cells expanded much more than their $CD5^{low}$ counterparts. This suggests that cells with high tonic signaling contribute more to the immune response to infection than lower-affinity cells. Similar to the $CD4^+$ T cell data, $CD5^{high}$ $CD8^+$ T cells were present at higher ratios than their $CD5^{low}$ counterparts when adoptively transferred and subjected to an LM infection model [4]. Functional differences between Nur77-GFP^{high} and Nur77-GFP^{low} cells have not been explored yet. These data suggest that $CD4^+$ and $CD8^+$ T cells with high tonic signaling dominate in the immune response to infection.

Treg cells with different degrees of self-reactivity have also been shown to have distinct functional roles *in vivo*. A recent publication from Ed Palmer's group [22] demonstrated that expression levels of CD25, PD-1, and GITR reflect populations of Tregs with different degrees of self-reactivity: $Triple^{hi}$ Treg (high expression of all three markers) had increased CD5 and Nur77-GFP levels compared to $Triple^{lo}$ Tregs (low expression of these three markers). Using B3K508 TCR transgenic T cells (that recognize peptides of different affinities), it was shown that ligands at the threshold of negative selection select for $Triple^{lo}$ cells, whereas very high-affinity peptides select $Triple^{hi}$ cells, suggesting that these two populations differ in their degree of affinity for self. These cells are maintained *in vivo* by self (and not foreign) antigens, as this population persists in "antigen free" mice which lack infectious, microbial and dietary antigens but do contain self-antigens. Functionally, self-reactive Tregs ($Triple^{hi}$) proliferated more *in vivo* than $Triple^{lo}$ cells, as measured by Brdu incorporation. Furthermore, $Triple^{hi}$ cells were more suppressive than $Triple^{lo}$ cells, whereas these lower affinity cells were better at inducing iTregs in the periphery than their $Triple^{hi}$ counterparts [22].

Collectively, these data suggest that the degree of self-reactivity in $CD4^+$ conventional T cells, $CD8^+$ T cells, and $CD4^+$ regulatory T cells impacts their functional ability to respond to infection and control immune responses. How tonic signaling contributes to other aspects of an immune response, such as helper T cell differentiation and metabolic reprogramming is still an open question.

Tonic Signals and Transcriptional Programs – a Role for LAT

The linker for activation of T cells (LAT) is a transmembrane adapter protein involved in proximal TCR signaling. LAT is phosphorylated at four tyrosine residues in response to TCR crosslinking and this leads to the recruitment of signaling molecules that allow for full T cell activation. One of these is PLCγ1, discussed in Chapter 1, which is critical for calcium signaling and DAG-dependent activation of the Ras-Erk pathway. LAT-deficient mice, or mice where all four tyrosine have been mutated, have a severe block in thymocyte development and lack peripheral T cells [23,24]. The fact that loss or mutation of LAT cannot be compensated for by other molecules suggests that LAT is a central adapter protein in T cells. Recently, three patients harboring homozygous loss-of-function LAT mutations were identified. Intriguingly, some T cells did develop in these individuals, and *ex vivo* studies showed that the patients' T cells, surprisingly, were able to flux calcium and activate the NFkB pathway. Erk phosphorylation was impaired, as expected from murine and cell line studies. Interestingly, reconstitution of a LAT-deficient Jurkat line with a construct harboring the patient variant of LAT showed impaired calcium flux and activation of downstream signaling pathways, consistent with data from the LAT-deficient mice [25]. It is not yet clear how to explain these differences between the patient cells and the mouse studies.

Additional studies also reveal an important role for basal LAT signals: when LAT is point-mutated at the tyrosine residue where PLCγ1 docks (Y136F), the mice have an intriguing phenotype: they have a severe (yet incomplete) block in thymocyte development, but despite a lower thymic output, T cells do populate the peripheral lymphoid organs and greatly expand over time [26,27]. The LAT^{Y136F} (also referred to at $LAT^{m/m}$ here) mice develop lymphadenopathy and splenomegaly, and the $CD4^+$ T cells have an activated phenotype ($CD44^{hi}$ $CD62L^{lo}$). They also produce high levels of the Th2-cytokine interleukin 4 (IL-4) even without *ex vivo* restimulation with PMA and ionomycin. Interestingly, cells from one of the patients harboring a loss-of-function LAT mutant also produced high levels of IL-4 (with and without *ex vivo* α-CD3/28 or PMA/ionomycin stimulation) [28]. This Th2-biased lymphoproliferation is also observed in mice where LAT is inducibly deleted or point mutated: these two systems involve either (1) using a $Lat^{flox/dtr}$ mouse combined with diphtheria toxin treatment [29], or (2) Cre-ER expressing mice with one floxed allele and one null or mutant allele ($LAT^{f/m}$ or $LAT^{f/-}$) treated with tamoxifen [30]. This indicates that the Th2 lymphoproliferation phenotype is not due to altered thymocyte development and selection defects, and instead points to LAT as having an important control function in peripheral $CD4^+$ T cells. Paradoxically, despite the activated, differentiated, and proliferative phenotype, T cells from LAT^{Y136F} mice were refractory to *ex vivo* stimulation through the T cell receptor with α-CD3/CD28, and displayed an inability to flux calcium, proliferate, and secrete IL-2 [27,29]. We interpreted that these findings may indicate that the LAT-PLCγ1 pathway is important for transmitting a low-level, tonic signal, and that loss of this tonic signal somehow is permissive for spontaneous T cell activation and differentiation.

The cellular outputs of tonic signals are also starting to become elucidated. Work from our lab and others has proposed that tonic TCR signals control gene expression [6,31]. Microarray analysis of WT Jurkat T cells compared to a Jurkat line deficient for the adapter LAT (J.CaM2), and thus lacking LAT-dependent tonic signals, revealed unique changes in gene

expression. These cell line arrays, as well as mouse thymocyte studies, revealed a LAT-dependent tonic pathway that represses transcription of the *Rag-1* and *Rag-2* genes. Inhibitor studies showed that PLCγ1, PI3K, PKC, calcineurin and MEK also participate in this LAT-dependent tonic pathway, leading to the basal phosphorylation of the MAPK effector kinase ERK [6]. In this study, it was also shown that the tyrosine 132 on LAT (Y136 in murine LAT) was crucial for repression of *Rag* gene expression by basal LAT signaling.

Work from our lab and others supports the hypothesis that LAT-dependent tonic signals control gene expression programs. In addition to the aforementioned basal LAT signal that represses *Rag1* and *Rag2* gene expression, there is evidence that tonic LAT can also maintain expression of some genes. Peripheral $CD4^+$ T cells from mice where LAT is inducibly deleted for 4 weeks (Cre-ER^+ $LAT^{f/m}$) have reduced levels of surface TCR and lose *Tcrα* transcripts over time [31]. J.CaM2 cells also have reduced TCR/CD3 surface levels, due to reduced *TCRα* transcripts. Intriguingly, treatment of J.CaM2 cells with trichostatin A (TSA), an inhibitor of class I and II histone deacetylaces (HDACs), increased the levels of *TCRα* and *TCRβ* transcripts [31]. This result suggested that a tonic LAT signaling pathway maintains gene expression programs in naïve T cells by modulating the activity of HDACs, a class of epigenetic modifiers that de-acetylate histone tails, leading to gene repression [32]. In Chapter 5, I will present my work delineating a tonic LAT-HDAC7-gene expression pathway and the insights we have gained into how altered gene expression in LAT-perturbed cells contributes to the Th2-biased lymphoproliferation seen in the LAT^{KO} and LAT^{Y136F} mouse models.

The Ras activator Rasgrp1 (introduced in Chapter 1) is another signaling protein involved in transmitting tonic signals. The Rasgrp1-low (10% of WT levels) Jurkat line JPRM441 has reduced *TCRα* and *TCRβ* transcript levels. The second messenger diacylglycerol (DAG) appears to be important for this gene expression effect as well, as overexpression of DGKζ

(which limits DAG availability in cells by converting DAG to PA) also leads to reduced *CD3* transcripts [31]. As of yet, these findings have not been recapitulated in peripheral mouse T cells, as there is no mouse model in which Rasgrp1 can be inducibly deleted. Fully Rasgrp1-deficient animals have a profound block in T cell development and peripheral T cell lymphopenia, so they cannot be used to study the role of Rasgrp1 in peripheral T cell biology. Nevertheless, the data from these cell lines points to a tonic DAG-Rasgrp1 pathway that has a role in controlling basal transcription in T cells.

Rasgrp1-Dependent Tonic Signals and Translational Programs

The above-mentioned studies provide a strong link between tonic signals and gene expression. However, it is plausible that tonic signals control other cellular outputs, such as mRNA translation and metabolism. Gene expression profiling of $CD8^+$ $CD5^{low}$ vs $CD5^{high}$ T cells did not reveal many differences in transcription, as only 57 genes were increased by two-fold or more [4]. RNA-Seq on WT naïve $CD4^+$ $CD5^{low}$ and $CD5^{high}$ cells only revealed ~110 genes altered by two-fold or more (Myers and Roose, unpublished data). Interestingly, data from our lab utilizing a mouse model with a point mutation in *Rasgrp1* supports the notion that a tonic Rasgrp1-mTOR-mRNA translation pathway has a control function in naïve T cells.

A connection between Rasgrp1 and mTOR has been identified in T cells [10,33], though precisely how mechanistically Rasgrp1 participates in mTOR signaling is still unknown. Thymocytes and T cells stimulated through the TCR or with PMA activate the mTOR pathway, and this requires Rasgrp1, as mTOR signaling is abrogated in Rasgrp1-deficient thymocytes. mTOR signaling is also reduced when Rasgrp1-Ras signals are dampened via DGKζ overexpression. Interestingly, this study also showed that phosphorylation of S6 (at S235/236), 4E-BP1 (at T37/41) and Akt (at S473) were reduced in unstimulated Rasgrp1-deficient

thymocytes compared to WT [33]. This suggests that Rasgrp1 signals to mTOR in a tonic fashion as well as in a TCR-inducible one.

Additional evidence for tonic Rasgrp1-mTOR signals in T cells comes from our lab's characterization of mice with an *N*-ethyl-*N*-nitrosourea (ENU)-mutated Rasgrp1 allele called Rasgrp1^{Anaef} which has a single nucleotide substitution leading to the missense variant R519G [10]. The initial characterization of these mice will be presented in Chapter 6, but briefly: Rasgrp1^{Anaef} mice exhibit features of T cell autoreactivity and autoimmunity that become more prominent with age. T cells from these mice express elevated levels of the activation marker CD44 on otherwise naïve (CD62L^{hi}) cells, and T cells aberrantly stimulate B cells to produce anti-nuclear antibodies (ANA). Thymocytes and T cells exhibit elevated levels of basal P-S6 (S235/236). This elevated basal mTOR signaling is responsible for the autoimmune features in these animals. Pharmacological inhibition of mTOR (with rapamycin) *in vivo* reduces CD44 levels on thymocytes. Genetic complementation by crossing Rasgrp1^{Anaef} mice to mTOR^{chino} mice (an mTOR variant that has reduced mTOR-S6 signaling and lower CD44 levels on T cells) resolves the T cell CD44 phenotype and the ANAs. Interestingly, CD44 has been shown to be a translational target of mTOR [34], and CD44 protein levels appear to be under tonic control as well. CD5^{high} WT cells have lower CD44 mRNA and higher CD44 protein levels compared to their CD5^{low} counterparts (Myers et al., unpublished data). These studies indicate that tonic Rasgrp1-mTOR signals impact basal mRNA translation in T cells. This will be discussed at greater length in Chapter 7.

Conclusions and Perspectives

Several mouse models have been published wherein single nucleotide changes in signaling genes lead to breaks in immune tolerance and autoimmunity: the LAT^{Y136F} and Rasgrp1^{Anaef}

models discussed above are two relevant examples. While these mutations may impact the ability of T cells to engage signaling pathways downstream of TCR ligation, it is now becoming more and more clear that they impact tonic signaling pathways as well. Given that humans inherit ~12000 missense gene variants [35], understanding how subtle changes in signaling proteins impact immune cell homeostasis will be critical for our full understanding of the molecular basis of autoimmunity. We propose that it will be critical to fully understand tonic and TCR-inducible signaling pathways in T cells as we move forward with sophisticated treatments for autoimmune diseases and other diseases in which T cell immunotherapies will play a role.

REFERENCES

1 van Oers, N.S. *et al.* (1993) Constitutive tyrosine phosphorylation of the T-cell receptor (TCR) zeta subunit: regulation of TCR-associated protein tyrosine kinase activity by TCR zeta. *Mol. Cell. Biol.* 13, 5771–5780

2 van Oers, N.S. *et al.* (1994) ZAP-70 is constitutively associated with tyrosine-phosphorylated TCR zeta in murine thymocytes and lymph node T cells. *Immunity* 1, 675–685

3 Mandl, J.N. *et al.* (2012) T Cell-Positive Selection Uses Self-Ligand Binding Strength to Optimize Repertoire Recognition of Foreign Antigens. *Immunity* DOI: 10.1016/j.immuni.2012.09.011

4 Fulton, R.B. *et al.* (2014) The TCR's sensitivity to self peptide–MHC dictates the ability of naive CD8+ T cells to respond to foreign antigens. *Nat. Immunol.* 16, 107–117

5 Lam, K.P. *et al.* (1997) In vivo ablation of surface immunoglobulin on mature B cells by inducible gene targeting results in rapid cell death. *Cell* 90, 1073–1083

6 Roose, J.P. *et al.* (2003) T Cell Receptor-Independent Basal Signaling via Erk and Abl Kinases Suppresses RAG Gene Expression. *Plos Biol* 1, e3

7 Germain, R.N. (2002) T-cell development and the CD4-CD8 lineage decision. *Nature Reviews Immunology* 2, 309–322

8 Azzam, H.S. *et al.* (1998) CD5 expression is developmentally regulated by T cell receptor (TCR) signals and TCR avidity. *J. Exp. Med.* 188, 2301–2311

9 Stefanová, I. *et al.* (2002) Self-recognition promotes the foreign antigen sensitivity of naive T lymphocytes. *Nature* 420, 429–434

10 Daley, S.R. *et al.* (2013) Rasgrp1 mutation increases naive T-cell CD44 expression and drives mTOR-dependent accumulation of Helios^{+} T cells and autoantibodies. *eLife* 2, e01020

11 Stefanová, I. *et al.* (2003) TCR ligand discrimination is enforced by competing ERK positive and SHP-1 negative feedback pathways. *Nat. Immunol.* 4, 248–254

12 Bhandoola, A. *et al.* (2002) Peripheral expression of self-MHC-II influences the reactivity and self-tolerance of mature CD4(+) T cells: evidence from a lymphopenic T cell model. *Immunity* 17, 425–436

13 Srinivasan, L. *et al.* (2009) PI3 Kinase Signals BCR-Dependent Mature B Cell Survival. *Cell* 139, 573–586

14 Polic, B. *et al.* (2001) How alpha beta T cells deal with induced TCR alpha ablation. *Proc Natl Acad Sci U S A* 98, 8744–8749

15 Takeda, S. *et al.* (1996) MHC class II molecules are not required for survival of newly generated CD4+ T cells, but affect their long-term life span. *Immunity* 5, 217–228

16 Tanchot, C. *et al.* (1997) Differential requirements for survival and proliferation of CD8 naïve or memory T cells. *Science* 276, 2057–2062

17 Vahl, J.C. *et al.* (2014) Continuous T Cell Receptor Signals Maintain a Functional Regulatory T Cell Pool. *Immunity* DOI: 10.1016/j.immuni.2014.10.012

18 Levine, A.G. *et al.* (2014) Continuous requirement for the TCR in regulatory T cell function. *Nat. Immunol.* 15, 1070–1078

19 Moran, A.E. *et al.* (2011) T cell receptor signal strength in Treg and iNKT cell development demonstrated by a novel fluorescent reporter mouse. *Journal of Experimental Medicine* 208, 1279–1289

20 Zikherman, J. *et al.* (2012) Endogenous antigen tunes the responsiveness of naive B cells but not T cells. *Nature* 489, 160–164

21 Persaud, S.P. *et al.* (2014) Intrinsic CD4+ T cell sensitivity and response to a pathogen are set and sustained by avidity for thymic and peripheral complexes of self peptide and MHC.

Nat. Immunol. 15, 266–274
22 Wyss, L. *et al.* (2016) Affinity for self antigen selects Treg cells with distinct functional properties. *Nat. Immunol.* 17, 1093–1101
23 Zhang, W. *et al.* (1999) Essential role of LAT in T cell development. *Immunity* 10, 323–332
24 Sommers, C.L. *et al.* (2001) Knock-in mutation of the distal four tyrosines of linker for activation of T cells blocks murine T cell development. *J. Exp. Med.* 194, 135–142
25 Keller, B. *et al.* (2016) Early onset combined immunodeficiency and autoimmunity in patients with loss-of-function mutation in LAT. *Journal of Experimental Medicine* 213, 1185–1199
26 Aguado, E. *et al.* (2002) Induction of T helper type 2 immunity by a point mutation in the LAT adaptor. *Science* 296, 2036–2040
27 Sommers, C.L. (2002) A LAT Mutation That Inhibits T Cell Development Yet Induces Lymphoproliferation. *Science* 296, 2040–2043
28 Keller, B. *et al.* (2016) Early onset combined immunodeficiency and autoimmunity in patients with loss-of-function mutation in LAT. *Journal of Experimental Medicine* 213, 1185–1199
29 Mingueneau, M. *et al.* (2009) Loss of the LAT adaptor converts antigen-responsive T cells into pathogenic effectors that function independently of the T cell receptor. *Immunity* 31, 197–208
30 Shen, S. *et al.* (2009) The essential role of LAT in thymocyte development during transition from the double-positive to single-positive stage. *The Journal of Immunology* 182, 5596–5604
31 Markegard, E. *et al.* (2011) Basal LAT-diacylglycerol-RasGRP1 Signals in T Cells Maintain TCRα Gene Expression. *PLoS ONE* 6, e25540
32 Haberland, M. *et al.* (2009) The many roles of histone deacetylases in development and physiology: implications for disease and therapy. *Nat Rev Genet* 10, 32–42
33 Gorentla, B.K. *et al.* (2011) Negative regulation of mTOR activation by diacylglycerol kinases. *Blood* 117, 4022–4031
34 Hsieh, A.C. *et al.* (2012) The translational landscape of mTOR signalling steers cancer initiation and metastasis. *Nature* DOI: 10.1038/nature10912
35 Auton, A. *et al.* (2015) A global reference for human genetic variation. *Nature* 526, 68–74

Chapter 3

mTOR Signaling in T Cells

Introduction

The mechanistic/mammalian target of rapamycin (mTOR) is classically known to be a critical regulator of cell growth, proliferation, and mRNA translation. The biochemical details of this pathway have been largely characterized in cell lines, and the physiological role of mTOR signaling has been widely studied in a number of model organisms and disease states such as cancer. Recently, there has been a great deal of interest in the role of mTOR signaling in T cell biology, in particular its role in T cell growth, activation, and proliferation, but also its role in differentiation, metabolism, and trafficking. Most of our knowledge of mTOR signaling is based on receptor-induced studies, e.g. with stimulation by insulin, amino acids, other growth factors, or pMHC) performed through *in vitro* manipulations, often in cell lines: however, we have noted that the mTOR pathway appears to be particularly robust in freshly-isolated murine primary $CD4^+$ T cells, suggesting that tonic mTOR signals exist and are relevant for T cell biology (1,2). This chapter will outline the mTOR signaling pathway in T lymphocytes and discuss recent work that expands our understanding of how mTOR signaling contributes to helper T cell differentiation, mRNA translation, and metabolism.

Canonical mTOR Signaling

The mTOR pathway has been well-characterized using established cell line systems. mTOR is a serine/threonine kinase that associates with several cofactors to form two distinct complexes, mTORC1 and mTORC2 **(Figure 3.1)**. The accessory protein regulatory-associated protein of mTOR (RAPTOR) is a critical component of complex 1, whereas rapamycin-insensitive companion of mTOR (RICTOR) is a critical component of mTORC2. RAPTOR and RICTOR function as scaffolds to bring the complexes together and for binding substrates (1-3). mTORC1 can be activated by diverse signal inputs such as nutrients and growth factors from the

microenvironment (reviewed in (4-6)), and these inputs have also been shown to couple to the lipid kinase phosphatidylinositol 3-kinase (PI3K). PI3K produces phosphatidylinositol (3,4,5)-triphosphate (PIP3), which activates phosphoinositide-dependent protein kinase-1 (PDK1). PDK1 subsequently activates Akt at the plasma membrane. Akt phosphorylates and inhibits the Ras homolog enriched in brain (Rheb) GTPase activating protein (GAP) complex tuberous sclerosis complex 1/2 (TSC1/2). The net result is activation of the small GTPase Rheb, and GTP-bound Rheb in turn activates mTORC1. mTOR activation is contingent upon its relocalization to the lysosome, a process which is regulated by amino acids and the Rag GTPases. In response to amino acid import, The Rag GTPases exist as heterodimers between either RagA or RagB with either RagC or RagD. In response to amino acid stimulation, the RagA/B becomes GTP loaded and RagC/D GDP-loaded, which is the active conformation. Rag GTPases then induce the localization of mTOR to the lysosome, via binding to RAPTOR. mTOR is also able to localize with Rheb at the lysosomal surface, facilitating its activation (3,7-9).

Following activation, mTORC1 directly phosphorylates its substrates: the S6 kinases (S6K1 and S6K2), which phosphorylate the ribosomal S6 protein, and the eukaryotic translation initiation factor 4E (eIF4E) binding proteins (4E-BP1, 2, and 3) **(Figure 3.1)**. It is still relatively unclear what upstream cues activate mTORC2, but it is firmly established that mTORC2 activity results in the phosphorylation and activation of AGC-family kinases such as Akt and SGK1 (6,10-12). Interestingly, it seems that T cells may have a distinct pathway for turning on mTORC1, as mTORC1 activation in $CD8^+$ T cells occurs independently of PI3K or Akt. Treatment with the Akt inhibitor Akti-1/2 or with the p110δ inhibitor IC87114 does not impact phosphorylation of downstream mTORC1 effectors S6K, S6, and 4E-BP1 (10,13).

mTOR signaling is balanced by the AMP-activated protein kinase (AMPK) pathway. AMPK senses when ATP levels in cells drop (and the AMP/ATP ratio rises) and AMPK

phosphorylates TSC2. Phospho-TSC2 has increased GAP activity towards Rheb·GTP, effectively shutting off mTOR signaling (14-16). Overall, AMPK signals to promote catabolic processes instead of the anabolic ones utilized in highly metabolic, glycolytic cells (15,17,18).

A striking cell biological effect of active mTOR signaling is the alteration in cell metabolism, including the increase in cell growth, cap-dependent translation and elongation, ribosome biogenesis, and switches in metabolic programs (3,6). In T cells, there has been a great deal of recent interest in mTOR signaling and its role in peripheral T cell biology, including in helper T cell differentiation (2,3,5-7,19,20) and lymphocyte metabolism (5,15,17,21,22). Important work has also revealed a role for mTOR in B:T cell interactions in the germinal center and the expression of adhesion molecules that mediate lymphocyte trafficking (23,24), though these topics are outside the scope of this chapter. These distinct functional outputs of mTOR activation, and what is known about them in T lymphocytes, will be discussed subsequently.

mTOR-dependent Growth and Proliferation in Animal Models

mTOR has been well-established as a regulator of cell mass and proliferation. Fruit flies that harbor crippling mutations in PI3K, Akt, and mTOR have reduced cell, organ, and organism size, and conversely mutations in PTEN, an important negative regulator of PI3K signaling, lead to increased cell growth (summarized in (18,23)). mTOR is important in embryonic development, as mTOR-deficient flies die in the pupal stage (18,25), and a whole-body knockout of mTOR in mice is embryonic lethal (26,27). Mice with reduced mTOR levels, caused by a *neo* cassette insertion that partially disrupts mTOR transcription, have reduced overall size and weight. We found that $mTOR^{chino}$ mice with I205S substitution in the Raptor-binding domain of mTOR resulting in a hypomorphic mTOR allele show reduced body mass as well (2,7).

Global deletion of S6K1, a downstream effector of mTOR, also effects growth and proliferation, as S6K1-deficient mice have reduced overall mass and a developmental delay (1,20).

mTOR-related Growth Defects in Lymphocytes

With respect to the immune system, mice with a neo insertion in mTOR have reduced spleen size and reduced numbers of T and B cells. T cells exhibited impaired proliferation in response to stimulation with α-CD3 and α-CD28, which activate the T cell receptor and provide costimulation, respectively (4,19). Another group generated a T-cell specific mTOR knockout mouse by crossing $mTOR^{fl/fl}$ animals to CD4-Cre, and T cells from these animals showed impaired TCR-induced proliferation as well (7,11). Impairing mTOR kinase activity in mouse T or B cells with a kinase-dead knock-in allele (mTOR-KI CD4-Cre or CD19-Cre) profoundly reduced cell size and impaired proliferation, as did T cell specific knockout of Raptor, one of the critical components of mTORC1 (10,28,29). Interestingly, T and B cells from S6K1/2 double-deficient mice grew and proliferated normally, indicating that the S6Ks are not essential for these processes. Instead, this study proposed that the 4E-BPs predominantly regulate growth and proliferation in lymphocytes. This study also revealed that 4E-BP2 is the dominant isoform expressed in lymphocytes, as opposed to 4E-BP1 which is more abundant in other cell types such as fibroblasts (10,30).

mTOR Regulates mRNA Translation

When cells are in nutrient-rich environments that support the growth and proliferation described above, they need to increase their cell size. To meet the biosynthetic demands of this growth, cells need to be able to produce new proteins through a process known as translation. Translation is energetically costly to the cell, and as such it is very tightly regulated and only

occurs when conditions are favorable. mTOR is a key integrator of environmental cues (including nutrient and growth factor availability), and thus it is a key facet of this regulation. Another energy sensor is AMPK, and when conditions are favorable AMPK signaling is turned off, which in turn increases mTOR signaling.

Translation is typically divided into four phases: initiation (the rate-limiting step wherein an elongation-competent 80S ribosome is assembled and pairs with an mRNA), elongation (where new amino acids are joined to the nascent polypeptide), termination, and recycling (14,16,31). Mechanistically, mTOR regulates translation initiation through its action on the 4E-BPs and the S6Ks. Ribosomes do not directly bind to mRNAs but are recruited to mRNAs by eukaryotic translation initiating factors, or eIFs. One of these eIFs, eIF4E, binds to the 5' cap present on all transcribed mRNAs. However, in non-activated cells, eIF4E is not bound to the 5' cap but complexes with hypo-phosphorylated 4E-BPs. When cellular conditions are favorable and mTORC1 signaling is activated, mTORC1 phosphorylates 4E-BP, leading to dissociation of 4E-BP from eIF4E. eIF4E can subsequently bind to the 5' cap of mRNAs. At this point it also associates with two other proteins: eIF4G (a scaffold) and eIF4A (an RNA helicase that unwinds complex 5'UTR structures in the mRNAs). eIF4G also interacts with eIF3, an important ribosome-initiation factor, and the "ternary complex" (eIF2, Met-tRNA, and GTP) are also recruited to the mRNA (15,18,19). Once these effectors are in place, the ribosome can then scan the mRNA in a 5' to 3' direction, generating a new polypeptide. Active S6K1 also phosphorylates and interacts with several effector proteins that promote translation, including elongation factors and cap-binding proteins (3,16).

mTOR Substrates

mTORC1-S6K signaling has also been shown to play a role in both translation initiation and ribosome biogenesis, which is essential for efficient translation. mTORC1 phosphorylates S6K1 at threonine 389, which results in the formation of a docking site for the kinase PDK1, which phosphorylates S6K1 at T229, fully activating S6K. S6K can phosphorylate another initiation factor, eIF4B, and in turn eIF4B enhances the helicase activity of eIF4A (15,32,33). This process is particularly important for the translation of mRNAs that have long and highly structured 5' untranslated regions (UTRs). A notorious example is c-Myc, which will be discussed subsequently in this Chapter as well as in Chapter 7. The particular nature of the 5' UTR structures of potential mTOR targets is an area of active investigation. Some groups previously documented that mTOR targets have long 5'UTRs, whereas a study from the Ruggero lab revealed mTOR-dependent mRNAs have short 5'UTRs (23,34). Interestingly, in prostate cancer cell lines, 68% of mTOR-responsive mRNAs appear to contain a structural element called a 5' terminal oligopyrimidine (5' TOP) motif, 63% possess a pyrimidine-rich translational element (PRTE), and 89% encompass either a 5'TOP or a PRTE (23,35). Whether these elements are indicative of mTOR-responsiveness in cell types other than prostate cancer cell lines, such as T lymphocytes, is still unknown.

Helper T Cell Differentiation is Controlled by mTORC1 and mTORC2

When a naïve $CD4^+$ T cell receives TCR input in the appropriate cytokine milieu, the cell becomes activated and can begin a program of proliferation and differentiation into effector subsets (25,36). Th1 cells produce IFNγ, express the transcription factor T-bet, and are important for immunity to intracellular pathogens; Th2 cells (discussed below for being regulated in part by mRNA translation) express Gata3, produce IL-4 and IL-13, and are important for immunity to helminths yet are pathogenic in atopic diseases. Th17 cells are pro-inflammatory and produce IL-17. Follicular helper T cells (Tfh) express the transcription factor Bcl6 and

important helper cells for B cells in the germinal center response. For example, Tfh-derived IL-4 can promote class switching to IgG1 and IgE in mice (26,37). Regulatory T cells, which suppress effector T cell responses, can be generated in the thymus, as well as induced in the periphery as a means to ensure tolerance.

Recently, it has been appreciated that mTOR signaling plays an important role in the above-described helper T cell activation and fate determination. TCR-stimulated mTOR-deficient T cells do not upregulate activation markers or proliferate well. Additionally, mTOR-deficient T cells preferentially become regulatory, and not effector T cells (7,38). Abrogating either mTORC1 signaling (via T cell specific Rheb KO) or mTORC2 signaling (via T cell-specific Rictor KO) in $CD4^+$ T cells revealed that mTORC1 is essential for Th1 and Th17 differentiation, whereas Th2 cells require mTORC2 (20,39). A separate study revealed a role for mTORC1 in Th2 differentiation, using T cell-specific Raptor knockout to eliminate mTORC1 signaling (19,40,41). T cell-specific deletion of the AGC kinase family member SGK1, which, just like its family member Akt, is downstream of mTORC2, led to a modest reduction in T cell proliferation but a profound defect in the generation of Th2 cells as measured by IL-4, -5, and -13 production (11,42). Recently, two groups independently identified a role for both mTORC1 and mTORC2 signaling in the generation of Tfh cells ($PD1^{hi}$ $CXCR5^+$) and the germinal center reaction, finding that Raptor-, Rictor- and mTOR-deficient T cells could not differentiate to Tfh, had impaired GC B cell formation and those B cells exhibited reduced antibody production (28,29,43,44). In sum, it has become evident that mTOR signaling is closely tied to $CD4^+$ T cell fate decisions, and in the next sections we discuss how this may occur through mTOR's effects on mRNA translation and metabolism.

mTOR and Translation in Lymphocytes

It appears that T cells with different activation states, that is naïve vs. *ex vivo* TCR-stimulated, and with different effector functions, such as conventional vs. regulatory $CD4^+$ T cells, have different translational programs. Bjur and colleagues compared the translational landscapes of aforementioned populations by isolating polysome-associated mRNAs from ribosomes (17,30,39), and documented that the translational programs in these cell populations were distinct from each other and also different from the characterized transcriptional profiles. Thus, mRNA translation is distinct in different T cell populations.

The transcription factor c-Myc has been shown to be regulated at the level of mRNA translation. Biochemically, c-Myc is induced downstream of PI3K, mTOR, and Erk signaling, as its induction can be blocked with inhibitors of these pathways (31,42). Raptor-deficient $CD4^+$ T cells also do not upregulate c-Myc protein (19,37). Interestingly, c-Myc expression is regulated in a sensitive manner: first, it appears that Myc mRNA and protein are induced in a digital fashion downstream of TCR signaling, yet c-Myc protein levels are regulated at the post-transcriptional level in an analog fashion downstream of IL-2R signaling. This was revealed by stimulating OT-1 T cells with agonist peptides of varying affinities and by culturing cells in different amounts of IL-2. This data suggests that TCR-activating signals generate some c-Myc expression in cells, and then its levels are fine-tuned based on environmental cues such as the presence of cytokines.

Several genes important for Th2 and Tfh biology have been shown to be regulated at the translational level, including Gata3, IL-4, and ICOS (16). Gata3 is the master transcription factor for Th2 cells, which produce IL-4. Naïve T cells differentiate into Th2 cells in the presence of TCR stimulation and IL-4 cytokine input. Gata3 gets induced and then binds to the IL-4, -5, and -13 locus, inducing the transcription of these cytokines (32,33). Cook and Miller showed that IL4R signaling can increase Gata3 mRNA levels somewhat, but not to a degree that is sufficient

for Th2 differentiation. Only with TCR stimulation, activating the mTOR pathway, do Gata3 protein levels rise sufficiently. Furthermore, TCR stimulation together with IL-4 increases Gata3 translation in T cells, as protein levels increase in a radio-labeled methionine assay, while mRNA levels stay constant (34). IL-4, a cytokine secreted by Th2 and Tfh cells, is under translational control in Th2 cells that are re-activated after initial priming, leading to increased polysomes and increased IL-4 protein production (35). Lastly, the ICOS costimulatory molecule is under translational control. ICOS costimulation augments IL-4 mRNA translation, as IL-4 was enriched in polysome fractions following stimulation through the TCR and through ICOS compared to stimulation through the TCR alone (36). This was dependent on ICOS-PI3K signaling, as no increase in polysome association was observed in mice with a $ICOS^{Y181F}$ mutation that abrogates the ability of ICOS to activate PI3K. The ICOS-PI3K loop was suggested to be important for targeted delivery of IL-4 cytokine to B cells by Tfh cells during the germinal center response. In sum, the role of mRNA translation regulating T cell function requires further studies, but results thus far point to an interesting link with Th2 differentiation.

Metabolic Programs in Naïve and Activated T Cell Subsets

Recently there has been an outpouring of research into the role of metabolic programs used by $CD4^+$ T cells (and other immune cells), and the role of mTOR therein. By now it is well established that T cells in different activation states dynamically adopt different metabolic programs to meet their functional needs. Naïve, quiescent T cells that are not actively dividing or producing cytokines generate most of their energy by converting glucose to pyruvate and oxidizing that pyruvate in the mitochondria (TCA cycle), a process referred to as oxidative phosphorylation or OXPHOS. Once T cells become activated, their metabolic demand greatly increases, and as such they respond by primarily utilizing a different metabolic pathway: aerobic glycolysis. Glycolysis is not an energy-efficient process as it yields only two molecules of ATP

per input molecule of glucose, but it is advantageous to rapidly dividing cells because it generates many biosynthetic precursors for cell growth. Several of the different effector T cell subsets (Th1, Th2, and Th17) have been shown to utilize aerobic glycolysis (37). Additionally, cells can obtain energy through the oxidation of lipids instead of glucose. Tregs primarily gain energy via lipid oxidation and have higher levels of AMPK, though Tregs do utilize glycolysis when proliferating. Interestingly, it seems that there are tradeoffs between metabolism and function, as Tregs utilizing a more glycolytic metabolic program have reduced suppressive capabilities (38). At the end of an immune response, memory cells form, and these typically utilize lipid oxidation (39). Inhibiting mTOR with rapamycin, or activating AMPK with metformin, can promote the generation of memory $CD8^+$ T cells, suggesting an additional link between T cell metabolism and function (40,41).

The reprogramming from OXPHOS to aerobic glycolysis involves several cell-biological changes. First, activated cells upregulate transporters to bring in glucose, amino acids, and other nutrients. These include the glucose receptor Glut1 (42), the trophic receptors CD71 (transferrin receptor), CD98, and Slc7a5, which heterodimerizes with CD98 to form a large neutral amino acid transporter (43,44). Additionally, activated T cells upregulate certain transcription factors, such as ERRα and c-Myc, which in turn enhance expression of metabolic genes (17,39).

The glucose transporter Glut1 is expressed at low levels in resting T cells, but Glut1 protein expression dramatically increases and is accompanied by increased trafficking of Glut1 to the surface when T cells are activated *in vitro* (42). Surface Glut1 is also induced on T cells *in vivo* in response to immunization (37). Treatment of *in vitro* activated T cells with PI3K and mTOR inhibitors demonstrated that these kinases are required for Glut1 induction. Interestingly, it seems that Glut1 is important for sustaining mTORC1 signaling once T cells are already

activated, as cultured Glut1-deficient T cells exhibit reduced P-S6 levels and increased P-AMPK levels (indicating metabolic stress) compared to WT, suggesting a positive feedback loop (3,8,9,42).

Mouse models of Glut1 overexpression (6,11,12,37) or deficiency (13,42) revealed an important functional role for Glut1 in T cell proliferation, survival, and cytokine production. Additionally, measuring OXPHOS levels via the oxygen consumption rate and aerobic glycolysis via the extracellular acidification rate revealed that Glut1-deficient cells could not undergo metabolic reprogramming from OXPHOS to glycolysis. These studies reveal a critical role for cellular import of glucose in lymphocyte activation, proliferation, and metabolism.

The process of aerobic glycolysis itself is important for T cell effector function, as naïve $CD4^+$ T cells stimulated in media containing galactose (which cannot be metabolized using aerobic glycolysis) were dramatically impaired in their ability to produce the cytokines IFNγ and IL-2. Mechanistically, it was shown that cells utilizing aerobic glycolysis increase the translation of IFNγ mRNA, likely mediated by preventing inhibitory GAPDH binding to IFNγ transcripts. Aerobic glycolysis has also been shown to be important in modulating T cell proliferation. Inhibiting glucose metabolism with 2-deoxyglucose (2-DG) *in vivo* partially inhibits T cell proliferation in an adoptive transfer experiment (15,31), and 2-DG treatment was also shown to protect mice from EAE (17,45). Perhaps unexpectedly, T cells were shown use OXPHOS in addition to aerobic glycolysis to aid their activation and proliferation. Treatment of cells with the ATP synthase inhibitor oligomycin impaired T cell activation and proliferation (6,46).

In addition to Glut1 and glucose enabling mTOR signals, amino acid signaling also activates mTOR (3,9). Recent work has uncovered an important role for amino acid uptake in T cell function. T cell-specific deletion of Slc7a5, a protein that heterodimerizes with CD98 to form

a system L transporter, has profound effects on T cell biology. System-L transporters are critical for the import of leucine and other large neutral amino acids into cells. CD98 is an mTOR target, as Raptor-deficient T cells show impaired TCR-induced CD98 upregulation (19). Slc7a5-deficient T cells cannot proliferate, fail to differentiate into Th1 and Th17 effector subsets, and cannot efficiently undergo metabolic reprogramming to aerobic glycolysis (43). Slc7a5-deficient T cells cannot activate the mTOR pathway or induce c-Myc protein, despite expressing robust c-Myc transcript. Interestingly, mTOR translocates to the lysosome in $CD8^+$ T cells following *in vitro* TCR stimulation, and mTOR-lysosome colocalization was stronger in cells that expressed higher levels of Slc7a5 (5,17,21,22,47). These studies suggests that TCR signals and amino acid uptake are coupled in T cells to promote mTOR signaling, metabolism, and effector function in T cells.

c-Myc as a Critical Decider

As discussed above, c-Myc is a translational target of mTOR. c-Myc itself also plays a critical role in metabolic reprogramming of T cells. Conditional deletion of Myc using a floxed allele crossed to a tamoxifen-inducible Cre profoundly alters T cell biology (24,31). Myc-deficient cells showed impaired proliferation *in vitro* and *in vivo* and did not increase their cell size upon T cell activation like WT lymphocytes do. Myc deficiency has a selective effect on distinct metabolic programs, as glycolysis and glutamine metabolism were impaired in Myc-deficient T cells, but mitochondrial oxidation of glucose (OXPHOS) and fatty acids were not affected. Myc is induced early in T cell activation, prior to upregulation of metabolic genes, suggesting that Myc itself could play a role in inducing the glycolytic program (18,31). Functionally, Myc expression correlates with and controls upregulation of the transferrin receptor CD71, revealing an intimate link between c-Myc and nutrient import (18,48).

In two very recent studies, it was shown that the decisive function of c-Myc is inherited in an asymmetric manner. Specifically, in the process of cell division, the daughter cell more proximal to the original parental cell receives more c-Myc protein than the distal daughter cell (27,47,49). This finding was extended to mTOR pathway components such as P-S6 and metabolic transporters such as CD98: these were also enriched in the c-Myc^{high}, proximal daughter cells when compared to the c-Myc^{low} distal daughter cells. Intriguingly, inheritance of c-Myc in the first cell division also appeared to correlate with the differentiation state of the CD8^{+} T cell. Sorted c-Myc^{high} cells transferred into recipients that were subsequently immunized with influenza A dominated the immune response, acting more like effector cells, while Myc^{low} cells dominated the memory response (2,49). It is still unclear how this effector/memory dichotomy with respect to c-Myc inheritance is explained, as the cells continue to divide during the course of an immune response.

Closing Remarks

In sum, mTOR signaling is critical for a number of cell biological processes in T cells, and here we focused on its role in activation, proliferation, differentiation into effector subsets, mRNA translation, and metabolism. Despite the outpouring of research into this topic in recent years, the biochemical details of how exactly the TCR couples to mTOR is still unknown. Additionally, whether mTOR signaling is regulated and activated similarly in naïve and effector T cells, and how mTOR activation contributes to the cellular transition with respect to changes in gene expression, mRNA translation, and metabolic reprogramming remain open questions. These topics are, in part, the subject of our research presented in Chapters 6-8 of this dissertation.

FIGURES

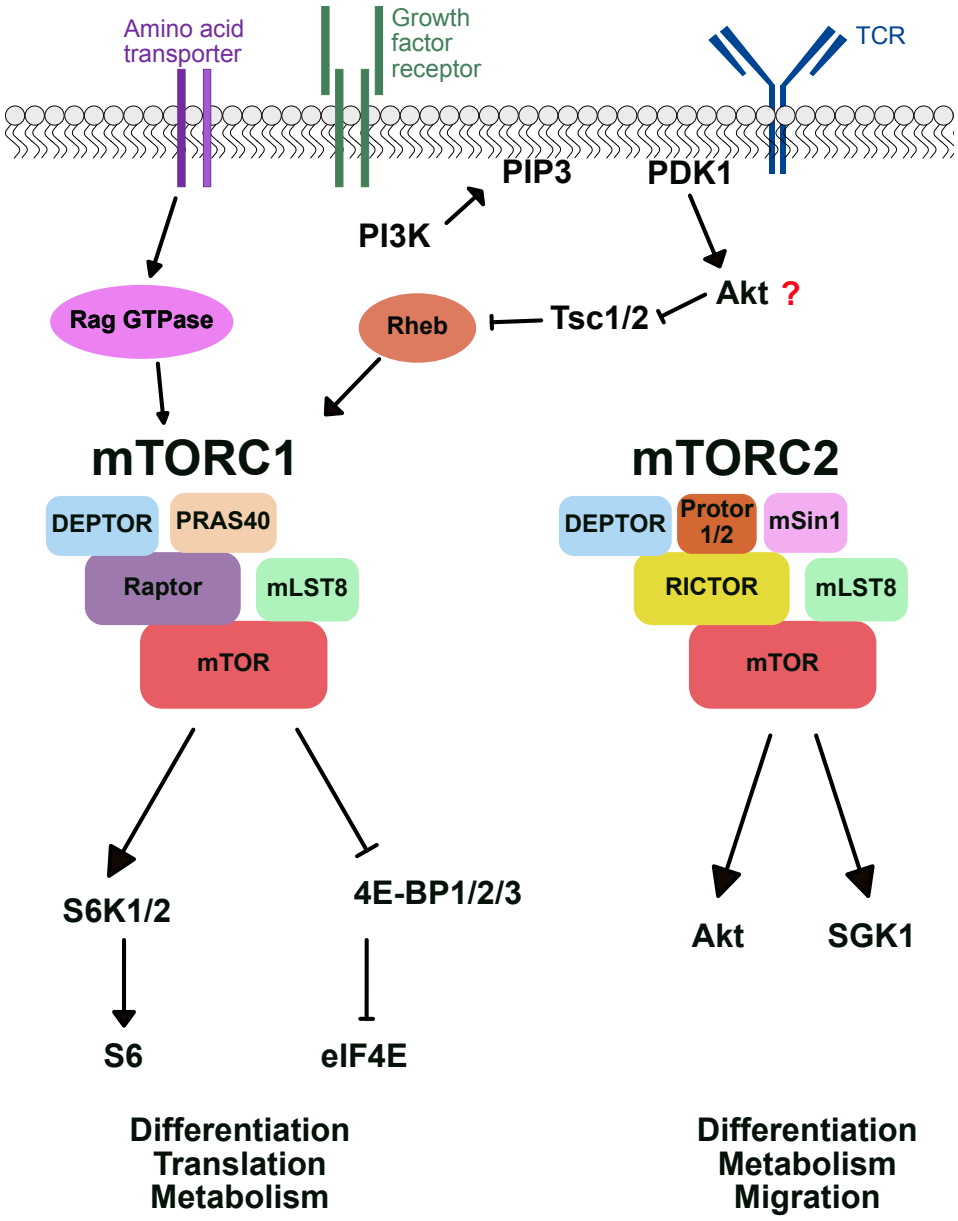

Amino acid transporter
Growth factor receptor
TCR
PIP3
PDK1
PI3K
Rag GTPase
Rheb
Tsc1/2
Akt ?
mTORC1
DEPTOR
PRAS40
Raptor
mLST8
mTOR
mTORC2
DEPTOR
Protor 1/2
mSin1
RICTOR
mLST8
mTOR
S6K1/2
4E-BP1/2/3
Akt
SGK1
S6
eIF4E
Differentiation
Translation
Metabolism
Differentiation
Metabolism
Migration

Figure 3.1: Schematic of mTOR Signaling. mTOR forms two distinct complexes with different cofactors, deemed mTORC1 (Raptor, mLST8, DEPTOR, Pras40) and mTORC2 (Rictor, mLST8, DEPTOR, Protor1/2, mSin1). Upstream activators of mTORC1 include amino acids, growth factor receptors, and the T cell receptor. Amino acids activate the Rag GTPases. PI3K activation leads to activation of the GTPase Rheb, and the combined activity of the Rags and Rheb activate mTORC1. Active mTORC1 phosphorylates its substrates S6K1/2 and 4E-BP1/2/3. This leads to cell biological effects such as helper T cell differentiation, ribosome biogenesis and mRNA translation, and metabolic reprogramming. Upstream activators of mTORC2 are still being determined, but once activated, mTORC2 phosphorylates its substrates which include Akt and SGK1. This leads to helper T cell differentiation, changes in metabolism, and cell migration.

REFERENCES

1. Shima H, Pende M, Chen Y, Fumagalli S, Thomas G, Kozma SC. Disruption of the p70(s6k)/p85(s6k) gene reveals a small mouse phenotype and a new functional S6 kinase. *EMBO J* (1998) **17**:6649–6659. doi:10.1093/emboj/17.22.6649

2. Daley SR, Coakley KM, Hu DY, Randall KL, Jenne CN, Limnander A, Myers DR, Polakos NK, Enders A, Roots C, et al. Rasgrp1 mutation increases naive T-cell CD44 expression and drives mTOR-dependent accumulation of Helios$^+$ T cells and autoantibodies. *eLife* (2013) **2**:e01020. doi:10.7554/eLife.01020

3. Zoncu R, Efeyan A, Sabatini DM. mTOR: from growth signal integration to cancer, diabetes and ageing. *Nat Rev Mol Cell Biol* (2010) **12**:21–35. doi:10.1038/nrm3025

4. Zhang S, Readinger JA, DuBois W, Janka-Junttila M, Robinson R, Pruitt M, Bliskovsky V, Wu JZ, Sakakibara K, Patel J, et al. Constitutive reductions in mTOR alter cell size, immune cell development, and antibody production. *Blood* (2011) **117**:1228–1238. doi:10.1182/blood-2010-05-287821

5. Powell JD, Pollizzi KN, Heikamp EB, Horton MR. Regulation of Immune Responses by mTOR. *Annu Rev Immunol* (2012) **30**:39–68. doi:10.1146/annurev-immunol-020711-075024

6. Laplante M, Sabatini DM. mTOR signaling in growth control and disease. *Cell* (2012) **149**:274–293. doi:10.1016/j.cell.2012.03.017

7. Delgoffe GM, Kole TP, Zheng Y, Zarek PE, Matthews KL, Xiao B, Worley PF, Kozma SC, Powell JD. The mTOR Kinase Differentially Regulates Effector and Regulatory T Cell Lineage Commitment. *Immunity* (2009) **30**:832–844. doi:10.1016/j.immuni.2009.04.014

8. Sancak Y, Peterson TR, Shaul YD, Lindquist RA, Thoreen CC, Bar-Peled L, Sabatini DM. The Rag GTPases Bind Raptor and Mediate Amino Acid Signaling to mTORC1. *Science* (2008) **320**:1496–1501. doi:10.1126/science.1157535

9. Perera RM, Zoncu R. The Lysosome as a Regulatory Hub. *Annu Rev Cell Dev Biol* (2016) **32**:223–253. doi:10.1146/annurev-cellbio-111315-125125

10. So L, Lee J, Palafox M, Mallya S, Woxland CG, Arguello M, Truitt ML, Sonenberg N, Ruggero D, Fruman DA. The 4E-BP-eIF4E axis promotes rapamycin-sensitive growth and proliferation in lymphocytes. *Science Signaling* (2016) **9**:ra57. doi:10.1126/scisignal.aad8463

11. Heikamp EB, Patel CH, Collins S, Waickman A, Oh M-H, Sun I-H, Illei P, Sharma A, Naray-Fejes-Toth A, Fejes-Toth G, et al. The AGC kinase SGK1 regulates TH1 and TH2 differentiation downstream of the mTORC2 complex. *Nat Immunol* (2014) **15**:457–464. doi:10.1038/ni.2867

12. Ebner M, Sinkovics B, Szczygieł M, Ribeiro DW, Yudushkin I. Localization of mTORC2 activity inside cells. *The Journal of Cell Biology* (2017) **8**:jcb.201610060. doi:10.1016/j.cell.2009.01.032

13. Finlay DK, Rosenzweig E, Sinclair LV, Feijoo-Carnero C, Hukelmann JL, Rolf J, Panteleyev AA, Okkenhaug K, Cantrell DA. PDK1 regulation of mTOR and hypoxia-inducible factor 1 integrate metabolism and migration of CD8+ T cells. *Journal of Experimental Medicine* (2012) **209**:2441–2453. doi:10.1084/jem.20112607

14. Jackson RJ, Hellen CUT, Pestova TV. The mechanism of eukaryotictranslation initiation and principlesof its regulation. (2010)1–15. doi:10.1038/nrm2838

15. Ma XM, Blenis J. Molecular mechanisms of mTOR-mediated translational control. *Nat Rev Mol Cell Biol* (2009) **10**:307–318. doi:10.1038/nrm2672

16. Piccirillo CA, Bjur E, Topisirovic I, Sonenberg N, Larsson O. Translational control of immune responses: from transcripts to translatomes. *Nat Immunol* (2014) **15**:503–511. doi:10.1038/ni.2891

17. MacIver NJ, Michalek RD, Rathmell JC. Metabolic Regulation of T Lymphocytes. *Annu Rev Immunol* (2013) **31**:130108114109008. doi:10.1146/annurev-immunol-032712-095956

18. Gingras AC, Raught B, Sonenberg N. Regulation of translation initiation by FRAP/mTOR. *Genes & Development* (2001) **15**:807–826. doi:10.1101/gad.887201

19. Yang K, Shrestha S, Zeng H, Karmaus PWF, Neale G, Vogel P, Guertin DA, Lamb RF, Chi H. T Cell Exit from Quiescenceand Differentiation into Th2 Cells Dependon Raptor-mTORC1-Mediated Metabolic Reprogramming. *Immunity* (2013) **39**:1043–1056. doi:10.1016/j.immuni.2013.09.015

20. Delgoffe GM, Pollizzi KN, Waickman AT, Heikamp E, Meyers DJ, Horton MR, Xiao B, Worley PF, Powell JD. The kinase mTOR regulates the differentiation of helper T cells through the selective activation of signaling by mTORC1 and mTORC2. *Nature Publishing Group* (2011) **12**:295–303. doi:10.1038/ni.2005

21. Pearce EL, Pearce EJ. Metabolic pathways in immune cell activation and quiescence. *Immunity* (2013) **38**:633–643. doi:10.1016/j.immuni.2013.04.005

22. Waickman AT, Powell JD. mTOR, metabolism, and the regulation of T-cell differentiation and function. *Immunol Rev* (2012) **249**:43–58. doi:10.1111/j.1600-065X.2012.01152.x

23. Hsieh AC, Liu Y, Edlind MP, Ingolia NT, Janes MR, Sher A, Shi EY, Stumpf CR, Christensen C, Bonham MJ, et al. The translational landscape of mTOR signalling steers cancer initiation and metastasis. *Nature* (2012)1–10. doi:10.1038/nature10912

24. Finlay D, Cantrell DA. Metabolism, migration and memory in cytotoxic T cells. *Nature Reviews Immunology* (2011) **11**:109–117. doi:10.1038/nri2888

25. O'Shea JJ, Paul WE. Mechanisms underlying lineage commitment and plasticity of helper CD4+ T cells. *Science* (2010) **327**:1098–1102. doi:10.1126/science.1178334

26. Crotty S. Follicular Helper CD4 T Cells (T FH). *Annu Rev Immunol* (2011) **29**:621–663. doi:10.1146/annurev-immunol-031210-101400

27. Murakami M, Ichisaka T, Maeda M, Oshiro N, Hara K, Edenhofer F, Kiyama H, Yonezawa K, Yamanaka S. mTOR is essential for growth and proliferation in early mouse embryos and embryonic stem cells. *Mol Cell Biol* (2004) **24**:6710–6718. doi:10.1128/MCB.24.15.6710-6718.2004

28. Zeng H, Cohen S, Guy C, Shrestha S, Neale G, Brown SA, Cloer C, Kishton RJ, Gao X, Ben Youngblood, et al. mTORC1 and mTORC2 Kinase Signaling and Glucose Metabolism Drive Follicular Helper T Cell Differentiation. *Immunity* (2016) **45**:540–554. doi:10.1016/j.immuni.2016.08.017

29. Yang J, Lin X, Pan Y, Wang J, Chen P, Huang H, Xue H-H, Gao J, Zhong X-P. Critical roles of mTOR Complex 1 and 2 for T follicular helper cell differentiation and germinal center responses. *eLife* (2016) **5**: doi:10.7554/eLife.17936

30. Bjur E, Larsson O, Yurchenko E, Zheng L, Gandin V, Topisirovic I, Li S, Wagner CR, Sonenberg N, Piccirillo CA. Distinct Translational Control in CD4+ T Cell Subsets. *PLoS Genet* (2013) **9**:e1003494. doi:10.1371/journal.pgen.1003494.s008

31. Wang R, Dillon CP, Shi LZ, Milasta S, Carter R, Finkelstein D, McCormick LL, Fitzgerald P, Chi H, Munger J, et al. The Transcription Factor Myc Controls Metabolic Reprogramming upon T Lymphocyte Activation. *Immunity* (2011) **35**:871–882. doi:10.1016/j.immuni.2011.09.021

32. Zeng W-P. “All things considered”: transcriptional regulation of T helper type 2 cell differentiation from precursor to effector activation. *Immunology* (2013) **140**:31–38. doi:10.1111/imm.12121

33. Ho I-C, Tai T-S, Pai S-Y. GATA3 and the T-cell lineage: essential functions before and after T-helper-2-cell differentiation. *Nature Publishing Group* (2009) **9**:125–135. doi:10.1038/nri2476

34. Cook KD, Miller J. TCR-Dependent Translational Control of GATA-3 Enhances Th2 Differentiation. *The Journal of Immunology* (2010) **185**:3209–3216. doi:10.4049/jimmunol.0902544

35. Scheu S, Stetson DB, Reinhardt RL, Leber JH, Mohrs M, Locksley RM. Activation of the integrated stress response during T helper cell differentiation. *Nat Immunol* (2006) **7**:644–651. doi:10.1038/ni1338

36. Gigoux M, Lovato A, Leconte J, Leung J, Sonenberg N, Suh W-K. Molecular Immunology. *Molecular Immunology* (2014) **59**:46–54. doi:10.1016/j.molimm.2014.01.008

37. Michalek RD, Gerriets VA, Jacobs SR, Macintyre AN, MacIver NJ, Mason EF, Sullivan SA, Nichols AG, Rathmell JC. Cutting Edge: Distinct Glycolytic and Lipid Oxidative Metabolic Programs Are Essential for Effector and Regulatory CD4+ T Cell Subsets. *The Journal of Immunology* (2011) **186**:3299–3303. doi:10.4049/jimmunol.1003613

38. Gerriets VA, Kishton RJ, Johnson MO, Cohen S, Siska PJ, Nichols AG, Warmoes MO, de Cubas AA, MacIver NJ, Locasale JW, et al. Foxp3 and Toll-like receptor signaling balance Treg cell anabolic metabolism for suppression. *Nat Immunol* (2016) **17**:1459–1466. doi:10.1038/ni.3577

39. Pearce EL, Poffenberger MC, Chang C-H, Jones RG. Fueling immunity: insights into metabolism and lymphocyte function. *Science* (2013) **342**:1242454. doi:10.1126/science.1242454

40. Araki K, Turner AP, Shaffer VO, Gangappa S, Keller SA, Bachmann MF, Larsen CP, Ahmed R. mTOR regulates memory CD8 T-cell differentiation. *Nature* (2009) **460**:108–112. doi:10.1038/nature08155

41. Pearce EL, Walsh MC, Cejas PJ, Harms GM, Shen H, Wang L-S, Jones RG, Choi Y. Enhancing CD8 T-cell memory by modulating fatty acid metabolism. *Nature* (2009) **460**:103–107. doi:10.1038/nature08097

42. Macintyre AN, Gerriets VA, Nichols AG, Michalek RD, Rudolph MC, Deoliveira D, Anderson SM, Abel ED, Chen BJ, Hale LP, et al. The Glucose Transporter Glut1Is Selectively Essentialfor CD4 T Cell Activation and Effector Function. *Cell Metabolism* (2014) **20**:61–72. doi:10.1016/j.cmet.2014.05.004

43. Sinclair LV, Rolf J, Emslie E, Shi Y-B, Taylor PM, Cantrell DA. Control of amino-acid transport by antigen receptors coordinates the metabolic reprogramming essential for T cell differentiation. *Nat Immunol* (2013) **14**:500–508. doi:10.1038/ni.2556

44. Edinger AL. Akt Maintains Cell Size and Survival by Increasing mTOR-dependent Nutrient Uptake. *Mol Biol Cell* (2002) **13**:2276–2288. doi:10.1091/mbc.01-12-0584

45. Shi LZ, Wang R, Huang G, Vogel P, Neale G, Green DR, Chi H. HIF1alpha-dependent glycolytic pathway orchestrates a metabolic checkpoint for the differentiation of TH17 and Treg cells. *Journal of Experimental Medicine* (2011) **208**:1367–1376. doi:10.1084/jem.20110278

46. Chang C-H, Curtis JD, Maggi LB Jr, Faubert B, Villarino AV, O'Sullivan D, Huang SC-C, van der Windt GJW, Blagih J, Qiu J, et al. Posttranscriptional Control of T Cell Effector Function by Aerobic Glycolysis. *Cell* (2013) **153**:1239–1251. doi:10.1016/j.cell.2013.05.016

47. Pollizzi KN, Sun I-H, Patel CH, Lo Y-C, Oh M-H, Waickman AT, Tam AJ, Blosser RL, Wen J, Delgoffe GM, et al. Asymmetric inheritance of mTORC1 kinase activity during division dictates CD8. *Nat Immunol* (2016)1–10. doi:10.1038/ni.3438

48. Preston GC, Sinclair LV, Kaskar A, Hukelmann JL, Navarro MN, Ferrero I, MacDonald HR, Cowling VH, Cantrell DA. Single cell tuning of Myc expression by antigen receptor signal strength and interleukin-2 in T lymphocytes. *EMBO J* (2015) **34**:2008–2024. doi:10.15252/embj.201490252

49. Verbist KC, Guy CS, Milasta S, Liedmann S, Kamiński MM, Wang R, Green DR. Metabolic maintenance of cell asymmetry following division in activated T lymphocytes. *Nature* (2016) **532**:389–393. doi:10.1038/nature17442

Chapter 4

Aims of My Ph.D. Studies

It is becoming more and more appreciated that naïve T cells receive different degrees of tonic signal input, and this heterogeneity has distinct functional outcomes for the cells. My working hypothesis has been that tonic signals in T cells represent an active, intrinsic control mechanism to keep these cells quiescent yet able to rapidly respond when they do encounter foreign antigen. In our studies, we utilized mouse models in which perturbations in tonic signaling pathways led to a loss of T cell tolerance. In Chapters 5, 6, 7, and 8 I present how basal control of transcriptional, translational, and metabolic programs in T cells are critical mechanisms by which naïve T cells stay in a primed-yet-quiescent state.

In Chapter 5, I will present a manuscript being prepared for publication in which we identified a tonic signaling pathway through the adapter LAT. This tonic LAT signal controls the phosphorylation and sub-cellular localization of HDAC7, an epigenetic regulator that represses gene expression by de-acetylating histones on DNA. This pathway is critical for T cell tolerance. Crippling LAT function via gene knockout or point-mutating the PLCγ1 binding site in LAT leads to loss of tonic signals to HDAC7 and repression of HDAC7 target genes. These genes function to curb T cell proliferation and activation.

In Chapter 6 I will present our identification of a tonic Rasgrp1-mTOR pathway. Point mutating the EF-hand of Rasgrp1 weakens autoinhibition and leads to elevated basal signaling by Rasgrp1 to the mTOR pathway and autoimmune features in mice. Given the role of mTOR in controlling translational programs, we have tested the hypothesis that regulation of basal mTOR signaling sets the translational landscape of naïve T cells and that altering this pathway leads to loss of controlled T cell function. These results will be presented in Chapter 7.

In Chapter 8, I will present our preliminary evidence that tonic and inducible Rasgrp1-mTOR signals are critical for T cell metabolic reprogramming and will discuss our hypotheses

for how Rasgrp1 may regulate this. mTOR also is an important regulator of basal T cell metabolism (which primarily relies on oxidative phosphorylation in the mitochondria), as well as the switch to aerobic glycolysis following TCR stimulation. Thus, we were interested in using the Rasgrp1^{Anaef} mice to uncover a role for Rasgrp1-mTOR signals in T cell metabolism.

Chapter 5

Tonic LAT-HDAC7 signals sustain *Nur77* and *Irf4* expression to tune naïve $CD4^+$ T cells

ABSTRACT

$CD4^+$ T cells differentiate into T helper cell subsets in feed-forward manners with synergistic signals from the T cell receptor (TCR), cytokines, and lineage-specific transcription factors. Naïve $CD4^+$ T cells avoid spontaneous engagement of feed-forward mechanisms but retain a prepared state. T cells lacking the adapter molecule LAT demonstrate impaired TCR-induced signals yet cause a spontaneous lymphoproliferative T helper 2 (T_H2) cell syndrome in mice. Thus, LAT constitutes an unexplained maintenance cue. Here we demonstrate that tonic signals through LAT constitutively export the repressor HDAC7 from the nucleus of $CD4^+$ T cells. Without such tonic signals, HDAC7 target genes *Nur77* and *Irf4* are repressed. We reveal that *Nur77* suppresses $CD4^+$ T cell proliferation and uncover a novel suppressive role for *Irf4 in* T_H2 polarization; halving *Irf4* gene-dosage leads to increases in $GATA3^+$ and $IL4^+$ cells. Our studies reveal that naïve $CD4^+$ T cells are dynamically tuned by tonic LAT-HDAC7 signals.

INTRODUCTION

$CD4^+$ T cells can polarize into T helper cell (T_H) subsets, such as T_H1 and T_H2 (T helper 2) subsets that produce either interferon-γ (IFN-γ) or IL-4, -5, and-13 cytokines (Mosmann et al., 2005). T cell receptor (TCR) signals, cytokine receptor signals, and transcription factors cooperate to establish these lineages via a feed-forward loop (Zhu et al., 2010); TCR signals in the presence of IFN-γ result in the activation of STAT4 and induction of the transcription factor T-bet (*Tbx21*) that induces more IFN-γ expression (reviewed in (Ansel et al., 2006; Murphy and Reiner, 2002)). Analogously, in a IL-4/STAT6/GATA3/IL-4 induction-, reinforcement-, and maintenance- model for T_H2, an initial TCR signal leads to upregulation of *IL-4* (termed "early IL-4") so that subsequent TCR signals with a low-level IL-4/STAT6 signal lead to very robust induction of IL-4, -5, and -13 (Ansel et al., 2006; Paul, 2010). An initial model emerged with T-bet, GATA-3, Foxp3, Rorγt, and Bcl6 transcription factors directing T cells to T_H1, T_H2, T_{REG} (regulatory T cells), T_H17, and T_{FH} (follicular helper T cells) lineages (**Figure 5.1A**), though it is clear that additional modes of regulation must exist (Locksley, 2009; O'Shea and Paul; Zhou et al., 2009; Zhu and Paul, 2010).

It is not completely understood how $CD4^+$ T cells remain in a "resting", naïve state that is permissive to the above-mentioned feed-forward mechanisms of T_H cell differentiation. Epigenetic control mechanisms of cytokine loci can impact the effect of lineage transcription factors (Hirahara et al., 2011; Kanno et al., 2012), and additional transcription factors with broader expression patterns operate in transcriptional networks with the lineage-specific transcription factors (Li et al., 2014). One of these, Interferon regulatory factor 4 (Irf4), is expressed in different T_H subsets (Biswas et al., 2010; Huber and Lohoff, 2014). Irf4 plays a critical role in T_H2 differentiation; Irf4 cooperates with NFATc2 to promote IL-4 production, is

critical for GATA3 upregulation, and GATA3 overexpression partially rescues IL-4 production by Irf4-deficient T_H2 cells (Biswas et al., 2010; Huber and Lohoff, 2014).

Tonic or constitutive signals in B lymphocytes rely on surface IgM and are critical for survival (Lam et al., 1997). In T cells, tonic signaling also occurs (Monroe, 2006), but its physiological role is largely unknown (Hogquist et al., 2003). Survival of naïve $CD4^+$ T cells is only modestly impacted following inducible deletion of *TCRα* (T cell receptor α chain) (Polic et al., 2001). Instead, tonic signals in T cells have been reported as immuno-modulatory, either enhancing (Stefanova et al., 2002) or blunting (Bhandoola et al., 2002; Smith et al., 2001) subsequent TCR responses to foreign antigen. Biochemically, tonic signals such as TCRζ phosphorylation can be detected in T cells rapidly isolated from peripheral lymphoid organs but not when isolated from peripheral blood, and these tonic signals quickly dissipate when cells are culture *in vitro* in non-stimulatory conditions (Stefanova et al., 2002; van Oers et al., 1994; van Oers et al., 1993). We previously established that the adapter molecule LAT (Linker for Activation of T cells) is critical for sending tonic Ras-ERK kinase signals, which can repress (Roose et al., 2003) or maintain (Markegard et al., 2011) expression of genes.

Crippling LAT's phospho-tyrosine docking site for PLCγ in the mouse germline via mutation of tyrosine 136 into phenylalanine (termed LAT^{Y136F} here) results in a spontaneous T_H2 hyperproliferative syndrome (Aguado et al., 2002; Sommers et al., 2002). Sophisticated mouse models with inducible LAT deletion (termed LAT^{NEG} here) or inducible switching from wildtype LAT to LAT^{Y136F} demonstrated that the spontaneous T_H2 hyperproliferative syndrome also develops when these LAT perturbations occur exclusively in peripheral T cells (Mingueneau et al., 2009; Shen et al., 2009) (**Figure 5.1B**). T cells with perturbed LAT function demonstrate impaired TCR-induced PLCγ activation and decreased PLCγ-dependent calcium- and ERK-

signaling (Mingueneau et al., 2009; Shen et al., 2009), yet paradoxically take on a $CD44^{HIGH}CD62L^{LOW}$ activated/memory T cell phenotype and produce high levels of intracellular IL-4 (Chuck et al., 2010; Mingueneau et al., 2009; Shen et al., 2009). Whereas it is known that MHC class II and CD28 expression are required for the development of the T_H2 immune pathology (Mingueneau et al., 2009), no further mechanistic insights relating loss of LAT in naïve peripheral T cells to immune abnormalities have been established.

These new genetic mouse models ruled out altered T cell developmental or selection processes as the predominant causes for the T_H2 hyperproliferative syndrome, which implies that there is an unappreciated role for LAT in providing some cue to curb $CD4^+$ T cells in their naïve state (Brownlie and Zamoyska, 2009). Here we describe how tonic signals through LAT facilitate constitutive export of the transcriptional repressor histone deacetylase 7 (HDAC7) from the nucleus, and thereby promote expression of immune-modulatory genes like *Nur77* and *Irf4*. We reveal novel repressive roles for *Nur77* and *Irf4* and demonstrate that these act to tune the naïve state of CD4 T cells.

RESULTS

Progressively altered gene expression in naïve CD4 T cells with LAT perturbations.

$CD4^+$ T cells take on an activated/memory $CD44^{HIGH}CD62L^{LOW}$ phenotype when LAT is deleted or mutated via Tamoxifen-induced Cre recombination (Chuck et al., 2010). In search of a direct molecular mechanism that underlies the hyperproliferative T_H2 syndrome when T cells lack the adapter LAT or express LAT^{Y136F} (**Figure 5.1B**), we profiled gene expression in sorted naïve $CD4^+$ T cells that are $CD44^{LOW}$. Triplicate samples of purified naïve $CD4^+$ T cells from mice

treated for either 1- or 4- weeks with tamoxifen resulting in LAT-negative (LAT^{NEG}), or point-mutated LAT (LAT^{Y136F}) status revealed altered expression for 188 genes when compared to wild type naïve $CD4^+$ T cells. Naïve, $CD4^+$ T cells that express LAT^{Y136F} for 4 weeks demonstrated the most striking changes in gene expression (**Figure 5.1B and Supplemental Figure S1**). These changes could reflect selection of particular T cell clones that occurs over the 4-week period in the LAT^{Y136F} model with a diverse TCR repertoire. LAT protein turnover takes 4 days (Ou-Yang et al., 2012), therefore one week of tamoxifen treatment effectively results in 3 days of LAT^{NEG} or LAT^{Y136F}. In search of the immediate and direct effects of LAT perturbation in naïve CD4 T cells, we focused on this short period of LAT perturbation.

HDAC target genes are repressed 3 days after LAT deletion or Y136F mutation.

Examination of expression levels of transcription factors that regulate helper T cell differentiation (**Figure 5.2A**) revealed no conspicuous changes when $CD44^{LOW}CD4^+$ T cells are LAT^{NEG} or LAT^{Y136F} for three days. By contrast, expression of a cluster of genes including *Egr1*, *Egr2*, and *Egr3*, *Irf4*, as well as *Nr4a1* (encoding Nur77*), Nr4a2, and Nr4a3* was greatly attenuated in both LAT^{NEG} and LAT^{Y136F} T cells (**Figure 5.2B and Supplemental Figure S2**). These genes are immediate early response genes downstream of mitogenic signals in many cell types. Several of these, *Nr4a1* in particular, have also been described as target genes of HDAC7 in both thymocytes (Dequiedt et al., 2003) and in DO11.10 T cell hybridoma cells (Kasler and Verdin, 2007).

HDACs deacetylate histone tails, which correlates with gene repression. HDACs are subdivided into four classes (I, IIa, IIb, and IV) (Haberland et al., 2009) and class I and IIa can be inhibited by Trichostatin A (Verdin et al., 2003). We previously reported that gene repression in a Jurkat T cell lymphoma line without LAT could be reversed by Trichostatin A (Markegard et

al., 2011) and postulated that there may be a functional connection between LAT, HDACs and the unexplained T_H2 hyperproliferative syndrome. HDAC7 belongs to class IIa, and class IIa members (HDACs 4, 5, 7, and 9) display unique and tissue-specific expression patterns (Haberland et al., 2009; Verdin et al., 2003). Through Taqman analyses we established that HDAC7 is the predominant class IIa HDAC expressed in $CD4^+$ T cells (**Figure 5.2C**) and therefore centered our attention on HDAC7.

We confirmed the reduced expression of *Nr4a1* (Nur77) in sorted naïve, $CD4^+$ T cells by quantitative PCR (**Figure 5.2D**). We utilized our previously published gene expression sets from thymocytes that either lack HDAC7 or express HDAC7ΔP, a constitutively nuclear, super-repressor version of HDAC7 with mutated serine phosphorylation sites (Kasler et al., 2012; Kasler et al., 2011) to generate a list of potential thymic HDAC7 targets. We applied an arbitrary threshold of 2.0-fold differential expression between loss of HDAC7 and the HDAC7ΔP super-repressor, which resulted in 369 differentially expressed genes (**Supplemental table 1**). The Venn diagram in **Figure 5.2E** demonstrates that the cluster of immediate early response genes expressed at lower levels in LAT^{NEG} or LAT^{Y136F} naïve $CD4^+$ T cells overlap with HDAC7 targets in this analysis. In sum, the expression levels of a set immediate early response genes are maintained by LAT and repressed by HDAC7; we will focus on the functional roles of *Nur77* and *Irf4* in $CD4^+$ T cells later.

<u>HDAC7 effects, expression, and phosphorylation</u>

Early support for a role for HDAC's in T_H cell function came from studies where T cells were treated with HDAC inhibitors, which enhanced the expression of both IFN-γ and T_H2-type cytokines (Bird et al., 1998; Valapour et al., 2002). To test if HDAC7 may, in principle, impact T_H

cell function, we isolated T cells from mice with HDAC7 deletion or expression of HDAC7ΔP, the super-repressor version of HDAC7 (Kasler and Verdin, 2007; Kasler et al., 2011). Direct *ex vivo* stimulation followed by intracellular FACS staining for cytokines revealed that HDAC7 deficiency led to increased percentages of $CD4^+$ T cells producing IFN-γ (**Figure 5.3A and Supplemental Figure S3A**). Fewer HDAC7ΔP-expressing T cells expressed IFN-γ compared to WT (**Figure 5.3B and Figure S3B**). HDAC7ΔP did not cause spontaneous increases in IL-4-producing cells under short-term stimulatory conditions (**Figure 5.3B**). Transduced purified wildtype T cells with a retroviral construct for HDAC7ΔP-GFP also revealed suppression of IFN-γ production (**Supplemental Figure S3C**).

We next explored the possibility that HDAC7 levels could impact Th2 differentiation. Microarray expression data revealed no statistically significant differences in *HDAC7* mRNA levels between WT, LAT^{NEG}, and LAT^{Y136F} $CD44^{LOW}CD4^+$ T cells (**Figure 5.3C**). Relative HDAC7 protein levels fell when thymocytes developed into naïve T cells and rose when these were stimulated (T_H0) or stimulated and polarized into different effector populations (**Figure 5.3D**). Comparisons of HDAC7 levels between *in vitro* generated T_H2 versus T_H1, T_H2, T_H17, and T_{REG} or T_H0, populations did not show striking differences (**Figure 5.3D**). These results argue that altered expression levels of HDAC7 are not the source of the LAT^{NEG} and LAT^{Y136F} T cell abnormalities.

Both HDAC-5 and -7 are regulated via phosphorylation of N-terminally located serine residues; phosphorylation leads to nuclear export and cytoplasmic retention of HDAC-5 and -7 and counteracts their repressive effects on gene expression (Dequiedt et al., 2003; Parra et al., 2005; Vega et al., 2004; Verdin et al., 2003; Zhang et al., 2002). B cell receptor (BCR) induced phosphorylation of HDAC-5 and -7 had previously been reported in avian- and murine- B cell

lines and primary B cells (Matthews et al., 2006). We observed that TCR stimulation could induce phosphorylation of HDAC-5 or -7 transfected into a Jurkat T cell leukemia cell line (**Figure 5.3E and 5.3F**). However, we noted a substantial amount of tonic HDAC phosphorylation in the unstimulated Jurkat samples, which had also been observed in a B cell line system (Matthews et al., 2006). Examination of primary lymph node cells revealed that TCR-induced HDAC7 phosphorylation was very modest and contrasted with the robust induction of ERK phosphorylation. Instead, tonic HDAC-7 phosphorylation was very pronounced in these primary cells (**Figure 5.3G**). Given our previous studies on LAT's role in tonic signals in non-stimulated cells and gene regulation (Markegard et al., 2011; Roose et al., 2003), we next investigated if the adapter LAT regulates HDAC7 phosphorylation, localization, and function in a tonic fashion.

LAT-dependent, tonic nucleo-cytoplasmic shuttling of HDAC7

HDAC7 has nuclear (N) localization in $CD4^+CD8^+$ double positive thymocytes but becomes predominantly cytoplasmic (C) in more developed $CD4^+$ or $CD8^+$ single positive thymocytes (Kasler et al., 2011). Unstimulated, naïve $CD4^+$ T cells maintain the predominant cytoplasmic distribution of HDAC7 seen in their predecessor CD4-single positive thymoctes (**Figure 5.4A)**, which agrees with the evident tonic phosphorylation of HDAC7 in primary lymph node cells (**Figure 5.3G**). These data show that tonic signals in $CD4^+$ T cells constitutively keep HDAC7 phosphorylated and exported from the nucleus. Uniform cytoplasmic localization of HDAC7 in T_H0, T_H1, T_H2, T_H17, and T_{REG} cells demonstrated that nucleo-cytoplasmic trafficking occurs efficiently in all T_H subsets (**Figure 5.4A**).

Primary cells rapidly lose tonic signals *in vitro* (Stefanova et al., 2002; van Oers et al., 1993) making biochemical studies on tonic signaling and pathway mapping challenging and we

therefore used a model cell line to investigate biochemical details of the tonic signals. To examine LAT, we used a LAT-deficient Jurkat T cell line, J.CaM2. We determined that tonic phosphorylation of HDAC-5 and -7 is decreased when cells lack LAT and is partially restored when J.CaM2 are stably reconstituted with a wildtype LAT cDNA construct (**Figures 5.4B and 5.4C**). Our results with the LAT^{Y136F} mouse model point to a role for PLCγ1 in the tonic signaling pathway, since PLCγ1 normally docks at phosphorylated Y136. We previously utilized overexpression of DGKζ to reduce tonic PLCγ1-diacylglycerol (DAG) signals as DGKζ coverts DAG to phosphatidic acid (Markegard et al., 2011). Overexpression of FLAG-tagged DGKζ expression reduced tonic phosphorylation of HDAC-5 in unstimulated Jurkat T cells (**Figure 5.4D**), indicating that a LAT-PLCγ1-DAG pathway is an important component of the tonic signaling pathway. Concomitant with decreased tonic HDAC phosphorylation in LAT-deficient J.CaM2 cells, its nucleo/cytoplasmic ratio increased 4.8 fold when cells do not express the adapter LAT (**Figure 5.4E**).

Tonic regulation of HDAC7 impacts Nur77 expression and proliferation of $CD4^+$ T cells

To substantiate our findings in figure 4, we now exploited the fact that tonic signals rapidly dissipate when primary cells are rested *ex vivo* in non-stimulatory medium (Stefanova et al., 2002; van Oers et al., 1993). Resting lymph node cells for 30 or 60 minutes in PBS at 37 °C resulted in a 70-80% decrease of tonic HDAC7 phosphorylation as well as in previously reported decreases of tyrosine-phosphorylated proteins detected by 4G10 immunoblotting (**Figure 5.5A**). Analysis of HDAC7 with CD4-costaining on cytospins of cells fixed immediately after isolation revealed a predominantly cytoplasmic HDAC7 distribution in $CD4^+$ T cells (**Figure 5.5B**) with the highest pixel intensity for HDAC7 at the cell perimeter (**Figure 5.5C**). Resting cells for 30 minutes in PBS before fixation resulted in a translocation to predominantly nuclear

HDAC7 localization (**Figures 5.5D and 5.5E**), as expected based on our phosphorylation data (**Figure 5.5A**).

CD5 expression is a sensitive reporter of TCR affinity (Azzam et al., 1998) and can be used as a marker of tonic TCR signaling (Mandl et al., 2013). Naïve $CD4^+$ T cells display a range of CD5 expression in which $CD5^{HIGH}$ cells received most tonic signal input (Mandl et al., 2013). We used CD44 and CD5 markers to sort $CD44^{LOW}$ naïve $CD4^+$ T cells into the most bright and most dim for CD5 while keeping cells ice cold and established that $CD5^{HIGH}$ naïve $CD4^+$ T cells have substantially more tonic HDAC7 phosphorylation than $CD5^{LOW}$ naïve $CD4^+$ T cells (**Figure 5.5F**). Furthermore, $CD5^{HIGH}$ naïve $CD4^+$ T cells expressed significantly higher mRNA levels of the HDAC target *Nur77* compared to their $CD5^{LOW}$ counterparts (**Figure 5.5G**). Single deficiency for *Nur77* leaves T cell development largely intact (Lee et al., 1995). More recently it has been reported that loss of Nur77 results in increased proliferation of stimulated $CD8^+$ T cells (Nowyhed et al., 2015), implying that Nur77 has suppressive functions. In support of this notion, we found that stimulation of sorted naïve $CD4^+$ T cells resulted in more proliferation measured by CTV-dilution when these cells lack Nur77 (**Figure 5.5H**), indicating that Nur77 is not only simply under tonic signal control but provides a negative feedback loop to suppress T cell proliferation. In sum, by utilizing three systems – induced LAT perturbation, PBS rest, and CD5-based sorted populations – we demonstrate that naïve $CD4^+$ T cells constitutively export HDAC7 from the nucleus in a dynamic manner that relies on tonic LAT-PLCγ1-DAG signals. Loss of this tonic control signal results in reduced expression of immediate early response genes; one of these, *Nur77*, functions to suppress T cell proliferation (**Figure 5.5I**).

Tonic regulation of Irf4 expression limits T_H2 polarization of $CD4^+$ T cells

Our gene expression analyses also indicated that tonic LAT-HDAC7 signals maintain *Irf4*

expression in naïve T cells (**Figure 5.2**). Irf4 is a member of the Irf (interferon regulatory factor) family of transcription factors (Lohoff and Mak, 2005; Tamura et al., 2008) and plays a critical role in the function and homeostasis of mature but not developing T cells (Mittrucker et al., 1997). Irf4's function in T cells is complex. First, specific ablation of *Irf4* in Foxp3-positive regulatory T cells yielded the surprising phenotype of a spontaneous T_H2 immune disorder (Zheng et al., 2009); thus, Irf4 fulfills a T_{REG}-intrinsic role to prevent effector T cells from polarizing towards T_H2 (**Figure 5.6A**). Multiple studies identified Irf4 as a critical factor promoting differentiation of T_H2 cells and production of T_H2 cytokines under T_H2 polarizing conditions *in vitro* and demonstrated that Irf4 is required for T_H2 responses *in vivo* (reviewed in (Biswas et al., 2010; Huber and Lohoff, 2014)). However, it has also been observed that Irf4 inhibits IL-4 production in naïve $CD4^+$ T cells from BALB/c mice (Honma et al., 2008). Thus, Irf4 may have both T_H2-stimulatory and T_H2-suppressing functions in $CD4^+$ T cells depending on their state (**Figure 5.6B**).

TCR stimulation results in strong upregulation of Irf4 expression (Biswas et al., 2010; Huber and Lohoff, 2014). In $CD8^+$ T cells, Irf4 expression levels increase in a graded manner directly proportional to the strength of incoming TCR receptor signal (Nayar et al., 2012; Nayar et al., 2014; Yao et al., 2013). Taqman analysis revealed that *Irf4* levels are reduced by roughly 60% in both LAT^{NEG} and LAT^{Y136F} $CD44^{LOW}CD4^+$ T cells (**Figure 5.6C**). Using the CD5-sorting strategy, we confirmed that baseline Irf4 expression levels are impacted by tonic signaling; $CD5^{LOW}$ naïve $CD4^+$ T cells with the lowest level of tonic signaling reproducibly expressed roughly half of the *Irf4* mRNA and Irf4 protein compared to $CD5^{HIGH}$ naïve counterparts (**Figure 5.6D and 5.6E**).

To specifically address how decreases in Irf4 expression levels impact $CD4^+$ T cells, we generated an *Irf4* allelic series of two wildtype copies, one wildtype copy, or zero wildtype

copies of *Irf4* by crossing floxed Irf4 mice to CD4-Cre mice (**Figure 5.6F).** *Irf4* Taqman revealed a 40% reduction in *Irf4* expression in heterozygous $Irf4^{+/fl}$ CD4 T cells (**Figure 5.6G).** CD3/CD28 stimulation of sorted $Irf4^{+/+}$ naïve CD4+ T cells ($CD44^{LOW}$ with exclusion of $CD25^{+}$ cells) induced upregulation of Irf4 expression, in agreement with published work (Biswas et al., 2010; Huber and Lohoff, 2014), but Irf4 levels lagged behind in $Irf4^{+/fl}$ cells (HET), measured after 10 hours (**Figure 5.6H**). Functionally, an increased percentage of $Irf4^{+/fl}$ T cells expressed GATA3 compared to wildtype cells stimulated for 10 hours in T_H2-polarizing culture conditions (**Figure 5.6I)**. Thus, Irf4 plays a suppressive role during the T_H2 initiation phase, when cells are still more naïve. This suppressive effect of Irf4 was still detectable in 5-day polarization assays: while full *Irf4* deletion resulted in the complete absence of IL-4 induction, we observed an increase in percentage of IL-4 producing cells when the gene dose of *Irf4* is halved ($Irf4^{+/fl}$), compared to cells with WT levels of Irf4 (**Figure 5.6J)**. Using CD4-Cre, these results unequivocally demonstrate that some (expression level of) Irf4 is critical for any polarization towards T_H2 cells but also revealed that normal expression levels of Irf4 that are sustained by tonic signals function to curb T_H2 polarization.

DISCUSSION

Mouse models with T cell-specific LAT perturbation develop a T_H2 hyperproliferative syndrome through unknown mechanisms (Chuck et al., 2010; Mingueneau et al., 2009; Shen et al., 2009). Utilizing three distinct experimental systems, we demonstrate the existence of dynamic maintenance cues in the form of tonic signals in naïve $CD4^{+}$ T cells that rely on the presence of an intact LAT adapter molecule. We reveal that these tonic signals are critical for constitutive phosphorylation and nuclear export of the repressor HDAC7 in naïve $CD44^{LOW}CD4^{+}$ T cells; without tonic HDAC7 regulation, expression of target genes become repressed. We particularly

focused on the LAT-HDAC7 target genes *Nur77* and *Irf4* and revealed that these are immunosuppressive, which offers novel mechanistic insights how tonic signals tune the naïve state of $CD4^+$ T cells.

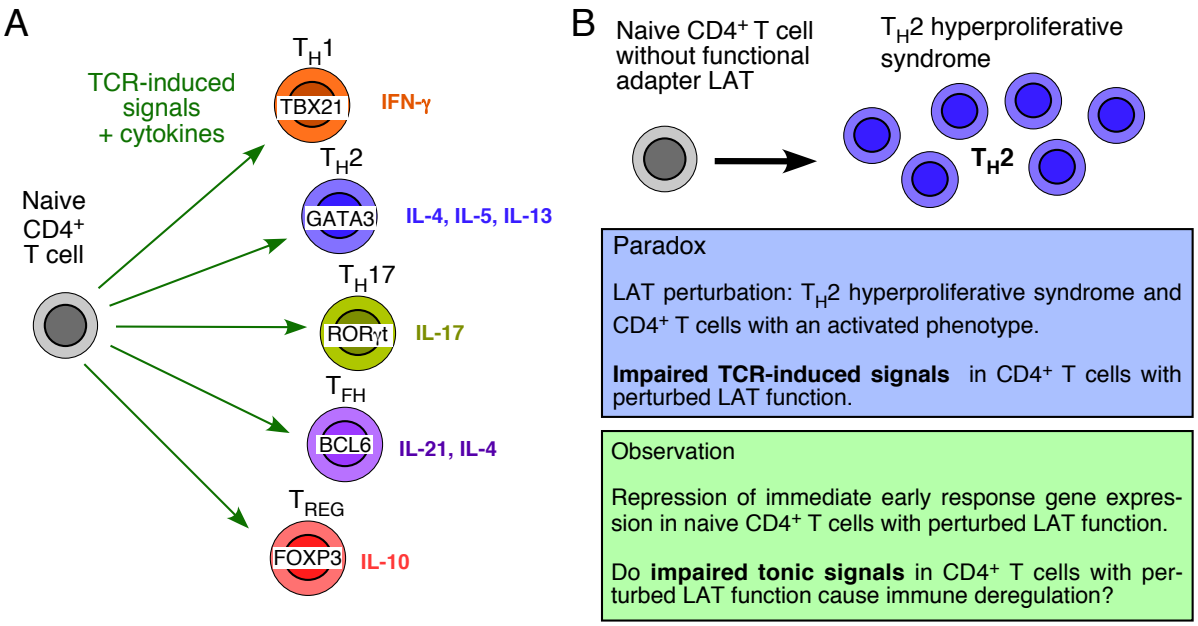
We show that Nur77 fulfills a negative feedback function to suppress proliferation of $CD4^+$ T cells. In addition, one of Nur77's reported targets is *FasL* (Fas ligand) (Rajpal et al., 2003), which regulates T cell homeostasis via induction of apoptosis of activated T cells. *FasL* is also a target of Egr transcription factors (Rengarajan et al., 2000) and we found *Egr-1*, *Egr-2*, and *Egr-3* expressed at reduced levels in T cells with perturbed LAT function (**Figure 5.2B**). LAT^{Y136F} T cells fail to upregulate FasL in response to TCR engagement (Ou-Yang et al., 2012; Sommers et al., 2002). The transcription factor Irf4 has received a lot of interest as a T cell fate-determining factor (Biswas et al., 2010; Huber and Lohoff, 2014)). We were inspired by the reported linear correlation between strength of TCR signal and Irf4 expression levels (Nayar et al., 2012; Nayar et al., 2014; Yao et al., 2013), and our studies revealed that Irf4 expression in naïve $CD4^+$ T cells is under tonic control. Sustained and optimal Irf4 expression functions to curb T_H2 differentiation, as a larger portion of $Irf4^{+/fl}$ T cells, which have a 40% reduction in *Irf4* mRNA, express GATA3 and IL-4. Recent work uncovered that Irf4 interacts with Fos/Jun heterodimers of the activator protein-1 (AP1) complex to regulate genes that contain AICE elements (AP-1/IRF composite elements) (Glasmacher et al., 2012; Li et al., 2012; Murphy et al., 2013). It is possible that reduced Irf4 levels result in altered composition of transcription factor complexes and/or altered regulation of AICE elements, which is an area for future investigation. Together, our studies with emphasis on Nur77 and Irf4 offer an explanation how perturbation of a tonic signal via LAT can cause a T_H2 hyperproliferative syndrome.

Our studies here focused on tonic LAT-HDAC signals in naïve $CD4^+$ T cells but it is possible that such signals are important for regulatory T cells as well. We previously

demonstrated that perturbations in LAT lead to impaired T_{REG} function (Chuck et al., 2010; Shen et al., 2010) and recent studies support the idea of functional constitutive signals in T_{REG}; deletion of the TCR in T_{REG} resulted in impaired homeostasis of T_{REG} (Levine et al., 2014; Vahl et al., 2014). Notably, TCR deletion in T_{REG} did not impact expression of FoxP3 or other T_{REG} signature genes, but instead, expression of *Egr1*, *Egr2*, *Nr4a1 (Nur77)*, *Irf4*, and *Ctla4* was reduced in the TCR-ablated T_{REG} (Levine et al., 2014; Vahl et al., 2014). Since we find that these same genes are under tonic LAT-HDAC7 tonic control in naïve $CD4^+$ T cells, this suggests that tonic LAT-HDAC7 signals may also regulate this gene set in T_{REG}. Furthermore, Nur77 and the two other Nr4a family members are critical for the generation of T_{REG} (Sekiya et al., 2013) and suppression of T_H2 by T_{REG} (Sekiya et al., 2015) and *Irf4* was shown to have a T_{REG}-intrinsic role to suppress T_H2 differentiation as well (Zheng et al., 2009).

Together, our studies presented here combined with the above-cited work put forth a model in which loss of tonic LAT-HDAC7 signals alters the tuning of naïve $CD4^+$ T cells (as well as the homeostasis of T_{REG}) and that tonic regulation of Nur77 and Irf4 levels are important mediators and feedback regulators for maintaining the naïve, undifferentiated state. We propose that dynamic maintenance cues in T cells should be considered in the context of immune-diseases and cancer immunotherapy where these tonic signals may either be influenced by checkpoint blockade therapy or be altered through single nucleotide polymorphisms (SNPs). In support of the latter idea, it is of interest to note that three *Nur77* SNPs have been associated with severity of bronchial hyperresponsiveness in asthma patients (Kurakula et al., 2015) and that a SNP in the 3'UTR region of *Irf4* has been associated with recurrent bronchitis in children (Pinto et al., 2013).

FIGURES

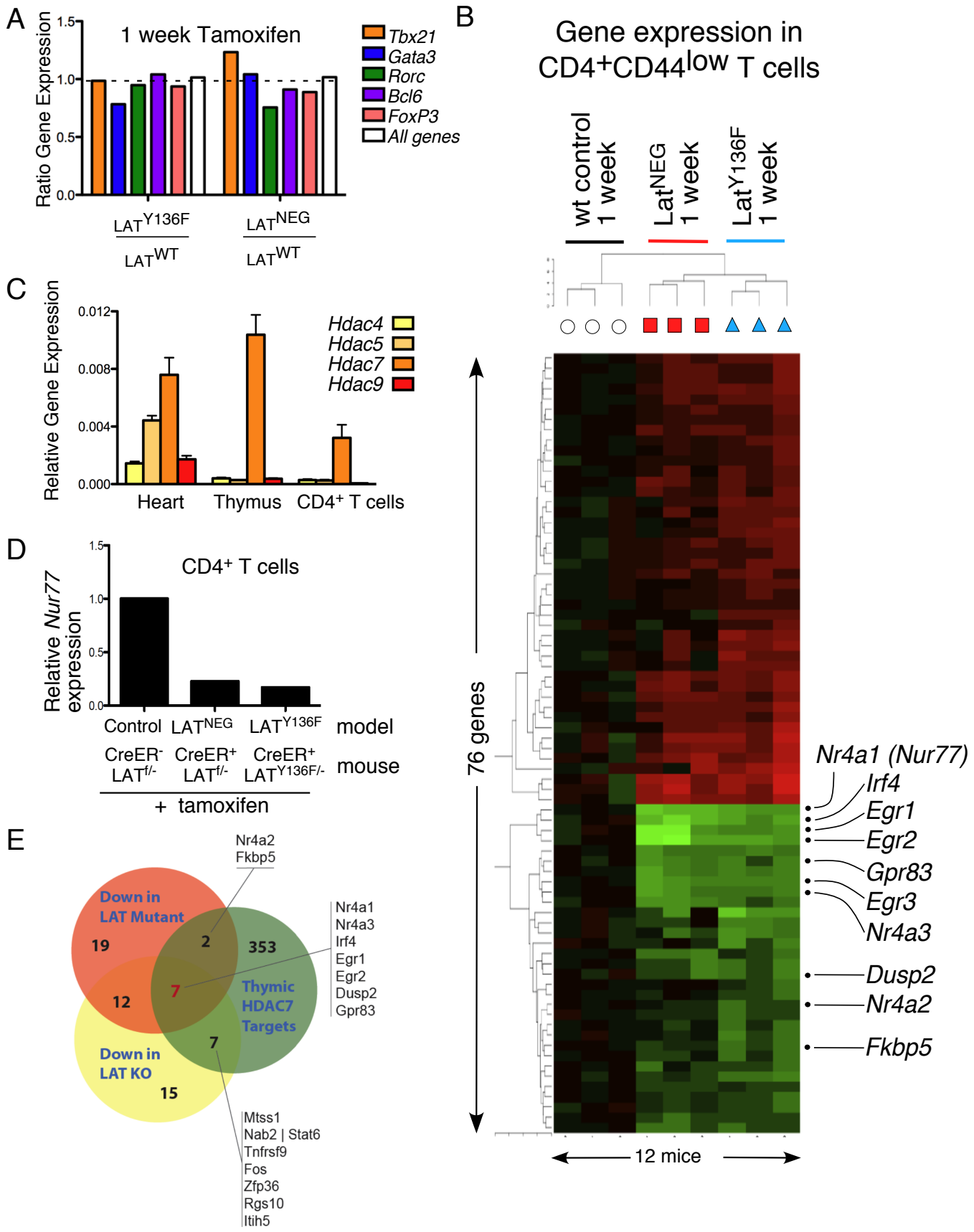


Myers, Figure 1

Figure 5.1: A paradoxical TH2 hyperproliferative syndrome

(A) Schematic of Th1-, Th2-, Th17-, Tfh-, and Treg- effector subset differentiation.

(B) Schematic of the Th2-biased hyperproliferative syndrome that occurs following perturbations of LAT function and explanation of the apparent paradox.



Myers, Figure 2

Figure 5.2: A panel of immediate early response genes is maintained by LAT and repressed by HDAC7

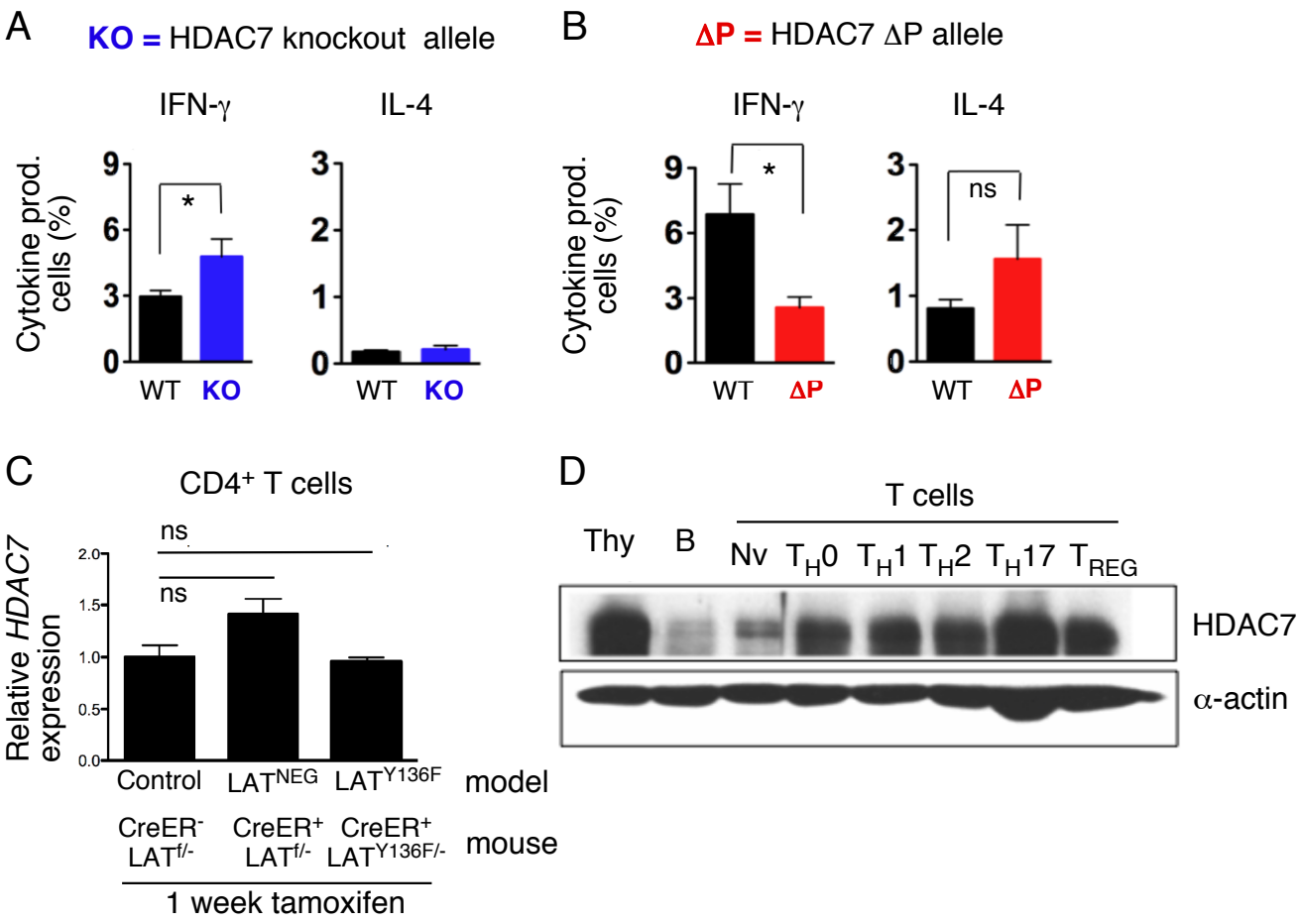
(A) Averaged gene expression levels of helper T_H cell transcription factors from microarray in Supplemental figure 1. Gene expression levels in LAT^{Y136F} and LAT^{NEG} were normalized to cells with intact, functional LAT (LAT^{WT}).

(B) Microarray analysis of gene expression changes in naïve $CD4^+$ T cells with short term LAT perturbation. A specific cluster of HDAC7 target genes including *Egr1, Egr2, Egr3, Irf4, Nurr77 or Nr4a1, Nr4a2, and Nr4a3* is highlighted. For more detail on the unsupervised clustering and all gene names, see Supplemental figures S1 and S2. Array data can be found in GEO (mouse array accession number GPL7207; human array accession number GPL18142).

(C) Taqman qPCR analysis of levels of class IIa HDAC transcripts in murine tissues, relative to *GAPDH* levels. Mean and error bars (SEM) are indicated of triplicate samples. A representative example of three independent experiments is shown.

(D) TaqMan qPCR analysis of *Nurr77* levels in purified $CD4^+$ T cells isolated from tamoxifen-treated WT, LAT^{NEG} and LAT^{Y136F} mice. Representative example of two independent assays on these three samples.

(E) Venn diagrams identifying genes with shared regulation by LAT and HDAC7. For a complete overview of the analyses see Supplemental table 1.



Myers, Figure 3

Figure 5.3: HDAC7 represses IFN-γ and is constitutively phosphorylated in $CD4^+$ T cells

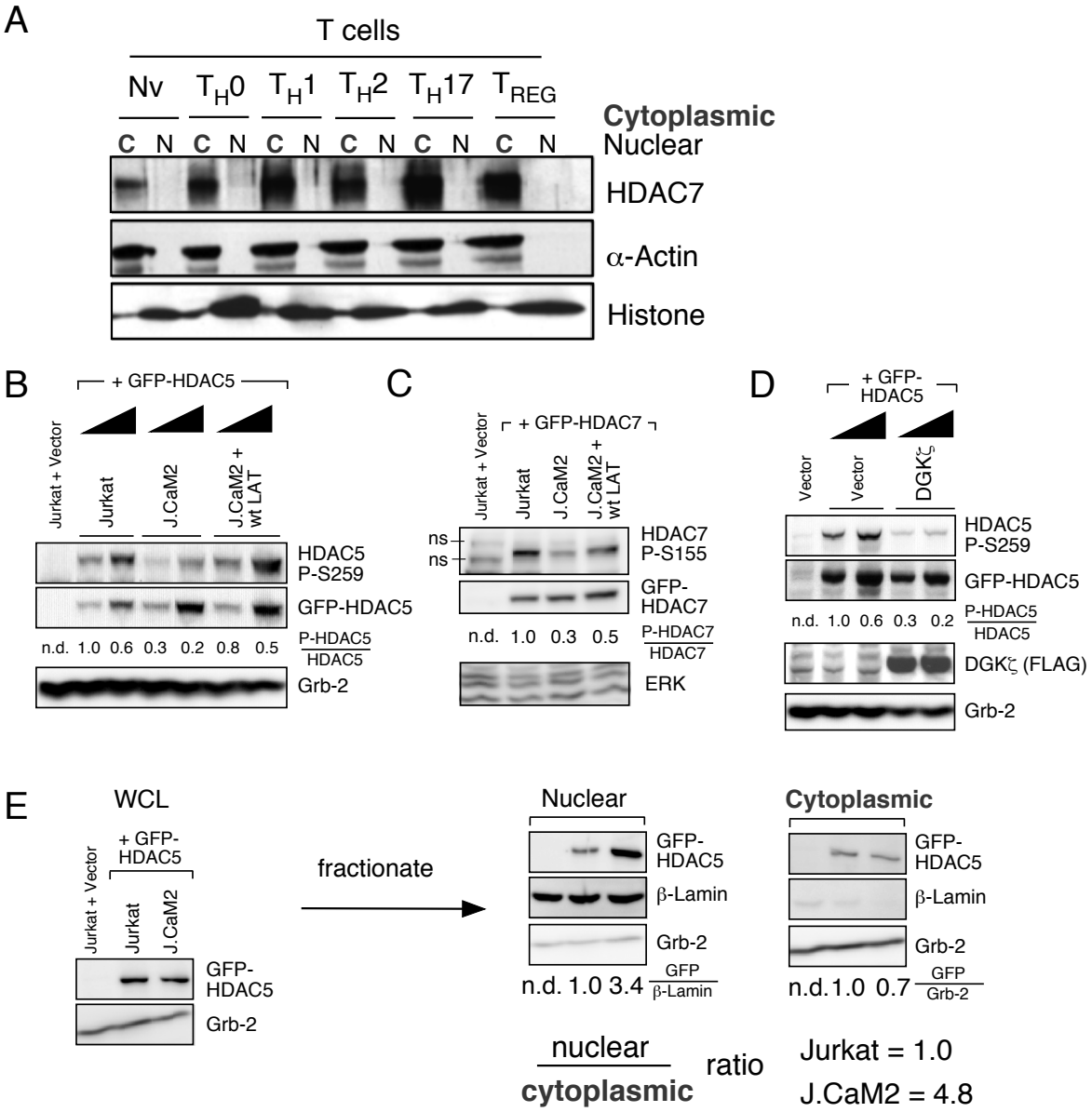
(A and B) Bargraph representation of percentages of cytokine-producing cells isolated from wildtype mice compared to HDAC7-deficient (KO in A) and HDAC7 ΔP-transgenic mice (ΔP in B) that were acutely stimulated with PMA and ionomycin for 4 hours *ex vivo* in the presence of Brefeldin A. Data are representative of 3-6 (A) or 5 (B) independent experiments with 1-2 mice/group, and error bars represent the SEM.

(C) Gene expression levels of HDAC7 in LAT^{WT}, LAT^{Y136F} and LAT^{NEG} mice. Gene expression levels (mean + SEM) were obtained from the 3 data points from the microarray with 1-week tamoxifen treatment. Ns = not significant.

(D) Immunoblot for HDAC7 levels in thymocytes (Thy), B cells (B), Naive T cells (Nv), and *in vitro* stimulated or polarized helper T cell subsets (T_H0, T_H1, T_H2, T_H17, T_{REG}). α-actin functions as loading control.

(E, F) Immunoblotting for phosphorylated HDAC-5 or -7 in Jurkat T cells transfected with vector alone, HDAC5-GFP (E) or HDAC7-GFP (F) and stimulated via the TCR for indicated time points. GFP indicates the level of transfected HDAC-GFP and Grb2- or ERK- blotting serves as loading control. The amount of phosphorylated HDAC was quantitated by normalizing for GFP levels, setting the unstimulated sample arbitrarily at 1.0.

(G) Immunoblotting of phosphorylated HDAC7 and phosphorylated ERK in primary $CD4^+$ T cells isolated from mouse lymph nodes and stimulated via the TCR for indicated time points. Quantitation of phospho-HDAC7 or –ERK was determined by normalizing for total HDAC7 or ERK. Blots in panels D-G are representative examples of at least three independent experiments for each panel.



Myers, Figure 4

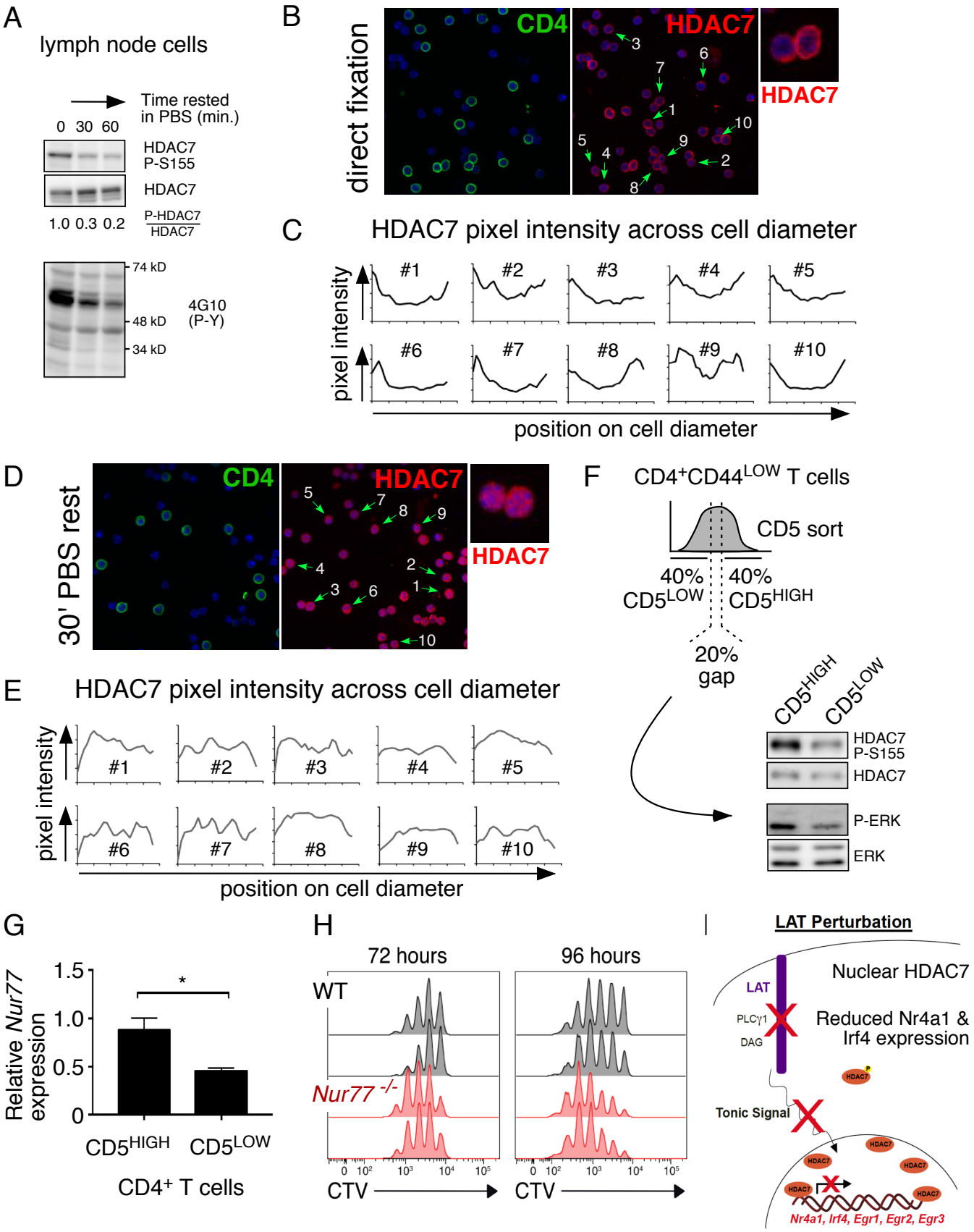
Figure 5.4: A tonic LAT-PLCγ1-DAG signal regulates constitutive phosphorylation and nuclear export of HDAC-5 and -7

(A) Immunoblotting for HDAC7 in cytoplasmic (C) and nuclear (N) fractions obtained from naive T cells (Nv), and *in vitro* polarized helper T cell subsets (T_H0, T_H1, T_H2, T_H17, T_{REG}).

(B, C) Analysis of basal phospho-HDAC5 (in B) or HDAC7 (in C) levels in unstimulated Jurkat, J.Cam2 (LAT-deficient Jurkat T cells), and J.Cam2 + a WT LAT cDNA construct. Cells were transfected and analyzed as in Figure 3.

(D) Immunoblotting for basal phospho-HDAC5 in cells transfected with FLAG-tagged DGKz to counteract basal PLCγ1-DAG signals.

(E) Analysis of basal HDAC5 localization in Jurkat and J.Cam2 cells transfected with HDAC5-GFP. Whole cell lysates (top) and nuclear (left) and cytoplasmic (right) fractions were assessed for HDAC5 by GFP blotting. β-lamin and Grb2 function as markers for the purity of the nuclear and cytoplasmic fractions, respectively. The fractions of GFP over β-lamin or Grb2 function were used to determine a nuclear/cytoplasmic ratio for HDAC5. This ratio was 1.0 for Jurkat and increased to 4.8 (3.4 over 0.7) for LAT-deficient J.CaM2 cells. Blots in panels 5.4A-E are representative examples of at least three independent experiments for each panel.



Myers, Figure 5

Figure 5.5: Tonic signals in $CD4^+$ T cells dynamically regulate HDAC7 and its target Nur77 to limit proliferation

(A) Immunoblotting for phosphorylated HDAC7 (top) and total phosphotyrosine (4G10, bottom) in lymph node cells isolated from mice that were lysed directly or first rested in PBS for the indicated time points.

(B, C) Immunofluorescence of HDAC7 localization in $CD4^+$ T cells in a cytospin preparation co-stained for HDAC7 (red) and CD4 (green). Quantification of pixel signal intensity across the diameter of the 10 $CD4^+$ T cells in B was obtained with Fiji image analysis software.

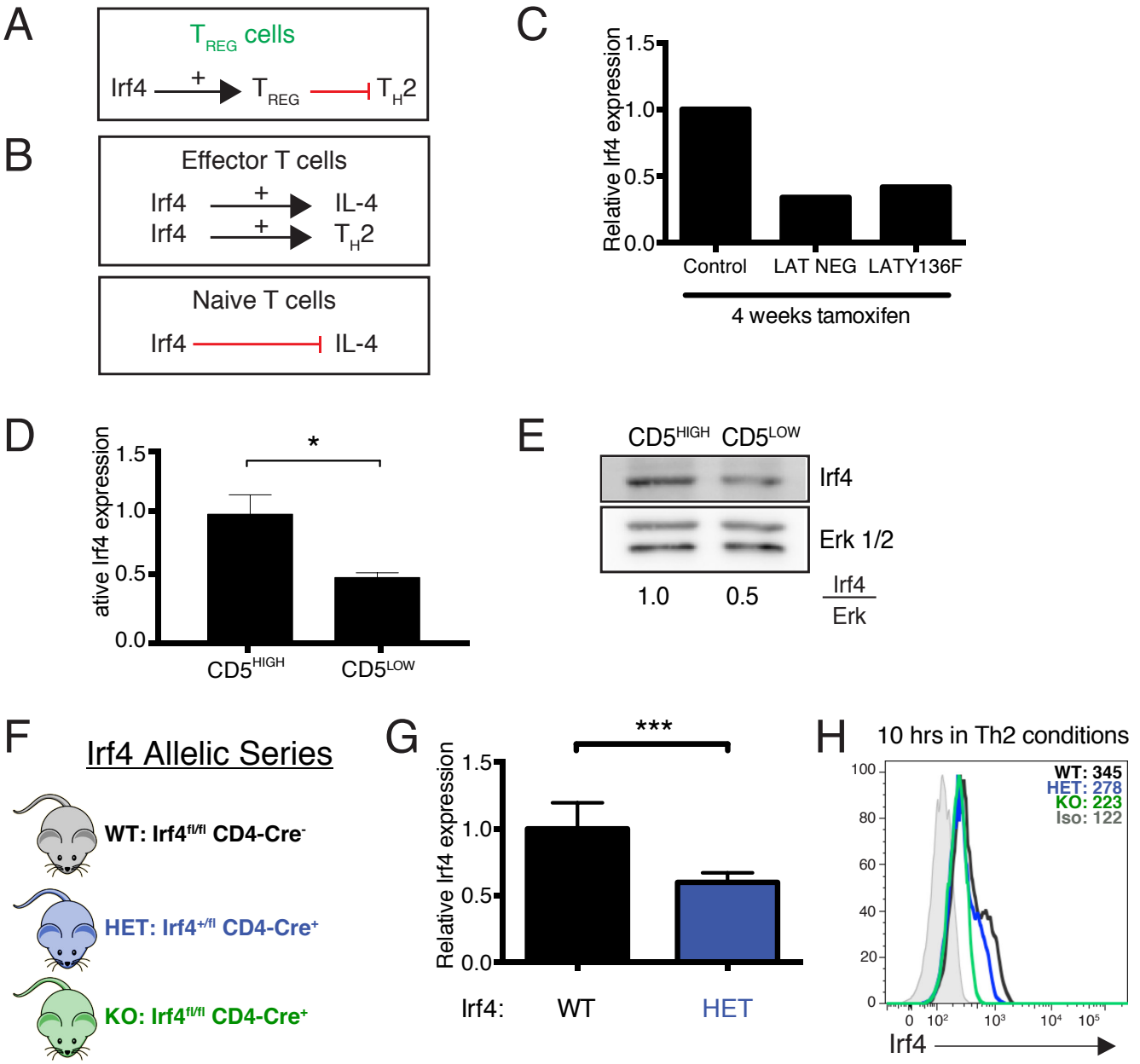
(D, E) Analysis of HDAC7 localization exactly as in B and C, except that lymph node cells were rested in PBS for 30 minutes prior to fixation and cytospin analysis. Note the switch to predominant nuclear HDAC7 localization following PBS rest.

(F) Schematic of CD5 sorting scheme of naïve $CD44^{low}$ $CD4^+$ T cells from lymph node and immunoblot analysis of phospho-HDAC7 and -ERK levels in sorted populations. An arbitrary 20% gap was chosen to segregate $CD5^{HIGH}$ from $CD5^{LOW}$ cells yet obtain sufficient cells for biochemistry. Total HDAC7 and ERK serve as loading controls.

(G) TaqMan qPCR analysis of *Nurr77* mRNA levels in CD5 sorted cells. Taqman samples were run in triplicate. *Nurr77* mRNA levels were arbitrarily set at 1.0 in one $CD5^{LOW}$ sample. Unpaired T test: $p = 0.018$ (indicated by *). All panels in A-G are representative examples of three independent experiments.

(H) Flow cytometric analysis of Cell Trace Violet (CTV) dilution in sorted (TCRb+ CD4+ CD25- CD44 low) naïve $CD4^+$ T cells from two WT and two $Nur77^{-/-}$ mice. Cells were cultured for 72 and 96 hours on CD3/CD28 coated plates (0.5ug/ml each) at which point viable $CD4^+$ cells were analyzed for CTV dilution by flow cytometry. Data is representative of two independent experiments.

(I) Cartoon summarizing how tonic signals through LAT influence phosphorylation and nucleo-cytoplasmic shuttling of HDAC7 and expression of HDAC7 target genes.



Myers, Figure 6

Figure 5.6: Irf4 expression is under tonic signal regulation and curbs T_H2 polarization of $CD4^+$ T cells

(A) Schematic of the role of Irf4 in regulatory T cells (T_{REG}) and T_{REG}-suppressive effects on T_H2 differentiation.

(B) Schematic of the role of Irf4 in effector (top) and naïve (bottom) $CD4^+$ T cells in controlling T_H2 differentiation and IL-4 production.

(C) TaqMan qPCR analysis of *Irf4* levels in T cells isolated from 4-week tamoxifen-treated WT, LAT^{KO} and LAT^{Y136F} mice**.** Representative example of three independent assays on these three samples.

(D) TaqMan qPCR analysis (n = 3) and (E) immunoblot analysis (n=2) of Irf4 levels in CD5 sorted cells. Taqman samples were run in triplicate. *Irf4* mRNA levels were arbitrarily set at 1.0 in one $CD5^{LOW}$ sample. Unpaired T test: p = 0.034 (indicated by *).

(F) Cartoon of *Irf4* allelic series.

(G) TaqMan qPCR analysis of *Irf4* levels in T cells isolated from $Irf4^{wt/wt}$ and $Irf4^{+/fl}$ CD4-Cre mice. Representative example of two independent experiments performed in triplicate. Unpaired T test: p = 0.0005 (indicated by ***).

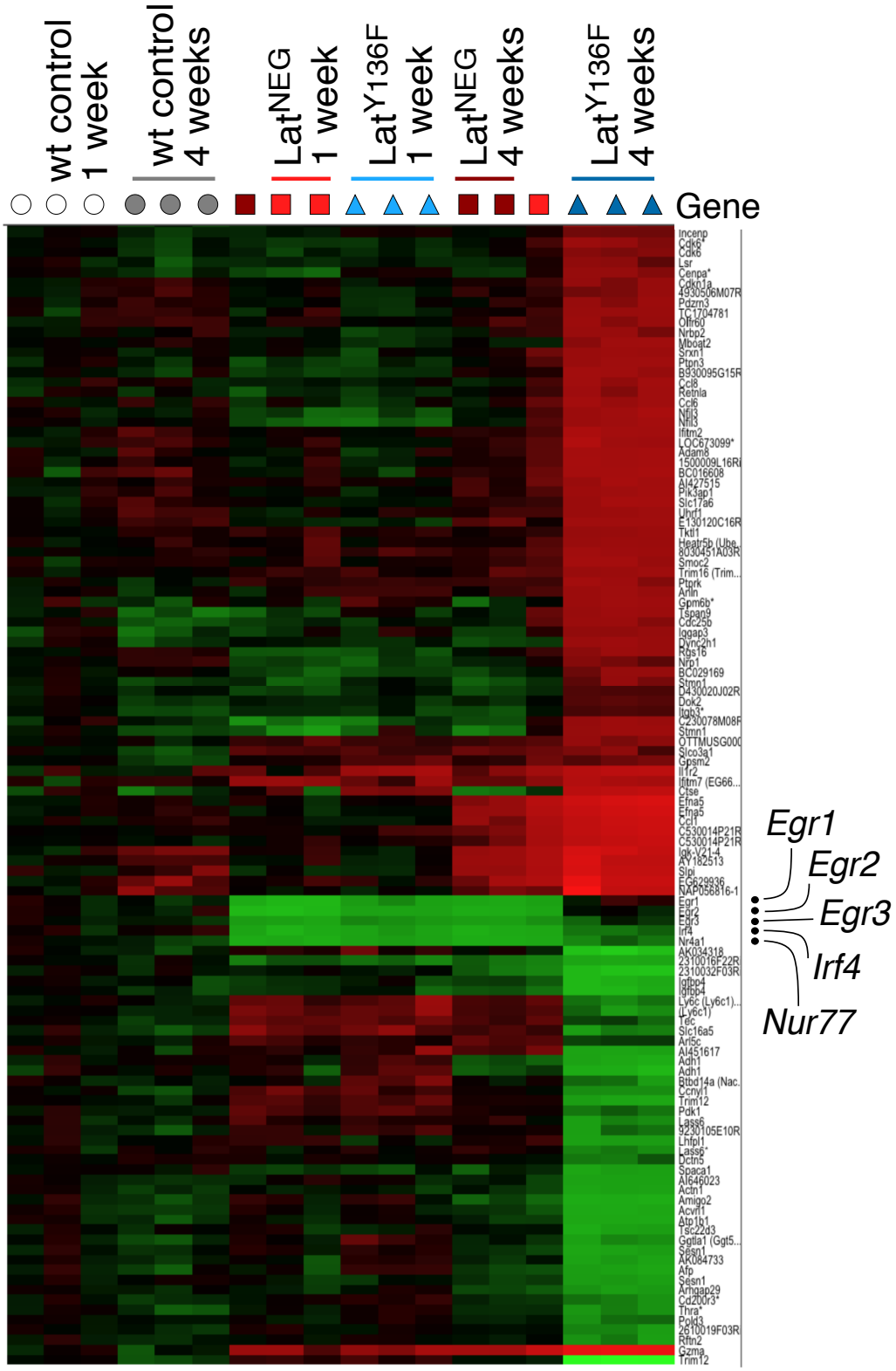
(H) Flow cytometry for Irf4 expression in sorted $CD4^+$ $CD25^-$ $CD44^{LOW}$ T cells from Irf4 WT and HET mice cultured for 10 hours in T_H2-polarizing conditions on α-CD3/CD28 coated plates (0.5ug/ml each). Data is representative of two independent experiments with 2 mice/group.

(I) Flow cytometry for Gata3 in MACS-purified $CD4^+$ $CD25^-$ $CD44^{LOW}$ T cells from Irf4 WT and HET mice cultured for 10 hours in T_H2-polarizing conditions. Data is representative of three independent experiments with 3-4 mice per group. Error bars represent SEM and significance was determined using an unpaired t-test, p=0.0056 (indicated by **).

(J) Flow cytometric analysis of IL-4 production in viable T_H2 polarized naïve $CD4^+$ $CD25^-$ $CD44^{LOW}$ T cells sorted from $Irf4^{wt/wt}$ CD4-Cre mice (WT), $Irf4^{+/fl}$ CD4-Cre mice (HET), or $Irf4^{fl/fl}$ CD4-Cre mice (KO) mice stimulated with 0.5ug/ml α-CD3 and α-CD28. Percentage of cytokine-

positive cells were calculated and data was normalized and compiled from three independent experiments with 2 mice per group per experiment. Error bars represent SEM and significance was determined using an unpaired t-test, with Th2 WT vs HET $p=0.0446$ (indicated by *) and WT vs KO $p<0.0001$.

S1 Gene expression in naive CD4+CD44low T cells



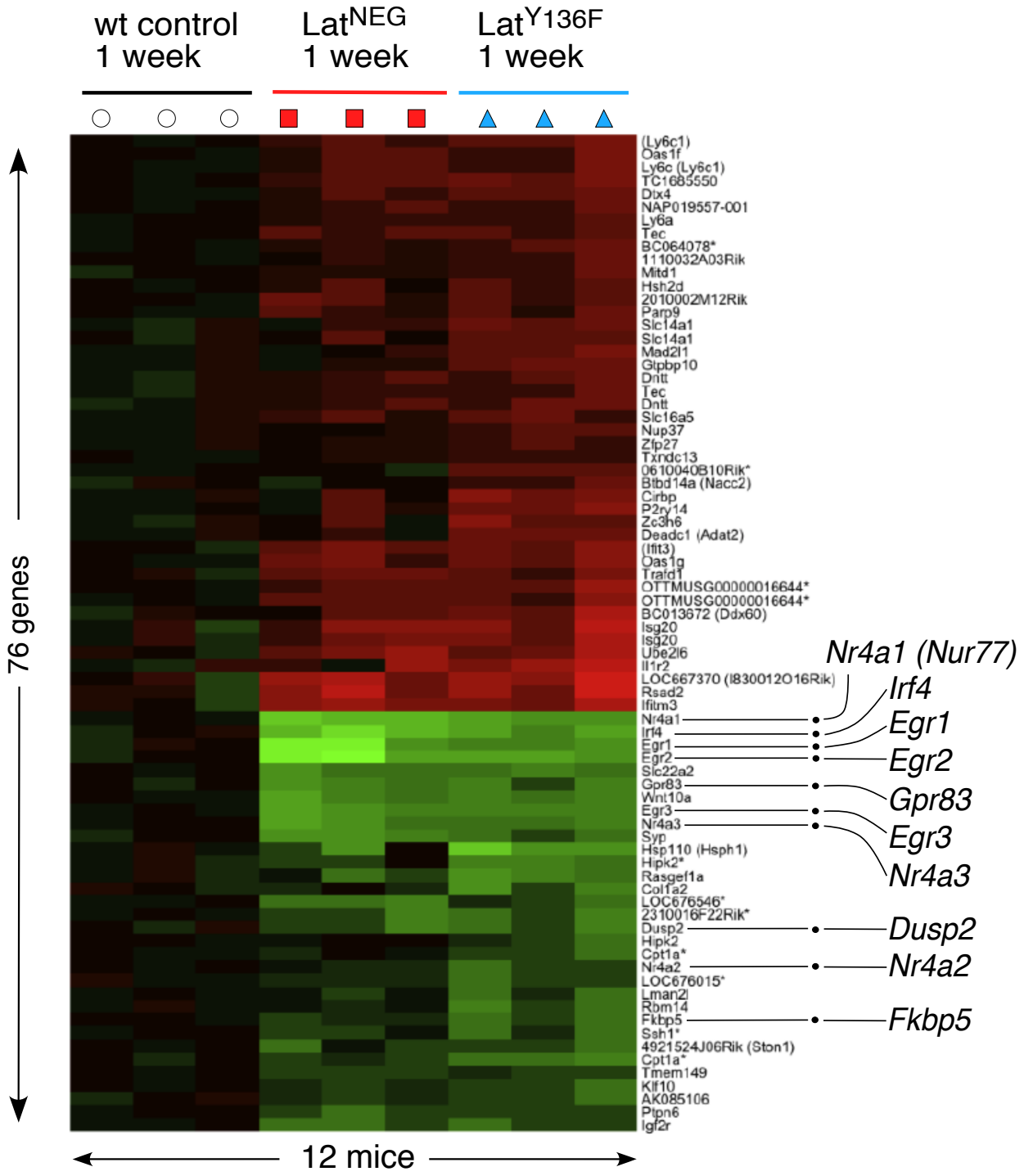
Myers, Supplemental Figure S1

Supplemental Figure S1 – Gene expression alterations in $CD44^{LOW}CD4^{+}$ T cells with LAT perturbations induced by either 1-week or 4-weeks of tamoxifen treatment

Unsupervised clustering of 188 gene expression changes and representation of dendrograms. Microarray analysis of gene expression changes in cells with short (1 week) or long (4 week) term LAT perturbation. Log2 fold changes are depicted in colorcoding and altered gene expression for 188 probe sets compared to averaged WT_1 (Wildtype, week one) are depicted. Array data can be found in GEO (mouse array accession number GPL7207; human array accession number GPL18142).

S2

Gene expression in
CD4+CD44low T cells



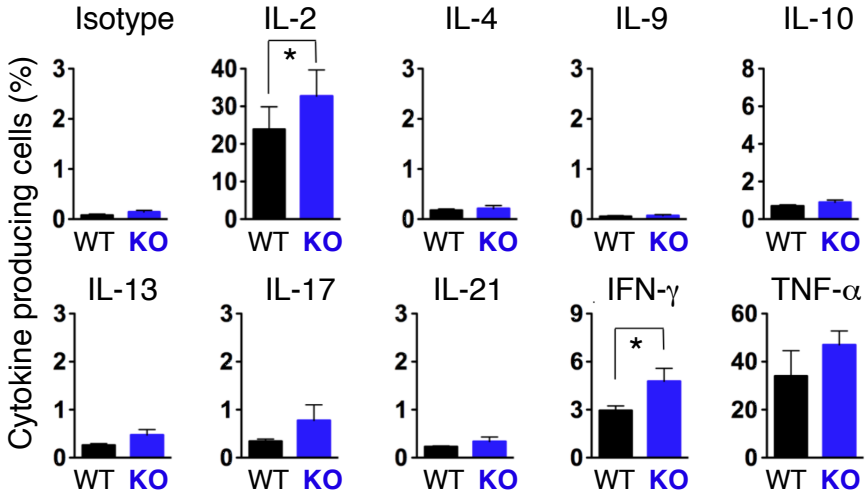
Myers,
Supplemental Figure S2

Supplemental Figure S2 – Gene expression alterations in $CD44^{LOW}CD4^{+}$ T cells with one week LAT perturbations

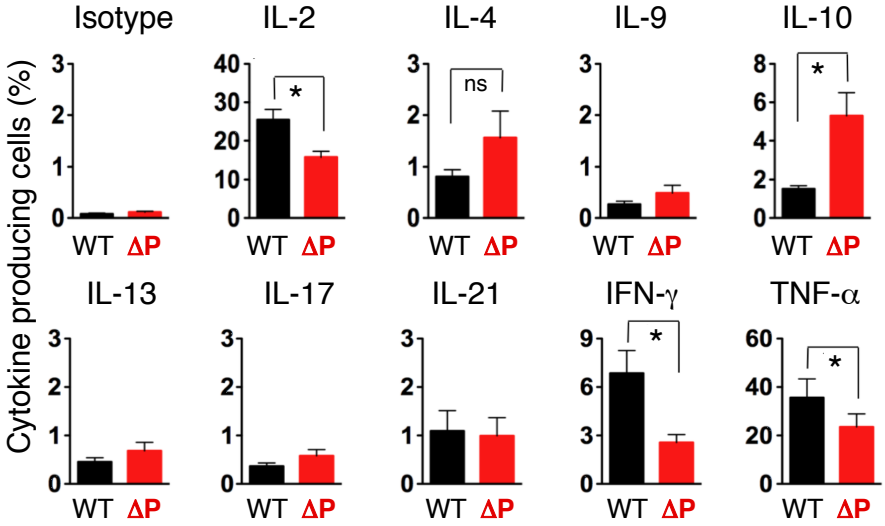
Unsupervised clustering of 76 gene expression changes. Microarray analysis of gene expression changes in cells with short (1 week) term LAT perturbation. Log2 fold changes are depicted in colorcoding and altered gene expression for 76 probe sets compared to averaged WT_1 (Wildtype, week one) are depicted. A specific cluster of HDAC7 target genes including *Egr1, Egr2, Egr3, Irf4, Nurr77 or Nr4a1, Nr4a2, and Nr4a3* is highlighted.

Array data can be found in GEO (mouse array accession number GPL7207; human array accession number GPL18142).

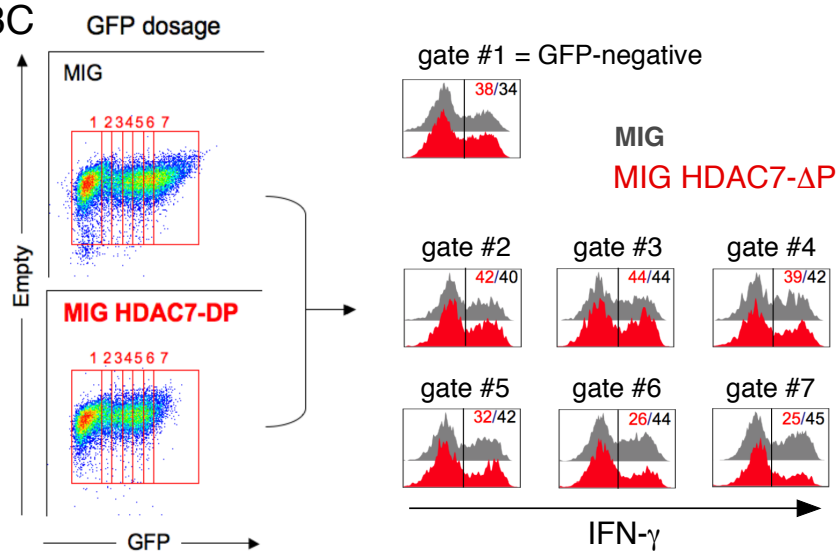
S3A **KO =** HDAC7 knockout allele



S3B **ΔP =** HDAC7 ΔP allele



S3C



Myers,
Supplemental Figure 3

Supplemental Figure S3 – Gene expression alterations in $CD44^{LOW}CD4^{+}$ T cells with one week LAT perturbations

(A and B) Bargraph representation of percentages of cytokine-producing cells isolated from wildtype mice compared to HDAC7-deficient (KO in A) and HDAC7 ΔP-transgenic mice (ΔP in B) that were acutely stimulated with PMA and ionomycin for 4 hours *ex vivo* in the presence of Brefeldin A. Data are representative of 3-6 (A) or 5 (B) independent experiments with 1-2 mice/group, and error bars represent the SEM.

(C) To address the caveat of altered thymocyte development in the transgenic HDAC7ΔP mice and to confirm the data with the genetic HDAC7 mouse models in an independent manner, we transduced purified wildtype T cells with a retroviral construct for HDAC7ΔP-GFP or control GFP vector (MIG) and measured IFN-γ following stimulation. Utilizing the GFP levels as a surrogate for increasing doses of HDAC7ΔP, we revealed that T cells with the highest level of HDAC7ΔP repressed IFNγ production the strongest.

METHODS

Mice

WT C57BL/6 mice were bred in house at UCSF. $LAT^{f/-}$ and LAT^{Y136F} mice crossed to ER-Cre (Chuck et al., 2010; Markegard et al., 2011) and HDAC7 KO mice and HDAC7-ΔP mice (Kasler et al., 2012; Kasler et al., 2011) have been described previously. *Nur77*$^{-/-}$ mice were obtained from The Jackson Laboratory. $Irf4^{fl/fl}$ (Jackson Labs) and CD4-Cre (Taconic Farms) mice were purchased and crossed. Mice were housed and treated in accordance with the guidelines of the Institutional Animal Care and Use Committee (IACUC) guidelines of the University of California, San Francisco (AN098375-03B for JPR and AN1110172-01 for EV) and Duke University (A160-14-06 for WZ).

Microarrays and gene expression data analysis

Microarray analysis of $CD4^+$ T cells was carried out using Agilent gene arrays using protocols optimized in our group and the UCSF Functional Genomics Core Facility. For details see the Supplemental Information.

Cell Lines, transfections, cell isolation, stimulations, and fractionations

Jurkat T cells and derived J.CaM2 cells were grown, transfected, and stimulated as described before (Das et al., 2009; Markegard et al., 2011). In short, cells were transfected with 10 μg of HDAC7-GFP, HDAC5-GFP, or GFP, rested overnight and stimulated with C305 antibody to trigger TCR signaling. For biochemical analysis, lymph node $CD4^+$ T cells were purified through MACS depletion (Miltenyi) using negative isolation. Cells were first incubated with biotinylated antibodies to non-CD4 T cells, followed by incubation with magnetically conjugated anti-biotin and anti-CD44 microbeads. Naïve $CD4^+$ T cells pass through the magnetic MACS Column while

other cell types are retained. MACS isolation yielded cells with >95% purity as assessed by FACS. $CD4^+$ T cells were stimulated *in vitro* with α-CD3 (2C11, UCSF mAb core) and α-CD4 (clone GK1.5, UCSF Monoclonal Antibody Core) as before (Das et al., 2009) and lysed with SDS lysis buffer. Nuclear and cytoplasmic fractions were prepared from indicated T cell subsets using NE-PER Nuclear and Cytoplasmic Extraction Kit (ThermoFisher Scientific, Cat#: 78838). For Primary T cell Isolation, Culture, and Analysis of Cytokines and Transcription Factors by Flow Cytometry, see the Supplemental Information.

Quantitative Real-Time PCR

RNA was extracted from harvested cells using Trizol, the RNeasy kit (QIAGEN) and treated with DNase I. Random primers (Invitrogen) and M-MLV Reverse Transcriptase (Invitrogen) were used to generate cDNA. For mRNA gene expression assays, TaqMan primers/probe were purchased from Life Technologies: *HDAC7*: Mm00469527_m1, *Nr4a1 (Nur77)*: Mm01300401_m1, *Irf4*: Mm00516431_m1, and *Actb*: Mm01205647_g1. TaqMan Real-Time PCR was performed using SensiMix II Probe Kit (Bioline). TaqMan reactions were run on a Mastercycler EP Reaplex system (Eppendorf) in triplicate. Values are represented as the difference in Ct values normalized to *Actb* for each sample.

Immunoblotting

Western blots analyses were performed and quantitated using a LAS3000 Imaging System (Fuji) and MultiGauge software as described previously (Das et al., 2009; Markegard et al., 2011). Antibodies to phosphorylated and total ERK, IRF4, and actin were from Cell Signaling; antibodies to HDAC7 and Grb2 were from Santa Cruz Biotechnology; antibody to GFP was from Clontech; antibody to lamin β was from Abcam, and antibody to histone 3 was from EMD

Millipore. Rabbit antiserum to phosphorylated HDAC7 (S259) was a gift from Dr. Timothy McKinsey.

Microscopy

For immunofluorescence analysis of fresh-frozen spleens, tissues were extracted and were immediately embedded in Tissue Tek Optimum Cutting Temperature (OCT) (Sakura) on dry ice. 6um cryostat sections of spleen were transferred to a superfrost plus microscope slide (Fisherbrand). Prior to staining, slides were fixed in cold acetone and permeabilized with 10% goat serum, 1:200 Fc block, 0.1% Triton-X100. The following primary antibodies were used for stainings: HDAC7 (30ug/mL, Abcam, 1441) and CD4 (4ug/mL, clone GK1.5, UCSF Hybridoma Core**)**. Primary antibody stainings were detected using 1:500 goat anti-rabbit antibody conjugated to Alexa Fluor 568 (Invitrogen, A-11036) for HDAC7 and goat anti-rat antibody conjugated to Alexa Fluor 488 (A-11006) for CD4. Nuclei were counterstained with DAPI (1ug/mL, Molecular Probes, D1306) and mounted with vectashield mounting medium (Vectashield Laboratories, H-1000). Tissue was analyzed at 100x zoom using an AR1+ Nikon confocal microscope and analyzed with Fiji.

Microarrays and gene expression data analysis

Microarray analysis of $CD4^+$ T cells was carried out using Agilent gene arrays $CD4^+$ T cells were lysed in Trizol and RNA was isolated using the RNeasy Minelute kit (Qiagen). RNA was processed using the RNA Clean and Concentrator-5 kit (Zymo Research) and amplified and labeled with Cy3-CTP using the Agilent low RNA input fluorescent linear amplification kits, according to the manufacturer's protocol. Equal amounts of labeled material were hybridized to Agilent whole mouse genome 4x44K Ink-jet arrays. Hybridizations were performed for 14 hours and the arrays were scanned using the Agilent microarray scanner in the UCSF Shared Microarray Core Facility. Raw signal intensities were extracted with Feature Extraction v10.5

software. The dataset was normalized using quantile normalization (Bolstad et al., 2003) and an ANOVA linear model was used to determine fold differences (Smyth, 2004). The false-discovery rate procedure, which adjusts for multiple comparisons, was used to determine statistical significance (Benjamini, 1995). All procedures were carried out by using R and Bioconductor (Gentleman et al., 2004; Smyth, 2004).

Microscopy on cytospins

For microscopic analysis of HDAC7 distribution in cytospins, single cell suspensions were prepared from lymph nodes, washed with PBS, and were either immediately fixed in 100ul 2% PFA or were rested in PBS for 30 minutes prior to fixation. Cells were then washed and spun onto slides using a Cytospin (700rpm, 4 minutes) and stained with primary antibodies to HDAC7 (Santa Cruz Biotechnology) and CD4 (clone GK1.5, UCSF Hybridoma Core**)** followed by secondary antibodies; goat-anti-rabbit antibody conjugated to Alexa Fluor 568 (Invitrogen, A-11036) for HDAC7 and goat anti-rat antibody conjugated to Alexa Fluor 488 (A-11006) for CD4. Cells were counterstained with DAPI. Images were acquired on a Zeiss spinning disk confocal microscope and analyzed using ImageJ software.

Primary T cell isolation, culture, and analysis of proliferation, cytokines and transcription factors by flow cytometry

Freshly collected total splenocytes from WT, HDAC7 KO, and HDAC7 ΔP were stimulated with PMA (10 ng/ml) and ionomycin (1μM) in the presence of Brefeldin A, and the cells were stained for CD4 (clone GK1.5). After fixation and permeabilization, cells were further stained with fluorophore-conjugated antibodies to the indicated cytokines or to an isotype control (all antibodies were purchased from eBioscience, Biolegend, or BD Pharmingen).

Cells used in polarization assays in Figure 6 were purified using MACS negative isolation (Miltenyi Biotec) and, where indicated, were subsequently sorted to >98% purity on a MoFlo

XDP cell sorter (Beckman Coulter) or a FACS Aria (BD Biosciences) in the UCSF flow cytometry core. Lymphocytes were stimulated in plates coated with α-CD3 (2C11) and α-CD28 (37.51) in the presence of Th1 (rIL-12 10ng/ml (Peprotech) and 10ug/ml α-IL-4 (11B11, UCSF mAb core) or Th2 (rIL-4 50ng/ml (Peprotech) and 10ug/ml α-IFN-γ (XMG1.2, UCSF mAb core)) polarizing media. After 5 days, cells were restimulated with PMA (5ng/ml) and ionomycin (0.67nM) in the presence of monensin (BD GolgiStop). Following restimulation, cells were stained with fixable viability dye (LifeTechnologies) and fluorophore-conjugated antibodies to CD4 (GK1.5), IFN-γ (XMG1.2), and IL-4 (11B11). All antibodies used were from eBioscience, BD, or Tonbo Biosciences. For Gata3 induction assays, cells were cultured for up to 48 hours in Th1 or Th2 media before fixation and permeabilization in Foxp3 / Transcription Factor buffer sets (eBioscience) and staining with Gata3 antibody (PE, clone TWAJ, eBioscience).

For Nur77 proliferation assays, lymph nodes from *Nur77*$^{-/-}$ and WT B6 mice were isolated and single cell suspensions were prepared. CD4^{+} cells were enriched using MACS isolation (Miltenyi), cells were labeled with cell trace violet (Thermo Fisher Scientific), and were stained with surface antibodies prior to sorting (for TCRb^{+} CD4^{+} CD25^{-} CD44^{low} naïve T cells). Sorted cells were cultured on CD3 (clone 2C11) and CD28 (clone 37.51) coated plates (0.5g/ml each) for up to 96 hours. Cells were labeled with a viability dye (Thermo Fisher Scientific), stained for CD4 prior to flow cytometric analysis.

All flow cytometry data was acquired on LSRII or Fortessa instruments (BD Biosciences) and analyzed using FlowJo software (Tree Star).

Retrovirus infection and IFN-γ producing cell analysis

To obtain recombinant virus, 10μg retrovirus encoding GFP and HDAC7-ΔP or control virus encoding GFP alone was transfected into phoenix-eco cells. Supernatants were collected 48 h

after transfection and were filtered through a 0.45-um membrane. Naïve mouse $CD4^+$ T cells were differentiated for 24 hours under Th1 condition [5μg/ml of plate bound α-CD3 (145-2C11, UCSF core facility), 2μg/ml of soluble α-CD28 (PV-1, UCSF core facility), 10ng/ml of IL-12 (Peprotech), and 10μg/ml of α-IL4 (clone#: 30340, R&D systems)], were infected twice with retroviral supernatant in the presence of polybrene (6 ug/ml) by 'spin-inoculation' at 2000 rpm for 90 minutes, and were further differentiated under Th1 condition. Three days after infection and differentiation, cells were activated with PMA (50ng/ml, Sigma) and ionomycin (1μM, Sigma) for 4 hours in the presence of brefeldin A (eBioscience) for last 1 hour. Cells were stained with α-CD4 (RM4-5, PerCP, eBioscience) and then further stained with α-IFN-γ (XMG1-2, APC, eBioscience) after fixation and permeabilization. Stained cells were acquired on a FACSCalibur, and the FlowJo program was used for data analysis.

REFERENCES

Aguado, E., Richelme, S., Nunez-Cruz, S., Miazek, A., Mura, A.M., Richelme, M., Guo, X.J., Sainty, D., He, H.T., Malissen, B., and Malissen, M. (2002). Induction of T helper type 2 immunity by a point mutation in the LAT adaptor. Science *296*, 2036-2040.

Ansel, K.M., Djuretic, I., Tanasa, B., and Rao, A. (2006). Regulation of Th2 differentiation and Il4 locus accessibility. Annu Rev Immunol *24*, 607-656.

Azzam, H.S., Grinberg, A., Lui, K., Shen, H., Shores, E.W., and Love, P.E. (1998). CD5 expression is developmentally regulated by T cell receptor (TCR) signals and TCR avidity. J Exp Med *188*, 2301-2311.

Bhandoola, A., Tai, X., Eckhaus, M., Auchincloss, H., Mason, K., Rubin, S.A., Carbone, K.M., Grossman, Z., Rosenberg, A.S., and Singer, A. (2002). Peripheral expression of self-MHC-II influences the reactivity and self-tolerance of mature CD4(+) T cells: evidence from a lymphopenic T cell model. Immunity *17*, 425-436.

Bird, J.J., Brown, D.R., Mullen, A.C., Moskowitz, N.H., Mahowald, M.A., Sider, J.R., Gajewski, T.F., Wang, C.R., and Reiner, S.L. (1998). Helper T cell differentiation is controlled by the cell cycle. Immunity *9*, 229-237.

Biswas, P.S., Bhagat, G., and Pernis, A.B. (2010). IRF4 and its regulators: evolving insights into the pathogenesis of inflammatory arthritis? Immunol Rev *233*, 79-96.

Brownlie, R., and Zamoyska, R. (2009). LAT polices T cell activation. Immunity *31*, 174-176.

Chuck, M.I., Zhu, M., Shen, S., and Zhang, W. (2010). The Role of the LAT-PLC-{gamma}1 Interaction in T Regulatory Cell Function. J Immunol *184*, 2476-2486.

Das, J., Ho, M., Zikherman, J., Govern, C., Yang, M., Weiss, A., Chakraborty, A.K., and Roose, J.P. (2009). Digital signaling and hysteresis characterize ras activation in lymphoid cells. Cell *136*, 337-351.

Dequiedt, F., Kasler, H., Fischle, W., Kiermer, V., Weinstein, M., Herndier, B.G., and Verdin, E. (2003). HDAC7, a thymus-specific class II histone deacetylase, regulates Nur77 transcription and TCR-mediated apoptosis. Immunity *18*, 687-698.

Glasmacher, E., Agrawal, S., Chang, A.B., Murphy, T.L., Zeng, W., Vander Lugt, B., Khan, A.A., Ciofani, M., Spooner, C.J., Rutz, S.*, et al.* (2012). A genomic regulatory element that directs assembly and function of immune-specific AP-1-IRF complexes. Science *338*, 975-980.

Haberland, M., Montgomery, R.L., and Olson, E.N. (2009). The many roles of histone deacetylases in development and physiology: implications for disease and therapy. Nature reviews *10*, 32-42.

Hirahara, K., Vahedi, G., Ghoreschi, K., Yang, X.P., Nakayamada, S., Kanno, Y., O'Shea, J.J., and Laurence, A. (2011). Helper T-cell differentiation and plasticity: insights from epigenetics. Immunology *134*, 235-245.

Hogquist, K.A., Starr, T.K., and Jameson, S.C. (2003). Receptor sensitivity: when T cells lose their sense of self. Curr Biol *13*, R239-241.

Honma, K., Kimura, D., Tominaga, N., Miyakoda, M., Matsuyama, T., and Yui, K. (2008). Interferon regulatory factor 4 differentially regulates the production of Th2 cytokines in naive vs. effector/memory CD4+ T cells. Proc Natl Acad Sci U S A *105*, 15890-15895.

Huber, M., and Lohoff, M. (2014). IRF4 at the crossroads of effector T-cell fate decision. Eur J Immunol *44*, 1886-1895.

Kanno, Y., Vahedi, G., Hirahara, K., Singleton, K., and O'Shea, J.J. (2012). Transcriptional and epigenetic control of T helper cell specification: molecular mechanisms underlying commitment and plasticity. Annu Rev Immunol *30*, 707-731.

Kasler, H.G., Lim, H.W., Mottet, D., Collins, A.M., Lee, I.S., and Verdin, E. (2012). Nuclear export of histone deacetylase 7 during thymic selection is required for immune self-tolerance. EMBO J *31*, 4453-4465.

Kasler, H.G., and Verdin, E. (2007). Histone deacetylase 7 functions as a key regulator of genes involved in both positive and negative selection of thymocytes. Mol Cell Biol *27*, 5184-5200.
Kasler, H.G., Young, B.D., Mottet, D., Lim, H.W., Collins, A.M., Olson, E.N., and Verdin, E. (2011). Histone deacetylase 7 regulates cell survival and TCR signaling in CD4/CD8 double-positive thymocytes. J Immunol *186*, 4782-4793.
Kurakula, K., Vos, M., Logiantara, A., Roelofs, J.J., Nieuwenhuis, M.A., Koppelman, G.H., Postma, D.S., van Rijt, L.S., and de Vries, C.J. (2015). Nuclear Receptor Nur77 Attenuates Airway Inflammation in Mice by Suppressing NF-kappaB Activity in Lung Epithelial Cells. J Immunol *195*, 1388-1398.
Lam, K.P., Kuhn, R., and Rajewsky, K. (1997). In vivo ablation of surface immunoglobulin on mature B cells by inducible gene targeting results in rapid cell death. Cell *90*, 1073-1083.
Lee, S.L., Wesselschmidt, R.L., Linette, G.P., Kanagawa, O., Russell, J.H., and Milbrandt, J. (1995). Unimpaired thymic and peripheral T cell death in mice lacking the nuclear receptor NGFI-B (Nur77). Science *269*, 532-535.
Levine, A.G., Arvey, A., Jin, W., and Rudensky, A.Y. (2014). Continuous requirement for the TCR in regulatory T cell function. Nat Immunol *15*, 1070-1078.
Li, P., Spolski, R., Liao, W., and Leonard, W.J. (2014). Complex interactions of transcription factors in mediating cytokine biology in T cells. Immunol Rev *261*, 141-156.
Li, P., Spolski, R., Liao, W., Wang, L., Murphy, T.L., Murphy, K.M., and Leonard, W.J. (2012). BATF-JUN is critical for IRF4-mediated transcription in T cells. Nature *490*, 543-546.
Locksley, R.M. (2009). Nine lives: plasticity among T helper cell subsets. J Exp Med *206*, 1643-1646.
Lohoff, M., and Mak, T.W. (2005). Roles of interferon-regulatory factors in T-helper-cell differentiation. Nat Rev Immunol *5*, 125-135.
Mandl, J.N., Monteiro, J.P., Vrisekoop, N., and Germain, R.N. (2013). T cell-positive selection uses self-ligand binding strength to optimize repertoire recognition of foreign antigens. Immunity *38*, 263-274.
Markegard, E., Trager, E., Yang, C.W., Zhang, W., Weiss, A., and Roose, J.P. (2011). Basal LAT-diacylglycerol-RasGRP1 Signals in T Cells Maintain TCRalpha Gene Expression. PloS one *6*, e25540.
Matthews, S.A., Liu, P., Spitaler, M., Olson, E.N., McKinsey, T.A., Cantrell, D.A., and Scharenberg, A.M. (2006). Essential role for protein kinase D family kinases in the regulation of class II histone deacetylases in B lymphocytes. Mol Cell Biol *26*, 1569-1577.
Mingueneau, M., Roncagalli, R., Gregoire, C., Kissenpfennig, A., Miazek, A., Archambaud, C., Wang, Y., Perrin, P., Bertosio, E., Sansoni, A.*, et al.* (2009). Loss of the LAT adaptor converts antigen-responsive T cells into pathogenic effectors that function independently of the T cell receptor. Immunity *31*, 197-208.
Mittrucker, H.W., Matsuyama, T., Grossman, A., Kundig, T.M., Potter, J., Shahinian, A., Wakeham, A., Patterson, B., Ohashi, P.S., and Mak, T.W. (1997). Requirement for the transcription factor LSIRF/IRF4 for mature B and T lymphocyte function. Science *275*, 540-543.
Monroe, J.G. (2006). ITAM-mediated tonic signalling through pre-BCR and BCR complexes. Nat Rev Immunol *6*, 283-294.
Mosmann, T.R., Cherwinski, H., Bond, M.W., Giedlin, M.A., and Coffman, R.L. (2005). Two types of murine helper T cell clone. I. Definition according to profiles of lymphokine activities and secreted proteins. 1986. J Immunol *175*, 5-14.
Murphy, K.M., and Reiner, S.L. (2002). The lineage decisions of helper T cells. Nat Rev Immunol *2*, 933-944.
Murphy, T.L., Tussiwand, R., and Murphy, K.M. (2013). Specificity through cooperation: BATF-IRF interactions control immune-regulatory networks. Nat Rev Immunol *13*, 499-509.

Nayar, R., Enos, M., Prince, A., Shin, H., Hemmers, S., Jiang, J.K., Klein, U., Thomas, C.J., and Berg, L.J. (2012). TCR signaling via Tec kinase ITK and interferon regulatory factor 4 (IRF4) regulates CD8+ T-cell differentiation. Proc Natl Acad Sci U S A *109*, E2794-2802.
Nayar, R., Schutten, E., Bautista, B., Daniels, K., Prince, A.L., Enos, M., Brehm, M.A., Swain, S.L., Welsh, R.M., and Berg, L.J. (2014). Graded levels of IRF4 regulate CD8+ T cell differentiation and expansion, but not attrition, in response to acute virus infection. J Immunol *192*, 5881-5893.
Nowyhed, H.N., Huynh, T.R., Thomas, G.D., Blatchley, A., and Hedrick, C.C. (2015). Cutting Edge: The Orphan Nuclear Receptor Nr4a1 Regulates CD8+ T Cell Expansion and Effector Function through Direct Repression of Irf4. J Immunol *195*, 3515-3519.
O'Shea, J.J., and Paul, W.E. (2010). Mechanisms underlying lineage commitment and plasticity of helper CD4+ T cells. Science *327*, 1098-1102.
Ou-Yang, C.W., Zhu, M., Fuller, D.M., Sullivan, S.A., Chuck, M.I., Ogden, S., Li, Q.J., and Zhang, W. (2012). Role of LAT in the granule-mediated cytotoxicity of CD8 T cells. Mol Cell Biol *32*, 2674-2684.
Parra, M., Kasler, H., McKinsey, T.A., Olson, E.N., and Verdin, E. (2005). Protein kinase D1 phosphorylates HDAC7 and induces its nuclear export after T-cell receptor activation. J Biol Chem *280*, 13762-13770.
Paul, W.E. (2010). What determines Th2 differentiation, in vitro and in vivo? Immunol Cell Biol *88*, 236-239.
Pinto, L.A., Michel, S., Klopp, N., Vogelberg, C., von Berg, A., Bufe, A., Heinzmann, A., Laub, O., Simma, B., Frischer, T.*, et al.* (2013). Polymorphisms in the IRF-4 gene, asthma and recurrent bronchitis in children. Clin Exp Allergy *43*, 1152-1159.
Polic, B., Kunkel, D., Scheffold, A., and Rajewsky, K. (2001). How alpha beta T cells deal with induced TCR alpha ablation. Proc Natl Acad Sci U S A *98*, 8744-8749.
Rajpal, A., Cho, Y.A., Yelent, B., Koza-Taylor, P.H., Li, D., Chen, E., Whang, M., Kang, C., Turi, T.G., and Winoto, A. (2003). Transcriptional activation of known and novel apoptotic pathways by Nur77 orphan steroid receptor. EMBO J *22*, 6526-6536.
Rengarajan, J., Mittelstadt, P.R., Mages, H.W., Gerth, A.J., Kroczek, R.A., Ashwell, J.D., and Glimcher, L.H. (2000). Sequential involvement of NFAT and Egr transcription factors in FasL regulation. Immunity *12*, 293-300.
Roose, J.P., Diehn, M., Tomlinson, M.G., Lin, J., Alizadeh, A.A., Botstein, D., Brown, P.O., and Weiss, A. (2003). T Cell Receptor-Independent Basal Signaling via Erk and Abl Kinases Suppresses RAG Gene Expression. PLoS Biol *1*, E53.
Sekiya, T., Kashiwagi, I., Yoshida, R., Fukaya, T., Morita, R., Kimura, A., Ichinose, H., Metzger, D., Chambon, P., and Yoshimura, A. (2013). Nr4a receptors are essential for thymic regulatory T cell development and immune homeostasis. Nat Immunol *14*, 230-237.
Sekiya, T., Kondo, T., Shichita, T., Morita, R., Ichinose, H., and Yoshimura, A. (2015). Suppression of Th2 and Tfh immune reactions by Nr4a receptors in mature T reg cells. J Exp Med *212*, 1623-1640.
Shen, S., Chuck, M.I., Zhu, M., Fuller, D.M., Yang, C.W., and Zhang, W. (2010). The importance of LAT in the activation, homeostasis, and regulatory function of T cells. J Biol Chem *285*, 35393-35405.
Shen, S., Zhu, M., Lau, J., Chuck, M., and Zhang, W. (2009). The essential role of LAT in thymocyte development during transition from the double-positive to single-positive stage. J Immunol *182*, 5596-5604.
Smith, K., Seddon, B., Purbhoo, M.A., Zamoyska, R., Fisher, A.G., and Merkenschlager, M. (2001). Sensory adaptation in naive peripheral CD4 T cells. J Exp Med *194*, 1253-1261.
Sommers, C.L., Park, C.S., Lee, J., Feng, C., Fuller, C.L., Grinberg, A., Hildebrand, J.A., Lacana, E., Menon, R.K., Shores, E.W.*, et al.* (2002). A LAT mutation that inhibits T cell development yet induces lymphoproliferation. Science *296*, 2040-2043.

Stefanova, I., Dorfman, J.R., and Germain, R.N. (2002). Self-recognition promotes the foreign antigen sensitivity of naive T lymphocytes. Nature *420*, 429-434.
Tamura, T., Yanai, H., Savitsky, D., and Taniguchi, T. (2008). The IRF family transcription factors in immunity and oncogenesis. Annu Rev Immunol *26*, 535-584.
Vahl, J.C., Drees, C., Heger, K., Heink, S., Fischer, J.C., Nedjic, J., Ohkura, N., Morikawa, H., Poeck, H., Schallenberg, S.*, et al.* (2014). Continuous T cell receptor signals maintain a functional regulatory T cell pool. Immunity *41*, 722-736.
Valapour, M., Guo, J., Schroeder, J.T., Keen, J., Cianferoni, A., Casolaro, V., and Georas, S.N. (2002). Histone deacetylation inhibits IL4 gene expression in T cells. J Allergy Clin Immunol *109*, 238-245.
van Oers, N.S., Killeen, N., and Weiss, A. (1994). ZAP-70 is constitutively associated with tyrosine-phosphorylated TCR zeta in murine thymocytes and lymph node T cells. Immunity *1*, 675-685.
van Oers, N.S., Tao, W., Watts, J.D., Johnson, P., Aebersold, R., and Teh, H.S. (1993). Constitutive tyrosine phosphorylation of the T-cell receptor (TCR) zeta subunit: regulation of TCR-associated protein tyrosine kinase activity by TCR zeta. Mol Cell Biol *13*, 5771-5780.
Vega, R.B., Harrison, B.C., Meadows, E., Roberts, C.R., Papst, P.J., Olson, E.N., and McKinsey, T.A. (2004). Protein kinases C and D mediate agonist-dependent cardiac hypertrophy through nuclear export of histone deacetylase 5. Mol Cell Biol *24*, 8374-8385.
Verdin, E., Dequiedt, F., and Kasler, H.G. (2003). Class II histone deacetylases: versatile regulators. Trends Genet *19*, 286-293.
Yao, S., Buzo, B.F., Pham, D., Jiang, L., Taparowsky, E.J., Kaplan, M.H., and Sun, J. (2013). Interferon regulatory factor 4 sustains CD8(+) T cell expansion and effector differentiation. Immunity *39*, 833-845.
Zhang, C.L., McKinsey, T.A., Chang, S., Antos, C.L., Hill, J.A., and Olson, E.N. (2002). Class II histone deacetylases act as signal-responsive repressors of cardiac hypertrophy. Cell *110*, 479-488.
Zheng, Y., Chaudhry, A., Kas, A., deRoos, P., Kim, J.M., Chu, T.T., Corcoran, L., Treuting, P., Klein, U., and Rudensky, A.Y. (2009). Regulatory T-cell suppressor program co-opts transcription factor IRF4 to control T(H)2 responses. Nature *458*, 351-356.
Zhou, L., Chong, M.M., and Littman, D.R. (2009). Plasticity of CD4+ T cell lineage differentiation. Immunity *30*, 646-655.
Zhu, J., and Paul, W.E. (2010). CD4+ T cell plasticity-Th2 cells join the crowd. Immunity *32*, 11-13.
Zhu, J., Yamane, H., and Paul, W.E. (2010). Differentiation of effector CD4 T cell populations (*). Annual review of immunology *28*, 445-489.

Chapter 6

Rasgrp1 mutation increases naïve T-cell CD44 expression and drives mTOR-dependent accumulation of Helios^{+} T cells and autoantibodies

ABSTRACT

Missense variants are a major source of human genetic variation. Here we analyze a new mouse missense variant, *Rasgrp1*^{Anaef}, with an ENU-mutated EF hand in the Rasgrp1 Ras guanine nucleotide exchange factor. *Rasgrp1*^{Anaef} mice exhibit anti-nuclear autoantibodies and gradually accumulate a CD44^{hi} Helios^{+} PD-1^{+} CD4^{+} T cell population that is dependent on B cells. Despite reduced Rasgrp1-Ras-ERK activation *in vitro*, thymocyte selection in *Rasgrp1*^{Anaef} is mostly normal *in vivo*, although CD44 is overexpressed on naïve thymocytes and T cells in a T-cell-autonomous manner. We identify CD44 expression as a sensitive reporter of tonic mTOR-S6 kinase signaling through a novel mouse strain, *chino*, with a reduction-of-function mutation in *Mtor*. Elevated tonic mTOR-S6 signaling occurs in *Rasgrp1*^{Anaef} naïve CD4^{+} T cells. CD44 expression, CD4^{+} T cell subset ratios and serum autoantibodies all returned to normal in *Rasgrp1*^{Anaef}*.Mtor*^{chino} double-mutant mice, demonstrating that increased mTOR activity is essential for the *Rasgrp1*^{Anaef} T cell dysregulation.

INTRODUCTION

Positive and negative selection of thymocytes generates a population of T lymphocytes with a broad spectrum of antigen-specific T cell receptors (TCR) (Kortum et al., 2013, Starr et al., 2003). It was recognized early on that the small GTPase Ras plays a role (Swan et al., 1995). Three Ras guanine exchange factor (RasGEF) families can activate Ras: SOS, RasGRP, and RasGRF (Stone, 2011). Following TCR engagement, *Son of Sevenless* (SOS)-1 and -2 are recruited to the plasma membrane via a Grb2-phospho-LAT interaction. Simultaneously, the second messenger diacylglycerol (DAG), generated via PLCγ, directly recruits Ras guanine nucleotide releasing protein 1 (Rasgrp1) to the plasma membrane (Ebinu et al., 1998). Biochemically, Rasgrp1 and SOS1 synergize to induce high-level Ras activation (Roose et al., 2007) and Rasgrp1 serves a critical role in priming SOS1 via Rasgrp1-produced RasGTP (Das et al., 2009). Consequentially, thymocyte development is severely impaired in *Rasgrp1*-deficient mice (Dower et al., 2000), and not compensated for by SOS RasGEFs. Additionally, there is only minimal compensation for loss of Rasgrp1 coming from Rasgrp3 or Rasgrp4 (Golec et al., 2013, Zhu et al., 2012). *Rasgrp1*-deficient mice exhibit a strong defect in positive selection and impaired ERK phosphorylation in thymocytes (Dower et al., 2000, Priatel et al., 2002). The importance of the canonical Rasgrp1-RasGTP-RAF-MEK-ERK pathway for developing thymocytes is further underscored by impaired positive selection in ERK-1 and -2 doubly deficient mice (Fischer et al., 2005).

Although Rasgrp1 plays a critical role in the activation of Ras, relatively little is known about its regulation in T lymphocytes or the *in vivo* importance of such regulation. In addition to membrane recruitment via its DAG-binding C1 domain (Ebinu et al., 1998), Rasgrp1's GEF activity is enhanced by inducible phosphorylation of threonine 184 (Zheng et al., 2005, Roose et

al., 2005). Phospholipase C γ (PLCγ) not only generates DAG but also inositol 1,4,5-trisphosphate (IP3), which binds to IP3 receptors on the endoplasmic reticulum to activate the calcium pathway (Feske, 2007). Interestingly, Rasgrp1 also contains a pair of EF hands, motifs that often bind calcium, which induces conformational changes (Gifford et al., 2007). Rasgrp1 has been reported to bind calcium *in vitro* (Ebinu et al., 1998). In chicken DT40 B cells, the first EF_1 domain enables the recruitment function of a C-terminal PT domain (plasma membrane targeting domain) that cooperates with the C1 domain to recruit Rasgrp1 to the membrane (Tazmini et al., 2009). Notably, the PT domain contribution is substantial in BCR-stimulated B cell lines, very modest in T cell lines, and negligible in fibroblasts (Beaulieu et al., 2007). Genetic deletion of Rasgrp1's 200 C-terminal amino acids reduces the formation of mature thymocytes in *Rasgrp1*$^{d/d}$ mice (Fuller et al., 2012). Our recent structural studies revealed that Rasgrp1's C terminus contains a coiled-coil dimerization domain (Iwig et al., 2013). Rasgrp1 dimerization plays an important role in controlling Rasgrp1's activity; the second EF hand of one Rasgrp1 molecule packs against the C1 domain of a second molecule in a manner that is incompatible with DAG-binding whereas calcium binding to the first EF hand is predicted to unlock this autoinhibitory dimer interface (Iwig et al., 2013). Lastly, it is unknown if Rasgrp1 may signal to pathways other than the canonical Rasgrp1-Ras-RAF-MEK-ERK cascade, although a link between Rasgrp1 and mTOR (mechanistic target of rapamycin) signaling has been proposed (Gorentla et al., 2011).

Older *Rasgrp1*-deficient (Coughlin et al., 2005) and *Rasgrp1*$^{d/d}$ mice (Fuller et al., 2012) develop splenomegaly and autoantibodies. In these mouse models, the complete deletion or truncation of Rasgrp1 greatly decreases T cell development in the thymus (Dower et al., 2000, Fuller et al., 2012), resulting in peripheral T cell lymphopenia followed by accumulation of $CD44^{hi}$ $CD62L^{lo}$ $CD4^{+}$ T cells (Priatel et al., 2007, Fuller et al., 2012). Autoimmune phenotypes caused by these mutations have been attributed to compromised T cell selection in the thymus

and compensatory expansion of peripheral T cells in response to lymphopenia and/or chronic infection. Hypomorphic missense alleles of the signaling molecules ZAP-70 and LAT also impair T cell development in the thymus and culminate in severe peripheral immune dysregulation. For example, an SKG allele of the kinase ZAP-70 has reduced binding-affinity for phospho-TCRζ and leads to autoimmune arthritis in mice (Sakaguchi et al., 2003). Point mutations in ZAP70's catalytic domain that reduce kinase activity to intermediate levels diminish thymic deletion and Foxp3^{+} Treg differentiation but preserve peripheral T cell activation, resulting in autoantibody formation and hyper-IgE production (Siggs et al., 2007). Mutation of a single tyrosine in LAT (LAT^{Y136F}) results in hyperproliferative lymphocytes of a T_H2 type (Aguado et al., 2002, Sommers et al., 2002). In each of these cases, peripheral T cell dysregulation is tied to, and potentially explained by, profound deficits in thymic T cell formation.

Single nucleotide variants that cause amino acid substitutions (missense variants; SNVs) or modify the level of gene expression rather than knocking out protein expression are a major form of human genetic variation: most people inherit ~12,000 missense gene variants (2010). Given the emerging examples of missense alleles having very different immunological consequences from null alleles, mouse models that analyze the consequences of missense variants in key immune genes are needed to understand the pathogenesis of complex human immune diseases. Common tag SNVs near *RASGRP1* are associated with susceptibility to autoimmune (Type 1) diabetes and to thyroid autoantibodies in Graves' disease (Plagnol et al., 2011, Qu et al., 2009), while 13 unstudied *RASGRP1* missense SNVs are currently listed in public databases. A fruitful approach for identifying missense gene variants that dysregulate immune function has been through *N*-ethyl-*N*-nitrosourea (ENU) mutagenesis (Nelms and Goodnow, 2001). Here we describe the analysis of a novel ENU-induced missense variant, *Rasgrp1^{Anaef}* that reveals an important *in vivo* regulatory function of Rasgrp1's EF hands. *Rasgrp1^{Anaef}* is distinct from previously described autoimmune mutations in *Rasgrp1*, *Zap70* or

Lat, as *Rasgrp1*^{Anaef} has no detectable effect on thymocyte development in mice with normal TCR repertoires, but results in peripheral accumulation of a distinct population of Helios^{+} PD-1^{+} T-helper cells and production of anti-nuclear autoantibodies. In contrast to *Rasgrp1* deletion, the *Rasgrp1*^{Anaef} missense variant increases tonic mTOR signaling in naïve CD4^{+} T cells. Genetic reduction of mTOR function in *Rasgrp1*^{Anaef} mice normalizes CD44 expression on naïve CD4^{+} T cells and abolishes excessive accumulation of effector T cells and autoantibodies, demonstrating a central role for increased mTOR activity in driving immune dysregulation in *Rasgrp1*^{Anaef} mice.

RESULTS

Identification of the *Rasgrp1*^{Anaef} mouse strain with a mutated EF hand in Rasgrp1

As part of a mouse genome-wide screen for immune phenotypes induced by ENU mutagenesis (Nelms and Goodnow, 2001), we identified a variant C57BL/6 (B6) pedigree displaying elevated frequencies of CD44^{hi} CD4^{+} cells (**Fig. 6.1a**), elevated CD44 expression on naïve FOXP3^{-} CD44^{lo} CD4^{+} cells (**Fig. 6.1b**) and antinuclear antibodies (ANAs) staining with a homogeneous nuclear pattern (**Fig. 6.1c, d**). The elevated frequency of CD44^{hi} cells trait, which occurred at a frequency consistent with inheritance of a recessive gene variant (**Fig. 6.1a**), was used to map the mutation in an F2 intercross to an interval between 114 and 121.2 Mb on chromosome 2 (**Supplementary Fig. S1a**).

Sequencing of the exons of *Rasgrp1*, the only gene within this interval with a known immune function, identified an A to G missense mutation in codon 519 within exon 13 (**Fig. 6.2a**). Whole-exome capture, sequencing and computational analysis of DNA from an affected mouse (Andrews et al., 2012) identified this mutation as the only novel single-nucleotide variant

within the interval of interest on chromosome 2 (data not shown). The mutant codon, located in Rasgrp1's second EF hand (EF_2), encodes a neutral amino acid glycine (G) instead of the normal arginine (R), a large polar molecule with a positive charge (Rasgrp1 R519G; **Figs. 6.2a and 6.2b**). Rasgrp1's arginine residue at 519 is also found in Rasgrp-2, and -4, and in EF_3 of calcium and integrin binding protein (CIB) (**Fig. 6.2b**). EF hands typically come in pairs separated by a linker and calcium binding subsequently alters the angle between helices E and F in proteins such as calmodulin (CaM) (**Fig. 6.2c**) (Gifford et al., 2007, Grabarek, 2006). Unique to Rasgrp1, this linker is unusually short. Furthermore, biophysical studies revealed that Rasgrp1's EF_2 does not bind calcium, that the E helix is non-existent in EF_2, but instead has evolved as a critical loop forming an autoinhibitory interface with the C1 domain (**Figs. 6.2d and 6.2e**) (Iwig et al., 2013).

The ENU-generated allele was named "*Rasgrp1*^{Anaef} " to reflect the combination of antinuclear antibody (ANA) production and the amino acid substitution in the EF hand. Genotyping of this mutation in multiple generations of B6 offspring (**Supplementary Fig. S1b and S1c**) demonstrated that inheritance of the *Rasgrp1*^{Anaef} allele was well correlated with the immunological abnormalities described above and below. ANAs were present in 70% of homozygous *Rasgrp1*$^{Anaef/Anaef}$ mice and 35% of heterozygous *Rasgrp1*$^{Anaef/+}$ mice (**Fig. 6.1d**), compared to 5% of wildtype B6 mice, indicating a gene dosage effect. The R519G substitution caused an approximate 40% decrease in Rasgrp1 protein levels in homozygous *Rasgrp1*$^{Anaef/Anaef}$ thymocytes (**Fig. 6.2f**). Since heterozygous *Rasgrp1*$^{+/-}$ thymocytes express half the Rasgrp1 dosage (**Fig. 6.2g**) but do not display an abnormal immune phenotype (Dower et al., 2000), whereas heterozygous *Rasgrp1*$^{Anaef/+}$ mice do exhibit abnormal immune phenotypes (**Fig. 6.1b and 6.1d**), we conclude that the immune dysregulation in mice bearing the *Rasgrp1*^{Anaef} allele is caused by the specific R519G alteration and not simply by a reduction of

Rasgrp1 protein levels. In the remainder of the manuscript we discuss the analysis of homozygous *Rasgrp1*$^{Anaef/Anaef}$ mice and refer to these as *Rasgrp1*^{Anaef} mice.

Rasgrp1^{Anaef} preserves Rasgrp1 function for T cell selection in the thymus

Analysis of *Rasgrp1*^{Anaef} mice revealed a striking contrast to the published *Rasgrp1*-deficient and *Rasgrp1*$^{d/d}$ mouse models, which have T cell developmental defects that result in low thymic T cell output (Priatel et al., 2007, Fuller et al., 2012, Dower et al., 2000). The frequency and number of mature CD4$^+$ and CD8$^+$ single positive (SP) thymocyte subsets was normal in *Rasgrp1*^{Anaef} mice, whereas these subsets were markedly decreased in *Rasgrp1*$^{-/-}$ knockout mice analyzed in parallel (**Fig. 6.3a and 6.3b)**. Unlike the knockout allele, the *Rasgrp1*^{Anaef} mutation did not decrease the frequency of CD69^{hi} TCRβ^{hi} cells amongst CD4$^+$CD8$^+$ double positive (DP) thymocytes (**Fig. 6.3c**) or the number of Foxp3$^+$ CD4SP cells in the thymus (**Fig. 6.3b**). Even in bone marrow chimeras reconstituted with a mixture of CD45.2$^+$ *Rasgrp1*^{Anaef} and CD45.1$^+$ wildtype marrow, the *Rasgrp1*^{Anaef} thymocytes exhibited no competitive disadvantage as they matured from DP to SP cells (**Fig. 6.3d**). Injection into mice of 5-bromo-2'-deoxyuridine (BrdU) to pulse-label a cohort of proliferating DP thymocytes followed by analysis on day 5 demonstrated that the kinetics of maturation into SP cells was unaffected by the *Rasgrp1*^{Anaef} mutation (**Fig. 6.3e, Supplementary Fig. S2a**). There was also normal deletion of Vβ5$^+$ and Vβ11$^+$ SP thymocytes upon self-superantigen/I-E^k recognition in B10.Br mice (**Fig. 6.3f**) and similar usage of TCRα Jα segments in wildtype and *Rasgrp1*^{Anaef} CD4SP thymocyte populations (**Fig. 6.3g and Supplementary Fig. S2b)**. Thus, analysis of the thymus of *Rasgrp1*^{Anaef} mice with a diverse TCR repertoire revealed no abnormalities in positive selection, Foxp3$^+$ T-regulatory (T-reg) cell differentiation or clonal deletion, in striking contrast to previously described *Rasgrp1* mutations.

Anaef diminishes canonical Rasgrp1-Ras-ERK signaling in response to *in vitro* stimulation

Despite the normal thymic development in *Rasgrp1*^{Anaef} animals, there was a striking biochemical effect of the *Rasgrp1*^{Anaef} mutation on activation of the canonical Rasgrp1-Ras-ERK signaling pathway in a range of *in vitro* stimulation assays. GFP-tagged wildtype- or *Anaef*-Rasgrp1 was transiently expressed in RasGRP1-deficient Jurkat cells (JPRM441) (Roose et al., 2005), which were either left unstimulated or stimulated with a combination of PMA (a synthetic analog of diacylglycerol) and ionomycin (a calcium ionophore). Gating on cells with different GFP intensities (**Supplementary Fig. S3a**) revealed that Rasgrp1^{Anaef} was hypomorphic (partial loss of function) for activating the Ras-ERK pathway: in GFP^{+} cells expressing Rasgrp1^{Anaef} there was only low ERK phosphorylation (P-ERK) and this was only modestly increased when PMA and ionomycin were added (**Fig. 6.4a**). By contrast, GFP^{+} cells expressing high levels of wildtype Rasgrp1 vector induced 5-times higher P-ERK spontaneously and this was doubled by PMA and ionomycin stimulation. Next, we stably reconstituted the JPRM441 cell line, which expresses ~10% of residual wildtype RasGRP1 protein (Roose et al., 2005) with *Rasgrp1*^{Anaef} or *Rasgrp1*^{wildtype} vectors and selected clones with Rasgrp1 expression levels similar to the parental Jurkat cell line (**Supplementary Fig. S3b**). Since JPRM441 cells do not express surface TCR (Roose et al., 2005), clonal cell lines were stimulated with PMA followed by RasGTP pull-down assays, which demonstrated that *Rasgrp1*^{Anaef} decreased PMA-induced GTP-loading of Ras to levels below that of the nontransfected JPRM441 cells (**Fig. 6.4b**). In the same transfected cell lines, PMA-induced P-ERK responses were decreased in *Rasgrp1*^{Anaef} expressing cells, most notable with the lower dose of PMA (PMA MED; 5ng/mL) and contrasted the effective induction of P-ERK signals in Jurkat and JPRM441-WT-Rasgrp1 cells (**Fig. 6.4c and 6.4d**). Similarly, *Rasgrp1*^{Anaef} expressing cells demonstrated less potent synergy in P-ERK

levels when ionomycin was combined with a very low PMA stimulus (2 ng/mL) (**Fig. 6.4e and Supplementary Fig. S3c**). In fact, P-ERK responses in JPRM441-Rasgrp1^{Anaef} cells were more impaired than in the parental JPRM441 cells, indicating a dominant negative effect, which was also observed at the level of Ras activation (**Fig. 6.4b**). We previously reported a dominant negative effect for ΔDAG-Rasgrp1, a form of Rasgrp1 lacking the DAG-binding C1 domain (ΔDAG) and we postulated that there may be competition with the residual ~10% of wildtype RasGRP1 (Roose et al., 2005). As Rasgrp1 is regulated by DAG-driven membrane recruitment (Ebinu et al., 1998, Roose et al., 2005) we examined this process for Rasgrp1^{Anaef}. EGFP-tagged wildtype or *Anaef* Rasgrp1-transfected JPRM441 cells were FACS sorted on low GFP expression to avoid overexpression artifacts and cells were allowed to adhere to coated slides. PMA stimulation resulted in membrane recruitment and cytoplasmic clearing of wildtype Rasgrp1; whereas these events were decreased for Rasgrp1^{Anaef} (**Fig. 6.4f**).

To test TCR-induced Ras-ERK signaling in thymocytes, we first stimulated thymocytes from wildtype or *Rasgrp1^{Anaef}* mice with anti-CD3 crosslinking antibodies and probed lysates for tyrosine-phosphorylated proteins to examine the global biochemical effects of the *Rasgrp1^{Anaef}* mutation. Both thymocyte populations demonstrated similar induction of total phospho-tyrosine patterns and similar activating phosphorylation of Lck and Zap-70 that lie upstream of Rasgrp1 **(Supplementary Fig. S4a)**. Rasgrp1's GEF activity is also enhanced by phosphorylation on T184 (Roose et al., 2005, Zheng et al., 2005). Using a new monoclonal antibody specific for P-T_{184}-Rasgrp1 **(Supplementary Fig. S4b**) we observed drastically impaired phosphorylation of T_{184}-Rasgrp1, and reduced ERK phosphorylation in *Rasgrp1^{Anaef}* thymocytes (**Fig. 6.5a**). By contrast, *Rasgrp1$^{+/-}$* thymocytes heterozygous for the null allele displayed readily detectable Rasgrp1- and ERK- phosphorylation (**Fig. 6.5b**), demonstrating that the signaling defects in the *Rasgrp1^{Anaef}* thymocytes are much greater than when the amount of Rasgrp1 is simply halved.

Thymocyte subset-specific P-ERK analyses revealed reduced anti-CD3- and PMA-induced responses in DP, CD4SP, and CD8SP *Rasgrp1*^{Anaef} thymocytes (**Fig. 6.5c and Supplementary Fig. S4c**), echoing the cell line conclusion that the *Anaef* mutation results in a partial loss of function with respect to induced Ras-ERK signaling. When pressure was placed on TCR-Ras-ERK signaling for positive selection *in vivo*, by introducing three different rearranged TCR transgenes that are prematurely expressed at higher than normal levels on DP thymocytes, a small decrease in positive selection was revealed in *Rasgrp1*^{Anaef} TCR-transgenic thymocytes compared to their wildtype controls (**Supplementary Fig. S5**). Collectively, these results lead to the surprising conclusion that the low affinity pMHC stimulation that drives physiological positive selection *in vivo* is remarkably robust to decreased Rasgrp1 activation of Ras-ERK.

Intrinsically dysregulated formation of Helios^{+} PD-1^{+} CD4^{+} T cells in *Rasgrp1*^{Anaef} mice

Given the evidence above for normal thymic formation of T cells in *Rasgrp1*^{Anaef} animals with normal TCR genes, we sought to define the peripheral CD4^{+} cell dysregulation that results in an expanded population of CD44^{hi} CD4^{+} T cells. Total splenocyte numbers and CD4 subsets were within the normal range in young *Rasgrp1*^{Anaef} animals, but between 50 and 150 days of age the frequencies of activated or memory CD44^{hi} Foxp3^{-} CD4^{+} cells increased, as did Foxp3^{+} CD4 cells, while the frequency of CD44^{low} Foxp3^{-} naïve CD4^{+} cells decreased (**Fig. 6.6a-c**).

Further resolution of CD4^{+} subsets based on intracellular cytokine staining revealed that interferon-γ producing cells were increased in frequency by a similar magnitude as CD44^{hi} cells as a whole (**Fig. 6.6d and data not shown**). Thus, there was no evidence that the Rasgrp1 mutation skewed T-helper cells towards a Th1 phenotype, but simply increased the number of activated or memory/effector CD4^{+} cells. Staining for PD-1 and CXCR5, whose high expression on CD4^{+} cells identifies T follicular helper (T_{FH}) cells (Ramiscal and Vinuesa, 2013) revealed a

dramatic expansion of these cells in *Rasgrp1*^{Anaef} mice (**Fig. 6.6e**). However most of the increase in CD44^{hi} Foxp3^{-} CD4^{+} cells in *Rasgrp1*^{Anaef} mice was due to a 600% increase in cells that expressed intermediate levels of PD-1 and CXCR5, and hence are unlikely to be T_{FH} cells, but were distinguished by high expression of the Helios transcription factor (**Fig. 6.6e**). Helios is highly expressed in Foxp3^{+} T-reg cells (Thornton et al., 2010), but in wildtype and *Rasgrp1*^{Anaef} mice Helios is also upregulated in a subset of Foxp3^{-} CD4^{+} cells, nearly all of which are CD44^{hi} (**Fig. 6.6f**). *Rasgrp1*^{Anaef} greatly increased this Helios^{+} CD44^{hi} Foxp3^{-} CD4^{+} population, which was also distinguished by high PD-1 expression in *Rasgrp1*^{Anaef} (**Fig. 6.6f**). *Rasgrp1*^{Anaef} mice had normal frequencies of CD95 (Fas)$^{+}$ GL-7^{+} germinal center B cells in the spleen (**Fig. 6.6g**), consistent with the conclusion that the accumulating Helios^{+} PD-1^{+} CXCR5^{int} Foxp3^{-} CD44^{hi} CD4^{+} cells were a distinct type of activated CD4^{+} cell but not fully differentiated T_{FH} cells.

To test if the dysregulated accumulation of Helios^{+} PD-1^{+} CXCR5^{int} CD44^{hi} CD4^{+} T cells in *Anaef* mice required B cells, *Rasgrp1*^{Anaef} animals were intercrossed with mice bearing a null mutation in the BCR subunit, CD79a (Yabas et al., 2011). In *Rasgrp1*^{Anaef} *Cd79a*^{null} animals lacking B cells, accumulation of PD-1^{+} Helios^{+} CD4^{+} T cells was profoundly suppressed (**Fig. 6.7a and 6.7b**). Indeed, the *Rasgrp1*^{Anaef}–driven distortion in relative frequencies of naïve, effector/memory and regulatory subsets of CD4 splenocytes was rectified by the absence of B cells in *Rasgrp1*^{Anaef} *Cd79a*^{null} mice (**Fig. 6.7c and 6.7d**). By contrast, the elevated CD44 expression on naïve CD4^{+} cells was still present (**Fig. 6.7e**) indicating this is a constitutive effect of the *Rasgrp1*^{Anaef} mutation.

The requirement for B cells could indicate they are needed as specialized antigen presenting cells, as is the case for T_{FH} cells (Ramiscal and Vinuesa, 2013), or that the *Anaef* mutation also acts in B cells since B cells also express Rasgrp1 (Stone, 2011). To resolve these alternatives, we used bone marrow from *Rasgrp1*^{Anaef} *Cd79a*^{null} animals mixed with wildtype *Rasgrp1*$^{+/+}$ marrow to generate chimeric mice where the *Rasgrp1*^{Anaef} mutation was excluded from B cells

but present in most of the T cells (experimental group B in **Fig. 6.7f-h**), and compared these with control chimeras where all hematopoietic cells were *Rasgrp1*^{Anaef} or *Rasgrp1*^{WT} (groups A, C and D in **Fig. 6.7**). Despite having the *Anaef* mutation in the T but not B cells of group B mice, a high proportion developed antinuclear autoantibodies comparable to the control group D where both B and T cells carried the *Anaef* mutation (**Fig. 6.7g**). Moreover, a high frequency and number of CD45.2^{+} *Rasgrp1*^{Anaef} CD4^{+} T cells acquired a Helios^{+} PD-1^{+} phenotype in Group B animals, unlike the co-resident CD45.1^{+} wildtype T cells (**Fig. 6.7i**). The accumulation of these activated CD4 T cells thus reflects a cell-autonomous effect of the *Anaef* mutation within the CD4 T cells and does not depend upon the *Anaef* allele being present in B cells.

CD44 expression is a sensitive reporter of mTOR activity in naïve T cells

Increased basal expression of the cell adhesion receptor, CD44, was a unique trait exhibited by naïve, CD62L-positive *Rasgrp1*^{Anaef} T cells (**Fig. 6.1b**). CD44 expression normally increases during differentiation of DP thymocytes into SP T cells, attains higher levels on naïve CD4 T cells than on naïve CD8 cells, and increases further on activated/memory T cells, but little was known about what determines the level of CD44 expressed. In cancer cells CD44 has been described as an mTOR target (Hsieh et al., 2012). In our ongoing peripheral blood screen of ENU mutagenized mouse pedigrees, we identified a strain, *chino*, with decreased CD44 expression on peripheral CD4^{+} CD62L^{hi} cells but relatively normal T cell numbers and subsets (**Fig 6.8a**). This unusual phenotype mapped to a single nucleotide change (T to G) in exon 5 of the mechanistic target of rapamycin (*Mtor*) gene, introducing serine in place of isoleucine at position 205 in the fifth predicted HEAT domain of the protein (Knutson, 2010) (**Fig. 6.8b**). This mTOR isoleucine residue is entirely conserved from mammals to yeast **(Supplementary Fig. S6)**. The mTOR HEAT-repeat domain forms a large superhelical structure that binds RAPTOR

to recruit substrates such as S6 kinase for phosphorylation by the mTOR kinase domain (Kim et al., 2002, Adami et al., 2007).

As the absence of *Mtor* is embryonic lethal in mice (Murakami et al., 2004, Gangloff et al., 2004), the fact that *Mtor*$^{chino/chino}$ (hereafter referred to as *Mtor*^{chino}) mice are viable but slightly smaller than wildtype (**Fig. 6.8c**) indicates that the *Mtor*^{chino} allele retains substantial function. Consistent with a subtle decrease in mTOR activity, TCR-induced phosphorylation of ribosomal protein S6 (P-S6) was modestly decreased but not abolished in *Mtor*^{chino} CD4^{+} splenocytes (**Fig. 6.8d**). The numbers of DP, CD4SP and CD8SP thymocytes were normal in *Mtor*^{chino} mice **(Fig 6.8e)**. Whereas expression of CD69, CD5 and TCRβ on DP and SP thymocytes was normal, CD44 expression was decreased on *Mtor*^{chino} CD4SP and CD8SP thymocytes **(Fig. 6.8f**). CD44 expression on peripheral blood CD4^{+} T cells decreased in an *Mtor*^{chino} allele dose-dependent manner **(Fig. 6.8g**), demonstrating that CD44 expression is a highly sensitive reporter of small changes in basal mTOR activity in CD4^{+} T cells. This conclusion is reinforced by supplementary data from two studies: mice with a *neo*-insertion in an *Mtor* intron that decreases *Mtor* mRNA approximately 70% show a similar selective lowering of CD44 on CD4^{+} T cells (Zhang et al., 2011) and CD44 levels are also reduced on naïve, CD62L-positive T cells that are deficient for the mTOR activator Rheb or deficient for the mTOR-interacting protein Rictor (Delgoffe et al., 2011). Furthermore, we found that pharmacological inhibition of mTOR with rapamycin in mice treated with low doses that avoid toxicity (Coenen et al., 2007, Araki et al., 2009), resulted in a dose-dependent decrease in CD44 expression on wildtype and *Rasgrp1*^{Anaef} thymocytes as well (**Fig. 6.8h**).

Rasgrp1^{Anaef} exaggerates basal mTOR-S6 signaling and CD44 expression in T cells

Our finding that tonic CD44 expression on naïve T cells sensitively reports small changes in mTOR activity prompted further analysis of this pathway in *Rasgrp1*^{Anaef} T cells. CD44 was elevated on *Rasgrp1*^{Anaef} DP and SP thymocytes, in diametric contrast to decreased CD44 on these cells in *Rasgrp1*$^{-/-}$ knockout mice (**Fig 6.9a and 6.9b**) (Priatel et al., 2007). A putative defect in regulatory T cells cannot explain the increased CD44 expression on naïve *Rasgrp1*^{Anaef} CD4^{+} cells, because in mixed chimeras bearing many wild-type Foxp3^{+} CD4 cells, CD44 expression was still increased on *Rasgrp1*^{Anaef} but not on co-resident wild-type CD62L^{+} FOXP3^{-} CD4^{+} splenocytes (**Fig 6.9c)**. The cell autonomous increase in CD44 expression was detectable on *Rasgrp1*^{Anaef} SP and DP thymocytes (**Supplementary Fig. S7a and S7b**) and even on CD4^{+} cells expressing a transgenic TCR (**Fig 6.9d**). Elevated CD44 expression on *Rasgrp1*^{Anaef} cells was selective: there were no distinguishable differences between wild type and *Rasgrp1*^{Anaef} cells in CD69 and TCRβ, which are markers of cumulative Ras signaling (D'Ambrosio et al., 1994, Genot and Cantrell, 2000, Starr et al., 2003), nor in CD5 expression, a sensitive reporter of TCR affinity and constitutive or tonic TCR signaling (Azzam et al., 1998, Mandl et al., 2013) (**Fig 6.9e and Supplementary Fig. S7a and S7b**), and rapamycin treatment *in vivo* selectively reduced the increased CD44 expression on *Rasgrp1*^{Anaef} cells (**Fig. 6.8h**) but did not impact TCR or CD69 expression (**data not shown**).

Consistent with the CD44 data, P-S6 levels in unstimulated TCRβ^{low} (pre-selection) DP thymocytes were modestly increased in *Rasgrp1*^{Anaef} mice whereas they were decreased in cells from *Rasgrp1*$^{-/-}$ mice (**Fig. 6.10a**). CD44 levels gradually rise as T cells mature from DP to SP and peripheral naïve T cells, suggesting that CD44 expression may reflect basal or tonic signaling. Such signals can be visualized by constitutive tyrosine-phosphorylation of the TCRζ chains and other proteins (van Oers et al., 1993), basal levels of ZAP70 recruitment to phosphorylated zeta chains (van Oers et al., 1994, Stefanova et al., 2002), and tonic

phosphorylation of ERK (Roose et al., 2003, Markegard et al., 2011). Furthermore, these signals dissipate when T cells are rested *in vitro* in non-stimulatory medium (van Oers et al., 1993, Stefanova et al., 2002). We investigated tonic mTOR-S6 signals and found substantial basal P-S6 levels in freshly isolated lymph node cells that decreased when cells were serum-starved *in vitro* (**Fig. 6.10b**). A recent study reported that naive $CD4^+$ T cells display a range of CD5 expression in which the $CD5^{high}$ cells receive most tonic signal input and are most immune reactive (Mandl et al., 2013). We first sorted $CD44^{low}$ naïve $CD4^+$ T cells into the most bright and most dim expression for CD5 and determined that $CD5^{high}$ naïve $CD4^+$ T cells have significantly more P-S6 than their $CD5^{low}$ counterparts (**Fig. 6.10c**). Next, dividing $CD5^{low}$ and $CD5^{high}$ naïve $CD4^+$ T cells in equal 50%-50% splits revealed that basal P-S6 was increased in *Rasgrp1*^{Anaef}, particularly in the $CD5^{low}$ subset compared to wild type cells (**Fig. 6.10d**). The exact origin of tonic signals in T cells and its function being either immune stimulatory or immune suppressive is still an area of debate (Stefanova et al., 2002, Smith et al., 2001, Polic et al., 2001, Hogquist et al., 2003, Bhandoola et al., 2002), but at least part of the tone appears to be generated by low affinity TCR binding to self pMHC (Stefanova et al., 2002). To examine if self-peptide/MHCII recognition plays a role in the increased CD44 expression on *Rasgrp1*^{Anaef} naïve $CD4^+$ T cells, we adoptively transferred a mixture of wild-type and *Rasgrp1*^{Anaef} splenocytes into wild-type or MHCII(*H2-Aa*)–deficient recipient mice (**Supplementary Fig. S8**). Maintenance of CD5 expression on T cells requires contact with self pMHC (Smith et al., 2001, Mandl et al., 2012) and, as expected, CD5 expression on wildtype $CD4^+$ $CD62L^+$ $Foxp3^-$ T cells decreased in MHCII-deficient hosts (**Fig. 6.10e**), consistent with the hypothesis that CD5 is a sensitive reporter of TCR signal strength. By contrast, CD44 levels were similar irrespective of MHCII expression in the adoptive hosts, and CD44 levels remained higher on *Rasgrp1*^{Anaef} than co-transferred wild-type cells in both contexts (**Fig. 6.10e**). These data reveal constitutively increased expression of two reporters of mTOR activity in *Rasgrp1*^{Anaef} naïve $CD4^+$ T cells: the well-established reporter P-S6 and the reporter clarified here, CD44. The fact that the

Rasgrp1^{Anaef}–driven increase in CD44 is retained in the absence of MHCII suggests that this tonic signal is at least partially independent of triggering of TCRs by self-pMHC.

CD44^{+} Helios^{+} PD-1^{+} CD4^{+} T cell accumulation and autoantibodies in *Rasgrp1*^{Anaef} mice are corrected by hypomorphic mTOR mutation.

To test the role of elevated mTOR signaling in the *Rasgrp1*^{Anaef}–induced overexpression of CD44 in naïve T cells and in the accumulation of activated CD44^{hi} PD-1^{+} CD4^{+} cells and autoantibodies, *Rasgrp1*^{Anaef} mice were intercrossed with the subtle loss-of-function *Mtor*^{chino} strain. Using a CD62L^{+} Foxp3^{-} gate to resolve naïve CD4^{+} splenocytes, we found that the *Mtor*^{chino} mutation abolished the *Rasgrp1*^{Anaef}–driven increase in CD44 expression in these naïve T cells (**Fig 6.11a**). The *Mtor*^{chino} mutation alone resulted in a decrease in numbers of splenocytes, including CD4^{+} cells, as was observed in mice with reduced *Mtor* mRNA (Zhang et al., 2011), but the relative proportions of the CD4^{+} subsets examined were normal (**Fig. 6.11b**). Whereas *Rasgrp1*^{Anaef} mice with normal mTOR accumulated a high frequency of CD44^{hi} Foxp3^{-} CD4^{+} splenocytes, including the prominent PD-1^{+} Helios^{+} subset, this was corrected down to normal numbers in *Rasgrp1*^{Anaef} *Mtor*^{chino} double mutants (**Fig 6.11b and 6.11c**). Moreover, in bone marrow chimeras bearing *Rasgrp1*^{Anaef} *Mtor*^{chino} double-mutant hematopoietic cells, the frequency of animals with antinuclear autoantibodies was corrected to the low frequency observed in control chimeras with wildtype *Rasgrp1* and *Mtor* (**Fig 6.11d**). Collectively, these results establish that accumulation of CD44^{hi} Helios^{+} PD-1^{+} CD4^{+} cells and autoantibodies induced by *Rasgrp1*^{Anaef} is sensitive to small differences in mTOR signaling.

DISCUSSION

The findings here reveal a new role for Rasgrp1 in the cell-intrinsic regulation of peripheral $CD4^+$ T cells. By analyzing a missense mutation in the Rasgrp1 EF-hand, the results dissociate this new function of Rasgrp1 from its well-known role in thymic positive selection. While the *Anaef* EF-hand mutation did decrease Rasgrp1 activation of Ras and ERK when thymocytes were stimulated acutely by antibodies to CD3 or with PMA *in vitro*, the activity of this pathway during physiological positive selection *in vivo* remained sufficient for normal numbers of single positive thymocytes and peripheral T cells to form even under competitive reconstitution conditions. T cell lymphopenia and sparse T cell repertoires secondary to defective positive selection potentially explain the autoantibodies observed in mice where Rasgrp1 is entirely absent or C-terminally deleted (Priatel et al., 2007, Dower et al., 2000, Coughlin et al., 2005, Fuller et al., 2012), and in animals with missense mutations in ZAP-70 or LAT (Sakaguchi et al., 2003, Siggs et al., 2007, Aguado et al., 2002, Sommers et al., 2002). By contrast, the normal thymic development coupled with experiments in mixed bone marrow chimeras where wild-type and mutant T cells co-exist rules out this possibility for the *Rasgrp1*^{Anaef} mutation, and shows that peripheral CD4 cells are intrinsically dysregulated. By a combination of biochemical and genetic studies, we identify overactive mTOR signaling within naïve CD4 T cells as a key component for *Rasgrp1*^{Anaef} to drive two abnormalities: 1) a constitutive increase in CD44 expression in naïve CD4 T cells and 2) a gradual accumulation of peripheral $Helios^+$ $CD44^{hi}$ CD4 cells and autoantibodies.

Rasgrp1^{Anaef}'s effect on Ras/ERK signaling *in vivo* was much milder than expected from its effects in *in vitro* assays. In response to relatively strong *in vitro* stimuli, the *Rasgrp1*^{Anaef} mutation results in impaired membrane recruitment and T_{184} phosphorylation of Rasgrp1 as well as reduced activation of Ras-ERK, establishing that *Rasgrp1*^{Anaef} is a hypomorphic (partial loss-of-function) allele under these conditions. By contrast, *in vivo*, *Rasgrp1*^{Anaef} did not alter CD69 and TCRβ induction or positive selection of thymocytes, unlike the C-terminally deleted

(*Rasgrp1*$^{d/d}$) and knockout (*Rasgrp1*$^{-/-}$) alleles which caused moderate and severe decreases in these processes, respectively. This may indicate that the cumulative Ras-ERK signals required for these events are sufficiently buffered or robust that they tolerate a modest reduction in Rasgrp1's Ras activating activity. Only when a TCR transgene was prematurely expressed at higher than normal levels in DP thymocytes was there a measurable deficit in positive selection, and even under these conditions there was a small decrease in positive selection compared even to the subtle *Zap70*^{murdock} mutation (Siggs et al., 2007). This is surprising given that the induction of these signals involves low affinity pMHC binding by the TCR, which might be expected to be particularly sensitive to small changes in Ras-ERK signal strength (Kortum et al., 2013).

CD44 expression on thymocytes is decreased in the complete absence of Rasgrp1 (**Fig. 6.9**) (Priatel et al., 2007) and increased by oncogenic Ras (Kindler et al., 2008, Zhang et al., 2009, Wang et al., 2011) establishing that CD44 expression in thymocytes is positively regulated by Ras. T-cell CD44 expression is also sensitive to mTOR activity, being reduced by the partial loss-of-function *Mtor*^{chino} (**Fig. 6.8**) and *Mtor*^{tm1Lgm} (Zhang et al., 2011) alleles, and dramatically decreased in the absence of Rictor (Delgoffe et al., 2011), a binding partner of mTOR. *Rasgrp1*^{Anaef} thymocytes and naïve CD4 T cells have increased CD44 and P-S6 expression, suggesting that the *Anaef* mutation increases either Rasgrp1/Ras/ERK signaling or PI-3-kinase/mTOR/S6 signaling, or both. Our recent biophysical studies revealed that Rasgrp1's EF hands keep the protein in an autoinhibited, dimeric state, and modeling indicates that calcium-binding to the EF domain would relieve autoinhibition (Iwig et al., 2013). Thus, Rasgrp1's EF hands play both stimulatory- and inhibitory- roles that may result in the EF2 substitution in *Rasgrp1*^{Anaef} decreasing maintenance of the autoinhibited state in the absence of strong TCR stimuli and decreasing RasGRP1 activation during strong TCR stimulation. Evidence exists for multiple intersections between the RasGRP1/Ras/ERK/RSK and PI-3-

kinase/mTOR/S6 pathways, including at the level of Ras with PI-3-kinase (Castellano and Downward, 2010) and at the level of RSK with S6 (Salmond et al., 2009). While the mechanism is currently unclear, the current evidence suggests that *Rasgrp1*^{Anaef}'s gain-of-function in naïve T cells in the absence of strong TCR stimulation – and apparently in the absence of MHC II ligands for the TCR (**Fig 6.10e**) - activates S6-CD44 more than it activates ERK-CD69.

In T cells, the mTOR pathway is activated by strong TCR stimulation (Gorentla et al., 2011) and is required for efficient differentiation of naïve CD4 cells into effector cells (Delgoffe et al., 2009). T-cell-specific deletion of Tsc1, a negative regulator of mTOR, results in increased levels of P-S6 and an exuberant response to TCR stimulation in naïve T cells (Yang et al., 2011). Increased mTOR stimulation by Rasgrp1^{Anaef} may allow self-antigens to activate some naïve CD4 cells, resulting in the gradual accumulation of activated CD62L^{low} CD44^{hi} PD-1^{+} HELIOS^{+} T cells and antinuclear autoantibodies. Because accumulation of PD-1^{+} HELIOS^{+} T cells in *Rasgrp1*^{Anaef} mice requires B cells (**Fig. 6.7**), these T cells might require B cells as specialized APCs or they might require Fc receptor-dependent enhancement of antigen presentation by antibodies (Silva et al., 2011).

Given the huge number of missense variants in each person (2010), patients with autoimmune diseases are more likely to have point mutations in various genes than complete loss of gene expression. This new *Rasgrp1*^{Anaef} mouse model adds to an emerging category of animal models with point mutations in TCR signaling proteins, along with *Zap70*^{skg} (Sakaguchi et al., 2003), *Zap70*^{murdock} and *Zap70*^{mrtless} hypomorphic alleles (Siggs et al., 2007), LAT^{Y136F} mice (Aguado et al., 2002, Sommers et al., 2002), and *Card11*^{unmodulated} mice (Jun et al., 2003), where a partial deficit in T cell signaling precipitates autoimmunity or allergy. *RASGRP1* splice variants have been documented for patients with SLE (Yasuda et al., 2007) and abnormal microRNA-driven downregulation of Rasgrp1 expression may play a role in aberrant DNA

methylation in Lupus $CD4^+$ T cells (Pan et al., 2010). In addition, *RASGRP1*-linked SNVs have been associated with autoimmune diabetes and thyroid disease (Plagnol et al., 2011, Qu et al., 2009). Of the 13 uncharacterized *RASGRP1* missense SNVs currently known, rs62621817 is of particular interest here since it causes a missense variation in RasGRP1's first EF hand, changing a conserved, negatively charged aspartic acid into a valine residue. We propose that *Rasgrp1*^{Anaef} mice may provide a useful model system for further studies to help elucidate how *RASGRP1* variants contribute to autoimmune disease, and to help target future efforts to modulate this pathway pharmacologically.

FIGURES

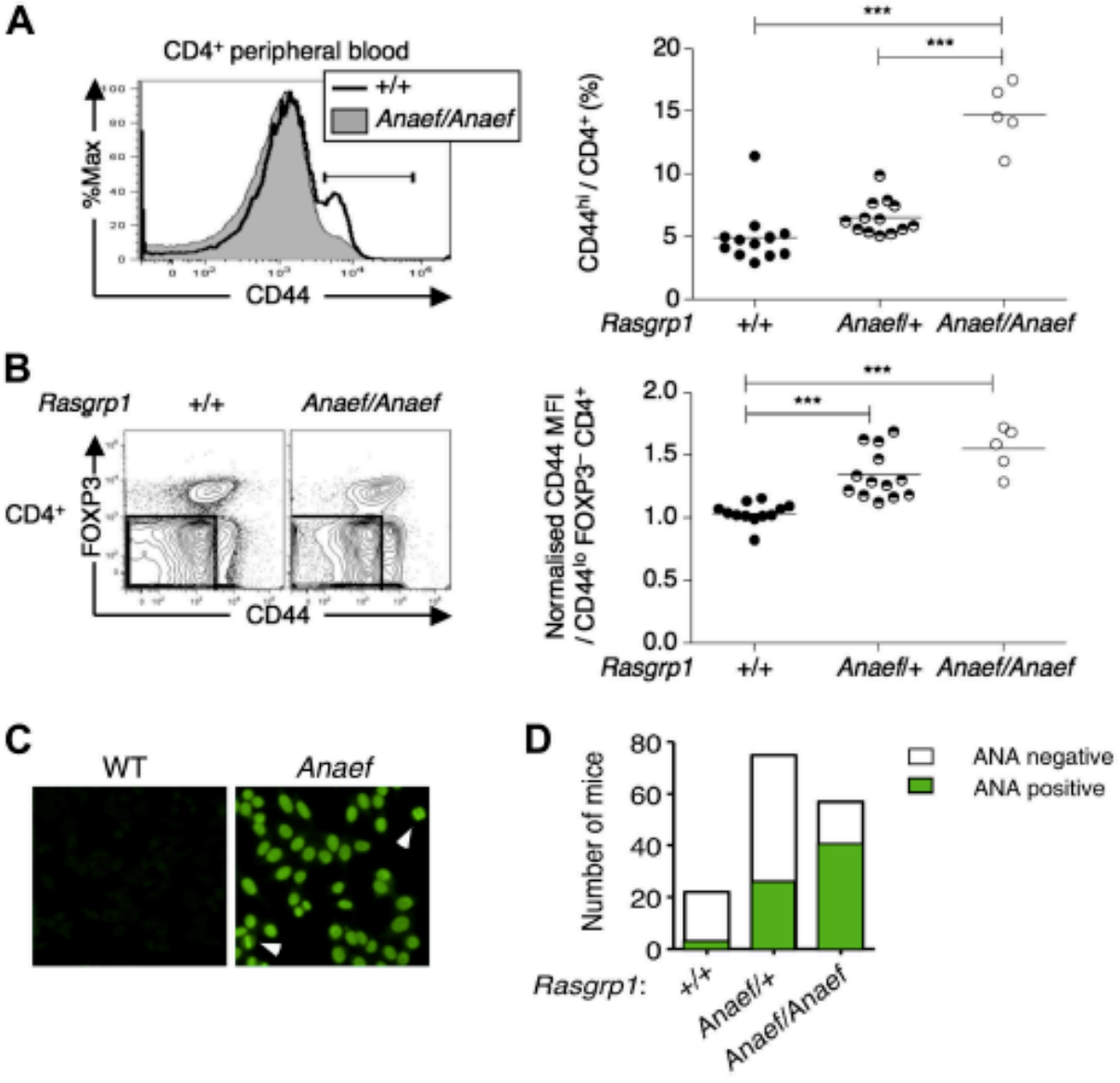

A
CD4+ peripheral blood
+/+
Anaef/Anaef
%Max
CD44
CD44hi / CD4+ (%)
Rasgrp1 +/+ Anaef/+ Anaef/Anaef
B
Rasgrp1 +/+ Anaef/Anaef
CD4+
FOXP3
CD44
Normalised CD44 MFI / CD44lo FOXP3− CD4+
C
WT
Anaef
D
Number of mice
ANA negative
ANA positive
Rasgrp1: +/+ Anaef/+ Anaef/Anaef

Figure 6.1: An ENU mouse mutant with increased CD44hi CD4 cells and anti-nuclear autoantibodies

(a, b) Representative flow cytometry showing on peripheral blood $CD4^+$ cells (a) CD44 expression with the gate used to define $CD44^{hi}$ cells and (b) FOXP3 vs CD44 phenotype including normalized CD44 Mean Fluorescence Intensity (MFI) of the gated $CD44^{lo}$ $FOXP3^-$ subset from *Rasgrp1*$^{+/+}$ (WT), heterozygous *Rasgrp1*$^{Anaef/+}$ or homozygous *Rasgrp1*$^{Anaef/Anaef}$ mice. Statistical analysis (right) used unpaired Student's T tests where each symbol represents an individual mouse; *** $p < 0.001$.

(c) Antinuclear antibodies (ANA) in diluted blood plasma from a B6xB10.*Rasgrp1*^{Anaef} mouse and wildtype littermate, measured by indirect immunofluorescence on HEp-2 cells. Note homogeneous nuclear staining of interphase cells and positive chromatin bars in dividing cells (marked with arrow). Magnification 20x.

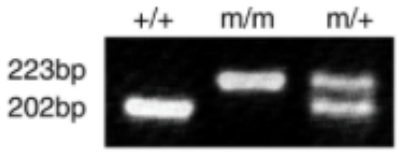
(d) Quantitation of positive ANA results for wildtype, *Rasgrp1*$^{Anaef/+}$ and *Rasgrp1*$^{Anaef/Anaef}$ C57Bl/6xC57Bl/10 siblings tested at 15 weeks of age.

A

	SNP Position (Mb)								
	101.9	104.9	114	115.3	117.7	121.2	121.6	145.7	
B6 Control	B6	B6	B6	B6	B6	B6	B6	B6	
CBA Control	CBA	CBA	CBA	CBA	CBA	CBA	CBA	CBA	
AnaefxCBA F2 #40	Het	Het	Het	Het	Het	Het	Het	Het	Unaffected Littermates
AnaefxCBA F2 #103	Het	Het	Het	Het	Het	Het	Het	Het	
AnaefxCBA F2 #66	CBA	CBA	CBA	CBA	CBA	CBA	CBA	CBA	
AnaefxCBA F2 #126	CBA	CBA	CBA	CBA	CBA	CBA	CBA	CBA	
AnaefxCBA F2 #10	B6	B6	B6	B6	B6	B6	B6	Het	Affected *Anaef*
AnaefxCBA F2 #74	Het	Het	B6	B6	B6	B6	B6	B6	
AnaefxCBA F2 #136	CBA	CBA	CBA	Het	Het	Het	Het	Het	
AnaefxCBA F2 #190	B6	B6	B6	B6	B6	Het	Het	Het	
AnaefxCBA F2 #234	Het	Het	B6	B6	B6	B6	B6	B6	
AnaefxCBA F2 #242	B6	B6	B6	B6	B6	B6	B6	B6	

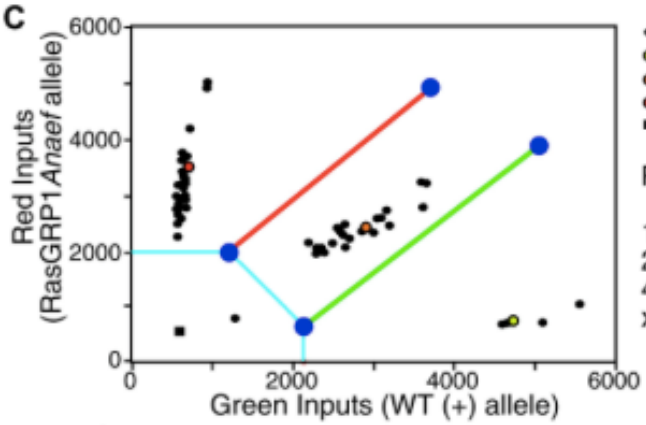
Region of Interest 114-121.2 Mb

B



Primer Sequences:
R519G Forward -
5'AGGCTGCCTCTCTTTCTCAC3'
R519G Reverse wild type -
5'TCATGAAGTAGGCCGTGATCTCG
TCGCT3'
R519G Reverse mutant -
5'TGGAATAGATGGAGCTGGCCCC
TATGAAGTAGGCCGTGATCTCGTA
TCC3'

C



- Individual mouse
- +/+ control
- *Anaef*/+ control
- *Anaef*/*Anaef* control
- no DNA control

Program Cycle:

10" 95°C
20" 60°C
40" 72°C
x 35 cycles

Primer Sequences:
8B6004-1 -
5'GAAGGTGACCAAGTTCATGCTGTAGGCCGTGATCTCGTCTCT3'
8B66004-2 -
5'GAAGGTCGGAGTCAACGGATTTAGGCCGTGATCTCGTCTCC3'
8B6004-R -
5'CCTGACCTCAATGACCTGACTAT3'

Figure 6.1 – Supplemental Figure 1: Mapping and genotyping of the Rasgrp1 mutation in ENU mutant mice with anti-nuclear antibodies and CD44hi phenotype

(S1a) SNP analysis of a cohort of F2 mice generated by outcrossing a B6 animal identified as "affected" with CBA, then incrossing F1 offspring to produce the (ENU.B6 x CBA/J)F2 animals listed. Phenotypes of affected mice tracked with a genomic region between 114-121.2 on chromosome 2. The Rasgrp1 gene lies in this interval.

(S1b) Genotyping of *Rasgrp1*$^{Anaef/Anaef}$, *Rasgrp1*$^{Anaef/WT}$, and wildtype mice in the Roose lab was performed using MS-PCR as described (Rust et al., 1993, Bottema and Sommer, 1993). Products are wt: 202bp and R519G: 223bp.

(S1c) Genotyping of *Rasgrp1*$^{Anaef/Anaef}$, *Rasgrp1*$^{Anaef/WT}$, and wildtype mice using Amplifluor PCR in the Goodnow Lab. The *Rasgrp1*^{Anaef} strain was established through ethylnitrosourea (ENU)-mediated mutagenesis of B6 mice at the Australian National University as previously described (Randall et al., 2009).

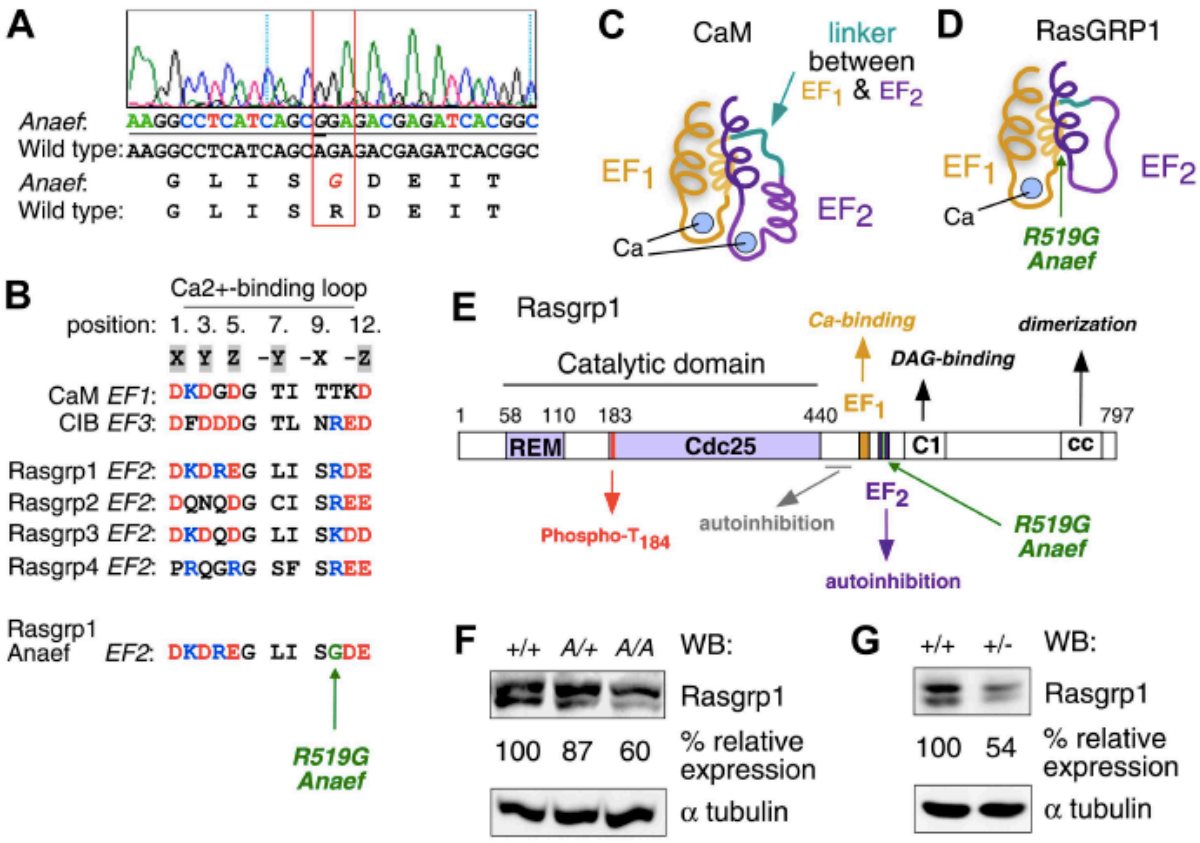

A
Anaef: AAGGCCTCATCAGCGGAGACGAGATCACGGC
Wild type: AAGGCCTCATCAGCAGAGACGAGATCACGGC
Anaef: G L I S G D E I T
Wild type: G L I S R D E I T
B
Ca2+-binding loop
position: 1. 3. 5. 7. 9. 12.
X Y Z -Y -X -Z
CaM EF1: DKDGDG TI TTKD
CIB EF3: DFDDDG TL NRED
Rasgrp1 EF2: DKDREG LI SRDE
Rasgrp2 EF2: DQNQDG CI SREE
Rasgrp3 EF2: DKDQDG LI SKDD
Rasgrp4 EF2: PRQGRG SF SREE
Rasgrp1 Anaef EF2: DKDREG LI SGDE
R519G Anaef
C
CaM
linker between EF1 & EF2
EF1
EF2
Ca
D
RasGRP1
EF1
EF2
Ca
R519G Anaef
E
Rasgrp1
Catalytic domain
Ca-binding
dimerization
DAG-binding
EF1
1 58 110 183 440 797
REM
Cdc25
C1
cc
Phospho-T184
autoinhibition
EF2
autoinhibition
R519G Anaef
F
+/+ A/+ A/A WB:
Rasgrp1
100 87 60 % relative expression
α tubulin
G
+/+ +/- WB:
Rasgrp1
100 54 % relative expression
α tubulin

Figure 6.2: Mapping of the ENU mutation to the autoinhibitory second EF hand domain in Rasgrp1

(a) Sequence trace of *Rasgrp1*^{Anaef} exon 13 aligned to wildtype Rasgrp1 sequence.

(b) Sequence comparison of CaM (calmodulin), CIB (calcium and integrin binding protein) and Rasgrp1, -2, -3 and -4 EF hands with conserved residues highlighted. (Acidic, red; Basic, blue; Calcium-binding residues, highlighted in grey; ENU-mutated residue in green).

(c, d) Model of a typical pair of EF hands with two calcium (Ca)-binding loops each flanked by N- and C-terminal α-helices based on CaM (c). Model including the atypical second EF hand in RasGRP1 (d). RasGRP1's second EF hand does not bind calcium and the E helix has evolved into an autoinhibitory domain (Iwig et al., 2013).

(e) Linear schematic of Rasgrp1 protein domains, phosphorylation site threonine 184, and position of R519G mutation in the second EF hand that evolved into a domain for autoinhibition.

(f, g) Western blot for Rasgrp1 protein in thymocytes from *Rasgrp1*$^{Anaef/Anaef}$ (A/A), heterozygous *Rasgrp1*$^{Anaef/WT}$ (A/+), heterozygous *Rasgrp1*$^{Null/WT}$ (+/-), and wildtype (+/+) mice. Blot was reprobed for α-tubulin as a loading control. Relative Rasgrp1 expression was calculated and is shown. Note the expression of Rasgrp1‘s typical doublet, thought to be due to alternative translation initiation (Poon and Stone, 2009). Representative blots of at least 3 independent experiments.

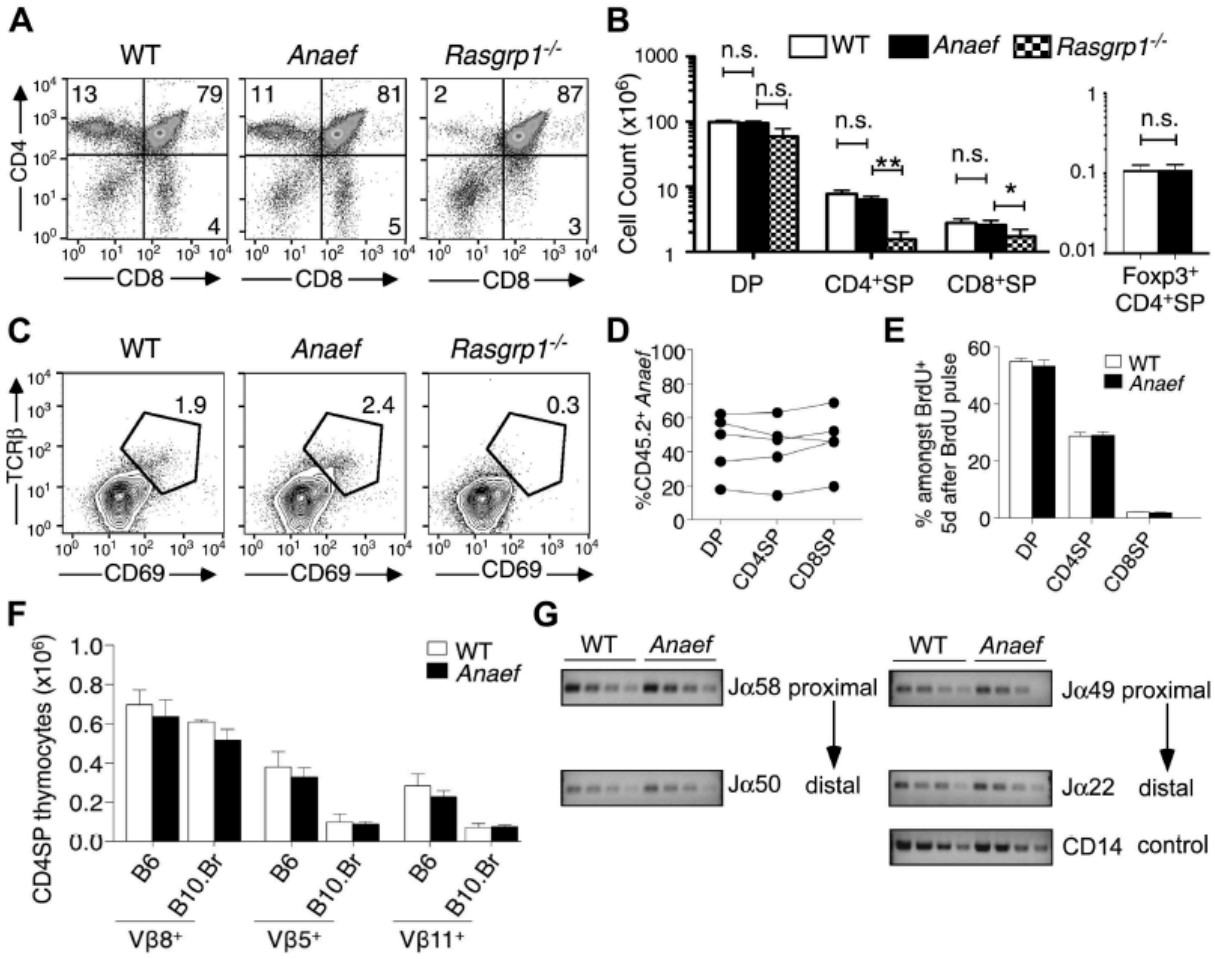

A
WT
Anaef
Rasgrp1-/-
CD4
CD8
13
79
4
11
81
5
2
87
3
B
WT
Anaef
Rasgrp1-/-
Cell Count (x10^6)
n.s.
**
*
DP
CD4+SP
CD8+SP
Foxp3+ CD4+SP
C
TCRβ
CD69
1.9
2.4
0.3
D
%CD45.2+ Anaef
DP
CD4SP
CD8SP
E
% amongst BrdU+ 5d after BrdU pulse
F
CD4SP thymocytes (x10^6)
B6
B10.Br
Vβ8+
Vβ5+
Vβ11+
G
Jα58 proximal
Jα50 distal
Jα49 proximal
Jα22 distal
CD14 control

Figure 6.3: *Rasgrp1*^{Anaef} differs from *Rasgrp1*^{null} by preserving T cell selection in the thymus

(a) CD4/CD8 phenotype of thymocytes in wildtype, *Rasgrp1*^{Anaef}, and *Rasgrp1*$^{-/-}$ mice.

(b) Number of DP, CD4SP and CD8SP as well as Foxp3+ CD4SP thymocytes in wildtype (n = 36), *Rasgrp1*^{Anaef} (n = 35), and *Rasgrp1*$^{-/-}$ (n = 3) mice. Student's t tests P value symbols: ** $p < 0.005$, * $p < 0.05$.

(c) Percentages of CD69^{hi} TCRβ^{hi} cells among DP cells. Representative of 3 mice per genotype.

(d) Competitive repopulation of thymic subsets in irradiated CD45.1^{+} B6 recipient mice reconstituted with a mixture of CD45.1^{+} WT and CD45.2^{+} *Rasgrp1*^{Anaef} bone marrow cells. The percentage of CD45.2^{+} cells amongst the indicated thymocyte subsets was determined 8 weeks after reconstitution. Lines connect measurements from individual mice. Data are representative of three separate chimera cohorts.

(e) Mixed bone marrow chimeras bearing CD45.1^{+} WT and either CD45.2^{+} WT or CD45.2^{+} *Rasgrp1*^{Anaef} hematopoietic cells were injected i.p. with 1 mg BrdU 5 days before analysis. The percentages of DP, CD4SP and CD8SP cells amongst BrdU-labelled CD45.2^{+} *Rasgrp1*^{Anaef} (black columns) or CD45.2^{+} WT (white columns) thymocytes were determined and the mean ± s.e.m (n=5 mice per group) is shown. See Supplementary Fig. 2a for flow cytometry gates.

(f) Mean ± s.e.m number of CD4SP thymocytes expressing TCR Vβ8, which is not superantigen reactive, or Vβ5 or Vβ11 that recognize endogenous retroviral superantigen presented by the I-E MHC II molecule, in B6 mice lacking I-E and in B10.BR expressing the I-E (n=3 mice per group compiled from 2 experiments).

(g) Analysis of Jα usage in sorted CD4SP thymocytes of wildtype or *Rasgrp1*^{Anaef} mice following published methods. PCR was performed using serial 1:2 dilutions of template DNA with primer sets that reveal rearrangements proximal (Jα58, Jα49) or distal (Jα50, Jα22) to the two

promoters. Figure 2g is representative of three independent experiments. See supplementary figure S2b for details on promoter use, additional Jα segments, and published methods.

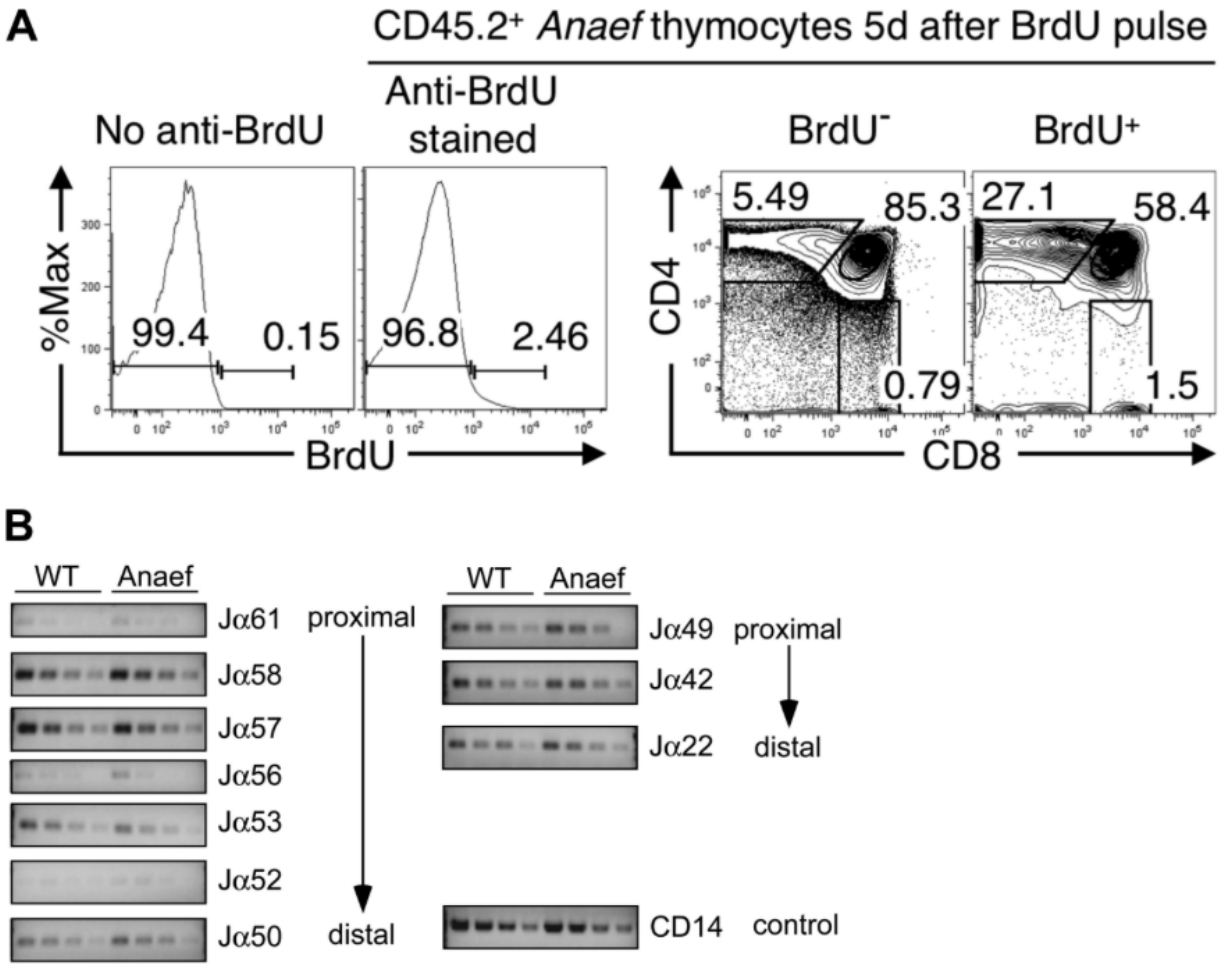

A
CD45.2+ Anaef thymocytes 5d after BrdU pulse
No anti-BrdU
Anti-BrdU stained
BrdU-
BrdU+
%Max
99.4
0.15
96.8
2.46
BrdU
CD4
5.49
85.3
0.79
27.1
58.4
1.5
CD8
B
WT
Anaef
Jα61
Jα58
Jα57
Jα56
Jα53
Jα52
Jα50
proximal
distal
WT
Anaef
Jα49
Jα42
Jα22
proximal
distal
CD14
control

Figure 6.3 – Supplemental Figure 2: Comparison of thymocyte maturation kinetics in WT and *Rasgrp1*^{Anaef}

(S2a) Gating strategy to analyze thymocyte maturation kinetics in Fig. 2E. Histograms and plots show CD45.2$^+$ *Anaef* thymocytes in mixed chimeras bearing CD45.1$^+$ WT plus CD45.2$^+$ *Anaef* hematopoietic cells. The histogram second from the left shows gates defining BrdU$^-$ and BrdU$^+$ subsets of CD45.2$^+$ *Anaef* thymocytes, each of which was analysed for CD4 versus CD8 expression in the right two plots. The CD4/CD8 plots indicate that the BrdU$^+$ subset has a higher frequency of SP cells, demonstrating the specificity of the BrdU$^+$ gate. Gating defining DP, CD4SP and CD8SP subsets amongst BrdU$^+$ cells (far right plot) were used to compile Fig. 2e.

(S2b) Analysis of Jα usage in sorted CD4$^+$ SP thymocytes of wildtype or Anaef mice following published methods (Abarrategui and Krangel, 2006). PCR was performed using serial 1:2 dilutions of template DNA with primer sets. Primer sequences for the PCR were identical to those formerly reported (identity of sequences between 129 mice and C57/Bl6 mice was verified in the databases). Two promoters regulate the rearrangements; TEA (T-Early-α), which regulated Jα61 to Jα50 and the Jα49 promoter that regulated Jα49 and more distal segments such as Jα22. As described, CD14 was used as control. A representative experiment with CD4$^+$ SP from three independent experiments is shown here. We did not observe significant differences in Jα segments between DP thymocytes from wildtype and *Rasgrp1*^{Anaef} mice either (not shown).

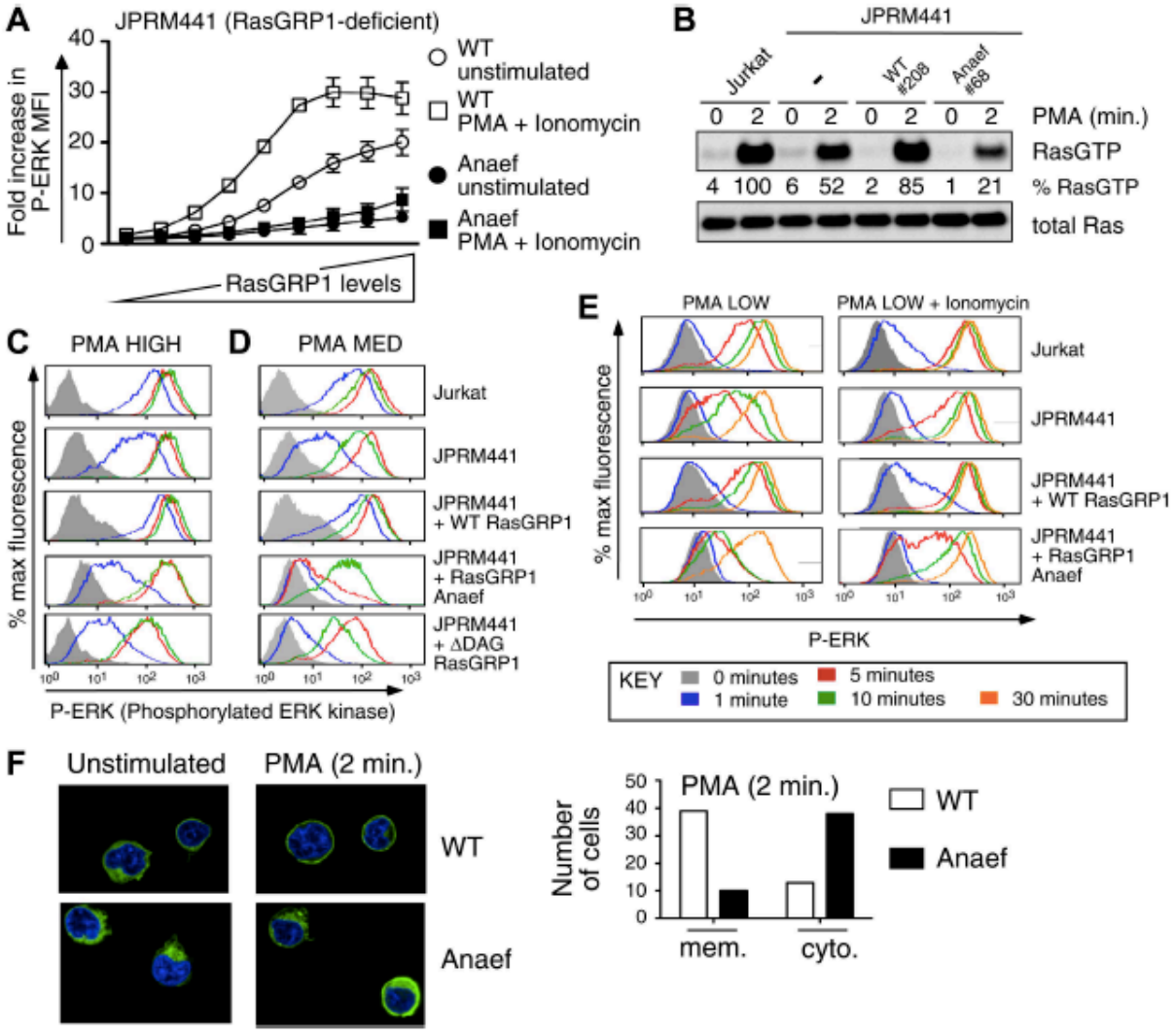

A
JPRM441 (RasGRP1-deficient)
Fold increase in P-ERK MFI
40
30
20
10
0
WT unstimulated
WT PMA + Ionomycin
Anaef unstimulated
Anaef PMA + Ionomycin
RasGRP1 levels
B
JPRM441
Jurkat
WT #208
Anaef #68
0 2 0 2 0 2 0 2
PMA (min.)
RasGTP
4 100 6 52 2 85 1 21
% RasGTP
total Ras
C
PMA HIGH
D
PMA MED
% max fluorescence
Jurkat
JPRM441
JPRM441 + WT RasGRP1
JPRM441 + RasGRP1 Anaef
JPRM441 + ΔDAG RasGRP1
P-ERK (Phosphorylated ERK kinase)
E
PMA LOW
PMA LOW + Ionomycin
% max fluorescence
Jurkat
JPRM441
JPRM441 + WT RasGRP1
JPRM441 + RasGRP1 Anaef
P-ERK
KEY
0 minutes
1 minute
5 minutes
10 minutes
30 minutes
F
Unstimulated
PMA (2 min.)
WT
Anaef
Number of cells
PMA (2 min.)
50
40
30
20
10
0
WT
Anaef
mem.
cyto.

Figure 6.4: Rasgrp1^{Anaef} diminishes *in vitro* signaling to Ras and ERK

(a) RasGRP-1 deficient Jurkat cells (JPRM441) were transiently transfected with EGFP-tagged wildtype- or Anaef- RasGRP1 and RasGRP1-dose/P-ERK responses were determined by FACS.

(b) Jurkat, JPRM441, and JPRM441 cells stably reconstituted with Anaef- or WT Rasgrp1 were left unstimulated or stimulated with 25 ng/ml PMA and RasGTP levels were determined through a RasGTP pull down assay.

(c, d, e) The indicated cell lines were stimulated for 0, 1, 5, 10, or 30 minutes (see key) with a high (25ng/mL, c), medium (5ng/mL, d), or low dose (2ng/mL, e) of PMA, or with 2ng/mL PMA with ionomycin (1μM) and stained for intracellular phosphorylated -ERK-1 and -2 (P-ERK), and analyzed by flow cytometry. Results for JPRM441-Rasgrp1Anaef clones #68 are shown, similar results were obtained with clone #69.

(f) EGFP-tagged constructs were transiently transfected into JPRM441 and RasGRP1 localization was determined for unstimulated and PMA-stimulated cells as described in the text. Fifty images for the two-minute PMA stimulation were scored in a blinded manner and plotted with RasGRP1-Anaef in the black columns.

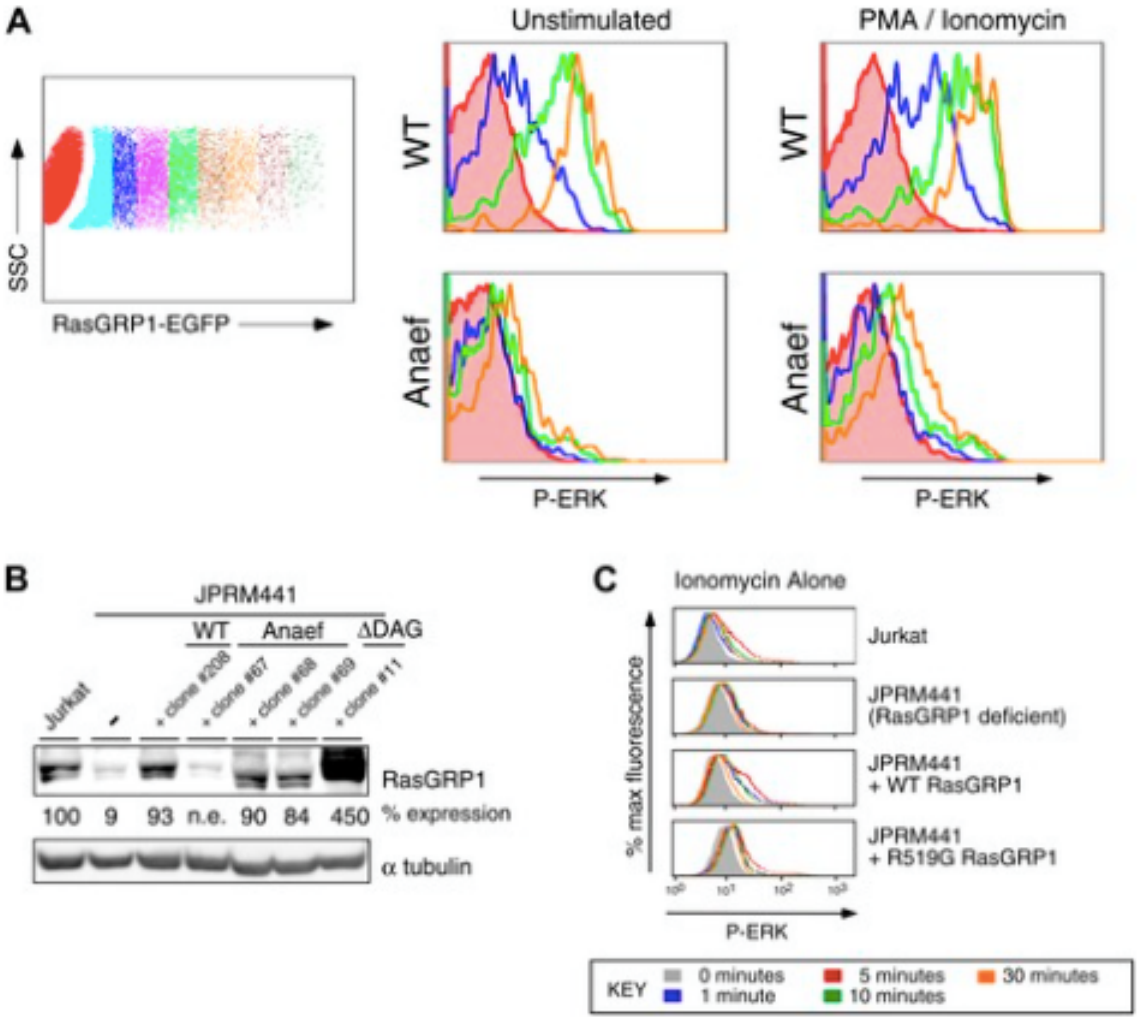

A
Unstimulated
PMA / Ionomycin
SSC
RasGRP1-EGFP
WT
Anaef
P-ERK
B
JPRM441
WT
Anaef
ΔDAG
Jurkat
+ clone #208
+ clone #67
+ clone #68
+ clone #69
+ clone #11
RasGRP1
100 9 93 n.e. 90 84 450 % expression
α tubulin
C
Ionomycin Alone
% max fluorescence
Jurkat
JPRM441
(RasGRP1 deficient)
JPRM441
+ WT RasGRP1
JPRM441
+ R519G RasGRP1
P-ERK
KEY
0 minutes
1 minute
5 minutes
10 minutes
30 minutes

Figure 6.4 – Supplemental Figure 3: Biochemical aspects of the *Rasgrp1*^{Anaef} allele

(S3a) Gating strategy for transiently expressed RasGRP1-EGFP in JPRM441 cells and analysis of ERK phosphorylation of cells expressing increasing doses of wildtype of Anaef RasGRP1 as depicted in the blue (2nd), green (4th), and orange (6th) color-coded cell populations, compared to ERK phosphorylation without transfected RasGRP1 in the filled brown histogram.

(S3b) JPRM441 were stably reconstituted with a construct expressing Rasgrp1^{Anaef} (clones #67, 68, 69). Protein lysates from an equivalent number of cells were probed for expression of Rasgrp1 and α tubulin (loading control). Percent expression of Rasgrp1 in each cell line (relative to the parental wildtype Jurkat) is shown. Rasgrp1Anaef protein levels in clones #68 and #69 were similar to those found in the parental Jurkat cell line and to expression of wildtype Rasgrp1 in a reconstituted JPRM441 clone 208 that we previously characterized (Roose et al., 2005) and were utilized in subsequent assays.

(S3c) Ionomycin-induced P-ERK responses. The depicted stable cell lines were stimulated with ionomycin (1μM) for the indicated times and stained for intracellular p-ERK. Representative histograms are shown.

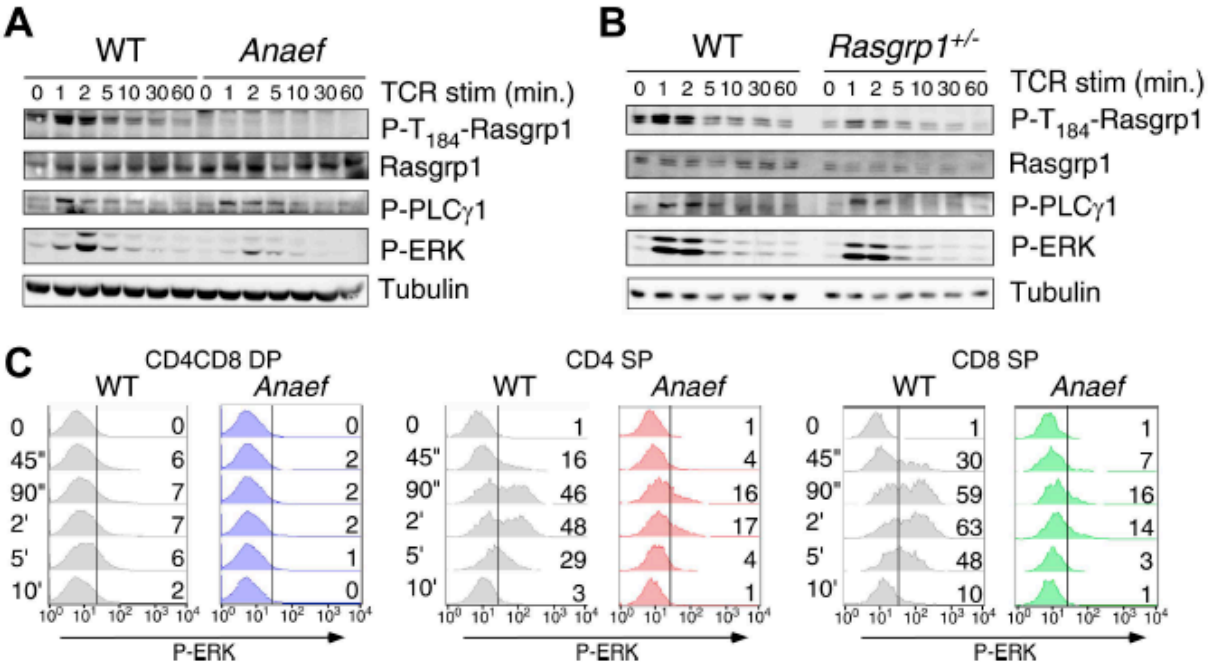

A
WT
Anaef
0 1 2 5 10 30 60 0 1 2 5 10 30 60
TCR stim (min.)
P-T184-Rasgrp1
Rasgrp1
P-PLCγ1
P-ERK
Tubulin
B
WT
Rasgrp1+/-
0 1 2 5 10 30 60 0 1 2 5 10 30 60
TCR stim (min.)
P-T184-Rasgrp1
Rasgrp1
P-PLCγ1
P-ERK
Tubulin
C
CD4CD8 DP
CD4 SP
CD8 SP
WT
Anaef
0
45"
90"
2'
5'
10'
0 0
6 2
7 2
7 2
6 1
2 0
1 1
16 4
46 16
48 17
29 4
3 1
1 1
30 7
59 16
63 14
48 3
10 1
P-ERK

Figure 6.5: *Rasgrp1*^{Anaef} signaling characteristics of *in vitro* stimulated thymocytes.

(a, b) Phosphorylation of PLCγ1, Rasgrp1, and ERK in total thymocytes from *Rasgrp1*^{Anaef} and age-matched WT mice or *Rasgrp1*$^{+/-}$ and age-matched WT mice stimulated with anti-CD3 antibodies.

(c) P-ERK induction by in vitro stimulation followed by intracellular flow cytometric staining and electronic gating on thymocyte subsets. Thymocytes from *Rasgrp1*^{Anaef} and age-matched WT mice were stimulated with anti-CD3 antibody (5μg/mL) and crosslinked using secondary antibody (Goat anti-hamster, 20μg/mL) for the indicated time points, fixed, and stained for intracellular p-ERK. Histograms show P-ERK staining on electronically gated DP, CD4SP or CD8SP thymocytes. These conditions yielded low-levels of ERK phosphorylation that is typically observed for wildtype DP thymocytes. Numbers indicate the percentages of cells above the arbitrarily set reference point in the histograms so that it can be appreciated how many cells within each population cross this P-ERK threshold. Data is representative of 3 independent experiments. For PMA-induced responses see figure S4d

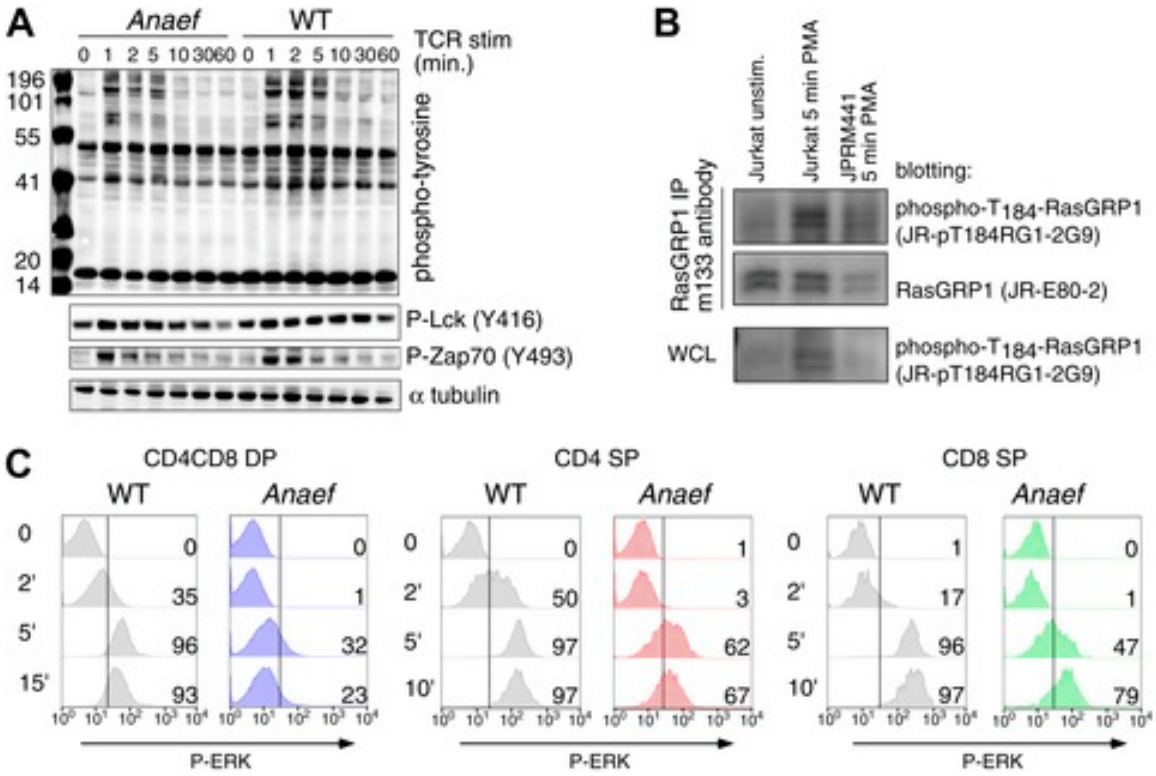

A
Anaef
WT
TCR stim (min.)
0 1 2 5 10 30 60 0 1 2 5 10 30 60
196
101
55
41
20
14
phospho-tyrosine
P-Lck (Y416)
P-Zap70 (Y493)
α tubulin
B
Jurkat unstim.
Jurkat 5 min PMA
JPRM441 5 min PMA
RasGRP1 IP m133 antibody
blotting:
phospho-T184-RasGRP1 (JR-pT184RG1-2G9)
RasGRP1 (JR-E80-2)
WCL
phospho-T184-RasGRP1 (JR-pT184RG1-2G9)
C
CD4CD8 DP
CD4 SP
CD8 SP
WT
Anaef
0
2'
5'
15'
10'
P-ERK

Figure 6.5 - Supplemental Figure 4: Signaling characteristics of *Rasgrp1^{Anaef}* thymocytes

(S4a) Thymocytes from *Rasgrp1^{Anaef}* and age-matched WT mice were stimulated with anti-CD3 antibody (clone 2C11, 10μg/mL) and whole cell lysates were analyzed for induction of tyrosine phosphorylated proteins (4G10) and for specific phospho-Lck and phospho-Zap70 residues. α-tubulin is a loading control. Surface TCR expression levels on *Rasgrp1^{Anaef}* thymocytes were indistinguishable from wildtype (data not shown).

(S4b) Characterization of JR-pT184RG1-2G9 monoclonal antibody. Whole cell lysates (WCL) or RasGRP1 immunoprecipitations with m133 monoclonal antibody of the indicated cell samples were subjected to western blot analysis with JR-pT184RG1-2G9 antibody. Note the induction of phosphorylated RasGRP1 in PMA-stimulated Jurkat cells and the reduction of this phosphor-RasGRP1 species in JPRM441 cells. Backblotting for total RasGRP1 levels was performed using a JR-E80-2 monoclonal antibody that recognizes human RasGRP1.

(S4c) P-ERK induction by intracellular flow cytometric staining and electronic gating on thymocyte subsets following in vitro stimulation. Thymocytes from *Rasgrp1^{Anaef}* and age-matched WT mice were stimulated with PMA (30ng/ml) for the indicated time points, fixed, and stained for intracellular p-ERK. Histograms show P-ERK staining on electronically gated $CD4^+CD8^+$ (double positive) and $CD4^+$ or $CD8^+$ single positive thymocytes.

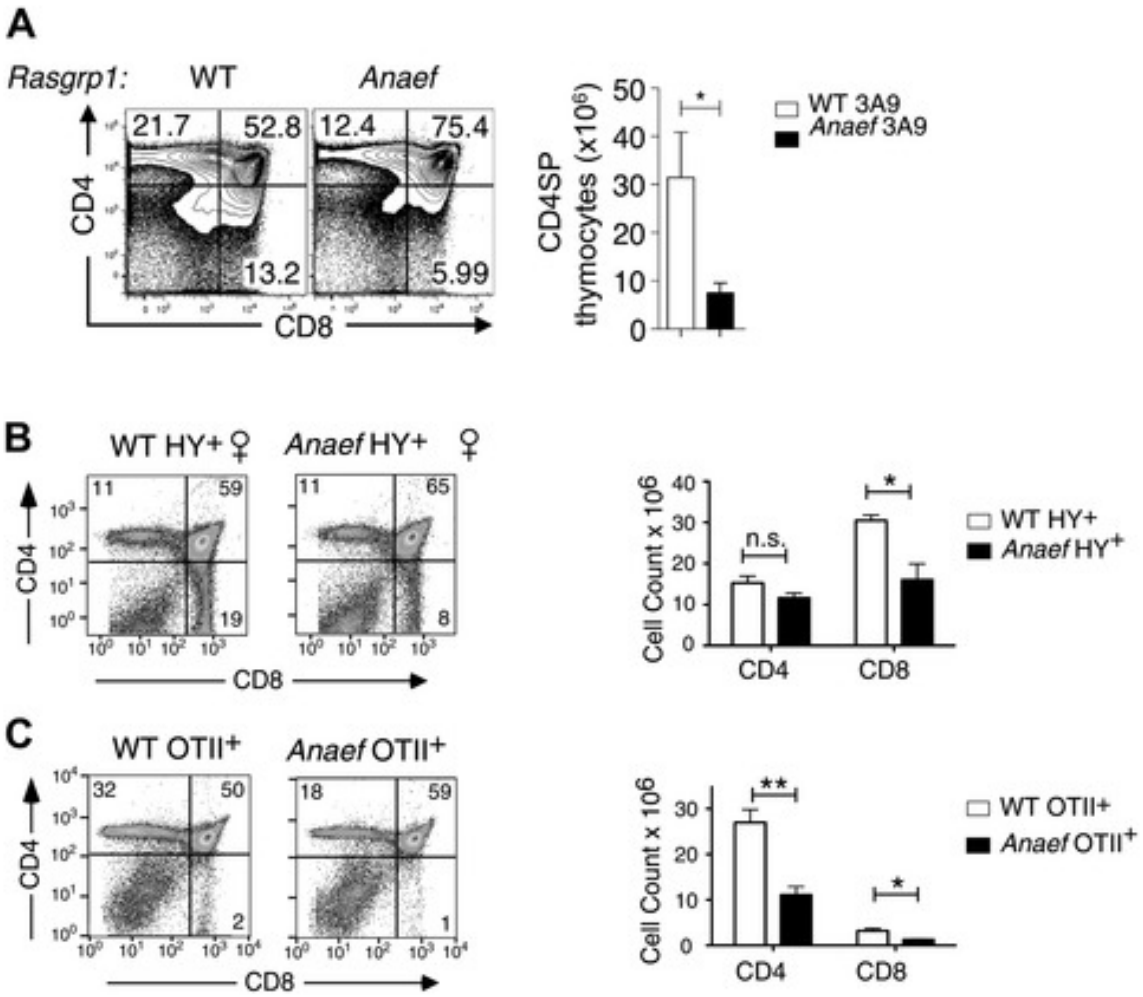

A
Rasgrp1:
WT
Anaef
21.7
52.8
13.2
12.4
75.4
5.99
CD4
CD8
CD4SP thymocytes (x10^6)
50
40
30
20
10
0
*
WT 3A9
Anaef 3A9
B
WT HY+ ♀
Anaef HY+ ♀
11
59
19
11
65
8
CD4
CD8
Cell Count x 10^6
40
30
20
10
0
n.s.
*
WT HY+
Anaef HY+
CD4
CD8
C
WT OTII+
Anaef OTII+
32
50
2
18
59
1
CD4
CD8
Cell Count x 10^6
30
20
10
0
**
*
WT OTII+
Anaef OTII+
CD4
CD8

Figure 6.5 - Supplemental Figure 5: Thymic selection in *Rasgrp1*^{Anaef} mice carrying transgenic TCRs

Rasgrp1^{Anaef} mice demonstrate a 2-6 fold decrease in positive selection in the context of three different transgenic TCRs that are uniformly and strongly expressed early on during thymocyte development.

(S5a) Representative CD4/CD8 phenotype of the thymus after reconstitution of irradiated B10.BR mice with 3A9 TCR transgenic bone marrow that was either WT or Anaef. Means and s.e.m. number of CD4SP cells are shown on the right. Statistics used unpaired Student's T test (n = 5 per group). * $p < 0.05$.

(S5b) Representative flow cytometry plots and quantitation of thymocytes in HY TCR transgenic females that facilitate positive selection of CD8 cells on MHCI. Total cell counts with mean and standard error are shown on the right (n=4 mice). * $p < 0.05$.

(S5c) Representative flow cytometry plots and quantitation of thymocytes in OTII TCR transgenic mice in which CD4 SP are selected on MHCII. Representative plots and total cell counts are shown (n=6 mice). Student's t tests P value symbols: ** $p < 0.005$, * $p < 0.05$

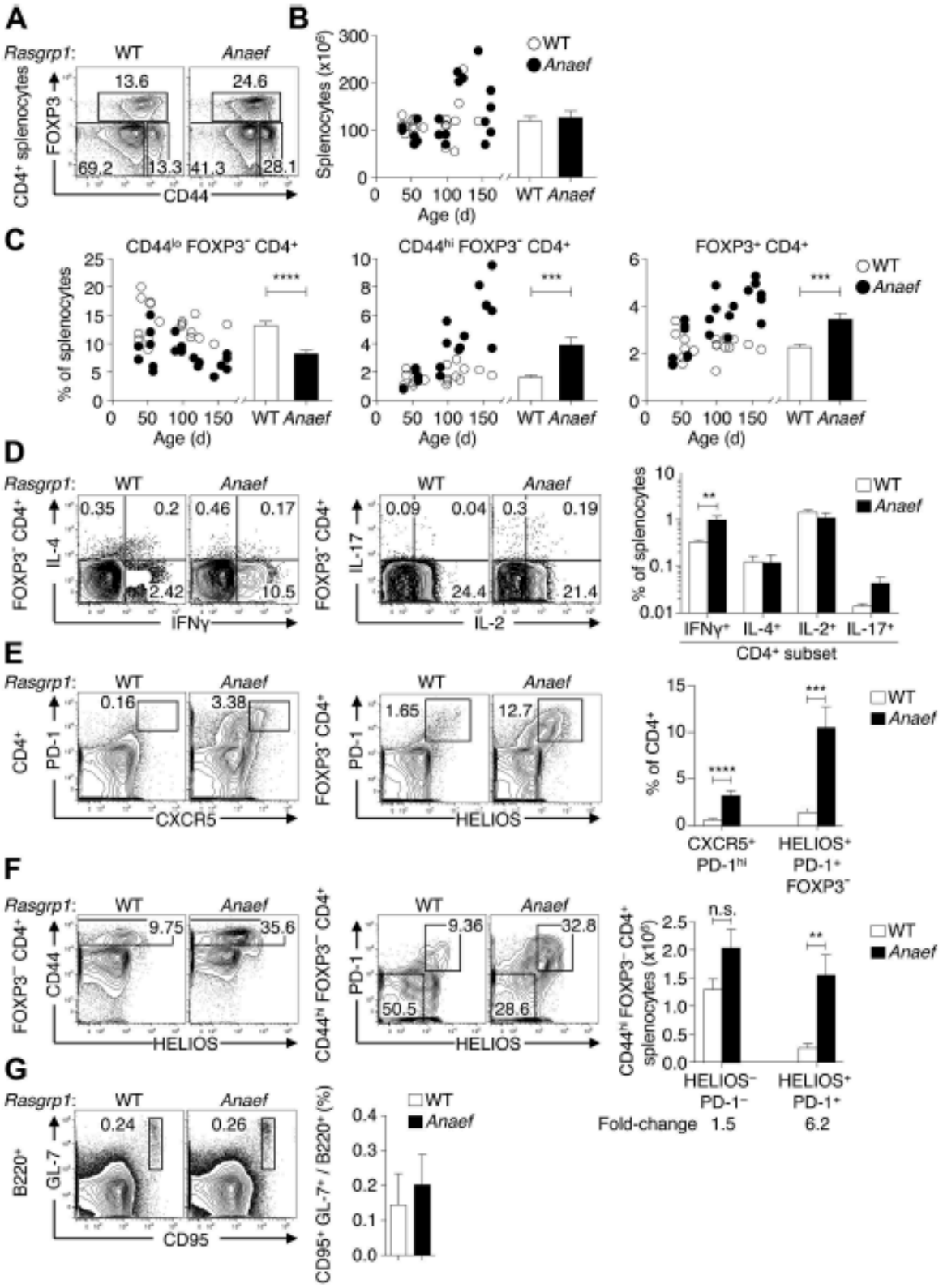

A
Rasgrp1: WT Anaef
CD4+ splenocytes
FOXP3
CD44
13.6
24.6
69.2
13.3
41.3
28.1
B
Splenocytes (x10^6)
WT
Anaef
Age (d)
C
CD44lo FOXP3- CD4+
CD44hi FOXP3- CD4+
FOXP3+ CD4+
% of splenocytes
Age (d)
****
***
D
FOXP3- CD4+
IL-4
IFNγ
IL-17
IL-2
0.35
0.2
0.46
0.17
2.42
10.5
0.09
0.04
0.3
0.19
24.4
21.4
IFNγ+ IL-4+ IL-2+ IL-17+
CD4+ subset
E
CD4+
PD-1
CXCR5
FOXP3- CD4+
HELIOS
0.16
3.38
1.65
12.7
CXCR5+ PD-1hi
HELIOS+ PD-1+ FOXP3-
F
FOXP3- CD4+
CD44
HELIOS
CD44hi FOXP3- CD4+
PD-1
9.75
35.6
9.36
32.8
50.5
28.6
n.s.
HELIOS- PD-1-
HELIOS+ PD-1+
Fold-change 1.5 6.2
G
B220+
GL-7
CD95
0.24
0.26
CD95+ GL-7+ / B220+ (%)

Figure 6.6: *Rasgrp1*^{Anaef} results in intrinsic dysregulation of peripheral CD4 T cells

(a) Representative plots of wildtype or *Rasgrp1*^{Anaef} CD4^{+} splenocytes subsetted into naïve (CD44^{lo} FOXP3^{-}), activated/memory (CD44^{hi} FOXP3^{-}), and T-reg (FOXP3^{+}) populations.

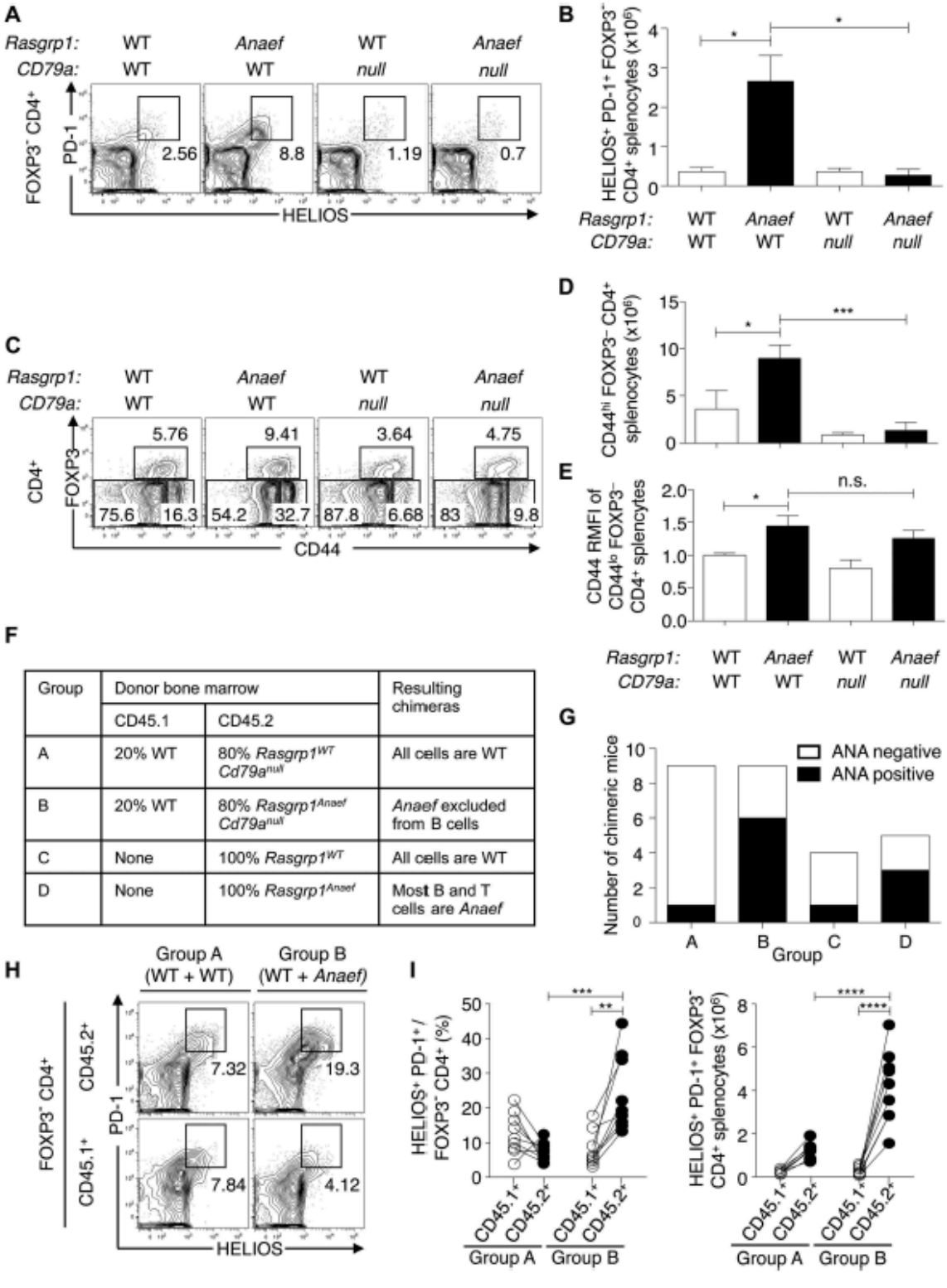
(b, c) Splenic cellularity and frequencies of the CD4^{+} subsets gated in (a) as a function of age in wildtype versus *Rasgrp1*^{Anaef} mice; each dot represents 1 mouse (WT in white; *Rasgrp1*^{Anaef} in black). Inset column graphs show the group mean ± s.e.m. Statistics obtained by unpaired Student's T test. *** $p < 0.001$, **** $p < 0.0001$.

(d) Representative intracellular labeling of IFNγ, IL-4, IL-2 or IL-17 on electronically gated Foxp3^{-} CD4^{+} wildtype or *Rasgrp1*^{Anaef} splenocytes that had been stimulated with PMA and ionomycin for 4 hours. Column graphs show mean ± s.e.m frequencies amongst all splenocytes. Statistical analysis of % IFNγ^{+} cells used an unpaired Student's T test (n = 7 WT, 6 *Anaef*) ** $p < 0.01$.

(e) Phenotype of CD4^{+} splenocytes showing a CXCR5^{+} PD-1^{hi} gate for the T_{FH} population (left) and a gate for the HELIOS^{+} PD-1^{+} population amongst Foxp3^{-} CD4^{+} splenocytes (right). Column graph shows mean ± s.e.m frequencies of these populations amongst CD4^{+} splenocytes in wildtype or *Rasgrp1*^{Anaef} mice. Statistical analyses used unpaired Student's T tests (n = 19 WT, 18 *Anaef*). *** $p < 0.001$, **** $p < 0.0001$.

(f) Helios versus CD44 phenotype of Foxp3^{-} CD4^{+} splenocytes (left plots) showing the gate for the CD44^{hi} population, which was analyzed for expression of Helios and PD-1 (right plots). Column graph shows the mean ± s.e.m number of splenocytes within the CD44^{hi} Foxp3^{-} CD4^{+} subpopulations gated in the right plots (n = 19 WT, 20 *Anaef* mice aged >70 days and compiled from 11 separate experiments). Unpaired Student's T test ** $p < 0.01$.

(g) Phenotype of B220^{+} splenocytes showing the CD95(Fas)^{hi} GL-7^{hi} gate used to define germinal center B cells (left), the mean ± s.e.m frequency of which is shown in the column graph (right) (n = 7 WT, 5 *Anaef*).



Group	Donor bone marrow		Resulting chimeras
	CD45.1	CD45.2	
A	20% WT	80% *Rasgrp1*^{WT} *Cd79a*^{null}	All cells are WT
B	20% WT	80% *Rasgrp1*^{Anaef} *Cd79a*^{null}	*Anaef* excluded from B cells
C	None	100% *Rasgrp1*^{WT}	All cells are WT
D	None	100% *Rasgrp1*^{Anaef}	Most B and T cells are *Anaef*

Figure 6.7: Role of B and T cells in *Rasgrp1*^{Anaef}-induced PD-1^{+} CD4^{+} T cell and autoantibody formation

(a-e) B6.*Cd79a*$^{-/-}$ mice lacking B cells were intercrossed with B6.*Rasgrp1*^{Anaef} mice to produce mice with the genotypes shown above the plots. Plots (left) display phenotype of *(a-b)* Foxp3^{-} CD4^{+} splenocytes and the gate used to define the PD-1^{+} HELIOS^{+} subpopulation and absolute numbers of these cells are shown on the column graphs (mean ± s.e.m). Statistical comparisons used unpaired Student's T tests (n = 4 WT, 5 *Anaef*, 2 *CD79a-null*, and 4 *Anaef.CD79a-null*) * $p < 0.05$.

(c) CD4^{+} splenocytes and the gates used to define FOXP3^{+} regulatory, CD44^{hi} FOXP3^{-} effector/memory, and CD44^{lo} FOXP3^{-} naïve subsets. Absolute numbers of effector/memory splenocytes *(d)* and Relative CD44 expression on naive splenocytes *(e)* are shown in the column graphs (mean ± s.e.m). Statistical comparisons used unpaired Student's T tests (n = 4 WT, 5 *Anaef*, 2 *CD79a-null*, and 4 *Anaef.CD79a-null*) * $p < 0.05$, *** $p < 0.001$.

(f) Experimental design to delineate role of *Rasgrp1*^{Anaef} in T and B cells. Irradiated mice received either 100% *Rasgrp1*^{WT} marrow, 100% *Rasgrp1*^{Anaef} marrow, or a 1:4 mixture of CD45.1^{+} wild-type marrow mixed with CD45.2^{+} marrow from either *Cd79a*$^{null/null}$*Rasgrp1*^{WT} or *Cd79a*$^{null/null}$ *Rasgrp1*^{Anaef} siblings.

(g) Incidence of homogeneous nuclear ANA in blood plasma in chimeric mice collected 18 weeks after irradiation, measured by immunofluorescence on HEp-2 cells and scored in a blinded manner.

(h) Representative plots (left), and quantification of frequency (middle) and number (right) of PD-1^{+} Helios^{+} cells among Foxp3^{-} CD4^{+} splenocytes from mixed chimeras in groups A and B as described in *(f)* 45 weeks after irradiation. Lines in *(i)* connect measurements from individual mice. Statistical analysis used paired Student's T-tests within groups and unpaired T-tests between groups. ** $p < 0.01$, *** $p < 0.001$, **** $p < 0.0001$.

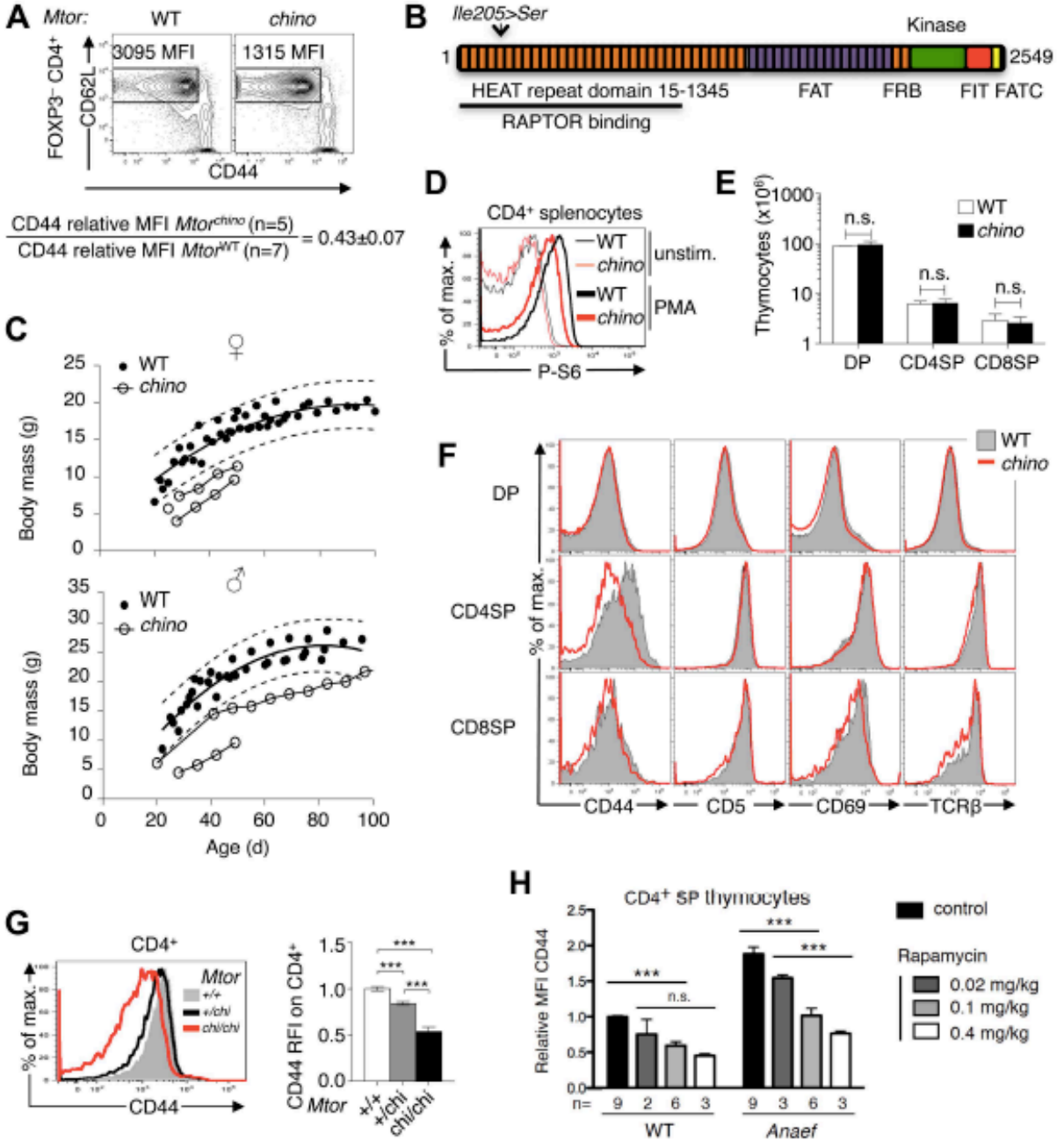

A
Mtor:
WT
chino
3095 MFI
1315 MFI
FOXP3⁻ CD4⁺
CD62L
CD44
CD44 relative MFI Mtor^chino (n=5) / CD44 relative MFI Mtor^WT (n=7) = 0.43±0.07
B
Ile205>Ser
Kinase
1
2549
HEAT repeat domain 15-1345
FAT
FRB
FIT FATC
RAPTOR binding
C
♀
♂
WT
chino
Body mass (g)
Age (d)
D
CD4⁺ splenocytes
WT
chino
unstim.
PMA
% of max.
P-S6
E
Thymocytes (x10⁶)
n.s.
WT
chino
DP
CD4SP
CD8SP
F
DP
CD4SP
CD8SP
% of max.
CD44
CD5
CD69
TCRβ
G
CD4⁺
Mtor
+/+
+/chi
chi/chi
% of max.
CD44
CD44 RFI on CD4⁺
H
CD4⁺ SP thymocytes
control
Rapamycin
0.02 mg/kg
0.1 mg/kg
0.4 mg/kg
Relative MFI CD44
n=
WT
Anaef

Figure 6.8: CD44 is a sensitive reporter of mTOR activity in immature and naïve CD4$^+$ T cells

(a) CD44^{lo} T cell phenotype upon which *Mtor*^{chino} mice were identified. Phenotype of Foxp3$^-$ CD4$^+$ splenocytes from *Mtor*$^{+/+}$ (WT) and *Mtor*$^{chino/chino}$ (*chino*) mice, showing the CD62L^{hi} subset on which CD44 expression was quantified and normalized to the mean of WT animals (mean ± s.e.m. from 3 experiments shown below).

(b) Schematic of mTOR protein showing functional domains and the *chino* I205S mutation in the fifth HEAT repeat.

(c) Reduced body size in *chino*. Body mass versus age of WT (black dots; 10 female (top), 11 male (bottom)) or *chino* (unfilled dots; 3 female, 2 male) mice. Curves were fitted to the WT datasets using second order polynomial equations; dotted lines show 95% prediction bands (the area expected to enclose 95% of future WT data points; GraphPad Prism version 5.0d for MAC OS X). Straight lines connect multiple measurements of individual *chino* mice.

(d) Splenocytes from WT or *chino* mice were left unstimulated or were stimulated with PMA (100ng/ml) for 10 minutes, fixed, and stained for intracellular phosphorylated-S6 (P-S6). Histogram overlay shows P-S6 staining on CD4$^+$ cells representative of 2 separate experiments.

(e) Number of DP, CD4SP and CD8SP cells per thymus of WT (n=7) or *chino* (n=7) mice compiled from 4 experiments.

(f) Selective reduction in CD44 expression on *chino* thymocytes. Histograms show CD44, CD5, CD69 or TCRβ expression on gated DP, CD4SP or CD8SP thymocytes from WT (solid gray) versus *chino* (red overlay) mice, representative of 4 separate experiments (n=7 mice per group in total).

(g) Histogram (left) and column graph (right, mean±s.e.m.) shows CD44 expression on CD4$^+$ CD3$^+$ B220$^-$ peripheral blood lymphocytes from littermate mice of the indicated *Mtor* genotypes, compiled from 5 separate experiments using a total of 20 *Mtor*$^{+/+}$, 49 *Mtor*$^{+/chi}$ and 7 *Mtor*$^{chi/chi}$

mice. CD44 relative fluorescence intensity (RFI) was calculated by dividing by the mean for the *Mtor*$^{+/+}$ group analysed in the same experiment. Unpaired Student's t tests: *** P<0.0001.

(h) CD44 RFI on unstimulated CD4SP thymocytes of WT or *Rasgrp1*^{Anaef} mice after 7 days of treatment with the indicated rapamycin doses. Untreated control was set at 1. *** p < 0.005, n.s. = non significant.

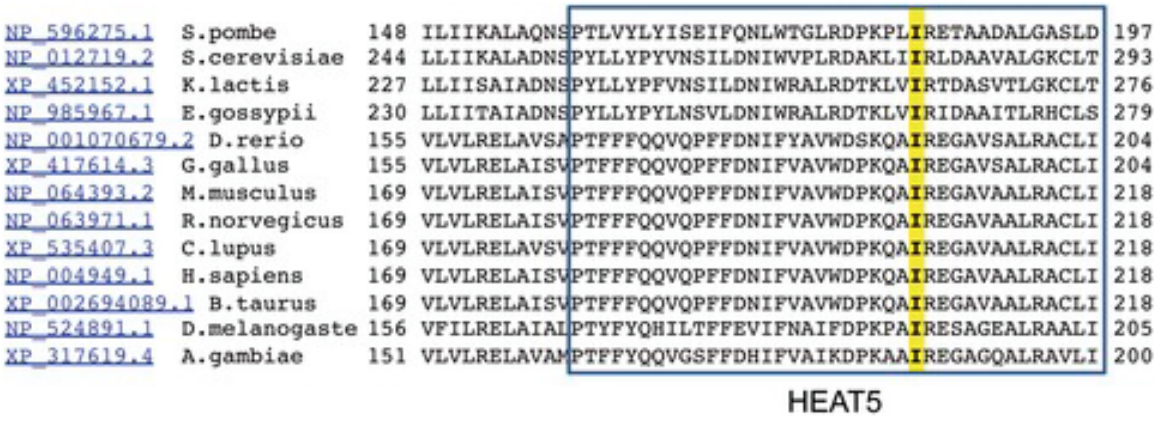

NP_596275.1 S.pombe 148 ILIIKALAQNSPTLVYLYISEIFQNLWTGLRDPKPLIRETAADALGASLD 197
NP_012719.2 S.cerevisiae 244 LLIIKALADNSPYLLYPYVNSILDNIWVPLRDAKLIIRLDAAVALGKCLT 293
XP_452152.1 K.lactis 227 LLIISAIADNSPYLLYPFVNSILDNIWRALRDTKLVIRTDASVTLGKCLT 276
NP_985967.1 E.gossypii 230 LLIITAIADNSPYLLYPYLNSVLDNIWRALRDTKLVIRIDAAITLRHCLS 279
NP_001070679.2 D.rerio 155 VLVLRELAVSAPTFFFQQVQPFFDNIFYAVWDSKQAIREGAVSALRACLI 204
XP_417614.3 G.gallus 155 VLVLRELAISVPTFFFQQVQPFFDNIFVAVWDPKQAIREGAVSALRACLI 204
NP_064393.2 M.musculus 169 VLVLRELAISVPTFFFQQVQPFFDNIFVAVWDPKQAIREGAVAALRACLI 218
NP_063971.1 R.norvegicus 169 VLVLRELAISVPTFFFQQVQPFFDNIFVAVWDPKQAIREGAVAALRACLI 218
XP_535407.3 C.lupus 169 VLVLRELAVSVPTFFFQQVQPFFDNIFVAVWDPKQAIREGAVAALRACLI 218
NP_004949.1 H.sapiens 169 VLVLRELAISVPTFFFQQVQPFFDNIFVAVWDPKQAIREGAVAALRACLI 218
XP_002694089.1 B.taurus 169 VLVLRELAISVPTFFFQQVQPFFDNIFVAVWDPKQAIREGAVAALRACLI 218
NP_524891.1 D.melanogaste 156 VFILRELAIALPTYFYQHILTFFEVIFNAIFDPKPAIRESAGEALRAALI 205
XP_317619.4 A.gambiae 151 VLVLRELAVAMPTFFYQQVGSFFDHIFVAIKDPKAAIREGAGQALRAVLI 200
HEAT5

Figure 6.8 - Supplemental Figure S6: Alignment of HEAT5 domains in mTOR

Amino acid sequences of the indicated 13 species were aligned to demonstrate the level of conservation in the HEAT5 domain. Note the isoleucine residue in yellow that is altered by the *chino* mutation to serine.

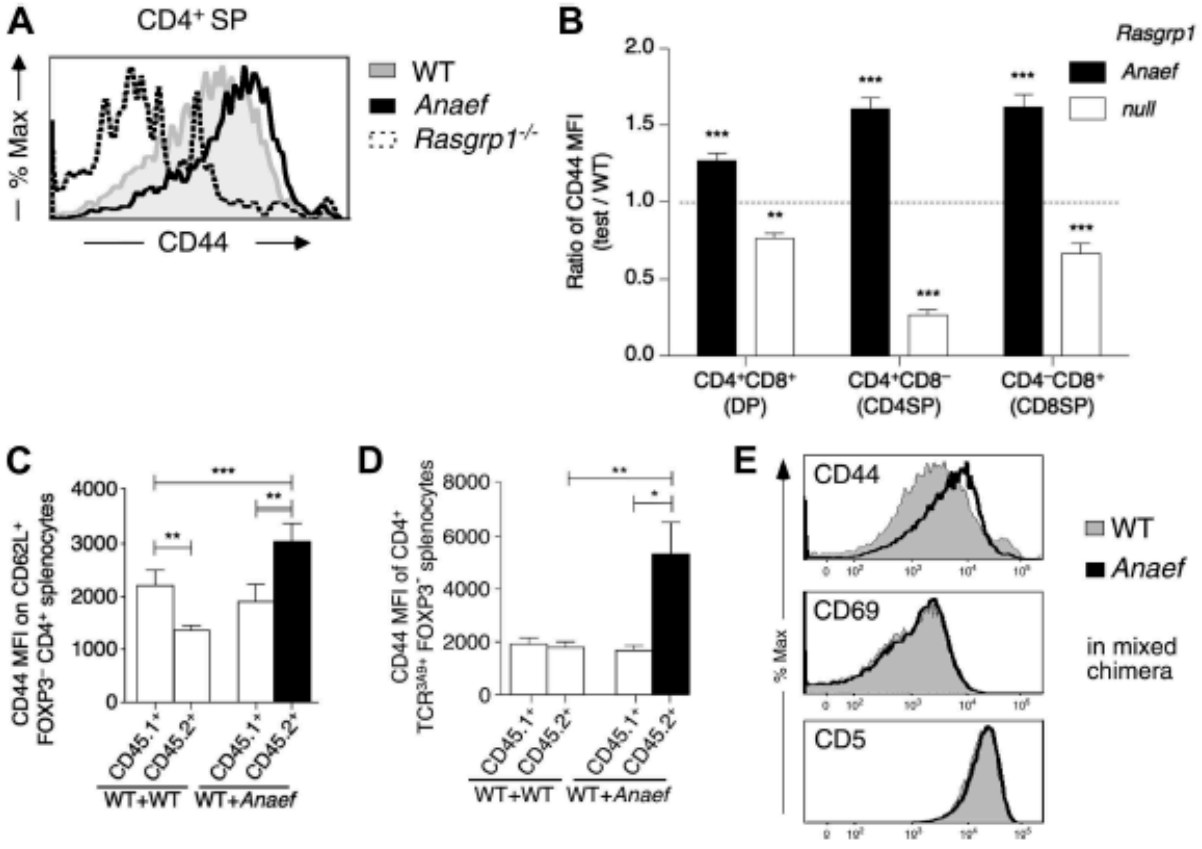

A
CD4+ SP
% Max
CD44
WT
Anaef
Rasgrp1-/-
B
Rasgrp1
Anaef
null
Ratio of CD44 MFI (test / WT)
2.0
1.5
1.0
0.5
0.0
CD4+CD8+ (DP)
CD4+CD8− (CD4SP)
CD4−CD8+ (CD8SP)
C
CD44 MFI on CD62L+ FOXP3− CD4+ splenocytes
4000
3000
2000
1000
0
CD45.1+
CD45.2+
WT+WT
WT+Anaef
D
CD44 MFI of CD4+ TCR3A9+ FOXP3− splenocytes
8000
6000
4000
2000
0
E
CD44
CD69
CD5
% Max
WT
Anaef
in mixed chimera

Figure 6.9: Selective and cell-autonomous increase in CD44 expression in *Rasgrp1*^{Anaef} CD4^{+} T cells

(a) Representative CD44 expression on unstimulated CD4SP thymocytes from wildtype, *Rasgrp1*^{Anaef} and *Rasgrp1*$^{-/-}$ mice.

(b) Mean relative CD44 from 22 *Rasgrp1*^{Anaef}, 13 wildtype, and 3 *Rasgrp1*$^{-/-}$ mice compiled from 7 experiments. In each experiment, the mean CD44 expression for the wildtype group was taken to be 1, and values for individual mice were normalized to this. Unpaired Student's T tests were used to compare *Rasgrp1*^{Anaef} and *Rasgrp1*$^{-/-}$ with the wildtype group. ** $p < 0.005$, *** $p < 0.0005$.

(c) CD44 MFI on CD62L^{+}Foxp3^{-}CD4^{+} splenocytes from mixed bone marrow chimeras described in Fig 7f. Statistical comparisons used paired T tests within, and unpaired T tests between, groups of chimeras (n = 9 for both groups); *** $p < 0.001$ ** $p < 0.01$.

(d) CD44 MFI on TCR3A9+ (clonotype positive) CD4^{+}Foxp3^{-} splenocytes from B10.BR mixed bone marrow chimeras containing CD45.1^{+} wildtype TCR3A9 plus either CD45.2^{+} wildtype (n=8) or CD45.2^{+} *Rasgrp1*^{Anaef} (n=7) 3A9 TCR-transgenic hematopoietic cells. Statistical comparisons in (c) and (d) used paired T tests within groups of chimeras and unpaired T tests between groups of chimeras. P value symbols: *** $p < 0.001$ ** $p < 0.01$, * $p < 0.05$.

(e) *Rasgrp1*^{Anaef} increases CD44 expression levels but does not affect CD69 or CD5 expression. CD4SP thymocytes are analysed from irradiated mice reconstituted with non-transgenic CD45.1^{+} wildtype mixed with CD45.2+ Rasgrp1^{Anaef} bone marrow.

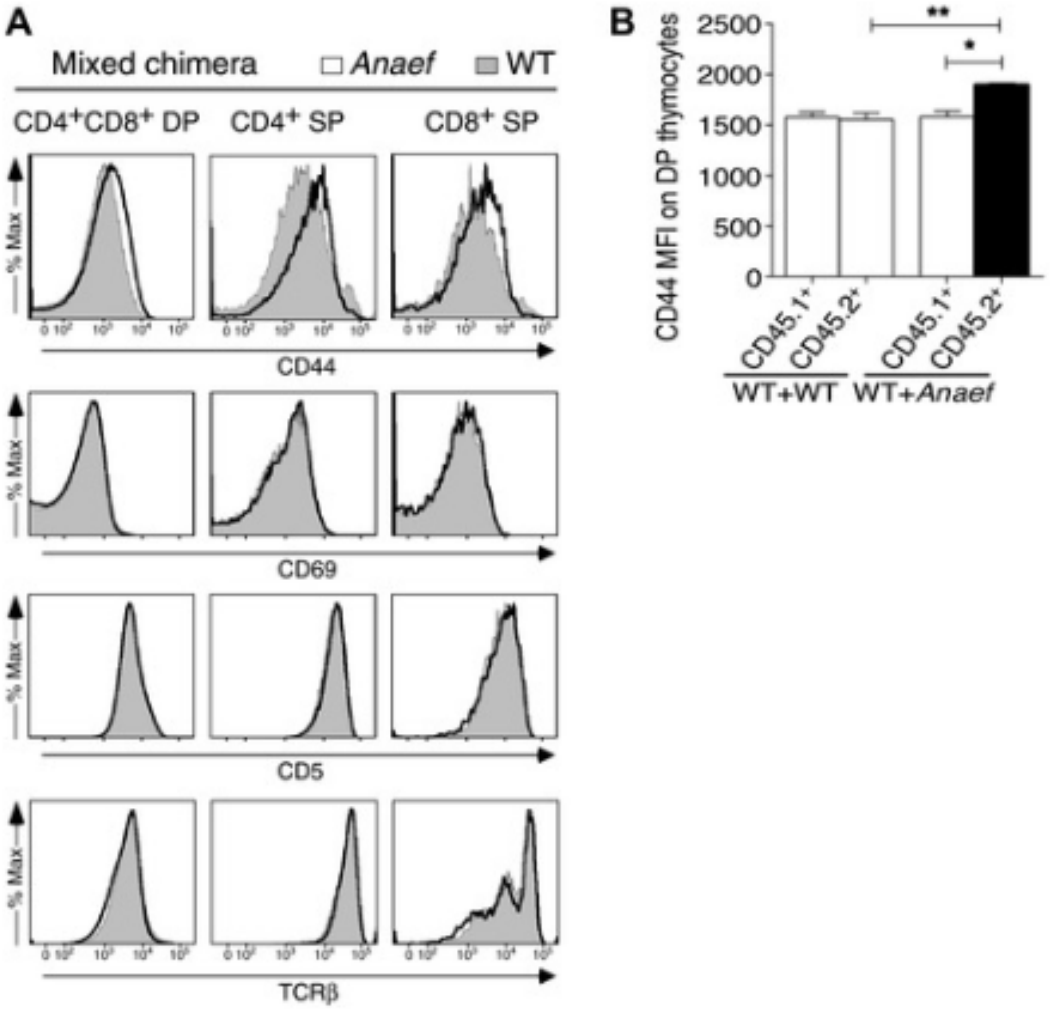

A
Mixed chimera
Anaef
WT
CD4+CD8+ DP
CD4+ SP
CD8+ SP
% Max
CD44
CD69
CD5
TCRβ
B
CD44 MFI on DP thymocytes
2500
2000
1500
1000
500
0
**
*
CD45.1+
CD45.2+
CD45.1+
CD45.2+
WT+WT
WT+Anaef

Figure 6.9 - Supplemental Figure S7: CD44 and P-S6 expression in thymocytes

(S7a) Selective effect of *Rasgrp1*^{Anaef} on CD44 expression during thymic maturation. Analysis of thymocytes from mixed chimeras (described in Fig. 9e bearing CD45.1^{+} WT (filled) plus CD45.2^{+} *Rasgrp1*^{Anaef} (black trace) hematopoietic cells. Histograms show CD44, CD69, CD5, TCRβ expression on DP, CD4SP and CD8SP thymocytes.

(S7b) Column graph shows CD44 MFIs on CD45.1^{+} or CD45.2^{+} DP thymocytes from the mixed chimeras (in S7a) as well as control WT + WT chimeras (n = 5 mice per group). P value symbols for unpaired T tests between groups and paired T tests within groups: ** p , 0.01, * p , 0.05.

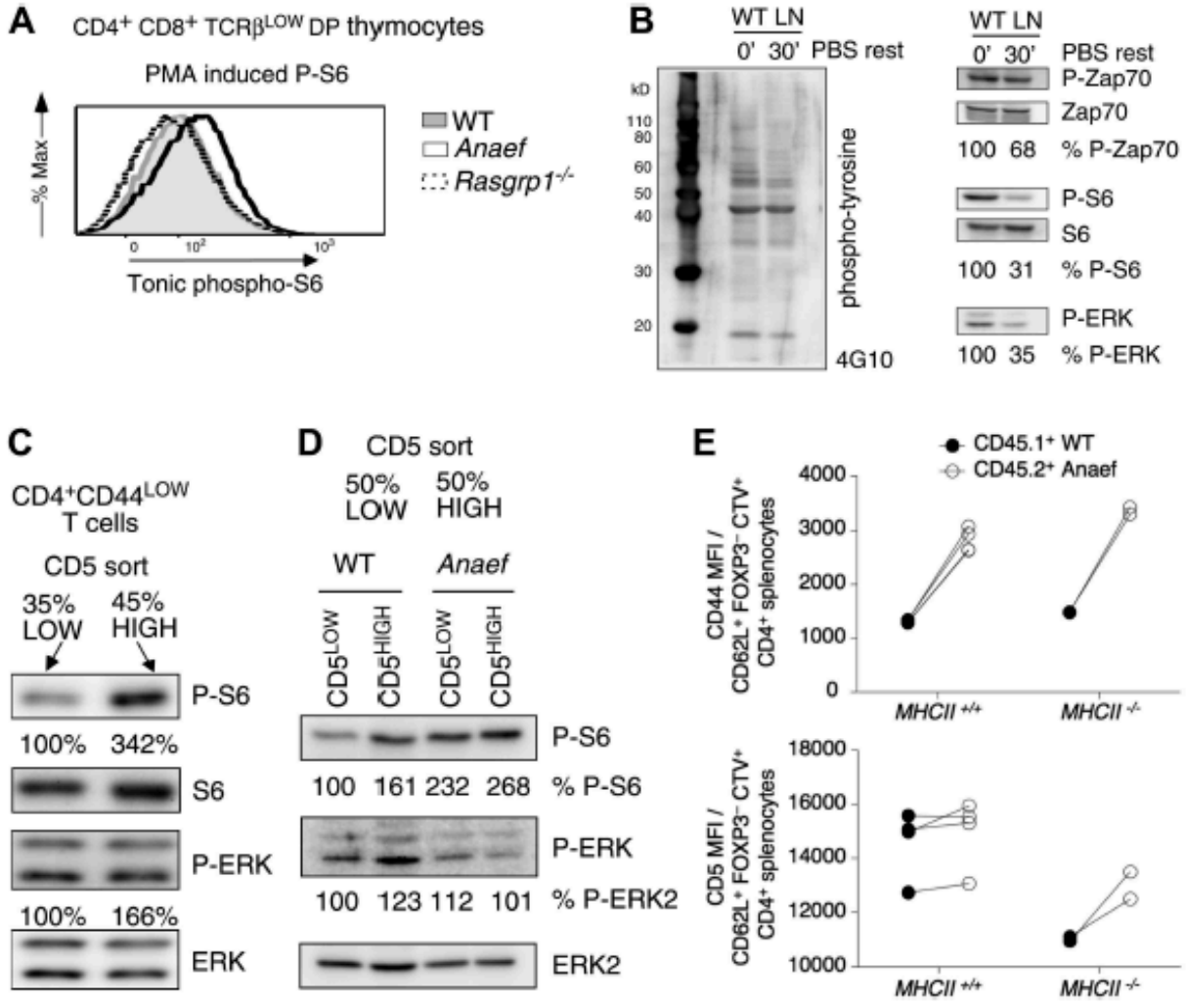

A
CD4+ CD8+ TCRβLOW DP thymocytes
PMA induced P-S6
% Max
WT
Anaef
Rasgrp1-/-
Tonic phospho-S6
B
WT LN
0' 30' PBS rest
kD
110
80
60
50
40
30
20
phospho-tyrosine
4G10
WT LN
0' 30' PBS rest
P-Zap70
Zap70
100 68 % P-Zap70
P-S6
S6
100 31 % P-S6
P-ERK
100 35 % P-ERK
C
CD4+CD44LOW T cells
CD5 sort
35% LOW
45% HIGH
P-S6
100% 342%
S6
P-ERK
100% 166%
ERK
D
CD5 sort
50% LOW
50% HIGH
WT
Anaef
CD5LOW
CD5HIGH
CD5LOW
CD5HIGH
P-S6
100 161 232 268 % P-S6
P-ERK
100 123 112 101 % P-ERK2
ERK2
E
CD45.1+ WT
CD45.2+ Anaef
CD44 MFI / CD62L+ FOXP3− CTV+ CD4+ splenocytes
4000
3000
2000
1000
0
MHCII +/+
MHCII -/-
CD5 MFI / CD62L+ FOXP3− CTV+ CD4+ splenocytes
18000
16000
14000
12000
10000
MHCII +/+
MHCII -/-

Figure 6.10: Increased tonic mTOR-S6 signals in *Rasgrp1*^{Anaef} thymocytes and T cells

(a) Tonic P-S6 levels in pre-selection DP thymocytes from wildtype, *Rasgrp1*^{Anaef} and *Rasgrp1*$^{-/-}$ mice. Representative histograms are shown for five independent experiments with n = 9 for WT, n = 7 for *Rasgrp1*^{Anaef} and n = 7 *Rasgrp1*$^{-/-}$ mice.

(b) Total lymph node cells were analyzed for the indicated phospho-proteins either immediatedly after extraction and single cell suspension generation (0') or after a 30 minute rest period in PBS at 37 degrees (30').

(c, d) Western blot measurements of basal P-S6 and P-ERK in unstimulated naive CD4^{+}CD44^{lo} T cells sorted into CD5^{low} and CD5^{high} subsets from wildtype and *Rasgrp1*^{Anaef} mice. Equal loading was confirmed with specific blotting for ERK2, which can be done without stripping. Panels c-e are representative results of at least 3 independent experiments.

(e) CD45.1 wild-type and *Rasgrp1*^{Anaef} splenocytes were mixed, labelled with CellTrace Violet and adoptively transferred into CD45.2 wild-type or MHCII–deficient recipient mice (Supplementary Fig. S8). 48h hours later, donor-derived CD4^{+}CD62L^{+}FOXP3^{-} cells in recipient spleens were resolved by flow cytometry and their CD44 (upper panel) and CD5 (lower panel) MFIs were plotted. Lines connect measurements from individual mice.

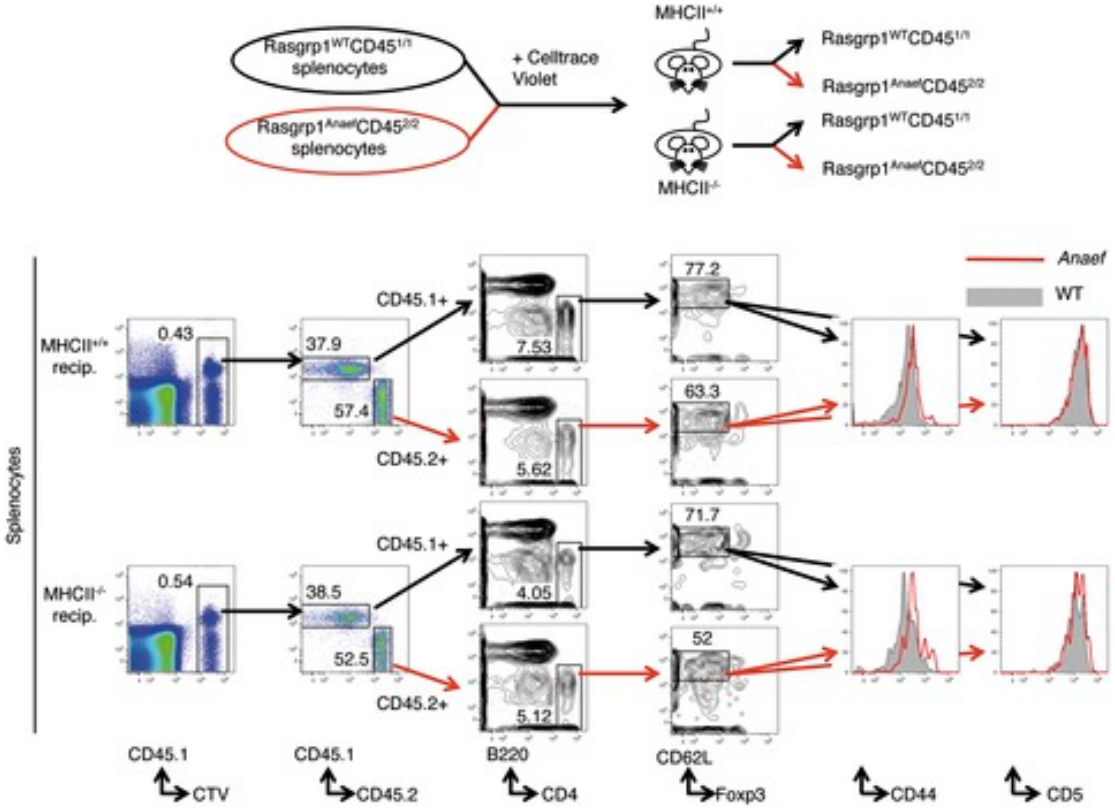

Rasgrp1WTCD451/1 splenocytes
Rasgrp1Anaef CD452/2 splenocytes
+ Celltrace Violet
MHCII+/+
MHCII-/-
Rasgrp1WTCD451/1
Rasgrp1Anaef CD452/2
Anaef
WT
Splenocytes
MHCII+/+ recip.
MHCII-/- recip.
0.43
37.9
57.4
CD45.1+
CD45.2+
7.53
5.62
77.2
63.3
0.54
38.5
52.5
4.05
5.12
71.7
52
CD45.1
CTV
CD45.1
CD45.2
B220
CD4
CD62L
Foxp3
CD44
CD5

Figure 6.10 - Supplementary Figure S8: Testing the role of MHCII recognition in constitutive CD44 overexpression by *Rasgrp1*^{Anaef} naive CD4 T cells

Schematic of experiment design as described in the text (top) and flow cytometric resolution of co-transferred (CTV^{+}) donor WT (CD45$^{1/1}$) and *Rasgrp1*^{Anaef} (CD45$^{2/2}$) naive CD4 T cells on which CD5 and CD44 expression were compared (bottom).

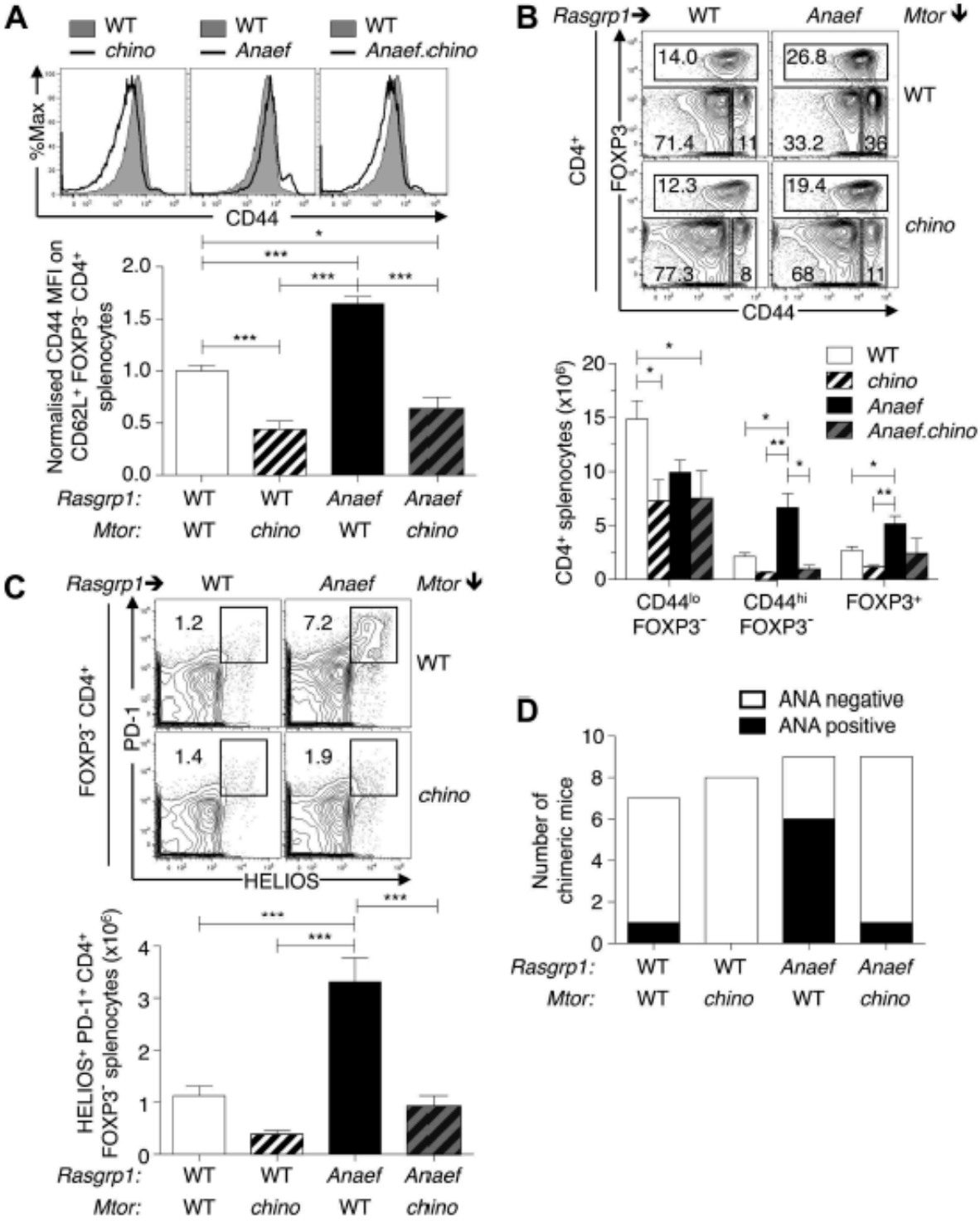

A
WT
chino
WT
Anaef
WT
Anaef.chino
%Max
CD44
Normalised CD44 MFI on CD62L+ FOXP3− CD4+ splenocytes
Rasgrp1:
Mtor:
B
Rasgrp1→
Mtor↓
WT
Anaef
14.0
26.8
71.4
11
33.2
36
12.3
19.4
77.3
8
68
11
CD4+
FOXP3
CD44
CD4+ splenocytes (x10⁶)
CD44lo FOXP3−
CD44hi FOXP3−
FOXP3+
C
1.2
7.2
1.4
1.9
FOXP3− CD4+
PD-1
HELIOS
HELIOS+ PD-1+ CD4+ FOXP3− splenocytes (x10⁶)
D
ANA negative
ANA positive
Number of chimeric mice

Figure 6.11: *Mtor* hypomorphic mutation corrects *Rasgrp1*^{Anaef}–induced increase in naive T-cell CD44 expression and accumulation of CD44^{+}Helios^{+}PD-1^{+}CD4^{+} cells and autoantibodies

(a) *B6.Rasgrp1*^{Anaef} mice were intercrossed with *B6.Mtor*^{chino} mice to generate the single and double-mutant mice. Representative CD44 histograms of CD62L^{+}FOXP3^{-}CD4^{+} splenocytes from these *chino*, *Anaef*, and *Anaef.chino* mutants were overlaid against wild-type cells and plotted. Below, CD44 MFI of mice was normalized against average CD44 MFI of wild-type mice across two independent experiments and graphed, with columns showing mean ± s.e.m. Significance indicated using a 1-way ANOVA and Tukey's post-test at n = 13 WT, 5 *chino*, 15 *Anaef*, and 4 *Anaef.chino*. * $p < 0.05$, ** $p < 0.01$, *** $p < 0.001$.

(b) Representative CD44 vs FOXP3 plots for these four genotypes from (a), which display CD4^{+} splenocytes gated into naïve (CD44^{lo} FOXP3^{-}), activated/memory (CD44^{hi} FOXP3^{-}), and T-reg (FOXP3^{+}) populations. Absolute numbers of these 3 subsets across all 4 genotypes is graphed below, with columns showing mean ± s.e.m. Significance indicated using a 1-way ANOVA and Tukey's post-test at n = 13 WT, 5 *chino*, 15 *Anaef*, and 4 *Anaef.chino*. * $p < 0.05$, ** $p < 0.01$.

(c) Bone marrow cells from sibling mice described in (a) and (b) were used to reconstitute irradiated *B6.SJL CD45*$^{1/1}$ mice, which were analysed 28 weeks after irradiation. Plots show HELIOS vs PD-1 expression on FOXP3^{-} CD4^{+} splenocytes, representative of both nonchimeric and chimeric mice. Absolute number of HELIOS^{+} PD-1^{+} FOXP3^{-} CD4^{+} splenocytes per mouse is graphed below, with columns showing mean ± s.e.m. Significance indicated using a 1-way ANOVA and Tukey's post-test at n = 11 WT, 10 *chino*, 10 *Anaef*, 11 *Anaef.chino*. *** $p < 0.001$.

(d) Chimeric mice from (c) were bled 27 weeks after irradiation and the presence of homogeneous nuclear ANA in blood plasma was measured by immunofluorescence on HEp-2 cells and scored in a blinded manner.

METHODS

Mice

Mice were housed in pathogen-free conditions and experiments approved by either the Australian University Animal Ethics and Experimentation Committee (Goodnow group, A2011/46) or the Institutional Animal Care and Use Committee of the University of California, San Francisco (Roose group, AN084051-01). C57BL/6 (B6), C57BL/6.SJL (CD45.1), B10Br, B10Br.CD45.1, B10Br TCR^{3A9}, *Cd79a*^{null} (also called *Cd79a*^{m1ANU}) and MHCII-deficient (*H2-Aa*^{tm1Blt}) mice were obtained from ANU Bioscience Services. The *Rasgrp1*^{Anaef} and *Mtor*^{chino} strains were established through ethylnitrosourea (ENU)-mediated mutagenesis of B6 mice at the Australian National University as previously described (Randall et al., 2009).

Genetic mapping of the *Anaef* mutation

Affected Rasgrp1^{Anaef} mice were crossed onto the CBA/J background to generate heterozygous F1 mice. F1 mice were intercrossed to yield mice homozygous for the *Anaef* mutation and carrying a mix of C57BL/6 and background CBA/J single nucleotide polymorphisms (SNPs). Genomic DNA isolated from both affected and unaffected mice was used as template for SNP mapping at the Genomics Institute of the Novartis Research Foundation (San Diego, CA). SNP markers were spaced approximately every 3-5 Mbp throughout the genome. Once a defined interval was established, the Rasgrp1 encoding gene was sequenced from genomic DNA from both affected *Anaef* and WT mice. All exons were amplified by PCR with primers spanning the whole exon and the flanking intronic regions. A single point mutation was identified in exon 13. Exome enrichment using the SureSelect Mouse Exome kit (G7550A-001: Agilent, CA), sequencing using the Illumina HiSeq 2000, and computational analysis to detect novel single-nucleotide variants were performed as described previously (Andrews et al., 2012).

Genotyping

Roose lab *Anaef* mice were genotyped using MS-PCR. Primers were combined in a single reaction with Taq, Taq buffer and dNTPs (all New England BioLabs). Goodnow lab *Anaef* mice were genotyped by APF Genomics Services following the manufacturer's instructions for Amplifluor PCR (SNP FAM/JOE; Millipore).

Transfections and stable cell lines

Transfections and creation of stable cell lines was performed as previously described (Roose et al., 2005).

Antinuclear antibody testing

Diluted mouse plasma was applied to HEp-2 slides (Inova, USA). AlexaFluor488-conjugated goat anti-mouse IgG (Invitrogen) was added and slides mounted with Dako fluorescence mounting medium. Photos were taken using an Olympus IX71 microscope and WIB filter with 20x lens and exposure time of 1/25 seconds.

Flow Cytometry

Suspensions of splenocytes (depleted of erythrocytes by brief osmotic lysis) or thymocytes were incubated with cocktails of anti-mouse antibodies specific for: CD44, CD4, CD45.1, CD45.2, CD5, CD62L, CD69, TCRβ, PD-1, TCR Vβ5, TCR Vβ8, TCR Vβ11, B220, CD95, GL-7, B220 (BD Pharmingen or BioLegend) or CD8 (BD Pharmingen and UCSF Monoclonal Antibody Core, clone YTS169.4) conjugated to AlexaFluor700, APC-780 or APCCy7, PE-Cy7, APC, PerCPCy5.5, FITC, PE, Pacific Blue or biotin. Biotinylated antibodies were detected in another incubation step with streptavidin conjugated to Qdot605 (Invitrogen) or BV605 (BioLegend). Cells expressing the 3A9 TCR transgene were detected using the 1G12 (mouse IgG1) antibody

(ATCC) followed by another incubation in anti-mouseIgG1 (A85.1). To detect intracellular proteins, cells were fixed and permeabilized using a Foxp3 staining kit (eBioscience), then labeled with antibodies specific for Foxp3 (FJK-16s, eBioscience), Helios (clone 22F6, Biolegend), IFNγ, IL-4, IL-2 or IL-17 (all BD Pharmingen). Flow cytometry data was acquired on a FACSort (Becton Dickinson) or an LSR Fortessa system and analyzed with FlowJo v8 (Treestar).

Cell Stimulations

Cells were stimulated using 25ng/mL (HIGH), 5ng/mL (MED), or 2ng/mL (LOW) PMA (Calbiochem) with/without ionomycin (10μM, Sigma), or with 100ng/mL PMA for Phospho-S6 assays. To mimic TCR engagement, cells were pre-labeled using anti-CD3 primary antibody (10μg/mL, UCSF Monoclonal Antibody Core, clone 2C11) and crosslinking was achieved using goat anti-hamster antibody (10μg/mL, Jackson ImmunoResearch). For intracellular cytokine detection by flow cytometry, splenocytes were stimulated in complete medium for 4 h at 37°C with PMA (100ng/mL; Sigma), ionomycin (500 ng/ml; Sigma) and GolgiStop (1/1000; BD), then labeled as described above.

Flow Cytometry for phosphorylated proteins

Procedure was performed as described in Das et al., 2009 (Das et al., 2009). Cells were fixed using Cytofix Cell Fixative (BD Biosciences). Cells were permeabilized using 90% Methanol. Primary staining for phospho-Erk occurred using rabbit anti-mouse p-Erk antibody (Cell Signaling, #4377S) followed by staining with goat anti-Rabbit PE (Jackson ImmunoResearch). For analysis of tonic and PMA induced S6 phosphorylation by FACS, single-cell suspensions were prepared from thymus. Half of the cells were fixed in warm cytofix (BD Biosciences) immediately after harvesting and reserved for tonic signaling analysis. The remaining cells were

then counted, and 10^6 cells/sample were stimulated PMA for 3 minutes, followed by fixation. Stimulated and unstimulated cells were then washed three times with cytoperm buffer (BD Biosciences) and incubated on ice in this buffer with a rabbit polyclonal antibody against phosphorylated S6 (cell signaling) for 45 minutes. The cells were then washed twice with cytoperm and incubated for an additional 45 minutes in cytoperm buffer containing an APC-conjugated goat anti-rabbit secondary antibody, as well as anti CD8-FITC, CD4, PE-Cy7 and TCRβ-PE. Cells were washed twice and analyzed in an LSR Fortessa system.

Ras Pulldown

Activation of Ras was analyzed using a RasGTP pulldown assay (Upstate) as previously described (Roose et al., 2005).

Western Blotting

Cells were lysed using Nonidet-P40 lysis buffer (1%) supplemented with protease and phosphatase inhibitors. Lysates were run on 10% acrylamide Bis-Tris gels and transferred onto PDVF filter (Millipore, Immobilon-P). Blots were probed for Rasgrp1 (Santa Cruz, M199), Alpha tubulin (Sigma), phospho-tyrosine (In house antibody prep, clone 4G10), phospho-Zap70 (Y493; Cell Signaling), phospho-PLCγ (Y783; Cell Signaling) and phospho-Lck (Y416; Cell Signaling), anti-ERK (pan-Erk) antibody (BD Transduction labs, clone 16/ERK). Rabbit anti- human Rasgrp1 (clone E80) was produced by Epitomics, Inc. (Burlingame, CA, USA). Mouse anti-Rasgrp1 p-T184 (clone JR-pT184RG1-4G7) was produced by AnaSpec (Fremont, CA, USA). Signal from primary antibodies detected using HRP conjugated secondary antibodies: Sheep anti-mouse HRP (GE Healthcare) and goat anti-rabbit HRP (SouthernBiotech). Blots were developed using Pierce ECL Western Blotting Substrate (ThermoScientific) and images recorded using a chemiluminescence imager (Fuji, LAS-4000).

Bone Marrow Chimeras

Bone marrow was collected, and in some experiments, depleted of T cells and NK cells by magnetic labelling using biotinylated anti-TCRβ and anti-NK1.1 and streptavidin microbeads followed by passage through a MACS LD column (Miltenyi Biotec). Recipient mice were irradiated with X-rays (2 doses of 4.5 Gy given 4 hrs apart) then injected i.v. with $2x10^6$ bone marrow cells that were either from single or multiple donors as described in the text.

Rapamycin treatment

Suboptimal doses of rapamycin (Coenen et al., 2007, Araki et al., 2009) were prepared on day 0 in sufficient quantity for all injections in one experiment. The appropriate rapamycin stock volume was diluted to the indicated concentrations in DMSO (15.4%), Cremaphor (15.4%) and water (69.2%), and aliquoted in six equal portions (one aliquot per injection) and frozen. Mice were injected on days 0, 1, 2, 3, 5 and 7, and then sacrificed on day 8. Thymocytes were harvested and analyzed as before.

BrdU labelling

1mg BrdU (BD) in PBS per mouse was injected i.p. to pulse label a cohort of dividing cells. Following surface staining of thymocytes as above, BrdU was detected following the BrdU Flow Kit (BD) protocol by fixing and permeabilizing cells with provided buffers, incubating for 1 hour at 37°C in DNase, then washing and staining with anti-BrdU antibody.

CellTrace Violet (CTV) labelling

CTV labeling was done at room temperature as described (Quah and Parish, 2010) with slight modifications. Splenocytes suspended at 10^8 cells/mL in RPMI containing HI-FCS (10% v/v) were transferred to the base of a fresh 15mL conical tube. 1μL of CTV (Life Technologies) stock

solution (10mM) per mL of cell suspension was placed on the dry wall of the tubes, then tubes were capped, inverted and briefly vortexed (final CTV concentration 10μM). After 5 minutes incubation in the dark, 10mL of 10%FCS/RPMI was added, then cells were sedimented by centrifugation before another wash in 10mL of the same medium. Cells were then resuspended in PBS and passed through a 70μm cell strainer (BD) before i.v. injection (200μL per mouse).

REFERENCES

ABARRATEGUI, I. & KRANGEL, M. S. 2006. Regulation of T cell receptor-alpha gene recombination by transcription. *Nat Immunol,* 7**,** 1109-15.

ADAMI, A., GARCIA-ALVAREZ, B., ARIAS-PALOMO, E., BARFORD, D. & LLORCA, O. 2007. Structure of TOR and its complex with KOG1. *Mol Cell,* 27**,** 509-16.

AGUADO, E., RICHELME, S., NUNEZ-CRUZ, S., MIAZEK, A., MURA, A. M., RICHELME, M., GUO, X. J., SAINTY, D., HE, H. T., MALISSEN, B. & MALISSEN, M. 2002. Induction of T helper type 2 immunity by a point mutation in the LAT adaptor. *Science,* 296**,** 2036-40.

ANDREWS, T. D., WHITTLE, B., FIELD, M. A., BALAKISHNAN, B., ZHANG, Y., SHAO, Y., CHO, V., KIRK, M., SINGH, M., XIA, Y., HAGER, J., WINSLADE, S., SJOLLEMA, G., BEUTLER, B., ENDERS, A. & GOODNOW, C. C. 2012. Massively parallel sequencing of the mouse exome to accurately identify rare, induced mutations: an immediate source for thousands of new mouse models. *Open Biol,* 2**,** 120061.

ARAKI, K., TURNER, A. P., SHAFFER, V. O., GANGAPPA, S., KELLER, S. A., BACHMANN, M. F., LARSEN, C. P. & AHMED, R. 2009. mTOR regulates memory CD8 T-cell differentiation. *Nature,* 460**,** 108-12.

AZZAM, H. S., GRINBERG, A., LUI, K., SHEN, H., SHORES, E. W. & LOVE, P. E. 1998. CD5 expression is developmentally regulated by T cell receptor (TCR) signals and TCR avidity. *J Exp Med,* 188**,** 2301-11.

BEAULIEU, N., ZAHEDI, B., GOULDING, R. E., TAZMINI, G., ANTHONY, K. V., OMEIS, S. L., DE JONG, D. R. & KAY, R. J. 2007. Regulation of RasGRP1 by B cell antigen receptor requires cooperativity between three domains controlling translocation to the plasma membrane. *Mol Biol Cell,* 18**,** 3156-68.

BHANDOOLA, A., TAI, X., ECKHAUS, M., AUCHINCLOSS, H., MASON, K., RUBIN, S. A., CARBONE, K. M., GROSSMAN, Z., ROSENBERG, A. S. & SINGER, A. 2002. Peripheral expression of self-MHC-II influences the reactivity and self-tolerance of mature CD4(+) T cells: evidence from a lymphopenic T cell model. *Immunity,* 17**,** 425-36.

BOTTEMA, C. D. & SOMMER, S. S. 1993. PCR amplification of specific alleles: rapid detection of known mutations and polymorphisms. *Mutat Res,* 288**,** 93-102.

CASTELLANO, E. & DOWNWARD, J. 2010. Role of RAS in the regulation of PI 3-kinase. *Curr Top Microbiol Immunol,* 346**,** 143-69.

COENEN, J. J., KOENEN, H. J., VAN RIJSSEN, E., KASRAN, A., BOON, L., HILBRANDS, L. B. & JOOSTEN, I. 2007. Rapamycin, not cyclosporine, permits thymic generation and peripheral preservation of CD4+ CD25+ FoxP3+ T cells. *Bone Marrow Transplant,* 39**,** 537-45.

CONSORTIUM*, T. G. P. 2010. A map of human genome variation from population-scale sequencing. *Nature,* 467**,** 1061-73.

COUGHLIN, J. J., STANG, S. L., DOWER, N. A. & STONE, J. C. 2005. RasGRP1 and RasGRP3 regulate B cell proliferation by facilitating B cell receptor-Ras signaling. *J Immunol,* 175**,** 7179-84.

D'AMBROSIO, D., CANTRELL, D. A., FRATI, L., SANTONI, A. & TESTI, R. 1994. Involvement of p21ras activation in T cell CD69 expression. *Eur J Immunol,* 24**,** 616-20.

DAS, J., HO, M., ZIKHERMAN, J., GOVERN, C., YANG, M., WEISS, A., CHAKRABORTY, A. K. & ROOSE, J. P. 2009. Digital signaling and hysteresis characterize ras activation in lymphoid cells. *Cell,* 136**,** 337-51.

DELGOFFE, G. M., KOLE, T. P., ZHENG, Y., ZAREK, P. E., MATTHEWS, K. L., XIAO, B., WORLEY, P. F., KOZMA, S. C. & POWELL, J. D. 2009. The mTOR kinase differentially regulates effector and regulatory T cell lineage commitment. *Immunity,* 30**,** 832-44.

DELGOFFE, G. M., POLLIZZI, K. N., WAICKMAN, A. T., HEIKAMP, E., MEYERS, D. J., HORTON, M. R., XIAO, B., WORLEY, P. F. & POWELL, J. D. 2011. The kinase mTOR regulates the differentiation of helper T cells through the selective activation of signaling by mTORC1 and mTORC2. *Nat Immunol,* 12**,** 295-303.

DOWER, N. A., STANG, S. L., BOTTORFF, D. A., EBINU, J. O., DICKIE, P., OSTERGAARD, H. L. & STONE, J. C. 2000. RasGRP is essential for mouse thymocyte differentiation and TCR signaling. *Nat Immunol,* 1**,** 317-21.

EBINU, J. O., BOTTORFF, D. A., CHAN, E. Y., STANG, S. L., DUNN, R. J. & STONE, J. C. 1998. RasGRP, a Ras guanyl nucleotide- releasing protein with calcium- and diacylglycerol-binding motifs. *Science,* 280**,** 1082-6.

FESKE, S. 2007. Calcium signalling in lymphocyte activation and disease. *Nat Rev Immunol,* 7**,** 690-702.

FISCHER, A. M., KATAYAMA, C. D., PAGES, G., POUYSSEGUR, J. & HEDRICK, S. M. 2005. The role of erk1 and erk2 in multiple stages of T cell development. *Immunity,* 23**,** 431-43.

FULLER, D. M., ZHU, M., SONG, X., OU-YANG, C. W., SULLIVAN, S. A., STONE, J. C. & ZHANG, W. 2012. Regulation of RasGRP1 function in T cell development and activation by its unique tail domain. *PLoS One,* 7**,** e38796.

GANGLOFF, Y. G., MUELLER, M., DANN, S. G., SVOBODA, P., STICKER, M., SPETZ, J. F., UM, S. H., BROWN, E. J., CEREGHINI, S., THOMAS, G. & KOZMA, S. C. 2004. Disruption of the mouse mTOR gene leads to early postimplantation lethality and prohibits embryonic stem cell development. *Mol Cell Biol,* 24**,** 9508-16.

GENOT, E. & CANTRELL, D. A. 2000. Ras regulation and function in lymphocytes. *Curr Opin Immunol,* 12**,** 289-94.

GIFFORD, J. L., WALSH, M. P. & VOGEL, H. J. 2007. Structures and metal-ion-binding properties of the Ca2+-binding helix-loop-helix EF-hand motifs. *Biochem J,* 405**,** 199-221.

GOLEC, D. P., DOWER, N. A., STONE, J. C. & BALDWIN, T. A. 2013. RasGRP1, but Not RasGRP3, Is Required for Efficient Thymic beta-Selection and ERK Activation Downstream of CXCR4. *PLoS One,* 8**,** e53300.

GORENTLA, B. K., WAN, C. K. & ZHONG, X. P. 2011. Negative regulation of mTOR activation by diacylglycerol kinases. *Blood,* 117**,** 4022-31.

GRABAREK, Z. 2006. Structural basis for diversity of the EF-hand calcium-binding proteins. *J Mol Biol,* 359**,** 509-25.

HOGQUIST, K. A., STARR, T. K. & JAMESON, S. C. 2003. Receptor sensitivity: when T cells lose their sense of self. *Curr Biol,* 13**,** R239-41.

HSIEH, A. C., LIU, Y., EDLIND, M. P., INGOLIA, N. T., JANES, M. R., SHER, A., SHI, E. Y., STUMPF, C. R., CHRISTENSEN, C., BONHAM, M. J., WANG, S., REN, P., MARTIN, M., JESSEN, K., FELDMAN, M. E., WEISSMAN, J. S., SHOKAT, K. M., ROMMEL, C. & RUGGERO, D. 2012. The translational landscape of mTOR signalling steers cancer initiation and metastasis. *Nature,* 485**,** 55-61.

IWIG, J. S., VERCOULEN, Y., DAS, R., BARROS, T., LIMNANDER, A., CHE, Y., PELTON, J. G., WEMMER, D. E., ROOSE, J. P. & KURIYAN, J. 2013. Structural analysis of autoinhibition in the Ras-specific exchange factor RasGRP1. *Elife,* 2**,** e00813.

JUN, J. E., WILSON, L. E., VINUESA, C. G., LESAGE, S., BLERY, M., MIOSGE, L. A., COOK, M. C., KUCHARSKA, E. M., HARA, H., PENNINGER, J. M., DOMASHENZ, H., HONG, N. A., GLYNNE, R. J., NELMS, K. A. & GOODNOW, C. C. 2003. Identifying the MAGUK protein Carma-1 as a central regulator of humoral immune responses and atopy by genome-wide mouse mutagenesis. *Immunity,* 18**,** 751-62.

KIM, D. H., SARBASSOV, D. D., ALI, S. M., KING, J. E., LATEK, R. R., ERDJUMENT-BROMAGE, H., TEMPST, P. & SABATINI, D. M. 2002. mTOR interacts with raptor to form a nutrient-sensitive complex that signals to the cell growth machinery. *Cell,* 110**,** 163-75.

KINDLER, T., CORNEJO, M. G., SCHOLL, C., LIU, J., LEEMAN, D. S., HAYDU, J. E., FROHLING, S., LEE, B. H. & GILLILAND, D. G. 2008. K-RasG12D-induced T-cell lymphoblastic lymphoma/leukemias harbor Notch1 mutations and are sensitive to gamma-secretase inhibitors. *Blood,* 112**,** 3373-82.

KNUTSON, B. A. 2010. Insights into the domain and repeat architecture of target of rapamycin. *J Struct Biol,* 170**,** 354-63.

KORTUM, R. L., ROUQUETTE-JAZDANIAN, A. K. & SAMELSON, L. E. 2013. Ras and extracellular signal-regulated kinase signaling in thymocytes and T cells. *Trends Immunol*.

MANDL, J. N., LIOU, R., KLAUSCHEN, F., VRISEKOOP, N., MONTEIRO, J. P., YATES, A. J., HUANG, A. Y. & GERMAIN, R. N. 2012. Quantification of lymph node transit times reveals differences in antigen surveillance strategies of naive CD4+ and CD8+ T cells. *Proc Natl Acad Sci U S A,* 109**,** 18036-41.

MANDL, J. N., MONTEIRO, J. P., VRISEKOOP, N. & GERMAIN, R. N. 2013. T cell-positive selection uses self-ligand binding strength to optimize repertoire recognition of foreign antigens. *Immunity,* 38**,** 263-74.

MARKEGARD, E., TRAGER, E., YANG, C. W., ZHANG, W., WEISS, A. & ROOSE, J. P. 2011. Basal LAT-diacylglycerol-RasGRP1 Signals in T Cells Maintain TCRalpha Gene Expression. *PLoS One,* 6**,** e25540.

MURAKAMI, M., ICHISAKA, T., MAEDA, M., OSHIRO, N., HARA, K., EDENHOFER, F., KIYAMA, H., YONEZAWA, K. & YAMANAKA, S. 2004. mTOR is essential for growth and proliferation in early mouse embryos and embryonic stem cells. *Mol Cell Biol,* 24**,** 6710-8.

NELMS, K. A. & GOODNOW, C. C. 2001. Genome-wide ENU mutagenesis to reveal immune regulators. *Immunity,* 15**,** 409-18.

PAN, W., ZHU, S., YUAN, M., CUI, H., WANG, L., LUO, X., LI, J., ZHOU, H., TANG, Y. & SHEN, N. 2010. MicroRNA-21 and microRNA-148a contribute to DNA hypomethylation in lupus CD4+ T cells by directly and indirectly targeting DNA methyltransferase 1. *J Immunol,* 184**,** 6773-81.

PLAGNOL, V., HOWSON, J. M., SMYTH, D. J., WALKER, N., HAFLER, J. P., WALLACE, C., STEVENS, H., JACKSON, L., SIMMONDS, M. J., BINGLEY, P. J., GOUGH, S. C. & TODD, J. A. 2011. Genome-wide association analysis of autoantibody positivity in type 1 diabetes cases. *PLoS Genet,* 7**,** e1002216.

POLIC, B., KUNKEL, D., SCHEFFOLD, A. & RAJEWSKY, K. 2001. How alpha beta T cells deal with induced TCR alpha ablation. *Proc Natl Acad Sci U S A,* 98**,** 8744-9.

POON, H. Y. & STONE, J. C. 2009. Functional links between diacylglycerol and phosphatidylinositol signaling systems in human leukocyte-derived cell lines. *Biochem Biophys Res Commun,* 390**,** 1395-401.

PRIATEL, J. J., CHEN, X., ZENEWICZ, L. A., SHEN, H., HARDER, K. W., HORWITZ, M. S. & TEH, H. S. 2007. Chronic immunodeficiency in mice lacking RasGRP1 results in CD4 T cell immune activation and exhaustion. *J Immunol,* 179**,** 2143-52.

PRIATEL, J. J., TEH, S. J., DOWER, N. A., STONE, J. C. & TEH, H. S. 2002. RasGRP1 transduces low-grade TCR signals which are critical for T cell development, homeostasis, and differentiation. *Immunity,* 17**,** 617-27.

QU, H. Q., GRANT, S. F., BRADFIELD, J. P., KIM, C., FRACKELTON, E., HAKONARSON, H. & POLYCHRONAKOS, C. 2009. Association of RASGRP1 with type 1 diabetes is revealed by combined follow-up of two genome-wide studies. *J Med Genet,* 46**,** 553-4.

QUAH, B. J. & PARISH, C. R. 2010. The use of carboxyfluorescein diacetate succinimidyl ester (CFSE) to monitor lymphocyte proliferation. *J Vis Exp*.

RAMISCAL, R. R. & VINUESA, C. G. 2013. T-cell subsets in the germinal center. *Immunol Rev,* 252**,** 146-55.

RANDALL, K. L., LAMBE, T., JOHNSON, A. L., TREANOR, B., KUCHARSKA, E., DOMASCHENZ, H., WHITTLE, B., TZE, L. E., ENDERS, A., CROCKFORD, T. L., BOURIEZ-JONES, T., ALSTON, D., CYSTER, J. G., LENARDO, M. J., MACKAY, F., DEENICK, E. K., TANGYE, S. G., CHAN, T. D., CAMIDGE, T., BRINK, R., VINUESA, C. G., BATISTA, F. D., CORNALL, R. J. & GOODNOW, C. C. 2009. Dock8 mutations cripple B cell immunological synapses, germinal centers and long-lived antibody production. *Nat Immunol,* 10**,** 1283-91.

ROOSE, J. P., DIEHN, M., TOMLINSON, M. G., LIN, J., ALIZADEH, A. A., BOTSTEIN, D., BROWN, P. O. & WEISS, A. 2003. T Cell Receptor-Independent Basal Signaling via Erk and Abl Kinases Suppresses RAG Gene Expression. *PLoS Biol,* 1**,** E53.

ROOSE, J. P., MOLLENAUER, M., GUPTA, V. A., STONE, J. & WEISS, A. 2005. A diacylglycerol-protein kinase C-RasGRP1 pathway directs Ras activation upon antigen receptor stimulation of T cells. *Mol Cell Biol,* 25**,** 4426-41.

ROOSE, J. P., MOLLENAUER, M., HO, M., KUROSAKI, T. & WEISS, A. 2007. Unusual interplay of two types of Ras activators, RasGRP and SOS, establishes sensitive and robust Ras activation in lymphocytes. *Mol Cell Biol,* 27**,** 2732-45.

RUST, S., FUNKE, H. & ASSMANN, G. 1993. Mutagenically separated PCR (MS-PCR): a highly specific one step procedure for easy mutation detection. *Nucleic Acids Res,* 21**,** 3623-9.

SAKAGUCHI, N., TAKAHASHI, T., HATA, H., NOMURA, T., TAGAMI, T., YAMAZAKI, S., SAKIHAMA, T., MATSUTANI, T., NEGISHI, I., NAKATSURU, S. & SAKAGUCHI, S. 2003. Altered thymic T-cell selection due to a mutation of the ZAP-70 gene causes autoimmune arthritis in mice. *Nature,* 426**,** 454-60.

SALMOND, R. J., EMERY, J., OKKENHAUG, K. & ZAMOYSKA, R. 2009. MAPK, phosphatidylinositol 3-kinase, and mammalian target of rapamycin pathways converge at the level of ribosomal protein S6 phosphorylation to control metabolic signaling in CD8 T cells. *J Immunol,* 183**,** 7388-97.

SIGGS, O. M., MIOSGE, L. A., YATES, A. L., KUCHARSKA, E. M., SHEAHAN, D., BRDICKA, T., WEISS, A., LISTON, A. & GOODNOW, C. C. 2007. Opposing functions of the T cell receptor kinase ZAP-70 in immunity and tolerance differentially titrate in response to nucleotide substitutions. *Immunity,* 27**,** 912-26.

SILVA, D. G., DALEY, S. R., HOGAN, J., LEE, S. K., TEH, C. E., HU, D. Y., LAM, K. P., GOODNOW, C. C. & VINUESA, C. G. 2011. Anti-islet autoantibodies trigger autoimmune diabetes in the presence of an increased frequency of islet-reactive CD4 T cells. *Diabetes,* 60**,** 2102-11.

SMITH, K., SEDDON, B., PURBHOO, M. A., ZAMOYSKA, R., FISHER, A. G. & MERKENSCHLAGER, M. 2001. Sensory adaptation in naive peripheral CD4 T cells. *J Exp Med,* 194**,** 1253-61.

SOMMERS, C. L., PARK, C. S., LEE, J., FENG, C., FULLER, C. L., GRINBERG, A., HILDEBRAND, J. A., LACANA, E., MENON, R. K., SHORES, E. W., SAMELSON, L. E. & LOVE, P. E. 2002. A LAT mutation that inhibits T cell development yet induces lymphoproliferation. *Science,* 296**,** 2040-3.

STARR, T. K., JAMESON, S. C. & HOGQUIST, K. A. 2003. Positive and negative selection of T cells. *Annu Rev Immunol,* 21**,** 139-76.

STEFANOVA, I., DORFMAN, J. R. & GERMAIN, R. N. 2002. Self-recognition promotes the foreign antigen sensitivity of naive T lymphocytes. *Nature,* 420**,** 429-34.

STONE, J. C. 2011. Regulation and Function of the RasGRP Family of Ras Activators in Blood Cells. *Genes Cancer,* 2**,** 320-34.
SWAN, K. A., ALBEROLA-ILA, J., GROSS, J. A., APPLEBY, M. W., FORBUSH, K. A., THOMAS, J. F. & PERLMUTTER, R. M. 1995. Involvement of p21ras distinguishes positive and negative selection in thymocytes. *EMBO J,* 14**,** 276-85.
TAZMINI, G., BEAULIEU, N., WOO, A., ZAHEDI, B., GOULDING, R. E. & KAY, R. J. 2009. Membrane localization of RasGRP1 is controlled by an EF-hand, and by the GEF domain. *Biochim Biophys Acta,* 1793**,** 447-61.
THORNTON, A. M., KORTY, P. E., TRAN, D. Q., WOHLFERT, E. A., MURRAY, P. E., BELKAID, Y. & SHEVACH, E. M. 2010. Expression of Helios, an Ikaros transcription factor family member, differentiates thymic-derived from peripherally induced Foxp3+ T regulatory cells. *J Immunol,* 184**,** 3433-41.
VAN OERS, N. S., KILLEEN, N. & WEISS, A. 1994. ZAP-70 is constitutively associated with tyrosine-phosphorylated TCR zeta in murine thymocytes and lymph node T cells. *Immunity,* 1**,** 675-85.
VAN OERS, N. S., TAO, W., WATTS, J. D., JOHNSON, P., AEBERSOLD, R. & TEH, H. S. 1993. Constitutive tyrosine phosphorylation of the T-cell receptor (TCR) zeta subunit: regulation of TCR-associated protein tyrosine kinase activity by TCR zeta. *Mol Cell Biol,* 13**,** 5771-80.
WANG, J., LIU, Y., LI, Z., WANG, Z., TAN, L. X., RYU, M. J., MELINE, B., DU, J., YOUNG, K. H., RANHEIM, E., CHANG, Q. & ZHANG, J. 2011. Endogenous oncogenic Nras mutation initiates hematopoietic malignancies in a dose- and cell type-dependent manner. *Blood,* 118**,** 368-79.
YABAS, M., TEH, C. E., FRANKENREITER, S., LAL, D., ROOTS, C. M., WHITTLE, B., ANDREWS, D. T., ZHANG, Y., TEOH, N. C., SPRENT, J., TZE, L. E., KUCHARSKA, E. M., KOFLER, J., FARELL, G. C., BROER, S., GOODNOW, C. C. & ENDERS, A. 2011. ATP11C is critical for the internalization of phosphatidylserine and differentiation of B lymphocytes. *Nat Immunol,* 12**,** 441-9.
YANG, K., NEALE, G., GREEN, D. R., HE, W. & CHI, H. 2011. The tumor suppressor Tsc1 enforces quiescence of naive T cells to promote immune homeostasis and function. *Nat Immunol,* 12**,** 888-97.
YASUDA, S., STEVENS, R. L., TERADA, T., TAKEDA, M., HASHIMOTO, T., FUKAE, J., HORITA, T., KATAOKA, H., ATSUMI, T. & KOIKE, T. 2007. Defective expression of Ras guanyl nucleotide-releasing protein 1 in a subset of patients with systemic lupus erythematosus. *J Immunol,* 179**,** 4890-900.
ZHANG, J., WANG, J., LIU, Y., SIDIK, H., YOUNG, K. H., LODISH, H. F. & FLEMING, M. D. 2009. Oncogenic Kras-induced leukemogeneis: hematopoietic stem cells as the initial target and lineage-specific progenitors as the potential targets for final leukemic transformation. *Blood,* 113**,** 1304-14.
ZHANG, S., READINGER, J. A., DUBOIS, W., JANKA-JUNTTILA, M., ROBINSON, R., PRUITT, M., BLISKOVSKY, V., WU, J. Z., SAKAKIBARA, K., PATEL, J., PARENT, C. A., TESSAROLLO, L., SCHWARTZBERG, P. L. & MOCK, B. A. 2011. Constitutive reductions in mTOR alter cell size, immune cell development, and antibody production. *Blood,* 117**,** 1228-38.
ZHENG, Y., LIU, H., COUGHLIN, J., ZHENG, J., LI, L. & STONE, J. C. 2005. Phosphorylation of RasGRP3 on threonine 133 provides a mechanistic link between PKC and RAS signaling systems in B cells. *Blood*.
ZHU, M., FULLER, D. M. & ZHANG, W. 2012. The role of Ras guanine nucleotide releasing protein 4 in Fc epsilonRI-mediated signaling, mast cell function, and T cell development. *J Biol Chem,* 287**,** 8135-43.

Chapter 7

Naïve CD4^{+} T Cells Feature Tonic Rasgrp1-mTORC1 Signals that Control mRNA Translation

ABSTRACT

T cells exhibit low-level, constitutive signals (tonic signals) in the basal state. Tonic signals through the mTORC1-S6 pathway are particularly robust in freshly-isolated naïve $CD4^+$ T cells. Here we explore the functional consequences of increased mTOR signals in T cells using a mouse model with a point mutation in the Ras activator Rasgrp1 (the $Rasgrp1^{Anaef}$ mouse) that drives elevated basal mTORC1 signaling. These mice develop mTOR-dependent T cell autoimmunity with age. Using the Nur77-GFP reporter system, we uncovered that the Anaef allele skews the TCR repertoire towards autoreactivity and increases differentiation to the Tfh and Th2 lineages. Mechanistically, we uncovered a role for basal Rasgrp1-mTOR signals in regulating mRNA translation: protein levels, but not transcript levels, of the Th2 master transcription factor Gata3 are elevated in naïve $CD4^+$ T cells with high tonic signaling. We are extending our findings to uncover what global translation programs are regulated by tonic Rasgrp1-mTOR signals in naïve T cells. Overall, our results provide novel insights into the role of tonic signaling pathways in $CD4^+$ T cells and how point mutations in signaling proteins can disrupt these tonic pathways, leading to perturbed immune function.

INTRODUCTION

$CD4^+$ T cells that encounter foreign antigen presented on MHC class II molecules elicit a strong signal through the T cell receptor (TCR) and, in the context of the appropriate cytokine milieu, trigger T cell activation and differentiation into specialized effector subsets such as Th1, Th2, Th17, iTreg, and Tfh. The signaling pathways turned on downstream of the TCR in response to cognate antigen have been well-described (see Chapter 1).

Naïve $CD4^+$ T cells continuously survey the peripheral lymphoid organs and, in the absence of infection, the antigens encountered are derived from self peptides. It has been observed that both $CD4^+$ and $CD8^+$ lymphocytes exhibit constitutive, low-level signaling in the absence of cognate foreign antigen when immediately investigated *ex vivo*, a phenomenon is referred to as "basal" or "tonic" signaling (Fulton et al., 2014; Hogquist et al., 2003; Mandl et al., 2012; Markegard et al., 2011; Stefanová et al., 2002; van Oers et al., 1994; 1993). Naive T cells must somehow balance remaining in a controlled naïve state while being able to be efficiently activated via foreign peptide MHC (pMHC). Early work characterizing this tonic pathway revealed that there is low-level phosphorylation of proximal TCR signaling components such as the TCRζ chain immunoreceptor tyrosine-based activation motifs (ITAMs) (van Oers et al., 1993), and association of the kinase Zap70 with pTCRζ in the basal state (van Oers et al., 1994). This basal pTCRζ is reduced in T cells isolated from the blood, where T cells are not constantly surveying and contacting self pMHC, or when an MHC class II blocking antibody is administered to mice (Stefanová et al., 2002). When T cells are rested *in vitro* in PBS, the tonic signal dissipates, arguing that it is actively maintained *in vivo* (Daley et al., 2013; van Oers et al., 1993). A set of conflicting studies in which T cells were deprived of tonic signals postulate that these signals either desensitize the TCR (Bhandoola et al., 2002) by recruiting negative

regulators, raising the threshold required for activation, or that interactions with self-pMHC sensitize the TCR, lowering its activation threshold (Stefanová et al., 2002).

Naïve $CD4^+$ T cells express a diverse set of TCRs, and these receptors exhibit a range of self-reactivity. This is reflected by the broad expression of several markers that report the strength of tonic signals received by a given T cell, including the surface molecule CD5 and the orphan nuclear receptor *Nr4a1* (*Nur77*). The functional relevance of the heterogeneity is still relatively unclear. Several studies have used the CD5 marker to define the physiological role of these basal signals in several T cell subsets, including $CD4^+$ conventional T cells (Daley et al., 2013; Mandl et al., 2012; Persaud et al., 2014). Tetramer studies revealed that $CD4^+$ conventional T cells with high tonic signaling ($CD5^{high}$) bind to foreign antigen better than their $CD5^{low}$ counterparts, suggesting that the degree of affinity for self-antigen parallels the degree of affinity for foreign antigen. Consistent with this, when congenically marked, sorted $CD5^{low}$ and $CD5^{high}$ cells were transferred into recipients prior to bacterial or viral infection, the $CD5^{high}$ cells expanded much more than their $CD5^{low}$ counterparts. This suggests that cells with high tonic signaling contribute more to the immune response to infection than lower-affinity cells (Mandl et al., 2012). Similar results were observed for $CD8^+$ T cells (Fulton et al., 2014). How mechanistically tonic signals contribute to the apparent increased fitness has yet to be determined.

We previously noted tonic signals through the mechanistic/mammalian target of rapamycin (mTOR) pathway in naïve $CD4^+$ T cells that were freshly-isolated from mouse lymph nodes (Daley et al., 2013). mTOR is a critical regulator of cell growth, proliferation, and mRNA translation in most cell types (Chi, 2012; Laplante and Sabatini, 2012). Recently there has been increased interest in the role of mTOR signaling in many aspects of $CD4^+$ T cell biology, including helper T cell differentiation. The mTOR kinase itself has been shown to be

dispensable for the generation of induced regulatory T cells (Delgoffe et al., 2009). mTOR associates with cofactors and accessory proteins to form two complexes, mTORC1 and mTORC2, which phosphorylate different substrates (Zoncu et al., 2010). Distinct signaling through mTORC1 and mTORC2 is critical for differentiation to Th1, Th2, Th17, and Tfh (Delgoffe et al., 2011; Heikamp et al., 2014; J. Yang et al., 2016; K. Yang et al., 2013; Zeng et al., 2016). mTOR also regulates translation of mRNAs into proteins (Laplante and Sabatini, 2012). Polysome analysis of naïve vs. *ex vivo* TCR-stimulated $CD4^+$ T cells revealed that these cells, with different activation states, translate distinct mRNAs (Bjur et al., 2013). The functional role of translational regulation in naïve T cells, as well as how dysregulation of translational programs impacts the naïve state, has not been studied.

We and others reported that the Ras activator Rasgrp1 participates in the mTOR pathway both in the basal (Daley et al., 2013) and the TCR-inducible (Gorentla et al., 2011) states. Point mutating the EF hand of Rasgrp1 (the $Rasgrp1^{Anaef}$ variant) leads to increased basal mTOR signaling, which drives spontaneous T cell activation (elevated surface CD44 levels) and autoimmune features (ANAs) in mice (Daley et al., 2013). Here we demonstrate that Rasgrp1 robustly signals to mTORC1-S6 but not to Ras-Erk or mTORC2-Akt kinase pathways in unstimulated cells. $Rasgrp1^{Anaef}$ generates tonic mTORC1-S6 signals, which favor differentiation to Tfh and Th2. Cells with increased tonic mTORC1-S6 signaling have increased translation of Th2-relevant mRNAs such as Gata3. We are currently applying ribosome profiling coupled to direct RNA-Seq to determine the translational landscape of naïve $CD4^+$ T cells and determine how increasing tonic mTORC1 signals with the $Rasgrp1^{Anaef}$ variant alters these basal translational programs. Our findings reveal that tonic signals actively tune the naïve state of $CD4^+$ T cells and that proper control of tonic translational programs is important for maintaining the naïve T cell state.

RESULTS

Robust Tonic Rasgrp1-mTORC1 Signals in Naïve CD4$^+$ T Cells

Tonic TCR signals lead to low-level phosphorylation of proximal signaling molecules such as TCRζ (Mandal and Rossi, 2012; van Oers et al., 1994; 1993). We previously showed that resting cells in PBS *ex vivo* could bring down tonic mTOR signals. Additionally, cells with a high degree of tonic signaling (CD5^{high}) had increased basal P-S6 signaling compared to cells with low tonic signaling (Daley et al., 2013). We were intrigued by this and wanted to more fully analyze tonic mTOR signaling in T cells. We intend to immediately fix lymph node cells from WT and Anaef mice, or rest a single-cell suspension in PBS for 30 and 60 minutes *ex vivo* and perform phospho-flow cytometry in conjunction with relevant surface markers (CD4, CD62L, and CD5), to analyze basal kinase signals in naïve vs. activated/memory cells as a function of TCR affinity for self (marked by level of CD5). We will perform phospho-flow for P-S6S$^{235/236}$ as a measure of mTORC1 signaling, P-Akt^{S473} as a measure of mTORC2 signaling, and P-Erk$^{T202/Y204}$ as a measure of Ras-kinase signaling.

To study Rasgrp1 function, we have previously utilized a DT40 chicken B cell line with deletion of Rasgrp1 and Rasgrp3 (Das et al., 2009). In the absence of any BCR stimulation, WT DT40 cells exhibited robust phosphorylation of S6, whereas very little P-S6 is observed in Rasgrp1/3 double-deficient (DKO) cells (**Fig 7.1A**). Transient transfection of DKO cells with constructs containing WT and catalytic dead (R271E) Rasgrp1 revealed that P-S6 increases as Rasgrp1 dosage goes up. These effects were specific to S6 as we did not observe much basal phosphorylation of Akt or the downstream Ras effector Erk. Additionally, Rasgrp1 catalytic activity is required, as we observed very little P-S6 in cells transfected with Rasgrp1^{R271E}, even with very high overexpression (**Fig 7.1B)**. The Rasgrp1 signal to S6 could be blocked with the

mTORC1 inhibitor rapamycin (**Fig 7.1B**) and the dual mTORC1/mTORC2 inhibitor INK-128 (**Fig 7.1D**) , but not with the Rsk inhibitor BI-D1870 (**Fig 7.1B**), indicating that the P-S6 signal was due to mTORC1 signaling and not through a Rsk-S6 pathway (Roux et al., 2007). Transfection with an R519G construct shows that the Anaef allele is moderately hypermorphic in its signaling behavior to S6 in this DT40 DKO cell line assay (**Fig 7.1D**), in agreement with our analyses on primary $CD4^+$ T cells from Anaef mice (Daley et al., 2013). We did not observe any differences between WT, R271E, and R519G-transfected DT40 cells with respect to mTORC2-Akt signaling (**Figure 7.1D**). As expected given that mTORC2 activates Akt (Laplante and Sabatini, 2012), Akt phosphorylation could be reduced with INK-128, but not with the mTORC1 inhibitor rapamycin. We also intend to confirm these results *in vivo* by treating WT and Anaef mice with rapamycin and INK128 and analyzing the effect of inhibition on P-S6, P-Akt, and P-Erk levels in $CD4^+$ T cells. In sum, these assays solidify the proposed connection between Rasgrp1 and mTORC1 signaling, and we investigated the functional consequences of mTORC1-S6 signals in Anaef mice next.

Altered Selection and Autoimmune Features in Aging Anaef Mice

We previously reported that elevated basal mTOR signals in $Rasgrp1^{Anaef}$ T cells drive elevated levels of the activation marker CD44, the expansion of a population of follicular-helper like cells ($PD1^{hi}$ $Helios^+$) and autoantibody production (Daley et al., 2013). We aimed to more fully characterize the extent and kinetics of the autoreactive and autoimmune features in aging Anaef mice.

Despite having reduced *in vitro* activation of the Ras-ERK pathway, which is essential for thymocyte positive selection, thymocytes from Anaef mice exhibit relatively normal development

and selection in the thymus (Daley et al., 2013). Thus, we hypothesized that the T cells have an autoreactive TCR repertoire.

To test the hypothesis that Anaef thymocytes compensate for a Ras-Erk signal defect by selecting an autoreactive TCR repertoire, we utilized a mouse model that reports TCR affinity, wherein GFP is transgenically expressed under the control of the Nur77 regulatory region (Zikherman et al., 2012). Nur77 is induced early downstream of TCR signaling at a level proportional to the strength of signal, and the level of TCR self-reactivity can be read-out by the level of GFP expression. The cumulative GFP signal is the sum of the TCR's affinity for self and the efficiency of the intracellular TCR signaling machinery. To uncouple these two parameters, we compared GFP levels in WT and Anaef mice both with the OT-II transgene, where all $CD4^+$ T cells express the same TCR that recognizes the protein ovalbumin in the context of MHC class II, as well as mice with a polyclonal TCR repertoire. Anaef OT-II post-positive selection ($CD4^+$ $CD8^+$ $TCR\beta^+$ $CD69^+$; **Supplemental Figure 1A)** and CD4 SP ($CD4^+$ $CD8^-$, **Figure 7.2A**) thymocytes, as well as splenic $CD4^+$ T conventional cells ($CD4^+$ $CD25^-$) had reduced GFP levels compared to WT, consistent with our *in vitro* data that Anaef cells have reduced TCR-induced P-Erk levels (Daley et al., 2013). In mice on a polyclonal background, Anaef $CD4^+$ SP thymocytes had reduced GFP levels compared to WT, but Anaef splenocytes had comparable or higher GFP levels than WT cells (**Figure 7.2B**), proving the selection of a more autoreactive TCR repertoire in Anaef mice, which likely contributes to the autoimmune features.

Using the HE-p2 assay to screen serum from WT and Anaef mice, we determined that the appearance of ANA already becomes fully penetrant in the Anaef mice at 28 weeks of age, though ANAs can be observed in some mice as early as 8 weeks **(Figure 7.2C)**. The ANAs in the Anaef mice represent a variety of isotypes, including IgM, IgG1, IgG2, IgG3, and IgE, but not IgA (**Figure 7.2D)**. Thus, the B cells in Anaef mice have undergone class-switching, an event

that requires T cell help. Of note, T cell derived IL-4 can promote switching to IgG1 (Crotty, 2011). H&E stained sections of kidneys from 28 and 66 week old mice revealed patchy, prominent lymphoid aggregates in the kidneys of three out of five 66 week old Anaef mice, while none of the other mice show abnormalities (data not shown).

Anaef $CD4^+$ T cells Exhibit Aberrant Helper T Cell Differentiation

The fact that that Anaef T cells are autoreactive and can aberrantly stimulate B cells to class-switch suggests that they are competent at producing cytokines that facilitate isotype switching. We previously verified that Anaef mice have an expanded population of T-follicular helper (Tfh)-like cells ($PD\text{-}1^{hi}$ $Helios^{hi}$) in the spleen (Daley et al., 2013). The mTOR kinase was recently shown to be important for differentiation to Tfh (J. Yang et al., 2016; Zeng et al., 2016). Given that the Anaef allele signals more strongly to mTORC1, we asked whether Tfh cells arise in unimmunized Anaef mice. Flow cytometric analysis of splenic $CD4^+$ $CD25^-$ T cells revealed that Anaef cells had increased protein levels of surface markers associated with Tfh cells, including ICOS, PD-1, and CXCR5 (**Figure 7.3A)**. Furthermore, Anaef mice had increased percentages of Tfh cells in the Peyer's Patches, a natural anatomical site where Tfh cells arise in otherwise naïve mice (**Figure 7.3B**).

In addition to its role in Tfh cell biology, mTOR is required for differentiation to other effector lineages yet is dispensable for regulatory T cell (Treg) generation (Delgoffe et al., 2009). Genetic perturbations of mTORC1 by deleting the GTPase Rheb in T cells revealed a role for mTORC1 in Th1 and Th17 differentiation (Delgoffe et al., 2011) and disrupting mTORC2 by deleting Rictor in T cells revealed a role for mTORC2 signaling in Th2 differentiation. An independent study in which mTORC1 signaling was perturbed by genetically deleting Raptor in T cells revealed a role for mTORC1 in Th2 differentiation (K. Yang et al., 2013). We

hypothesized that the increased basal mTORC1 signaling in Anaef T cells might impact their ability to differentiate to these effector subsets. To test this, we *in vitro* polarized WT and Anaef $CD4^+$ cells into Th1, Th2, Th17, and iTreg cells. Anaef cells were able to generate IFNγ-producing Th1 cells at WT levels in strongly-polarizing Th1 conditions. Similarly, we observed no difference in Th17 and iTreg generation by Anaef T cells as measured by IL-17A production and FoxP3/CD25 co-expression, respectively. Interestingly, we found that Anaef $CD4^+$ T cells were enhanced in their ability to differentiate into Th2 cells and produce IL-4 (**Fig 7.3C)**. To determine whether this was due to the elevated basal mTORC1 signaling in Anaef T cells, we intend to treat mice with INK128 *in vivo* to bring down tonic mTOR signals. We will perform *in vitro* polarization assays on cells from these inhibitor-treated animals (as well as vehicle controls) and expect that INK128 treatment will impair the ability of WT cells to differentiate to Th2 and will reduce the percentage of IL-4 producing Anaef cells to WT levels or lower.

Tonic mTORC1 Signals Affect Th2 Differentiation

As an independent approach to the Anaef model, we used the marker CD5 to test the impact of tonic mTORC1 signals on effector T cell differentiation. Freshly-isolated naïve WT cells that express high levels of CD5 (30% highest CD5 expression) exhibited increased P-$S6K^{T389}$ and P-$S6^{S235/236}$ compared to the 30% lowest CD5 expressing cells, and this difference was even more exaggerated in Anaef cells sorted based on CD5 (**Figure 7.4A).** In agreement with increased Th2 polarization of Anaef T cells, naïve $CD4^+$ $CD5^{high}$ cells, with highest tonic signaling, generated ~1.4 fold more IL-4 producing cells than CD5 low counterparts from the same sort. In strongly-polarizing Th1 conditions, we did not observe differences in IFNγ production between the $CD5^{low}$ and $CD5^{high}$ cells (**Figure 7.4B)**. To determine whether the ability to differentiate to Th2 depends on tonic mTOR signals, we will perform these *in vitro* Th2 differentiation assays on $CD5^{low}$ and $CD5^{high}$ cells in the presence of the mTOR inhibitor INK128. We will use the EC25,

50, and 75 doses of INK128 to test whether cells with different degrees of tonic signaling are differentially sensitive to mTOR inhibition. We will also add the inhibitor at different time points in the Th2 culture to determine what point during differentiation mTOR signaling is required.

Tonic mTORC1 Signals Control Translation of Specific Targets

We next sought to understand the mechanistic effects of tonic mTOR signals on helper T cell differentiation. Pilot RNA-Seq experiments revealed very few changes in RNA levels between naïve $CD4^+$ T cells sorted from WT and Anaef mice (data not shown). mTOR is known to be a key regulator of mRNA translation, and we hypothesized that translational programs may be regulated in a tonic fashion in naïve T cells. Interestingly, several genes important for Th2 and Tfh biology have been shown to be regulated at the translational level: these include the Th2 transcription factor Gata3, the Tfh and Th2 cytokine IL-4, and the costimulatory molecule ICOS (Cook and Miller, 2010; Gigoux et al., 2014; Piccirillo et al., 2014; Scheu et al., 2006).

CD44 is a translational target of mTOR in prostate cancer cells (Hsieh Nature 2012). We previously published that surface levels of CD44 protein on Anaef T cells decrease when mice are treated *in vivo* with the pharmacological inhibitor of mTOR, rapamycin (Daley et al., 2013). To more closely link this to effects on tonic translation, we compared basal mRNA and protein levels from cells freshly isolated from mice. Sorted WT cells with low and high levels of tonic signaling were lysed in Trizol, RNA was extracted, and we performed qPCR, normalizing the data to an internal control housekeeping gene, PPIA. To look at protein levels in a sensitive manner, we immediately fixed cells directly after lymph node isolation and homogenization and then performed cellular barcoding (Ksionda et al., 2016): cells from individual mice were labeled with different concentrations of fluorophore-conjugated succinimidyl ester dyes, subsequently combined into the same tube and stained with the target of interest and relevant surface

markers for gating. This method ensures that differences in expression of lowly expressed proteins are not due to staining artifacts. $CD5^{high}$ cells had lower CD44 mRNA levels than cells with lower tonic signaling, but the $CD5^{high}$ cells had higher CD44 protein levels (**Figure 7.5A**). To extend this to additional known translational targets of mTOR, we analyzed c-Myc mRNA and protein levels in $CD5^{low}$ and $CD5^{high}$ naïve $CD4^+$ T cells. c-Myc mRNA was lower in $CD5^{high}$ cells compared to $CD5^{low}$ (**Fig 7.5B)**. We will also examine c-Myc protein levels by immunoblotting, using lysates from WT naïve CD4+ T cells that were sorted based on CD5 (and kept ice-cold throughout the sorting procedure).

Gata3 is the master transcription factor for Th2 differentiation (O'Shea and Paul, 2010). It has been reported that Gata3 is regulated at the translational level in cells undergoing Th2 polarization (Cook and Miller, 2010). To determine if Gata3 is translationally regulated in the basal state, we compared mRNA levels by qPCR and protein levels by barcoding flow cytometry. As for CD44 and c-Myc, Gata3 mRNA levels were lower in $CD5^{high}$ cells, yet Gata3 protein levels were highest in the cells with high tonic signaling (**Figure 7.5C).** This suggests that tonic signals increase Gata3 mRNA translation.

We extended this finding to $CD4^+$ T cells from WT and Anaef mice. Samples for Taqman were prepared from MACS-purified $CD4^+$ $CD25^-$ cells, and fluorescent barcoding was performed as above, gating on $CD4^+$ T cells. We found slightly elevated CD44 in Anaef cells **(7**.**5D)**, and we observed no difference in c-Myc **(7.5E)** and Gata3 **(7.5F)** mRNA levels between WT and Anaef mice. Protein levels of all three markers were elevated in Anaef T cells. To determine whether tonic input into translation is due to mTOR signaling *in vivo*, we will treat mice with the INK128 inhibitor to bring down tonic mTOR signals. We expect to see reduced protein levels of these targets in inhibitor-treated animals. Collectively, these data indicate that tonic signaling

affects protein levels, but not mRNA levels, of the mTOR targets CD44 and c-Myc and the putative mTOR target Gata3.

We also analyzed the kinetics of Gata3 induction early in Th2 polarizing conditions. An increased percentage of WT $CD5^{high}$ cells (compared to $CD5^{low}$) and Anaef $CD4^+$ T cells (compared with WT) express Gata3 early on during the Th2 differentiation-phase and sustain Gata3 during the first 24 hours of culture (**Figures 7.5G, 7.5H)**. This indicates that these cells with high tonic signaling increase the production of Gata3 and/or better stabilize it early on in culture, and we hypothesize that this contributes to the ability of these cells to differentiate more efficiently to Th2 *in vitro*.

FUTURE DIRECTIONS

Paired RNA Seq and Ribosome Profiling Allow for Genome-wide Assessment of the $CD4^+$ T Cell Translational Landscape

We wanted to establish whether tonic signals control translational programs in T cells in the basal state. To test this, we will use a global, unbiased approach called ribosome profiling (Brar and Weissman, 2015; Hsieh et al., 2012; Ingolia et al., 2012), a technique in which mRNAs that are actively being translated by ribosomes (ribosome-protected fragments, or RPFs) are isolated and sequenced. In parallel, prior to RPF isolation we will take a fraction of the same cell population and perform RNA-Seq. Collectively, this will allow us to determine which mRNAs are more highly translated in $CD4^+$ T cells. As such, we will compare the translational landscapes of WT and $Rasgrp1^{Anaef}$ $CD4^+$ T cells, and we expect to find that Gata3, CD44, and c-Myc translation will be increased in Anaef cells. This method will also allow us to identify additional

mRNAs that are differentially translated in the Anaef cells compared to WT. To determine if translation of target mRNAs is under tonic control, we will validate our findings using our $CD5^{low/high}$ WT cell system and analyzing mRNAs in polysome fractions isolated from these cell populations. We expect these studies to aid our understanding of how tonic signals control basal translation in T cells and how dysregulation of basal translational programs contributes to autoimmunity.

DISCUSSION

$CD4^+$ T cells from $Rasgrp1^{Anaef}$ mice exhibit elevated mTORC1 signaling that drives T cell autoreactivity and autoimmunity. Additional mouse models in which point mutations lead to loss of T cell tolerance have been described, including the LAT^{Y136F} mouse that develops Th2 lymphoproliferation due in part to a tonic LAT-HDAC7-Irf4/Nur77 signal (Aguado et al., 2002; Sommers, 2002, Chapter 5 of this dissertation), and the $Zap70^{SGK}$ allele, which impairs the ability of Zap70 to bind to TCRζ leads to murine autoimmune arthritis (Sakaguchi et al., 2003). This suggests that tonic TCR signals provide an active control mechanism to keep T cells in the naïve state. However, these are all loss of function systems; the $Rasgrp1^{Anaef}$ variant is a weak gain-of-function allele, and thus it provides an interesting model to study the role of increased basal signals in T cells. Using $Rasgrp1^{Anaef}$ $CD4^+$ T cells as well as WT $CD4^+$ T cells sorted based on CD5, we reveal that tonic Rasgrp1-mTOR signals set a basal translational landscape in $CD4^+$ T cells. Increases in mTORC1-driven basal translation results in increased differentiation to the Tfh and Th2 lineages. These results provide novel mechanistic insights into the functional role for tonic signals in peripheral T cell homeostasis.

We show that tonic mTOR signals are particularly robust in lymphocytes, and that Rasgrp1 catalytic activity is specifically important for mTORC1, but not mTORC2, signaling in the basal state. Why the mTOR pathway seems to be particularly sensitive to differences in tonic signaling is unclear. mTOR is known to be an integrator of multiple upstream inputs (in addition to the TCR), including nutrients such as glucose and amino acids (Macintyre et al., 2014; MacIver et al., 2013; Pearce et al., 2013). Whether Rasgrp1-driven downstream mTOR activation relies on some of these other factors, and whether this signal is important for T cell metabolic programs, is still being worked out. Our preliminary results linking Rasgrp1-mTOR signaling to metabolic reprogramming will be discussed in Chapter 8.

Given the role of mTORC1 signaling in differentiation to Th1, Th17 (Delgoffe et al., 2011), Th2 (K. Yang et al., 2013), and Tfh (J. Yang et al., 2016; Zeng et al., 2016), and our observation that Rasgrp1^{Anaef} mice have a population of Tfh-like cells that expands in an mTOR-dependent manner (Daley et al., 2013) (**Figure 7.3**), we hypothesized that CD4^{+} T cells from Rasgrp1^{Anaef} mice may exhibit altered differentiation. We uncovered that Anaef T mice had increased Tfh cells in the Peyer's Patches, and that Anaef CD4^{+} T cells were enhanced in their ability to differentiate to Th2 *in vitro*. WT cells with high tonic signaling (CD5^{high}) also show the increased differentiation to Th2 compared to CD5^{low} cells. A recent publication found that CD5^{high} CD4^{+} T cells out-proliferate their CD5^{low} counterparts using *in vivo* bacterial and viral infection models. It will be interesting to determine whether Anaef CD4^{+} T cells, or CD5^{high} CD4^{+} T cells are better able to clear helminth infections (which require Th2 cytokines) or have more exacerbated features in allergic asthma models in which Th2 cells have been shown to be pathogenic (Seumois et al., 2016).

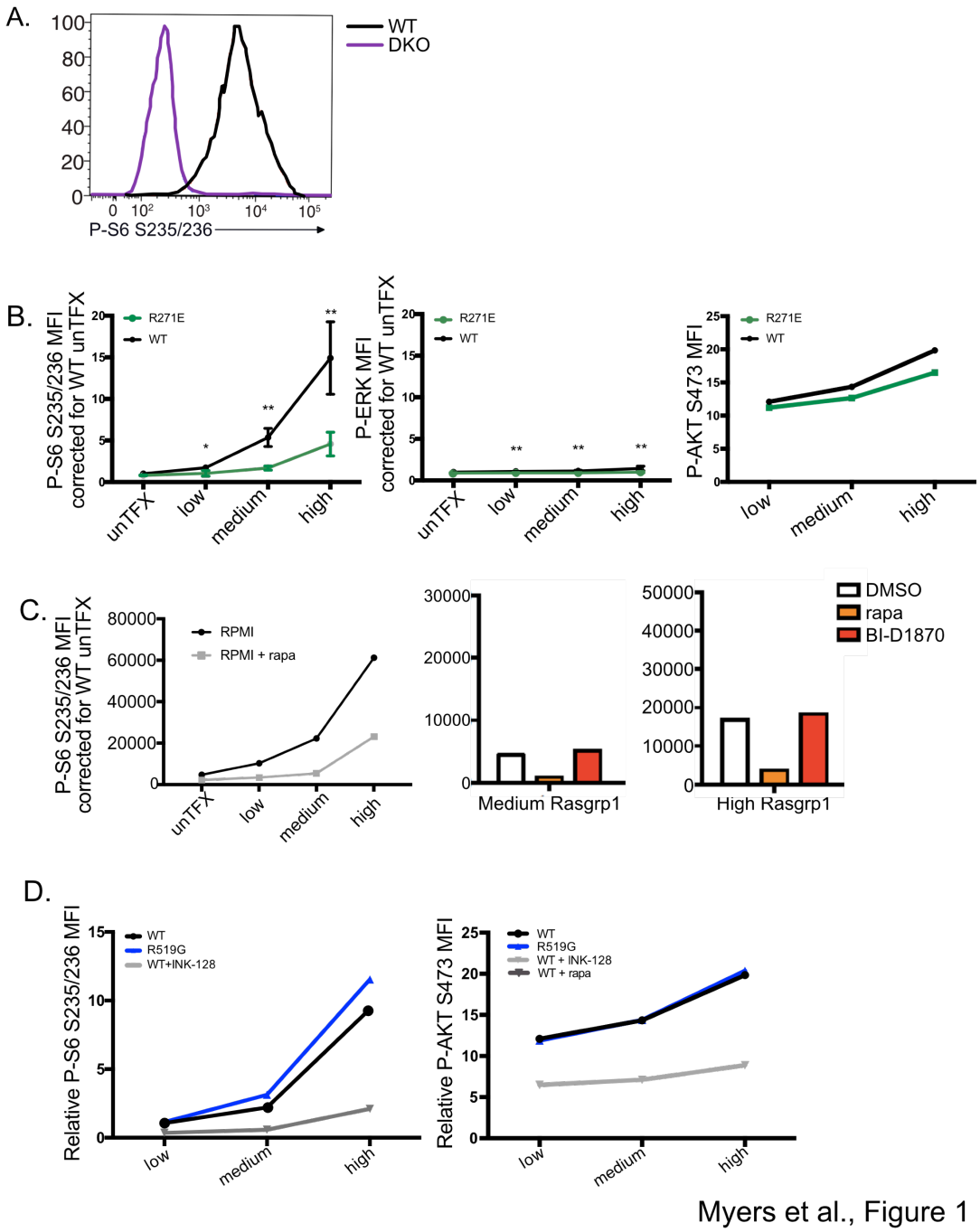
Recent work has shown that Gata3 is regulated at the translational level (Cook and Miller, 2010), and translation of IL-4, a cytokine produced by both Tfh and Th2 cells, is also

regulated in primed T cells (Scheu et al., 2006). Mechanistically, cells with high tonic signaling (Rasgrp1^{Anaef} and CD5^{high}) expressed increased protein but not mRNA levels of the Th2 master transcription factor Gata3 compared to cells with low tonic signaling (Rasgrp1^{WT} and CD5^{low}), demonstrating that tonic signals can control basal translational programs in T cells.

Together, our results put forth a novel model in which Rasgrp1-mTOR signaling controls basal protein translation in T cells. Increasing this basal translation may contribute to the autoreactive and autoimmune features observed in the mice. In addition, the slightly altered TCR repertoire in Anaef T cells that we revealed using the Nur77-GFP allele may further exacerbate the already increased mTORC1 signal from the Anaef variant, because CD4^{+} cells will intrinsically have a higher affinity for self-antigens.

Gain-of-function tonic signaling alleles such as Rasgrp1^{Anaef} may be useful tools to study the collateral damage from immune checkpoint blockade as a cancer treatment. Relieving the "brake" on T cells by blocking inhibitory receptors such as PD-1 and CTLA-4 will likely increase activity through tonic signaling pathways in these cells and thus increase the degree of sensitivity to self (Kong and Flynn, 2014; Michot et al., 2016). Moving forward, it will be important to understand what tonic signaling pathways are active in naïve CD4^{+} T cells and how altering these pathways can contribute to autoimmunity.

FIGURES



Myers et al., Figure 1

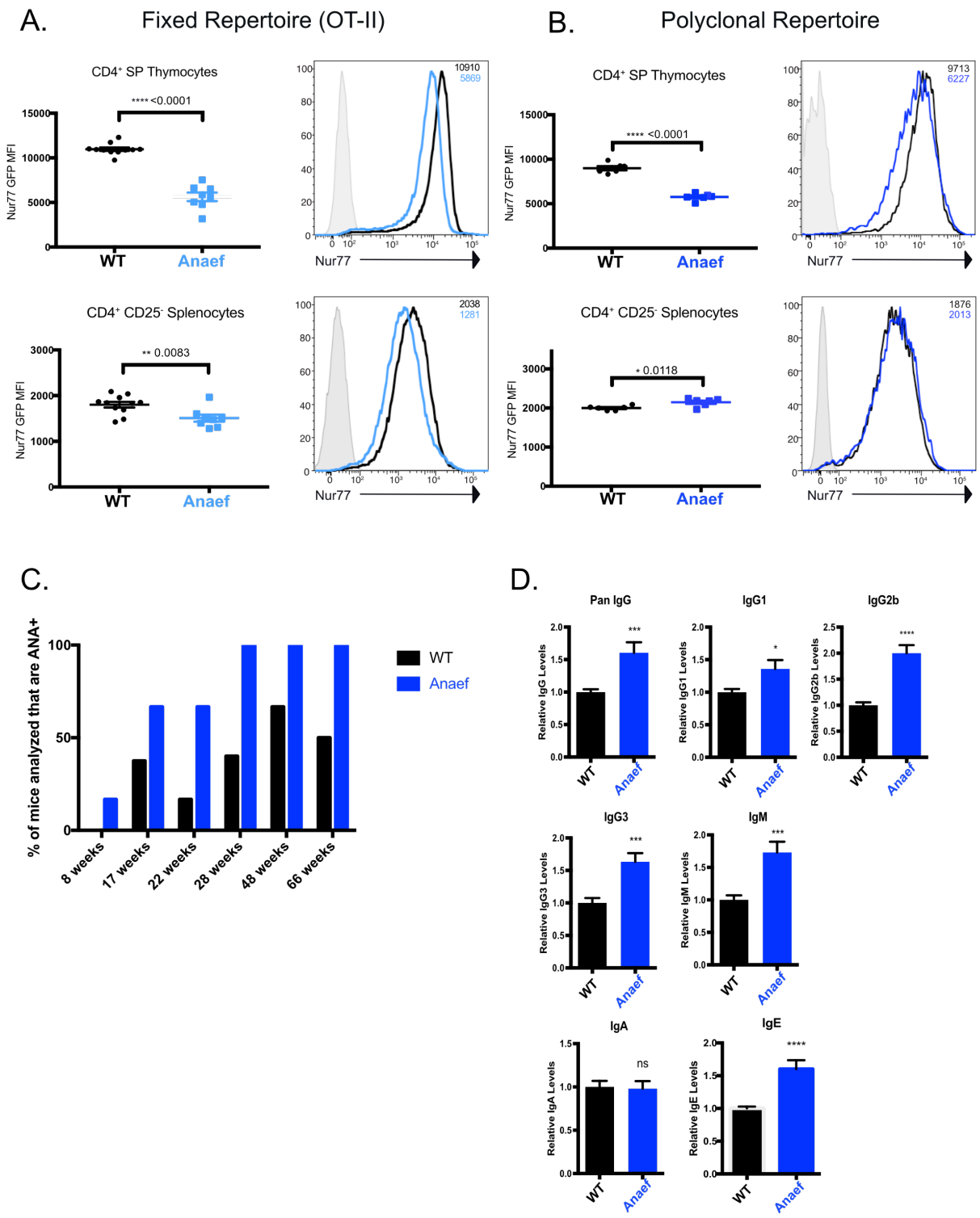
Figure 7.1: Robust Tonic Rasgrp1-mTORC1-S6 Signals in Naïve CD4$^+$ T Cells

(A) Flow cytometric analysis of basal P-S6 in WT and Rasgrp1/3 DKO DT40 cells.

(B) Flow cytometric analysis of P-S6 and P-Erk in Rasgrp1/3 DKO DT40 cells transiently transfected with WT or R271E Rasgrp1-EGFP.

(C) Flow cytometric analysis of P-S6 and P-Erk in Rasgrp1/3 DKO DT40 cells transiently transfected with WT or R271E Rasgrp1-EGFP and treated for 15 minutes with DMSO, rapamycin (20nM), or BI-D1870 (2μM).

(D) Flow cytometric analysis of P-S6 and P-Akt S473 in Rasgrp1/3 DKO DT40 cells transiently transfected with WT or R519G Rasgrp1-EGFP and treated for 30 minutes with rapamycin (20nM) or INK-128 (100nM) for 30 minutes.



Myers et al., Figure 2

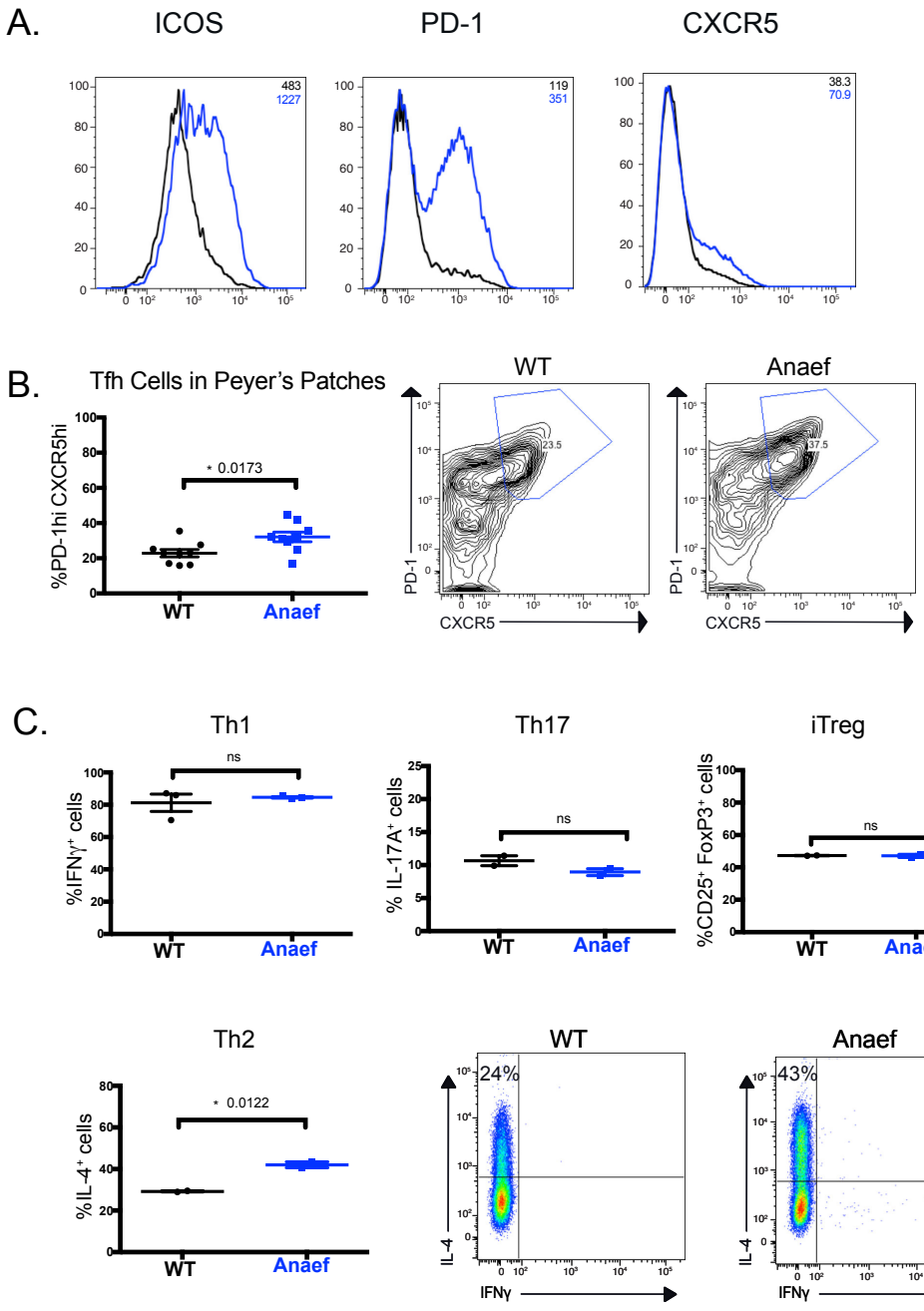
Figure 7.2: Altered Selection and Autoimmune Features in Aging Anaef Mice

(A) Flow cytometric analysis of Nur77-GFP levels in OTII WT and OTII Anaef CD4 SP thymocytes and $CD4^+$ $CD25^-$ splenocytes.

(B) Flow cytometric analysis of Nur77-GFP levels in polyclonal WT and Anaef CD4 SP thymocytes and $CD4^+$ $CD25^-$ splenocytes.

(C) Percentage of mice positive for anti-nuclear antibodies identified using the HEp-2 assay on serum from WT and Anaef mice at the indicated ages.

(D) ELISA for indicated antibody isotypes in serum from WT and Anaef mice.



Myers et al., Figure 3

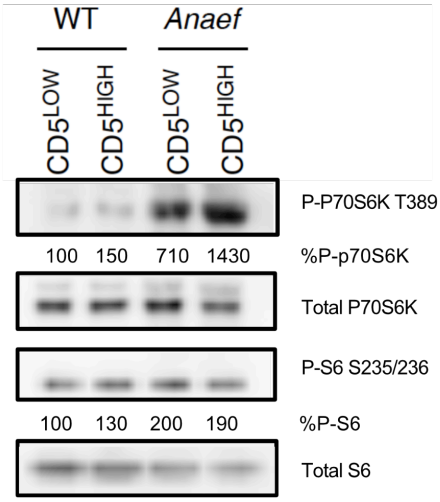
Figure 7.3: Anaef T Cells Exhibit Altered Helper T Cell Differentiation

(A) Flow cytometric analysis of ICOS, PD-1, and CXCR5 on $CD4^+$ splenocytes from WT and Anaef mice.

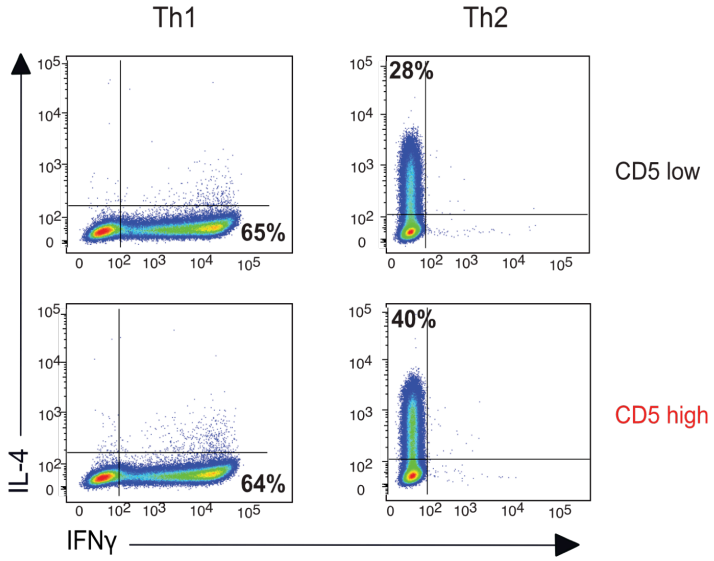
(B) Flow cytometric analysis of Tfh cells ($CD4^+$ $CD25^-$ PD-1^{hi} $CXCR5^{hi}$) in the peyer's patches of WT and Anaef mice.

(C) *in vitro* polarization assay on $CD4^+$ cells from WT and Anaef mice. Percentage of cytokine-producing cells (IFNγ for Th1, IL-4 for Th2, IL-17A for Th17) or percentage of $CD25^+$ $FoxP3^+$ (for iTreg) are shown. Th1 and Th2 cells were polarized for 5 days *in vitro* prior to analysis; Th17 and iTreg cells were polarized for 4 days prior to analysis.

A.



B.

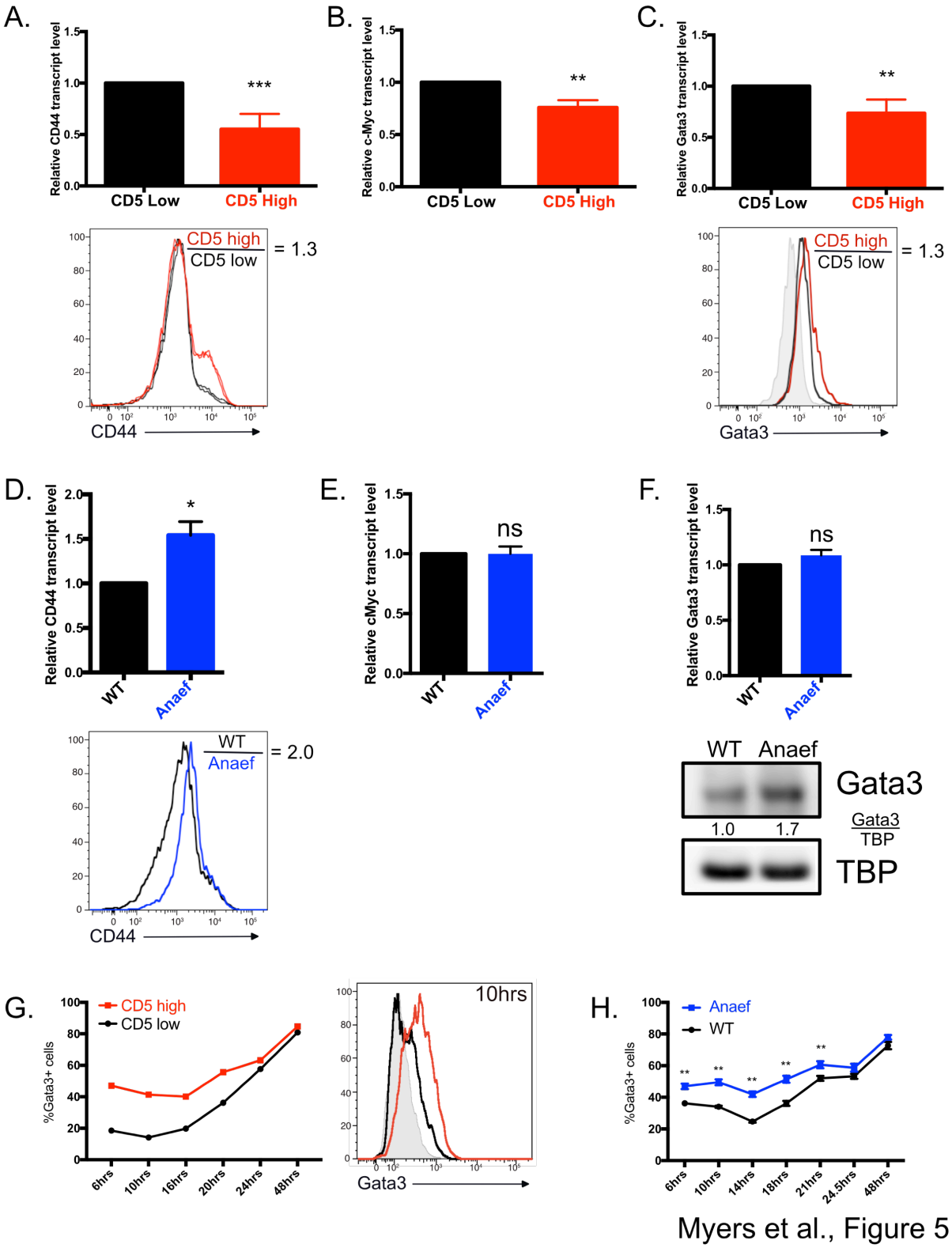


Myers et al., Figure 4

Figure 7.4: Tonic mTORC1 Signals Affect Th2 Differentiation

(A) Immunoblot for the indicated proteins on lysates from WT and Anaef naïve T cells ($CD4^+$ $CD25^-$ $CD44^{low}$) sorted into the 30% lowest and 30% highest CD5 expressers.

(B) *in vitro* polarization assay on $CD4^+$ $CD25^-$ $CD44^{low}$ WT cells sorted into the 30% lowest and 30% highest CD5 expressers. Percentage of cytokine-producing cells (IFNγ for Th1, IL-4 for Th2) are shown. Cells were polarized for 5 days.



Myers et al., Figure 5

Figure 7.5: Tonic mTORC1 Signaling Controls Translation of Specific Targets

(A) Taqman qPCR for CD44 on cDNA generated from $CD4^+$ $CD25^-$ $CD44^{low}$ WT cells sorted into the 30% lowest and highest CD5 expressers. CD44 mRNA levels were normalized to PPIA (top). Barcoding flow cytometry for surface CD44 levels on the indicated cell populations.

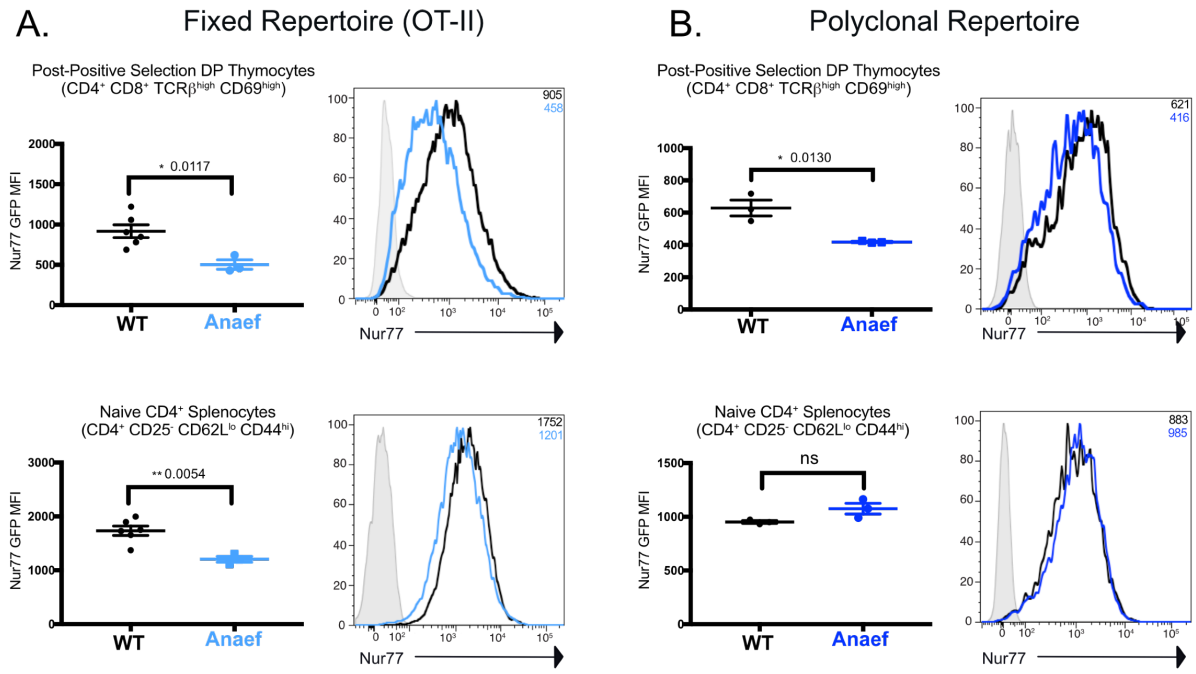
(B) Taqman qPCR for c-Myc, as in (A).

(C) Taqman qPCR for Gata3 as in (A); Barcoding flow cytometry for intracellular Gata3 levels on the indicated cell populations.

(D) As in A, but comparing $CD4^+$ WT and Anaef cells.

(E) As in B, but comparing $CD4^+$ WT and Anaef cells.

(F) As in C, but comparing $CD4^+$ WT and Anaef cells. Protein levels were measured by immunoblotting for Gata3 and the loading control TBP.



Myers et al., Supplemental Figure 1

Supplemental Figure 1: Rasgrp1^{Anaef} Thymocytes and T Cells have an Autoreactive TCR Repertoire

(A) Flow cytometric analysis of Nur77-GFP levels in OTII WT and OTII Anaef post-positive selection double positive (DP) thymocytes ($CD4^+$ $CD8^+$ $TCR\beta^{hi}$ $CD69^{hi}$) and naïve $CD4^+$ splenocytes.

(B) Flow cytometric analysis of Nur77-GFP levels in polyclonal WT and Anaef post-positive selection double positive (DP) thymocytes ($CD4^+$ $CD8^+$ $TCR\beta^{hi}$ $CD69^{hi}$) and naïve $CD4^+$ splenocytes.

METHODS

Mice

WT C57BL/6 mice and OT-II TCR transgenic mice were bred in house at UCSF. Nur77-GFP mice were obtained from Drs. Arthur Weiss and Julie Zikherman and have been described previously (Zikherman et al., 2012). Rasgrp1^{Anaef} mice have been described previously (Daley et al., 2013) and were bred at UCSF. Mice were housed and treated in accordance with the guidelines of the Institutional Animal Care and Use Committee (IACUC) guidelines of the University of California, San Francisco (AN098375-03B).

HEp-2 ANA Assays

HEp-2 assays were performed utilizing the Nova-Lite kit from INOVA diagnostics. Diluted serum was applied to slides, washed, then slides were stained with IgG-FITC (Jackson Labs) and DAPI (500ng/ml, LifeTechnologies). Slides were sealed with mounting medium (Dako) and imaged on a Keyensce BZ-X710 microscope. Sera were scored as ANA negative or ANA positive based on a no serum negative control or a CD45 Wedge B6-129 F1 positive control serum (a gift from Michelle Hermiston's lab) present on each slide.

Enzyme-Linked Immunosorbent Assay (ELISA)

96-well plates were coated overnight with Goat anti-Mouse Ig (Southern Biotech, 1010-01, [1:1000]). After washing plates 3x with DI water, plates were blocked with 15 ul PBS-BB (500 mL PBS w/o Ca/Mg + 250 uL Tween 20 (0.05%) + 5g BSA (1%)) for 45 minutes, then washed again 3X with DI water. Serum was diluted into small FACS tubes, distributed to the top row of 96-well plates, diluted accordingly throughout the remaining wells, and incubated for 120 minutes. (IgA (1:100, 5f), IgG3 (1:500, 4f), IgG1 (1:1000, 3f) IgM (1:2000, 3f), IgG2b (1:5000, 3f), IgG (1:10000, 3f)). HRP conjugated secondary antibodies were applied at a 1:2000 dilution

for 60 minutes (anti-IgA-HRP (SB1040-05), anti-IgG3-HRP (SB1100-05), anti-IgG1-HRP (SB1070-05), anti-IgM-HRP (SB1020-05), anti-IgG2b-HRP (SB1090-05), anti-IgG-HRP (SB1020-05)). HRP conjugated secondary antibodies were exposed with a slow kinetic TMB solution (Sigma, T4319) for 10 minutes. The reaction was terminated with 1N HCL. Absorbance was measured at 450 nm on a SpectraMax 340 PC plate reader and analyzed using SoftMax Pro 4.8 Software.

Comparison of isotype levels between WT and Anaef serum was done at a dilution within linear range in duplicates (IgA (1:135000), IgG3(1:128000), IgG1(1:81000), IgM (1:62000), IgG2b (1:405000), IgG (1:810000), IgE (1:40)). Three separate cohorts of 3 WT and 3 Anaef serum (n=9) were normalized to the mean absorbance of WT (n=3) serum within respective experiments/ plates. Significance was calculated using an Unpaired T-test.

Haemotoxylin and Eosin (H&E) Staining of Kidneys

Mouse kidneys were isolated, bisected, and fixed in 4% paraformaldehyde (PFA; Electron Microscopy Sciences) overnight. The next day the kidneys were put into 70% ethanol. Sectioning and H&E staining were performed by the UCSF Pathology Core. Slides were evaluated by Dr. Zoltan Laszik using a light microscope.

Cell Isolation and Stimulation

Cells were isolated from cervical, brachial, axillary, inguinal, and mesenteric lymph nodes and single cell suspensions were prepared by mashing cells through a 70μm strainer. Cells were counted and $CD4^+$ T cells were isolated by MACS negative isolation (Miltenyi) or by fluorescent activated cell sorting (FACS; staining for CD4, CD25, CD44, and CD5). Cells were counted and plated on 96 well plates that had been pre-coated with α-CD3 and α-CD28 at the concentrations indicated. T cells were cultured in RPMI (Hyclone) supplemented with 10% fetal calf serum, 1%

sodium pyruvate, 1% nonessential amino acids, 1% HEPES, 1% pen-strep glutamine, and 0.1% beta mercaptoethanol.

Flow Cytometry

Tfh cell analysis: Peyer's Patches were isolated from mice, mashed through 70μm strainers, and washed in FACS buffer (2% FCS, 2mM EDTA, 0.09% NaN_3). Cells were stained for antibodies to B220, CD4, PD-1, CXCR5 (Biolegend, clone L138D7) for 1 hour at room temperature. Cells were washed and analyzed by flow cytometry.

Intracellular cytokine staining: cells were harvested, restimulated in complete media supplemented with 5ng/ml PMA (Calbiochem) and 670nM ionomycin (Sigma Aldrich) for 1 hour at 37ºC, at which point monensin (BD Golgi Stop) was added and cells were incubated at 37ºC for an additional 3 hours. Cells were washed in FACS buffer, stained with Live/Dead Fixable Violet dye (BD, 1:1000) for 10 minutes, washed, stained for relevant surface markers where applicable, and then were fixed in BD Cytofix/Cytoperm buffer for 10 minutes. Cells were washed in BD Perm/Wash buffer 3 times to permeabilize cell membranes. Cells were then stained with anti-cytokine antibodies (eBioscience IFNγ XMG1.2; BD IL-4 11B11; eBioscience IL-17A eBio17B7) for 20 minutes and washed once with permeabilization buffer and once with FACS buffer prior to analysis by flow cytometry.

Transcription factor staining: in cellular barcoding and Gata3 time course experiments, cells were harvested at indicated time points, washed once in FACS buffer, and fixed for 10 minutes in FoxP3 Fixation buffer (eBiosciences). Cells were then washed twice with FoxP3 permeabilization buffer (eBiosciences) to permeabilize membranes. Where applicable, the permeabilized cells were stained with Pacific Blue succinimidyl ester (Molecular Probes) diluted in FoxP3 permeabilization buffer (final dye concentrations of 40, 6.5, 0.6, and 0.075ug/ml**)**, and

washed. Cells were stained with antibodies to transcription factors (e.g. Gata3 and FoxP3) and relevant isotype control (eBiosciences), washed, and analyzed by flow cytometry.

Phospho-flow cytometry: Cells were harvested at indicated time points, washed once in FACS buffer, and fixed for 20 minutes in 2% PFA at room temperature. For some experiments, cells were fixed in 2% PFA immediately after being isolated from mice and prepared into single cell suspensions. Cells were then washed twice with FACS buffer and permeabilized with ice-cold 90% methanol at -20ºC (minimum of 30 minutes, but typically overnight). Cells were washed with FACS buffer and stained with antibodies to P-S6 S235/236, P-44/42 MAPK (Erk1/2), and P-Akt S473 for 1 hour at room temperature, washed, and where applicable stained with donkey anti-rabbit secondary for 15 minutes on ice, washed, and analyzed by flow cytometry.

All flow cytometry data was acquired on a BD LSRII or Fortessa and analyzed using FlowJo (Treestar).

DT40 Cell Lines and Transfection Experiments

Rasgrp1/3 deficient DT40 chicken B cells were maintained in RPMI supplemented with 10%FBS, 1% chicken serum, 1% pen-strep-glutamine, and 2.5% HEPES. For transfection experiments, 20 million cells were washed twice in RPMI and resuspended in a 0.4cm cuvette (Invitrogen P460-50) info transfection media (same as above, excluding pen-strep). 67ug/ml of plasmid (pEGFP-N1-Rasgrp1-EGFP, with either WT Rasgrp1 or the point mutations for R271E or R519G) was added to the cuvette. Cells were electroporated using a Biorad Gene Pulser XCell and allowed to recover for 6hrs at 37ºC. Cells were then treated with vehicle or the indicated inhibitor for 30 minutes, fixed for 20 minutes with 2% paraformaldehyde, washed, and permeabilized overnight at -20ºC in 90% methanol. The following day cells were prepared for flow cytometry as described above.

Inhibitors

MLN128 (INK128) was purchased from Selleckchem and dissolved in DMSO, and it was used at 100nM. Rapamycin was purchased from Sigma Aldrich (R8781) and used at 20nM. BI-D1870 was purchased from Enzo Life Sciences (BML-EI407-0001) and used at 2uM.

Immunoblotting

Relevant cell populations were isolated by MACS purification (Miltenyi) or sorting (BD FACS Aria) as indicated. Cells were kept ice-cold throughout the entire procedure. Following purification of the cell population of interest, cells were washed twice in PBS, and then cell suspensions in PBS were directly lysed in 4X Laemmli buffer. Samples were boiled, ultracentrifuged for 30 minutes at 100,000rpm. Lysates were run on NuPAGE Novex 4-12% gradient Bis-Tris gels (ThermoFisher), transferred to PVDF membranes, blocked for 1 hour in 3% BSA, and probed for indicated proteins. Signal from primary antibodies was detected using HRP-conjugated secondary antibodies and blots were developed using Supersignal West Pico Chemiluminescent Substrate (Pierce) and images were recorded with a chemiluminescent imager (Fuji LAS-4000).

Antibodies

ICOS, PD1, CXCR5, CD4, TCRβ, CD44, CD62L, CD25, IFNγ, IL-4, IL-17A, FoxP3, Gata3 were purchased from eBioscience, BD Biosciences, BioLegend, and Tonbo Biosciences. Antibodies for phospho-flow cytometry were purchased from Cell Signaling Technologies: P-ERK (4377S), P-S6 (2211S), and P-Akt (4058L). Antibodies for western blotting were purchased from Cell Signaling (P-p70S6K T389 #9234P; Total p70S6K #2708S, P-S6 S235/236 #2211, Total S6 #2317, TBP #8515S). Gata3 antibody was purchased from Santa Cruz Biotechnologies (cat # SC-268).

TaqMan qPCR

Lymphocytes were extracted from 3 WT B6 mice, 8-10 weeks of age, and cells from 3 mice were pooled. Naive $CD4^+$ T cells were isolated using purified using negative isolation (Miltenyi Biotec). Cell were stained with fluorophore conjugated antibody for CD4 (Tonbo Biosciences, APC, clone: RM4-5), CD25 (Biolegend, Pacific Blue, clone: PC61), CD44 (BD Pharmingen, FITC, IM7), and CD5 (BD Pharmingen, PE, clone: 53-7). $CD4^+/CD25^-/CD44^{low}$ cells were subsequently sorted on a FACsAriaII cell sorter (BD Biosciences) in the UCSF flow cytometry core to >95% purity by CD5 protein level, 30% $CD5^{low}$ and 30% $CD5^{high}$.

Total RNA was extracted from sorted cells using Trizol, the PicoPure® RNA Isolation Kit (ThermoFisher Scientific, KIT0214), and treated with DNase I (ThermoFisher Scientific,12185010). RNA concentration was measured on a NanaoDrop spectrophotometer. cDNA was generated by reverse transcriptase using 500ng RNA per sample and the Super Script IV first-strand synthesis kit (ThermoFisher Scientific,18091050). For mRNA gene expression assays, TaqMan primers/probes were purchased from Life Technologies (*CD44* (Mm01277161_m1), *Gata3* (Mm00484683_m1), and *Myc* (Mm00487804_m1)).

TaqMan real-Time PCR was performed using TaqMan Fast Advanced Master Mix (Applied Biosciences, 4444963). Multiplex Taqman reactions were run on a QuantStudio 12K Flex Real-Time PCR System (ThermoFisher) in triplicate, taqman primer/probe for Ppia (Mm02342430_g1) was used as an endogenous control. The level of transcript expression is presented as a comparison of between $CD5^{low}$ and $CD5^{high}$ populations, of the same sort, calculated as $2^{-\Delta CT}$, where ΔCT is equal to the difference of the proband cycle threshold (CT) between $CD5^{high}$ - $CD5^{low}$, after being normalized to *Ppia* levels respective to each sample.

REFERENCES

Aguado, E., Richelme, S., Nuñez-Cruz, S., Miazek, A., Mura, A.-M., Richelme, M., Guo, X.-J., Sainty, D., He, H.-T., Malissen, B., Malissen, M., 2002. Induction of T helper type 2 immunity by a point mutation in the LAT adaptor. Science 296, 2036–2040. doi:10.1126/science.1069057

Bhandoola, A., Tai, X., Eckhaus, M., Auchincloss, H., Mason, K., Rubin, S.A., Carbone, K.M., Grossman, Z., Rosenberg, A.S., Singer, A., 2002. Peripheral expression of self-MHC-II influences the reactivity and self-tolerance of mature CD4(+) T cells: evidence from a lymphopenic T cell model. Immunity 17, 425–436.

Bjur, E., Larsson, O., Yurchenko, E., Zheng, L., Gandin, V., Topisirovic, I., Li, S., Wagner, C.R., Sonenberg, N., Piccirillo, C.A., 2013. Distinct Translational Control in CD4+ T Cell Subsets. PLoS Genet 9, e1003494. doi:10.1371/journal.pgen.1003494.s008

Brar, G.A., Weissman, J.S., 2015. Ribosome profiling reveals the what, when, where and how of protein synthesis. Nat Rev Mol Cell Biol 16, 651–664. doi:10.1038/nrm4069

Chi, H., 2012. Regulation and function of mTOR signalling in T cell fate decisions. Nature Reviews Immunology 12, 325–338. doi:10.1038/nri3198

Cook, K.D., Miller, J., 2010. TCR-Dependent Translational Control of GATA-3 Enhances Th2 Differentiation. The Journal of Immunology 185, 3209–3216. doi:10.4049/jimmunol.0902544

Crotty, S., 2011. Follicular Helper CD4 T Cells (T FH). Annu. Rev. Immunol. 29, 621–663. doi:10.1146/annurev-immunol-031210-101400

Daley, S.R., Coakley, K.M., Hu, D.Y., Randall, K.L., Jenne, C.N., Limnander, A., Myers, D.R., Polakos, N.K., Enders, A., Roots, C., Balakishnan, B., Miosge, L.A., Sjollema, G., Bertram, E.M., Field, M.A., Shao, Y., Andrews, T.D., Whittle, B., Barnes, S.W., Walker, J.R., Cyster, J.G., Goodnow, C.C., Roose, J.P., 2013. Rasgrp1 mutation increases naive T-cell CD44 expression and drives mTOR-dependent accumulation of Helios^{+} T cells and autoantibodies. eLife 2, e01020. doi:10.7554/eLife.01020

Das, J., Ho, M., Zikherman, J., Govern, C., Yang, M., Weiss, A., Chakraborty, A.K., Roose, J.P., 2009. Digital Signaling and Hysteresis Characterize Ras Activation in Lymphoid Cells. Cell 136, 337–351. doi:10.1016/j.cell.2008.11.051

Delgoffe, G.M., Kole, T.P., Zheng, Y., Zarek, P.E., Matthews, K.L., Xiao, B., Worley, P.F., Kozma, S.C., Powell, J.D., 2009. The mTOR Kinase Differentially Regulates Effector and Regulatory T Cell Lineage Commitment. Immunity 30, 832–844. doi:10.1016/j.immuni.2009.04.014

Delgoffe, G.M., Pollizzi, K.N., Waickman, A.T., Heikamp, E., Meyers, D.J., Horton, M.R., Xiao, B., Worley, P.F., Powell, J.D., 2011. The kinase mTOR regulates the differentiation of helper T cells through the selective activation of signaling by mTORC1 and mTORC2. Nature Publishing Group 12, 295–303. doi:10.1038/ni.2005

Fulton, R.B., Hamilton, S.E., Xing, Y., Best, J.A., Goldrath, A.W., Hogquist, K.A., Jameson, S.C., 2014. The TCR's sensitivity to self peptide–MHC dictates the ability of naive CD8+ T cells to respond to foreign antigens. Nat. Immunol. 16, 107–117. doi:10.1038/ni.3043

Gigoux, M., Lovato, A., Leconte, J., Leung, J., Sonenberg, N., Suh, W.-K., 2014. Molecular Immunology. Molecular Immunology 59, 46–54. doi:10.1016/j.molimm.2014.01.008

Gorentla, B.K., Wan, C.K., Zhong, X.P., 2011. Negative regulation of mTOR activation by diacylglycerol kinases. Blood 117, 4022–4031. doi:10.1182/blood-2010-08-300731

Heikamp, E.B., Patel, C.H., Collins, S., Waickman, A., Oh, M.-H., Sun, I.-H., Illei, P., Sharma, A., Naray-Fejes-Toth, A., Fejes-Toth, G., Misra-Sen, J., Horton, M.R., Powell, J.D., 2014. The AGC kinase SGK1 regulates TH1 and TH2 differentiation downstream of the mTORC2 complex. Nat. Immunol. 15, 457–464. doi:10.1038/ni.2867

Hogquist, K.A., Starr, T.K., Jameson, S.C., 2003. Receptor Sensitivity: When T cells Lose Their Sense of Self. Current Biology 13, R239–R241. doi:10.1016/S0960-9822(03)00161-1

Hsieh, A.C., Liu, Y., Edlind, M.P., Ingolia, N.T., Janes, M.R., Sher, A., Shi, E.Y., Stumpf, C.R., Christensen, C., Bonham, M.J., Wang, S., Ren, P., Martin, M., Jessen, K., Feldman, M.E., Weissman, J.S., Shokat, K.M., Rommel, C., Ruggero, D., 2012. The translational landscape of mTOR signalling steers cancer initiation and metastasis. Nature 1–10. doi:10.1038/nature10912

Ingolia, N.T., Brar, G.A., Rouskin, S., McGeachy, A.M., Weissman, J.S., 2012. The ribosome profiling strategy for monitoring translation in vivo by deep sequencing of ribosome-protected mRNA fragments. Nat Protoc 7, 1534–1550.

Kong, Y.-C.M., Flynn, J.C., 2014. Opportunistic Autoimmune Disorders Potentiated by Immune-Checkpoint Inhibitors Anti-CTLA-4 and Anti-PD-1. Frontiers in Immunology 5, 206. doi:10.3389/fimmu.2014.00206

Ksionda, O., Melton, A.A., Bache, J., Tenhagen, M., Bakker, J., Harvey, R., Winter, S.S., Rubio, I., Roose, J.P., 2016. RasGRP1 overexpression in T-ALL increases basal nucleotide exchange on Ras rendering the Ras/PI3K/Akt pathway responsive to protumorigenic cytokines. Oncogene 35, 3658–3668. doi:10.1038/onc.2015.431

Laplante, M., Sabatini, D.M., 2012. mTOR signaling in growth control and disease. Cell 149, 274–293. doi:10.1016/j.cell.2012.03.017

Macintyre, A.N., Gerriets, V.A., Nichols, A.G., Michalek, R.D., Rudolph, M.C., Deoliveira, D., Anderson, S.M., Abel, E.D., Chen, B.J., Hale, L.P., Rathmell, J.C., 2014. The Glucose Transporter Glut1Is Selectively Essentialfor CD4 T Cell Activation and Effector Function. Cell Metabolism 20, 61–72. doi:10.1016/j.cmet.2014.05.004

MacIver, N.J., Michalek, R.D., Rathmell, J.C., 2013. Metabolic Regulation of T Lymphocytes. Annu. Rev. Immunol. 31, 130108114109008. doi:10.1146/annurev-immunol-032712-095956

Mandal, P.K., Rossi, D.J., 2012. DNA-Damage-Induced Differentiation in Hematopoietic Stem Cells. Cell 148, 847–848. doi:10.1016/j.cell.2012.02.011

Mandl, J.N., Monteiro, J.P., Vrisekoop, N., Germain, R.N., 2012. T Cell-Positive Selection Uses Self-Ligand Binding Strength to Optimize Repertoire Recognition of Foreign Antigens.

Immunity 1–12. doi:10.1016/j.immuni.2012.09.011

Markegard, E., Trager, E., Yang, C.-W.O., Zhang, W., Weiss, A., Roose, J.P., 2011. Basal LAT-diacylglycerol-RasGRP1 Signals in T Cells Maintain TCRα Gene Expression. PLoS ONE 6, e25540. doi:10.1371/journal.pone.0025540.g005

Michot, J.M., Bigenwald, C., Champiat, S., Collins, M., Carbonnel, F., Postel-Vinay, S., Berdelou, A., Varga, A., Bahleda, R., Hollebecque, A., Massard, C., Fuerea, A., Ribrag, V., Gazzah, A., Armand, J.P., Amellal, N., Angevin, E., Noel, N., Boutros, C., Mateus, C., Robert, C., Soria, J.C., Marabelle, A., Lambotte, O., 2016. Immune-related adverse events with immune checkpoint blockade: a comprehensive review. Eur. J. Cancer 54, 139–148. doi:10.1016/j.ejca.2015.11.016

O'Shea, J.J., Paul, W.E., 2010. Mechanisms underlying lineage commitment and plasticity of helper CD4+ T cells. Science 327, 1098–1102. doi:10.1126/science.1178334

Pearce, E.L., Poffenberger, M.C., Chang, C.-H., Jones, R.G., 2013. Fueling immunity: insights into metabolism and lymphocyte function. Science 342, 1242454. doi:10.1126/science.1242454

Persaud, S.P., Parker, C.R., Lo, W.-L., Weber, K.S., Allen, P.M., 2014. Intrinsic CD4+ T cell sensitivity and response to a pathogen are set and sustained by avidity for thymic and peripheral complexes of self peptide and MHC. Nat. Immunol. 15, 266–274. doi:10.1038/ni.2822

Piccirillo, C.A., Bjur, E., Topisirovic, I., Sonenberg, N., Larsson, O., 2014. Translational control of immune responses: from transcripts to translatomes. Nat. Immunol. 15, 503–511. doi:10.1038/ni.2891

Roux, P.P., Shahbazian, D., Vu, H., Holz, M.K., Cohen, M.S., Taunton, J., Sonenberg, N., Blenis, J., 2007. RAS/ERK signaling promotes site-specific ribosomal protein S6 phosphorylation via RSK and stimulates cap-dependent translation. J. Biol. Chem. 282, 14056–14064. doi:10.1074/jbc.M700906200

Sakaguchi, N., Takahashi, T., Hata, H., Nomura, T., Tagami, T., Yamazaki, S., Sakihama, T., Matsutani, T., Negishi, I., Nakatsuru, S., Sakaguchi, S., 2003. Altered thymic T-cell selection due to a mutation of the ZAP-70 gene causes autoimmune arthritis in mice. Nature 426, 454–460. doi:10.1038/nature02119

Scheu, S., Stetson, D.B., Reinhardt, R.L., Leber, J.H., Mohrs, M., Locksley, R.M., 2006. Activation of the integrated stress response during T helper cell differentiation. Nat. Immunol. 7, 644–651. doi:10.1038/ni1338

Seumois, G., Zapardiel-Gonzalo, J., White, B., Singh, D., Schulten, V., Dillon, M., Hinz, D., Broide, D.H., Sette, A., Peters, B., Vijayanand, P., 2016. Transcriptional Profiling of Th2 Cells Identifies Pathogenic Features Associated with Asthma. The Journal of Immunology 197, 655–664. doi:10.4049/jimmunol.1600397

Sommers, C.L., 2002. A LAT Mutation That Inhibits T Cell Development Yet Induces Lymphoproliferation. Science 296, 2040–2043. doi:10.1126/science.1069066

Stefanová, I., Dorfman, J.R., Germain, R.N., 2002. Self-recognition promotes the foreign antigen sensitivity of naive T lymphocytes. Nature 420, 429–434. doi:10.1038/nature01146

van Oers, N.S., Killeen, N., Weiss, A., 1994. ZAP-70 is constitutively associated with tyrosine-phosphorylated TCR zeta in murine thymocytes and lymph node T cells. Immunity 1, 675–685.

van Oers, N.S., Tao, W., Watts, J.D., Johnson, P., Aebersold, R., Teh, H.S., 1993. Constitutive tyrosine phosphorylation of the T-cell receptor (TCR) zeta subunit: regulation of TCR-associated protein tyrosine kinase activity by TCR zeta. Mol. Cell. Biol. 13, 5771–5780. doi:10.1128/MCB.13.9.5771

Yang, J., Lin, X., Pan, Y., Wang, J., Chen, P., Huang, H., Xue, H.-H., Gao, J., Zhong, X.-P., 2016. Critical roles of mTOR Complex 1 and 2 for T follicular helper cell differentiation and germinal center responses. eLife 5. doi:10.7554/eLife.17936

Yang, K., Shrestha, S., Zeng, H., Karmaus, P.W.F., Neale, G., Vogel, P., Guertin, D.A., Lamb, R.F., Chi, H., 2013. T Cell Exit from Quiescenceand Differentiation into Th2 Cells Dependon Raptor-mTORC1-Mediated Metabolic Reprogramming. Immunity 39, 1043–1056. doi:10.1016/j.immuni.2013.09.015

Zeng, H., Cohen, S., Guy, C., Shrestha, S., Neale, G., Brown, S.A., Cloer, C., Kishton, R.J., Gao, X., Ben Youngblood, Do, M., Li, M.O., Locasale, J.W., Rathmell, J.C., Chi, H., 2016. mTORC1 and mTORC2 Kinase Signaling and Glucose Metabolism Drive Follicular Helper T Cell Differentiation. Immunity 45, 540–554. doi:10.1016/j.immuni.2016.08.017

Zikherman, J., Parameswaran, R., Weiss, A., 2012. Endogenous antigen tunes the responsiveness of naive B cells but not T cells. Nature 489, 160–164. doi:10.1038/nature11311

Zoncu, R., Efeyan, A., Sabatini, D.M., 2010. mTOR: from growth signal integration to cancer, diabetes and ageing. Nat Rev Mol Cell Biol 12, 21–35. doi:10.1038/nrm3025

Chapter 8: Future Directions

A Role for Tonic and Inducible Rasgrp1-mTOR Signals in T Cell Metabolism

INTRODUCTION

As discussed in Chapter 3, recently there has been a great deal of interest in the metabolic programs utilized by T cells and other immune cells, as well as in how metabolism impacts effector function. By now, it is well established that T cells in different activation states dynamically adopt different metabolic programs to meet their functional needs (Pearce et al., 2013; Powell et al., 2012). Naïve, quiescent T cells metabolize glucose using oxidative phosphorylation or OXPHOS. Once T cells become activated, their metabolic demand greatly increases, and as such they respond by primarily utilizing a different metabolic pathway, aerobic glycolysis. Aerobic glycolysis yields fewer ATP molecules than OXPHOS but is advantageous to cells because it generates many biosynthetic precursors for growth. The ability to bring glucose into the cell and to undergo metabolic reprogramming are critical for T cell activation and proliferation (Macintyre et al., 2014).

The serine/threonine kinase mechanistic/mammalian target of rapamycin (mTOR) is a key mediator of cellular metabolism and metabolic reprogramming in T cells (Chi, 2012; Powell et al., 2012). Acute stimulation of T cells with α-CD3 leads to mTOR activation (Gorentla et al., 2011). Within the first 10-24 hours of activation, which is before cell division, T cells experience a host of changes: they alter transcriptional and translational programs, including specific target genes like the transcription factor c-Myc, which is critical for proliferation (Macintyre et al., 2014; Verbist et al., 2016; Yang et al., 2013). Additionally, activation markers are upregulated at the cell surface: these include cytokine receptors such as the IL-2 receptor alpha (IL2Rα) chain (CD25), and nutrient receptors such as the glucose transporter Glut1, the transferrin receptor CD71, and CD98, a component of the leucine transporter. The ability to import nutrients is critical to support the bioenergetic demands of cell growth and division. Furthermore, the ability to import nutrients is important for sustaining mTOR signaling in activated T cells, as Glut1-

deficient and Slc7a5-deficient T cells fail to activate mTOR (Macintyre et al., 2014; Sinclair et al., 2013). This implies that there is some feedback mechanism that allows for sustained mTOR signaling and, ultimately, T cell activation, metabolic reprogramming, and proliferation. Interestingly, despite the outpouring of research into this topic in recent years, the biochemical details of how exactly the TCR couples to mTOR, as well as what effectors participate in the feedback loop, are still unknown.

We hypothesize that Rasgrp1 participates in this TCR-mTOR-metabolic reprogramming feedback loop. This is based on our characterization of the Rasgrp1^{Anaef} mouse and our biochemical studies in DT40 cell lines (discussed in Chapters 6 and 7), which point to a role for Rasgrp1 in basal mTOR signaling. Additionally, published work (Gorentla et al., 2011) and studies from our lab show that Rasgrp1 is required for TCR-induced mTOR activation. Interestingly, while the Rasgrp1^{Anaef} allele is hypermorphic in the basal state (leading to increased tonic mTORC1 signaling), it exhibits hypomorphic signaling to P-S6 and P-Erk upon TCR stimulation (Daley et al., 2013) This is likely due to the location of the mutation (R519G) in the EF hand of Rasgrp1, a region important for Rasgrp1's autoinhibition. Rasgrp1 exists as an autoinhibited dimer in resting lymphocytes, and we hypothesize that point-mutating the EF hand allows for a bit more "breathing" of this dimer, leading to increased tonic signaling (Iwig et al., 2013) (Jeff Iwig and Yvonne Vercoulen, personal communication). Upon receptor stimulation, we have demonstrated that Rasgrp1^{Anaef} does not get efficiently recruited to the plasma membrane, the site of Ras activation (Daley et al., 2013), potentially due to the inability of the autoinhibited dimer to fully open up in response to stimulation.

Here I will present our initial findings uncovering a role for Rasgrp1 in T cell activation, proliferation, and metabolism. I will also discuss our ideas for future experiments to more fully

elucidate how Rasgrp1 signals to mTOR and the consequences of perturbing Rasgrp1 expression or function in T cell metabolic reprogramming.

PRELIMINARY RESULTS

Rasgrp1^{Anaef} CD4^{+} T Cells have Impaired Acute TCR-induced mTORC1 Signaling

We performed *in vitro* stimulations with α-CD3 and α-CD28 on WT and Rasgrp1^{Anaef} CD4^{+} T cells isolated from mouse lymph nodes and utilized phospho-flow cytometry to examine phosphorylation of mTORC1 substrates. The Anaef cells were impaired in their ability to phosphorylate S6K at T389, 4E-BP1 at T37/41, and S6 at S235/236 over a time course of acute stimulation (2, 5, and 10 minutes) (**Figure 8.1A)**. This suggests that normal Rasgrp1 activity is involved in receptor-induced mTORC1 activation. We are presently unable to use primary mouse T cells to address whether Rasgrp1 itself is required for mTORC1 activation, as full-body Rasgrp1 KO mice have a block in thymocyte development and consequently lack peripheral T cells (Dower et al., 2000). The laboratory of Phil King is currently generating mice with a floxed Rasgrp1 allele. We intend to cross these mice to Cre-ERT2 and perform the above-described signaling assays on cells from these animals. This will allow us to more clearly address the role of Rasgrp1 in primary CD4^{+} T cells. We hypothesize that Rasgrp1-deficient peripheral T cells will exhibit impaired mTORC1 activation. This hypothesis is supported by results from experiments utilizing the DT40 chicken B cell line: WT DT40 cells are able to robustly activate mTORC1 in response to anti-chicken IgM stimulation (M4), whereas Rasgrp1/3 double-deficient cells exhibit impaired stimulation-induced mTORC1 activity (**Figure 8.1B**).

Rasgrp1^{Anaef} CD4^{+} T Cells have Impaired TCR-induced Activation and Proliferation

Given that mTOR has been shown to be important for T cell activation state, we were interested in analyzing the induction of activation markers on WT and Anaef $CD4^+$ T cells upon *in vitro* TCR stimulation. We purified $CD4^+$ T cells from WT and Anaef mice and stimulated them for 24 hours on α-CD3/CD28 coated plates. We found that Anaef $CD4^+$ T cells had a modest reduction in CD69 levels after 24 hours of stimulation (**Figure 8.2A**). CD69 is a target of Ras signaling, so this result is consistent with our previous studies that TCR-induced phosphorylation of Erk is reduced in Anaef cells. We also found that Anaef cells are impaired in their ability to upregulate the IL-2Rα subunit CD25 (**Figure 8.2A**). This could not be completely rescued with the addition of exogenous IL-2 (data not shown). These data indicate that Anaef T cells exhibit impaired TCR-induced activation.

We next wanted to determine whether proliferation was impacted by the Anaef mutation, as mTOR signaling has been shown to be important for T cell proliferation (Zhang et al., 2011). We purified $CD4^+$ T cells and labeled them with carboxyfluorescein succinimidyl ester (CFSE) prior to plating on α-CD3/CD28 coated plates. We analyzed CFSE dilution as a readout of proliferation after 72 and 96 hours of culture. Anaef cells had a proliferative delay compared to WT cells (**Figure 8.2B**). We found that Anaef cells do not make as much IL-2 as WT cells (data not shown), however this is not the cause of the observed proliferation defect, as the addition of exogenous IL-2 only partially restored proliferation by Anaef cells (**Figure 8.2B**). We also intend to measure induction of c-Myc, a target of mTOR signaling and an important factor for cellular proliferation, in TCR-stimulated Anaef cells.

<u>$Rasgrp1^{Anaef}$ $CD4^+$ T Cells have Impaired TCR-induced Upregulation of Trophic Receptors</u>

Given the role of mTOR signaling in T cell metabolism, we asked whether Anaef cells were capable of upregulating nutrient receptors, a critical step in their ability to support metabolic reprogramming upon activation. It has been previously shown that mTOR signaling is required for full upregulation of the glucose transporter Glut1 (Macintyre et al., 2014), so we were interested in analyzing the ability of Anaef cells to metabolize glucose. We isolated $CD4^+$ T cells from WT and Anaef mice and activated them *in vitro* with α-CD3 and α-CD28. Interestingly, WT and Anaef cells showed comparable Glut1 upregulation after 24 hours, but after 48 and 72 hours, the Anaef cells had reduced Glut1 levels compared to WT (**Figure 8.3A**). We also analyzed glucose uptake by these cells using (2-(N-(7-Nitrobenz-2-oxa-1,3-diazol-4-yl)Amino)-2-Deoxyglucose) (2-NBDG), a fluorescent glucose analog. We treated cells with 2-NBDG at the indicated time points and analyzed uptake of this analog by flow cytometry. Consistent with the Glut1 results, Anaef cells took up glucose at WT levels after 24 hours of culture, whereas Anaef cells exhibited impaired glucose uptake after 48 hours (**Figure 8.3B**). We intend to analyze hexokinase 2, the kinase that phosphorylates glucose upon its entry into cells, using this system as well.

We analyzed the induction of the transferrin receptor CD71 and the large neutral amino acid transporter CD98, both of which have been shown to be mTOR targets and are required for sustained mTOR activation (Macintyre et al., 2014; Sinclair et al., 2013). Anaef cells exhibited impaired upregulation of both of these molecules (**Figure 8.3C**). These results suggest that Rasgrp1 contributes to upregulation of trophic receptors, a key step in metabolic reprogramming. We plan on measuring basal and TCR-induced metabolic programs using Seahorse and expect that Anaef cells will have reduced extracellular acidification rate (ECAR, a readout of glycolysis) upon TCR stimulation. As Anaef cells exhibit increased basal mTORC1 signaling, we hypothesize that Anaef cells analyzed directly *ex vivo* may have elevated basal OCR (oxygen consumption rate, a readout of OXPHOS) and/or ECAR.

Rasgrp1 has a Role in Nutrient Sensing in Lymphocytes

We noted that our DT40 cell lines signaled differently to S6 when they were rested for 30 minutes in Hank's Buffered Saline (HBSS, "Hanks" in the figure), a nutrient-depleted medium, compared to RPMI, which contains some nutrients such as glucose and amino acids, prior to analysis. Rasgrp1-low Jurkat T cells (441zz) and DT40 B cells in HBSS exhibited very little basal P-S6 activity, whereas robust P-S6 is observed when cells are rested in RPMI prior to analysis (**Figure 8.4A**). Jurkat cells lack PTEN, the phosphatase that opposes PI3K, and as expected these cells have quite high P-S6 levels compared to the PTEN-sufficient DT40 cells. As observed in Chapter 7, some of this P-S6 signal is Rasgrp1-dependent, as we see higher P-S6 in WT DT40s in RPMI compared to Rasgrp1/3 DKO DT40s. Given that amino acids and glucose have been shown to activate mTORC1 (Laplante and Sabatini, 2012; Macintyre et al., 2014; Perera and Zoncu, 2016), we hypothesized that lack of P-S6 in HBSS was due to one of these nutrients being unavailable to cells. However, adding back glucose or non-essential amino acids to the HBSS did not restore P-S6 signaling (**Figure 8.4A**). We are currently investigating whether some essential amino acid is required, or some other component that differs between RPMI and HBSS. Overall, these data suggest that Rasgrp1-mTORC1 signals require some nutrient not present in HBSS. We hypothesize that Rasgrp1 may act as a sensor for this nutrient and intend to use our Rasgrp1-sufficient and -deficient cell line system to investigate this.

FUTURE DIRECTIONS

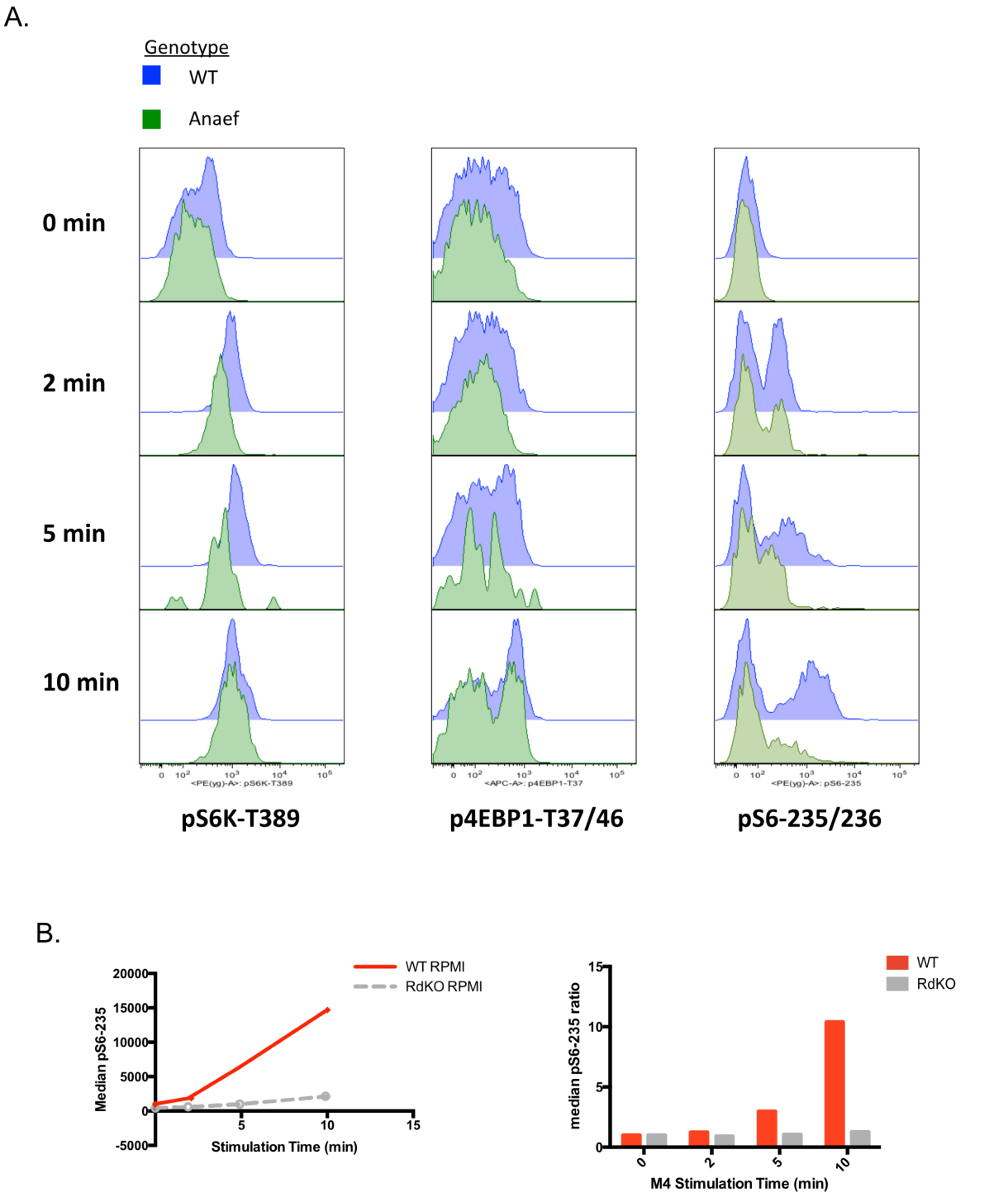
We are intrigued by these preliminary studies that suggest a link at the biochemical level between Rasgrp1 and mTORC1, both in the basal state and downstream of antigen receptor stimulation. We still do not know how Rasgrp1 couples to mTOR: mTORC1 activation requires the activity of two GTPases, the Rags and Rheb. Several proteins named the "Ragulator" complex act as guanine nucleotide exchange factors (GEFs) for the Rag GTPases, but there may be other GEFs involved, and to date no GEF has been identified that activates Rheb (Laplante and Sabatini, 2012). Rasgrp1 is a guanine nucleotide exchange factor (GEF), and Rasgrp catalytic function is required for mTORC1 signaling (**see Chapter 7, Figure 7.1A**). Rasgrp1 has also recently been reported to act as a GEF for Rhes, which is a GTPase expressed in the brain striatum that is very similar to Rheb (Shahani et al., 2016). Thus, we are interested in determining whether Rasgrp1 can act as a GEF for the Rags and/or for Rheb in lymphocytes and other cell types. We intend to perform transient transfections of Rasgrp1 and various GTPases into 293T cells and analyze mTORC1 activity by immunoblotting, and we can also look for co-localization of Rasgrp1 and Rheb in these transfected cells by immunoprecipitation (IP) followed by immunoblotting. We can also perform *in vitro* GEF assays to see if Rasgrp1 can serve as a GEF for Rheb or Rag. If Rasgrp1 is not a Rheb- or Rag-GEF, we can perform Rasgrp1 IPs followed by mass spectrometry analyses to identify novel interaction partners of Rasgrp1, which could also help us gain insights into how Rasgrp1 may activate mTOR.

We are also interested in furthering our understanding of how Rasgrp1-mTOR signals impact lymphocyte metabolism. We intend to use the Seahorse platform to determine what metabolic programs are used in WT and Anaef primary T cells, in both the basal and antigen receptor-induced states. We can also perform mass spectrometry analyses to determine what metabolites are being used by these cells in different activation states. To more fully probe where and when Rasgrp1 acts in the metabolic pathways, we can perform our *in vitro* signaling

assays using DT40 cells in the presence or absence of metabolic inhibitors of glycolysis (2DG) or OXPHOS (oligomycin), or in base media supplemented with various amino acids or other nutrients, as in Figure 8.4A.

Rasgrp1 is expressed in other immune cell types such as CD8 T cells (Coughlin et al., 2005), neutrophils (la Luz Sierra et al., 2010), NK cells (Lee et al., 2009), and mast cells (Liu et al., 2007), as well as non-hematopoietic cells such as regions of the brain (Kawasaki et al., 1998; Shahani et al., 2016), keratinocytes of the skin (Rambaratsingh et al., 2003), and intestinal (Depeille et al., 2015) and mammary (Samocha and Roose, unpublished findings) epithelial cells. As such, we would also like to apply our biochemical and metabolic assays to other immune and non-hematopoeitic cell types. We anticipate that these studies will yield novel insights as to how the antigen receptor and how Rasgrp1 couple to mTORC1 signaling, as well as how Rasgrp1-mTOR signals contribute to lymphocyte metabolism.

FIGURES



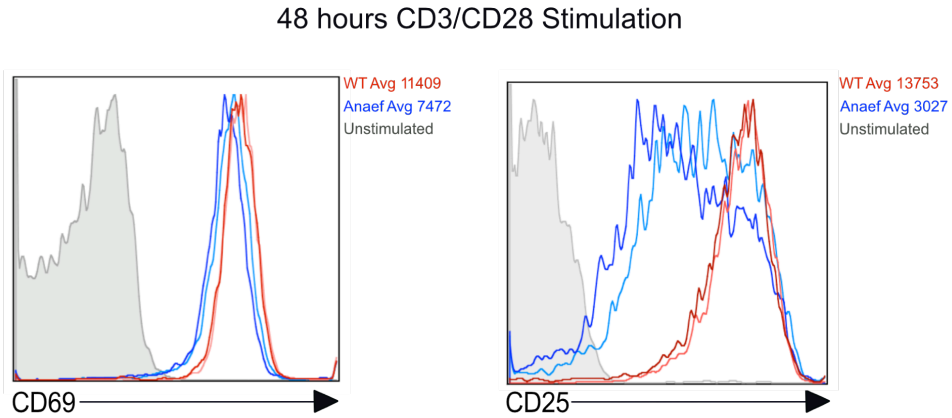
Myers et al., Figure 1

Figure 8.1: Rasgrp1^{Anaef} and Rasgrp1-deficient Cells have Impaired Receptor-induced mTORC1 Activation

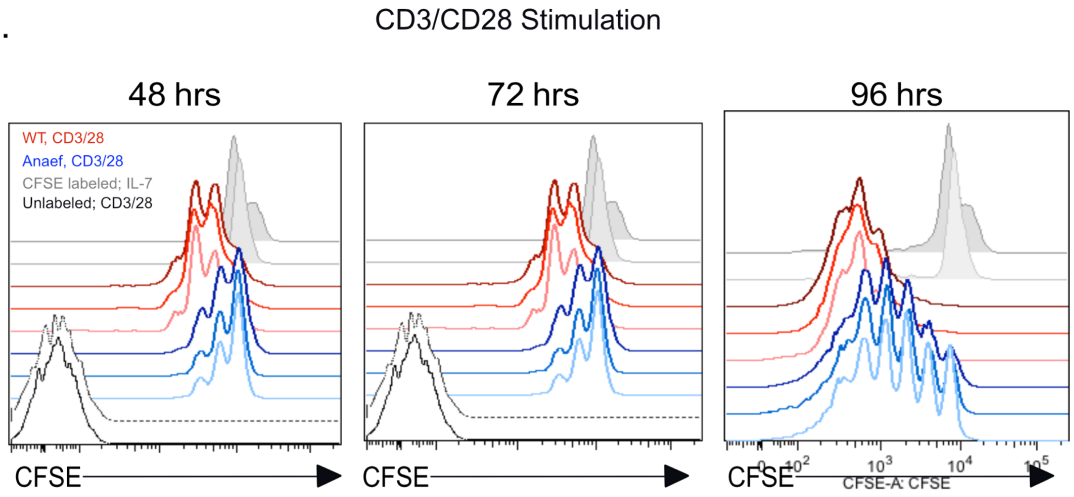
(A) Flow cytometric analysis of P-S6K^{T389}, P-4E-BP1$^{T37/41}$, and P-S6$^{S235/236}$ in WT and Anaef CD4^{+} T cells. Lymphocytes were purified from mouse lymph nodes, rested in RPMI for a minimum of 2 hours, and stimulated through the TCR with α-CD3 for the indicated time points prior to fixation.

(B) Flow cytometric analysis of P-S6$^{S235/236}$ in WT and Rasgrp1/3 DKO DT40 cells stimulated through the B cell receptor (BCR) with M4 for the indicated time points prior to fixation. Cells were rested for 30 minutes in RPMI prior to fixation.

A.



B.



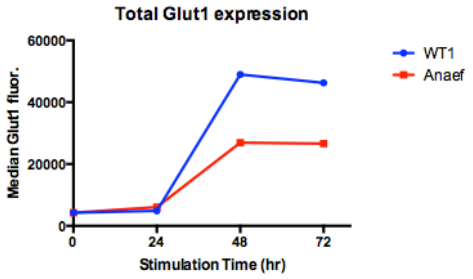
Myers et al., Figure 2

Figure 8.2: Rasgrp1^{Anaef} CD4^{+} T Cells have Impaired TCR-induced Activation and Proliferation

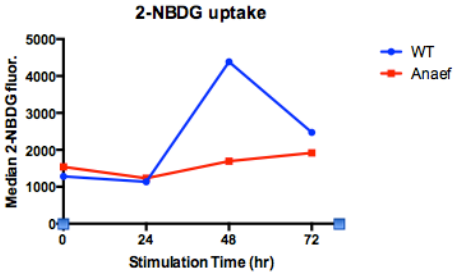
(A) Flow cytometric analysis of WT and Anaef CD4^{+} T cells for the induction of the activation markers CD69 and CD25. Cells were MACS-purified from mouse lymph nodes and cultured for 48 hours in complete media prior to FACS staining. Cells were labeled with DAPI immediately prior to FACS analysis and gated on live (DAPI-) CD4^{+} cells.

(B) Flow cytometric analysis of CFSE dilution by WT and Anaef CD4^{+} T cells. Cells were MACS-purified from mouse lymph nodes, cultured, and harvested at the indicated time points. Cells were labeled with DAPI immediately prior to FACS analysis and gated on live (DAPI-) cells.

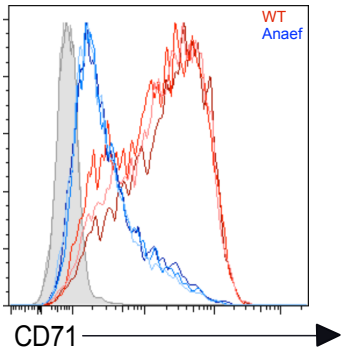
A.

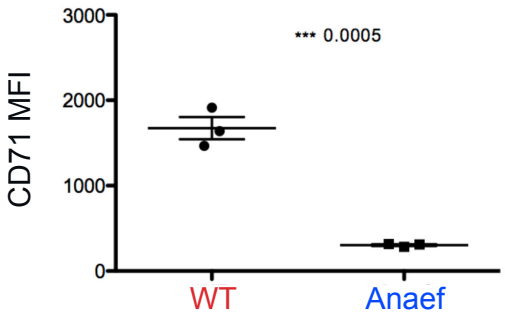


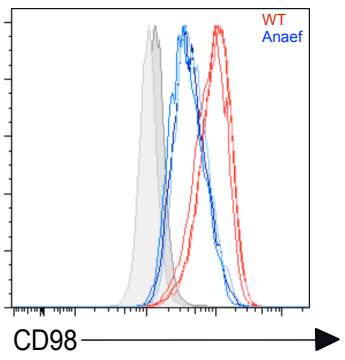
B.

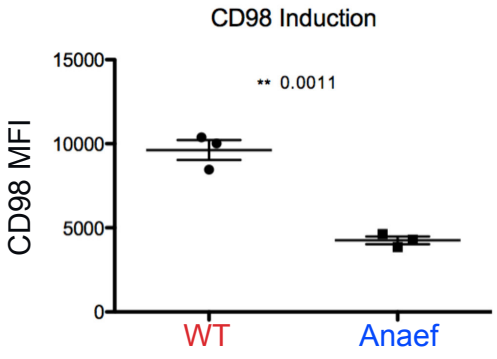


C.









Myers et al., Figure 3

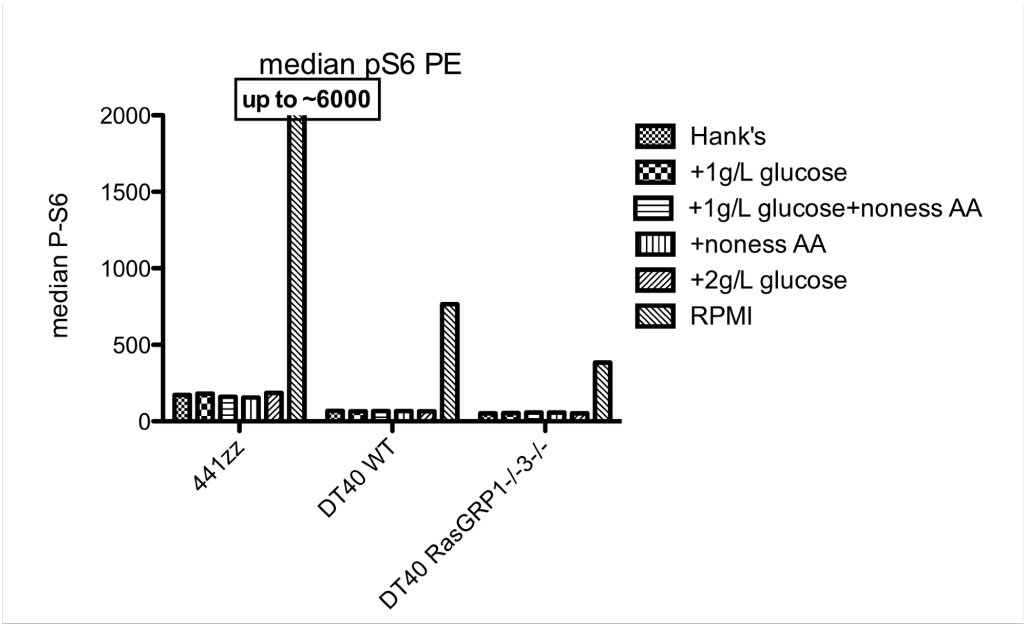
Figure 8.3: Rasgrp1^{Anaef} CD4^{+} T Cells have Impaired TCR-induced Upregulation of Trophic Receptors

(A) Flow cytometric analysis of WT and Anaef CD4^{+} T cells for the induction of the glucose transporter Glut1. Cells were MACS-purified from mouse lymph nodes and cultured for up to 72 hours in complete media prior to harvesting and fixation. Fixed cells from all indicated time points were stained with antibodies to Glut1 on the same day prior to FACS analysis.

(B) Flow cytometric analysis of WT and Anaef CD4^{+} T cells for glucose uptake using the fluorescent glucose analog 2-NBDG. Cells were MACS-purified from mouse lymph nodes and cultured for up to 72 hours in complete media prior to harvesting. Harvested cells were stained with 2-NBDG for 45 minutes at 37ºC prior to fixation. Fixed cells from all indicated time points were analyzed by FACS on the same day.

(C) Flow cytometric analysis of WT and Anaef CD4^{+} T cells for the induction of CD71 and CD98. Cells were MACS-purified from mouse lymph nodes and cultured for 24 hours in complete media prior to harvesting and FACS analysis.

A.



Myers et al., Figure 4

Figure 8.4: Rasgrp1 has a Role in Nutrient Sensing in Lymphocytes

(A) 441zz Jurkat, WT DT40, and Rasgrp1/3 DKO DT40 cells were rested in the indicated media for 30 minutes prior to FACS analysis for P-S6$^{S235/236}$.

METHODS

Mice

WT C57BL/6 mice and Anaef mice were bred in house at UCSF. Mice were housed and treated in accordance with the guidelines of the Institutional Animal Care and Use Committee (IACUC) guidelines of the University of California, San Francisco (AN098375-03B).

Primary T Cell Isolation and Stimulation

Cells were isolated from cervical, brachial, axillary, inguinal, and mesenteric lymph nodes and single cell suspensions were prepared by mashing cells through a 70μm strainer. Cells were counted and $CD4^+$ T cells were isolated by MACS negative isolation (Miltenyi). For short term stimulations, cells were rested in T cell media for a minimum of 2 hours or up to overnight. Cells were then resuspended in plain RPMI with inhibitors where applicable, rested for 30 minutes, and stimulated with 5ug/ml α-CD3 (clone 2C11). For long-term stimulations, cells were counted and plated on 96 well plates that had been pre-coated with 2ug/ml α-CD3 (2C11) and α-CD28 (37.51) (both from UCSF Monoclonal Antibody Core). T cells were cultured in RPMI (Hyclone) supplemented with 10% fetal calf serum, 1% sodium pyruvate, 1% nonessential amino acids, 1% HEPES, 1% pen-strep glutamine, and 0.1% beta mercaptoethanol.

Flow cytometry

Cells were harvested at indicated time points, washed once in FACS buffer, and fixed for 20 minutes in 2% PFA at room temperature. Cells were then washed twice with FACS buffer and permeabilized with ice-cold 90% methanol at -20ºC (for a minimum of 30 minutes but typically overnight). Cells were washed with FACS buffer and stained with antibodies to relevant surface markers and intracellular signaling proteins (P-S6K, P-S6, P-4EBP1) and receptors (Glut1) before flow cytometric analysis. For assays that do not require fixation, cells were harvested at

the indicated time points, washed, stained with surface markers to relevant antigens (CD71, CD98, CD69, CD25) for 30 minutes on ice, washed, and analyzed by flow cytometry. For proliferation assays, MACS-purified $CD4^+$ T cells were labeled with CFSE (2.5μM, Thermo Fisher Scientific), washed, and plated on α-CD3 (2C11) and α-CD28 (37.51) coated plates in complete media as above. All flow cytometry data was acquired on a BD LSRII or Fortessa and analyzed using FlowJo (Treestar).

DT40 cell lines and transfection experiments

Rasgrp1/3 deficient DT40 chicken B cells were maintained in RPMI supplemented with 10%FBS, 1% chicken serum, 1% pen-strep-glutamine, and 2.5% HEPES. Where applicable, cells were stimulated with M4 for the indicated times. Where applicable, cells were incubated in the indicated media (RPMI, HBSS, +/- nutrients) for 30 minutes. Cells were then fixed for 20 minutes with 2% paraformaldehyde, washed, and permeabilized overnight at -20ºC in 90% methanol. The following day cells were stained for intracellular signaling molecules as described above.

REFERENCES

Chi, H., 2012. Regulation and function of mTOR signalling in T cell fate decisions. Nature Reviews Immunology 12, 325–338. doi:10.1038/nri3198

Coughlin, J.J., Stang, S.L., Dower, N.A., Stone, J.C., 2005. RasGRP1 and RasGRP3 Regulate B Cell Proliferation by Facilitating B Cell Receptor-Ras Signaling. The Journal of Immunology 175, 7179–7184. doi:10.4049/jimmunol.175.11.7179

Daley, S.R., Coakley, K.M., Hu, D.Y., Randall, K.L., Jenne, C.N., Limnander, A., Myers, D.R., Polakos, N.K., Enders, A., Roots, C., Balakishnan, B., Miosge, L.A., Sjollema, G., Bertram, E.M., Field, M.A., Shao, Y., Andrews, T.D., Whittle, B., Barnes, S.W., Walker, J.R., Cyster, J.G., Goodnow, C.C., Roose, J.P., 2013. Rasgrp1 mutation increases naive T-cell CD44 expression and drives mTOR-dependent accumulation of Helios^{+} T cells and autoantibodies. eLife 2, e01020. doi:10.7554/eLife.01020

Depeille, P., Henricks, L.M., van de Ven, R.A.H., Lemmens, E., Wang, C.-Y., Matli, M., Werb, Z., Haigis, K.M., Donner, D., Warren, R., Roose, J.P., 2015. RasGRP1 opposes proliferative EGFR–SOS1–Ras signals and restricts intestinal epithelial cell growth. Nat Cell Biol 17, 804–815. doi:10.1038/ncb3175

Dower, N.A., Stang, S.L., Bottorff, D.A., Ebinu, J.O., Dickie, P., Ostergaard, H.L., Stone, J.C., 2000. RasGRP is essential for mouse thymocyte differentiation and TCR signaling. Nat. Immunol. 1, 317–321.

Gorentla, B.K., Wan, C.K., Zhong, X.P., 2011. Negative regulation of mTOR activation by diacylglycerol kinases. Blood 117, 4022–4031. doi:10.1182/blood-2010-08-300731

Iwig, J.S., Vercoulen, Y., Das, R., Barros, T., Limnander, A., Che, Y., Pelton, J.G., Wemmer, D.E., Roose, J.P., Kuriyan, J., 2013. Structural analysis of autoinhibition in the Ras-specific exchange factor RasGRP1. eLife 2, e00813–e00813. doi:10.7554/eLife.00813.032

Kawasaki, H., Springett, G.M., Toki, S., Canales, J.J., Harlan, P., Blumenstiel, J.P., Chen, E.J., Bany, I.A., Mochizuki, N., Ashbacher, A., Matsuda, M., Housman, D.E., Graybiel, A.M., 1998. A Rap guanine nucleotide exchange factor enriched highly in the basal ganglia. Proc Natl Acad Sci U S A 95, 13278–13283.

la Luz Sierra, de, M., Sakakibara, S., Gasperini, P., Salvucci, O., Jiang, K., McCormick, P.J., Segarra, M., Stone, J., Maric, D., Zhu, J., Qian, X., Lowy, D.R., Tosato, G., 2010. The transcription factor Gfi1 regulates G-CSF signaling and neutrophil development through the Ras activator RasGRP1. Blood 115, 3970–3979. doi:10.1182/blood-2009-10-246967

Laplante, M., Sabatini, D.M., 2012. mTOR signaling in growth control and disease. Cell 149, 274–293. doi:10.1016/j.cell.2012.03.017

Lee, S.H., Yun, S., Lee, J., Kim, M.J., Piao, Z.H., Jeong, M., Chung, J.W., Kim, T.D., Yoon, S.R., Greenberg, P.D., Choi, I., 2009. RasGRP1 Is Required for Human NK Cell Function. The Journal of Immunology 183, 7931–7938. doi:10.4049/jimmunol.0902012

Liu, Y., Zhu, M., Nishida, K., Hirano, T., Zhang, W., 2007. An essential role for RasGRP1 in

mast cell function and IgE-mediated allergic response. Journal of Experimental Medicine 204, 93–103. doi:10.1084/jem.20061598

Macintyre, A.N., Gerriets, V.A., Nichols, A.G., Michalek, R.D., Rudolph, M.C., Deoliveira, D., Anderson, S.M., Abel, E.D., Chen, B.J., Hale, L.P., Rathmell, J.C., 2014. The Glucose Transporter Glut1Is Selectively Essentialfor CD4 T Cell Activation and Effector Function. Cell Metabolism 20, 61–72. doi:10.1016/j.cmet.2014.05.004

Pearce, E.L., Poffenberger, M.C., Chang, C.-H., Jones, R.G., 2013. Fueling immunity: insights into metabolism and lymphocyte function. Science 342, 1242454. doi:10.1126/science.1242454

Perera, R.M., Zoncu, R., 2016. The Lysosome as a Regulatory Hub. Annu. Rev. Cell Dev. Biol. 32, 223–253. doi:10.1146/annurev-cellbio-111315-125125

Powell, J.D., Pollizzi, K.N., Heikamp, E.B., Horton, M.R., 2012. Regulation of Immune Responses by mTOR. Annu. Rev. Immunol. 30, 39–68. doi:10.1146/annurev-immunol-020711-075024

Rambaratsingh, R.A., Stone, J.C., Blumberg, P.M., Lorenzo, P.S., 2003. RasGRP1 Represents a Novel Non-protein Kinase C Phorbol Ester Signaling Pathway in Mouse Epidermal Keratinocytes. Journal of Biological Chemistry 278, 52792–52801. doi:10.1074/jbc.M308240200

Shahani, N., Swarnkar, S., Giovinazzo, V., Morgenweck, J., Bohn, L.M., Scharager-Tapia, C., Pascal, B., Martinez-Acedo, P., Khare, K., Subramaniam, S., 2016. RasGRP1 promotes amphetamine-induced motor behavior through a Rhes interaction network (“Rhesactome”) in the striatum. Science Signaling 9, ra111. doi:10.1126/scisignal.aaf6670

Sinclair, L.V., Rolf, J., Emslie, E., Shi, Y.-B., Taylor, P.M., Cantrell, D.A., 2013. Control of amino-acid transport by antigen receptors coordinates the metabolic reprogramming essential for T cell differentiation. Nat. Immunol. 14, 500–508. doi:10.1038/ni.2556

Verbist, K.C., Guy, C.S., Milasta, S., Liedmann, S., Kamiński, M.M., Wang, R., Green, D.R., 2016. Metabolic maintenance of cell asymmetry following division in activated T lymphocytes. Nature 532, 389–393. doi:10.1038/nature17442

Yang, K., Shrestha, S., Zeng, H., Karmaus, P.W.F., Neale, G., Vogel, P., Guertin, D.A., Lamb, R.F., Chi, H., 2013. T Cell Exit from Quiescenceand Differentiation into Th2 Cells Dependon Raptor-mTORC1-Mediated Metabolic Reprogramming. Immunity 39, 1043–1056. doi:10.1016/j.immuni.2013.09.015

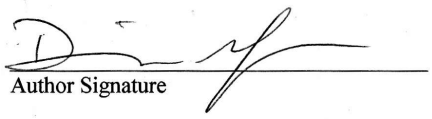
Zhang, S., Readinger, J.A., DuBois, W., Janka-Junttila, M., Robinson, R., Pruitt, M., Bliskovsky, V., Wu, J.Z., Sakakibara, K., Patel, J., Parent, C.A., Tessarollo, L., Schwartzberg, P.L., Mock, B.A., 2011. Constitutive reductions in mTOR alter cell size, immune cell development, and antibody production. Blood 117, 1228–1238. doi:10.1182/blood-2010-05-287821

Publishing Agreement

It is the policy of the University to encourage the distribution of all theses, dissertations, and manuscripts. Copies of all UCSF theses, dissertations, and manuscripts will be routed to the library via the Graduate Division. The library will make all theses, dissertations, and manuscripts accessible to the public and will preserve these to the best of their abilities, in perpetuity.

Please sign the following statement:

I hereby grant permission to the Graduate Division of the University of California, San Francisco to release copies of my thesis, dissertation, or manuscript to the Campus Library to provide access and preservation, in whole or in part, in perpetuity.



Author Signature

3/17/17

Date